The interaction of COMT genotype, tolcapone and acute stress, on brain activity and working memory performance



Marieke Annie Gerdine Martens

Wolfson College

Department of Psychiatry

University of Oxford

A thesis submitted for the degree of

Doctor of Philosophy

Trinity 2019

Abstract

An inverted-U-shaped relationship exists between dopamine and prefrontal cortex (PFC) dependent cognitive function, whereby either too little or too much dopamine signalling impairs cognitive performance. Genetic, pharmacological, pathological, and environmental factors can affect a person's position on the curve. In this thesis I explored three of such factors and their potential interactions. Interestingly, an inverted-U relationship also exists between acute stress and PFC-dependent cognitive performance, with moderate stress levels facilitating, and high levels impairing cognitive function. The enzyme catechol-O-methyltransferase (COMT) metabolises dopamine in the PFC. The human COMT gene contains a functional polymorphism (Val^{158}Met) that influences enzyme activity: the ancestral COMT-Val allele has ~40% greater activity than the COMT-Met allele. COMT activity can also be altered pharmacologically by inhibitors, like tolcapone. Previous research showed that COMT Val^{158}Met affects the functional connectivity of the PFC at rest and linked the COMT-Met allele with better PFC-dependent performance. Moreover, COMT genotype and tolcapone interact, with the drug having opposite effects on cognition in COMT-Met and COMT-Val homozygotes. The goal of this DPhil project is to extend these findings. In particular, there is evidence that stress also impacts dopamine signalling, and some indication that it interacts with COMT. However, it is unknown whether this interaction is modulated by COMT inhibition by tolcapone.

First, two stressors were explored, - a novel VR stressor and the Montreal Imaging Stress Task (MIST). Both induced a physiological and psychological stress response, however with a different magnitude and duration. The MIST induced a stronger and longer lasting physiological response, whilst the VR lift seemed to induce higher subjective ratings of stress and anxiety.

The main study of this thesis was a randomised, double-blind, placebo-controlled, between-subjects study of the effects of COMT genotype and tolcapone and their interaction, on behaviour and patterns of brain activity using MRI. I demonstrate that COMT and tolcapone influence cerebral blood flow, resting state functional connectivity, stress sensitivity and working memory related brain activation and performance. However, the majority of my findings are not compatible with a 'simple' inverted-U model, whereby stress acts only to increase central dopamine levels and thereby enhance (baseline) performance in COMT-Val homozygotes, and impair it in COMT-Met homozygotes. In future it would be of interest to further study these inverted-Us by investigating how different forms of PFC dependent cognitive functions are affected by different kinds of stressors. However, these relationships are complicated by the fact that some of the cognitive effects of stress are likely mediated by non-dopaminergic mechanisms, the context dependency of the different inverted-U relationships, the stress response not being a unitary concept, and the need for multidisciplinary approaches and falsifiable hypotheses.

Acknowledgements

There are not enough words to be able to thank everyone who helped me make this DPhil experience a success in the way that they deserve. First and foremost, my gratitude goes to my outstanding supervisors, Liz Tunbridge and Paul Harrison. Thank you for providing me with so many opportunities. Without your unlimited guidance, support, patience and faith in my abilities, I would not have been this successful. You have gone above and beyond in mentoring me over the last four years.

Deleted for privacy reasons.

Declarations

This dissertation is the result of my own work and includes nothing that is the outcome of work done in collaboration except as specified in the text. I state that no substantial part of my dissertation has already been submitted, or, is being currently submitted for any such degree, diploma or other qualification at the University of Oxford or other University or similar institution. I state that Chapter 2 of this thesis has been submitted for publication. None of my other work has been submitted or accepted for publication. All submitted papers are related directly to my field of study, and have been written whilst holding the status of a student for the DPhil.

In accordance with the guidelines, this thesis does not exceed 50,000 words, and it contains less than 150 figures.

Table of contents

Abstract I
Acknowledgements II
Declarations III
List of figures IX
List of tables X
Abbreviations XI

Chapter 1 Introduction 1
1.1 Dopamine 1
1.1.1 Dopamine and cognition 3
1.1.1.1 *Inverted-U between dopamine and PFC-dependent function* 3
1.2 COMT 6
1.2.1 COMT gene structure and expression 6
1.2.2 COMT Val^{158}Met polymorphism 7
1.2.3 COMT Val^{158}Met and behaviour 8
1.2.4 COMT inhibition with tolcapone 9
1.2.5 COMT inhibition and behaviour 10
1.3 The stress response 11
1.3.1 Autonomic nervous system 12
1.3.2 Hypothalamic-pituitary-adrenal (HPA) axis 12
1.3.3 Stress and virtual reality 15
1.3.4 The MIST: measuring stress effects in MRI paradigms 15
1.4 Interactions 16
1.4.1 Dopamine and stress 17
1.4.2 COMT Val^{158}Met and stress 18
1.5 Aims and objectives 19

Chapter 2 Physiological and psychological effects of a novel virtual reality stressor 22
2.1 Introduction 22
2.2 Methods 23
2.2.1 *Participants* 23
2.2.2 *Procedure* 23
2.2.3 *Virtual reality* 25
2.2.4 *Measurements of stress response* 26

2.2.5 *Tasks* 27
2.2.6 *Analyses* 27
2.3 Results 28
2.3.1 *Participants* 28
2.3.2 *Main analyses* 29
2.3.3 *Exploratory analyses* 31
2.4 Discussion 37
2.4.1 *Limitations* 39
2.4.2 *Conclusion* 39

Chapter 3 Physiological and psychological effects of the Montreal Imaging Stress Task (MIST). 40
3.1 Introduction 40
3.2 Methods 45
3.2.1 *Participants* 45
3.2.2 *Procedure* 45
3.2.3 *Tasks* 47
3.2.4 *Measurements of stress response* 48
3.2.5 *Analyses* 48
3.3 Results 50
3.3.1 *Participants* 50
3.3.2 *Analyses* 51
3.4 Discussion 61
3.4.1 *Limitations of the MIST* 62
3.4.2 *Conclusion* 63

Chapter 4 Overall methods for imaging study 65
4.1 Introduction 65
4.2 Methods 65
4.2.1 *Participants* 65
4.2.2 *Procedure* 67
4.2.3 *Tasks* 70
4.2.4 *Behavioural / MRI analyses* 70

Chapter 5 The interaction between COMT genotype and COMT inhibition on cerebral blood flow and brain structure 71
5.1 Introduction 71

5.1.1 *Catecholamines and blood flow* 71
5.1.2 *COMT and cerebral blood flow* 71
5.1.3 *Arterial spin labelling* 72
5.1.4 *COMT and brain structure* 73
5.2 Methods 74
5.2.1 *Participants, study design and procedure* 74
5.2.2 *Neuroimaging Protocol* 74
5.2.3 *Analysis methods* 75
5.3 Results 77
5.3.1 *Participants* 77
5.3.2 *Cerebral blood flow* 77
5.3.3 *Structural differences* 81
5.4 Discussion 81
5.4.1 *COMT genotype* 81
5.4.2 *COMT inhibition by tolcapone* 82
5.4.3 *Potential mechanisms* 82
5.4.4 *BOLD activations* 83
5.4.5 *Structural differences* 84
5.4.6 *Limitations* 84
5.4.7 *Conclusion* 84

Chapter 6 The interaction between COMT genotype and COMT inhibition on resting state connectivity 86
6.1 Introduction 86
6.1.1 *Resting state analysis* 86
6.1.2 *Effects of COMT genotype on rsFC* 87
6.2 Methods 88
6.2.1 *Participants, study design, and procedure* 88
6.2.2 *Neuroimaging Protocol* 88
6.2.3 *Analysis methods* 89
6.3 Results 92
6.3.1 *Participants* 92
6.3.2 *Identification of resting state networks* 93
6.3.3 *Group differences in rsFC* 93
6.3.4 *Exploratory analyses* 95
6.3.5 *Seed analysis* 100

6.4 Discussion 107
6.4.1 *Seed analysis* 107
6.4.2 *Results in relationship to other analysis methods* 107
6.4.3 *COMT inhibition* 108
6.4.4 *Conclusion* 109

Chapter 7 The interaction between COMT genotype and COMT inhibition on the stress response and stress related brain activity 111
7.1 Introduction 111
7.1.1 *MIST related brain activation* 111
7.1.2 *Dopamine and stress* 111
7.1.3 *COMT and stress* 112
7.1.4 *Aims and predictions* 112
7.2 Methods 117
7.2.1 *Participants, study design, and procedure* 117
7.2.2 *Task - MIST* 117
7.2.3 *Measurements of stress response* 118
7.2.4 *Behavioural analyses* 118
7.2.5 *Neuroimaging* 119
7.3 Results 121
7.3.1 *Participants* 121
7.3.2 *Physiological effects of the MIST - validation of the stress response* 121
7.3.3 *Group differences – main analyses* 125
7.3.4 *Group differences – exploratory analyses* 125
7.3.5 *Imaging results* 133
7.4 Discussion 140
7.4.1 *Validation of the MRI MIST* 140
7.4.2 *Effects of COMT genotype and COMT inhibition on the stress response* 141
7.4.3 *Effects of COMT genotype and COMT inhibition on stress related brain activity* 142
7.4.4 *MRI scanner induced stress response* 142
7.4.5 *Salivary amylase* 143
7.4.6 *Limitations* 143
7.4.7 *Conclusion* 144

Chapter 8 The interaction between COMT genotype and COMT inhibition on working memory related brain activity and performance under acute stress 145

8.1 Introduction 145
8.1.1 *Interactions between COMT, COMT inhibition and stress* 145
8.1.2 *Predictions* 146
8.2 Methods 149
8.2.1 *Participants, study design and procedure* 149
8.2.2 *Task* 149
8.2.3 *Behavioural analysis* 149
8.2.4 *Neuroimaging Protocol and structural MRI* 149
8.3 Results 151
8.3.1 *Participants* 151
8.3.2 *Behavioural results* 151
8.3.3 Group differences on N-back *performance* in cortisol responders 154
8.3.4 *Imaging results* 156
8.4 Discussion 163
8.4.1 *Effects on working memory performance* 164
8.4.2 *Effects on working memory related brain activity* 166
8.4.3 *Effects on working memory related brain activity – right dlPFC* 167
8.4.4 *Conclusion* 168

Chapter 9 Overall Discussion 169
9.1 Summary of the main findings 169
9.2 Strengths and limitations 175
9.2.1 *Strengths* 175
9.2.2 *Limitations* 175
9.3 Future studies 177
9.4 Broader considerations 180
9.5 Conclusion 181

Appendix I Protocol for the behavioural MIST 182
Appendix II Protocol for the MRI MIST 186
Appendix III Group differences in the effects of acute stress exposure in the MIST scenario on sAA and subjective stress in cortisol responders only 189

List of figures

Figure 1.1 - The synthesis and degradation of dopamine……2
Figure 1.2 - The inverted U-shaped relationship between dopamine and PFC-function……..4
Figure 1.3 - Inverted-U's……21
Figure 2.1 - Timeline of the experiment and VR lifts……24
Figure 2.2 - Summary of main analyses……30
Figure 2.3 - Effects of acute stress exposure in the VR scenario on physiological stress measures……32
Figure 2.4 - Effects of acute stress exposure in the VR scenario on psychological stress measures……34
Figure 3.1 - Timeline of the experiment……46
Figure 3.2 - Explanation of AUCG and AUCI……50
Figure 3.3 - Area under the curve cortisol data……52
Figure 3.4 - Effects of acute stress exposure by the MIST on N-back performance (percentage correct)……53
Figure 3.5 - Effects of acute stress exposure by the MIST on N-back performance (reaction times)……53
Figure 3.6 - Effects of acute stress exposure by the MIST on physiological stress measures – part 1……55
Figure 3.7 - Effects of acute stress exposure by the MIST on physiological stress measures – part 2……56
Figure 3.8 - Effects of acute stress exposure by the MIST on psychological stress measures……57
Figure 3.9 - Correlation between N-back performance and cortisol change……58
Figure 4.1 - Timeline of the imaging study……69
Figure 5.1 - Example of perfusion weighted images……78
Figure 5.2 - Differences in cerebral blood flow between COMT-Val and COMT-Met homozygotes……79
Figure 5.3 - Differences in cerebral blood flow between placebo and tolcapone……79
Figure 6.1 - Left vlPFC mask……92
Figure 6.2 - Right dlPFC mask……92
Figure 6.3 - Resting State Networks identified……94
Figure 6.4 - The effect of COMT-genotype on anterior DMN functional connectivity……95
Figure 6.5 - Effect of COMT inhibition on SMN functional connectivity……96
Figure 6.6 - Genotype by treatment interaction on SMN connectivity……97
Figure 6.7 - COMT-genotype by treatment interactions for the left vlPFC-seed……101
Figure 6.8 - Difference in FC between the right dlPFC for COMT-Met and COMT-Val homozygotes……104
Figure 6.9 - Interaction effect on FC between the right dlPFC and the middle temporal gyrus……104
Figure 7.1 - Effects of acute stress exposure by the MRI MIST on stress measures……123
Figure 7.2 - Effects of COMT genotype and COMT inhibition on stress measures……128
Figure 7.3 - Effects of acute stress exposure by the MRI MIST on cortisol levels in cortisol responders……129
Figure 7.4 - Effects of COMT genotype and COMT inhibition on cortisol levels in cortisol-responders……132
Figure 7.5 - Whole-brain fMRI MIST task activations and deactivations……134
Figure 7.6 - Whole-brain fMRI MIST task activations and deactivations – with GM and CBF maps……137
Figure 7.7 - Effects of COMT genotype on whole brain MIST deactivations……139
Figure 8.1 – Inverted-U's……148
Figure 8.2 - Effects of COMT-genotype and tolcapone on N-back performance (percentage correct……153
Figure 8.3 - Effects of COMT-genotype and COMT-inhibition on N-back reaction times……153
Figure 8.4 - Effects of COMT-genotype and tolcapone on N-back performance in cortisol responders……155
Figure 8.5 - Effects of COMT-genotype and tolcapone on N-back reaction times in cortisol responders……156
Figure 8.6 - Whole-brain fMRI MIST task activations and deactivations……157
Figure 8.7 - Effects of COMT inhibition on whole brain working memory related activity……162
Figure 8.8 - Small volume correction / ROI analysis - right dlPFC……163
Figure 9.1 - Inverted-U's……179
Figure I.1 - MIST examples……185

List of tables

Table 2.1 - Demographic and personality measures 29
Table 2.2 - Effects of acute stress exposure in the VR scenario on stress measures 29
Table 2.3 - Effects of acute stress exposure in the VR scenario on N-back performance 30
Table 2.4 - Correlations between different measures of the stress response and N-back performance. 35
Table 3.1 - Behavioural and imaging studies that used the MIST to induce stress 43
Table 3.2 - Demographic and personality measures. 51
Table 3.3 - Effects of acute stress exposure by the MIST on physiological and psychological stress measures 51
Table 3.4 - Effects of acute stress exposure by the MIST on N-back performance 52
Table 3.5 - Exploratory analyses - effects of acute stress by the MIST on stress measures. 54
Table 3.6 - Correlations between different measures of the stress response and N-back performance 59
Table 5.1 - Participant demographics and personality measures 77
Table 5.2 - Significant effects of COMT genotype and tolcapone on cerebral blood flow. 80
Table 6.1 - Resting state networks identified. 93
Table 6.2 - Effects of COMT genotype and COMT inhibition on resting state connectivity. 99
Table 6.3 - Left vlPFC seed connectivity. 102
Table 6.4 – Right dlPFC seed connectivity. 105
Table 6.5 - Summary of previous literature studying the effects of COMT genotype on rsFC. 110
Table 7.1 - Overview of studies that used the MIST in an MRI setting. 114
Table 7.2 - Overview of studies that used the MIST in a PET setting 115
Table 7.3 - Participant demographics and personality measures. 122
Table 7.4 - Correlations between different stress indices. 124
Table 7.5 - Effects of acute stress exposure by the MRI MIST on stress measures – main analyses 126
Table 7.6 - Effects of acute stress exposure by the MRI MIST on stress measures – exploratory analyses 127
Table 7.7 - Group differences on stress measures in cortisol responders only. 130
Table 7.8 - Whole brain fMRI MIST task activations and deactivations. 135
Table 7.9 - Whole brain fMRI MIST task activations and deactivations - with CBF and GM maps. 136
Table 8.1 - Hypotheses based on previous literature. 147
Table 8.2 - Effects of COMT genotype and COMT inhibition on N-back performance. 152
Table 8.3 - Effects of COMT genotype and COMT inhibition on N-back performance in cortisol responders.. 154
Table 8.4 - Whole brain fMRI N-back task activations and deactivations 159
Table 8.5 - Whole brain fMRI N-back task activations and deactivations - with CBF and GM maps 160
Table 8.6 - Effects of COMT inhibition on working memory related brain activity - with CBF and GM maps 161
Table 8.7 - Overview of predictions, hypotheses and actual findings. 165
Table 9.1 - Comparison between the VR lift stressor and the behavioural MIST stressor 170
Table 9.2 - Magnitude and duration of stress response induced by MRI MIST 170
Table 9.3 - Summary of the main results of this thesis. 171
Table 9.4 - Correlations between stress indices and N-back performance for the imaging study. 174

Abbreviations

3-MT	3-methoxytyramine
ACTH	adrenocorticotropin hormone
AD	aldehyde dehydrogenase
AH	aldehyde dehydrogenase
ANOVA	analysis of variance
ANS	autonomic nervous system
ASL	arterial spin labelling
AUC	area under the curve
AVP	arginine-vasopressin
BA	Brodmann Area
BET	FSL's Brain Extraction Tool
BOLD	blood-oxygen-level-dependent
BP	blood pressure
CASL	continuous ASL
CBF	cerebral blood flow
CNS	central nervous system
COMT	catechol-O-methyltransferase
CPT	continuous performance task
CRH	corticotrophin-releasing hormone
DA	dopamine
DAT	dopamine transporter
DBH	dopamine β-hydroxylase
DDC	dopamine decarboxylase
DHPA	3,4 dihydrophenylacetaldehyde
DMN	default mode network
DNA	deoxyribonucleic acid
DSM-IV	Diagnostic and Statistical Manual IV
ECG	electrocardiogram
ECN	executive control network
EMT	extraneuronal monoamine transporter
EPI	echo planar imaging
EV	explanatory variable
FA	flip angle
FC	functional connectivity
FEAT	FMRI expert analysis tool
FIX	FMRIB's ICA-based Xnoiseifier
FLAME	FMRIB's local analysis of mixed effects
FLIRT	FMRIB's linear image registration tool
fMRI	functional magnetic resonance imaging
FNIRT	FMRIB's non-linear image registration tool
FOV	field of view
FSL	FMRIB software library
FWE	family-wise error
GLM	generalized linear model
GM	grey matter
HPA	hypothalamic-pituitary-adrenal axis
HR	heart rate
HRF	haemodynamic response function
HRV	heart rate variability
HVA	homovanillic acid
ICA	independent component analysis
IQ	intelligence quotient
Kb	kilobases
LF-HF	low-frequency-high frequency
MAO	monoamine oxidase
MB-COMT	membrane-bound COMT
Melodic	Multivariate Exploratory Linear Decomposition into Independent Components
MHPA	3-methoxy-4-hydroxyphenlyacetaldehyde
mPFC	medial prefrontal cortex
MIST	Montreal Imaging Stress Task
MNI	Montreal Neurological Institute
MRI	magnetic resonance imaging
n	sample size
NAcc	nucleus accumbens
NART	National Adult Reading Test
NET	noradrenaline transporter
PASL	pulsed ASL
PCA	Principal Component Analysis
PE	parameter Estimates
PET	positron emission tomography
PFC	prefrontal cortex
PLD	post labelling delay
PVN	paraventricular nucleus
rCBF	regional cerebral blood flow
RF	radiofrequency
RMSSD	root mean square of successive differences
ROI	region of interest
Rpm	rounds per minute
rsFC	resting state functional connectivity
RSNs	resting state networks
sAA	salivary alpha-amylase
SC	skin Conductance
S-COMT	soluble COMT
SEM	standard error of the mean
SMN	superior motor network
SN	substantia nigra
SNP	single nucleotide polymorphism
SPSS	Statistical Package for the Social Sciences
TE	echo time
TFCE	threshold-free cluster enhancement
TH	tyrosine hydroxylase
TI	inversion delay
TR	repetition time
TSST	Trier Social Stress Test
VAS	visual analogue scale
VBM	voxel based morphometry
VR	virtual reality
VTA	ventral tegmental area
WCST	Wisconsin Card Sorting Test
WM	white matter

Chapter 1 Introduction

Dopaminergic abnormalities are significant in many psychiatric disorders and contribute substantially to their cognitive and emotional components. Moreover, stress is also implicated in a number of psychiatric disorders and is thought to have a dopaminergic component as well, with acute stress increasing dopamine in the brain. The enzyme catechol-O-methyltransferase (COMT) metabolises dopamine (DA) in the prefrontal cortex (PFC) and influences PFC dependent cognitive task performance. COMT genotype alters the cognitive and neural responses to stress. Moreover, there is evidence that the link between stress and PFC dopaminergic functioning is COMT-dependent. Clarification of these links will help to predict how real-world stressors in interaction with COMT genotype might impact on the therapeutic response to COMT inhibitors like tolcapone, as well as being of neuroscientific interest. This thesis investigates these interactions. First, following an introduction to the relevant literature, I will first present a novel virtual reality (VR) stressor and how it influences working memory performance in Chapter 2. Then, in Chapter 3, I will describe the stressor used in the main imaging study of this thesis, and, again, show its effect on working memory performance. In Chapter 4, I will describe the overall methods used for this main imaging study. Next, I will investigate the interaction between COMT genotype and COMT inhibition by tolcapone on resting state cerebral blood flow (Chapter 5) and functional connectivity (Chapter 6). Finally, I will examine the relationship between COMT with PFC-dependent cognitive function (working memory) and functional magnetic resonance imaging (MRI) signal under conditions of stress (Chapter 7 and 8).

1.1 Dopamine

Dopamine is a catecholamine critically involved in cognition, movement, reward, motivation and salience attribution (the assignment of importance to a stimulus) (Arnsten, 2009; Berridge and Robinson, 1998; Goldman-Rakic, 1998; Missale et al., 1998). Moreover, changes in brain dopamine function have been related to stress-related psychopathological conditions such as substance abuse (Robinson and Berridge, 1993) post-traumatic stress disorder (Hamner and Diamond, 1993) and psychosis (Howes and Kapur, 2009; Kambeitz et al., 2014).

In the brain, dopamine acts primarily on D1 (D1 and D5) and D2 (D2, D3, D4) receptor families (Goldman-Rakic, 1998; Missale et al., 1998). It is primarily synthesized in the ventral

tegmental area (VTA) and substantia nigra (SN) of the midbrain from its precursor tyrosine by the enzymes tyrosine hydroxylase (TH) and dopamine decarboxylase (DDC) (see **Figure 1.1).** From these regions, three major pathways extend to the PFC (mesocortical pathway), the nucleus accumbens (NAcc; mesolimbic pathway) and the basal ganglia (nigrostriatal pathway). A fourth pathway originates in the hypothalamus and projects to the pituitary gland (tuberoinfundibular pathway) (Arnsten, 2009; Goldman-Rakic, 1998; Marchese and Pani, 2002).

After dopamine is released, it may be removed from the extracellular space by the dopamine transporter (DAT), the extraneuronal monoamine transporter (EMT) or the NA transporter (NET) (which also has a high affinity for dopamine). Dopamine degradation may occur via a number of different enzymatic routes, the relative importance of which appears to vary between brain regions. Dopamine is degraded to homovanillic acid (HVA) by the enzymes catechol-o-methyltransferase (COMT), monoamine oxidase (MAO) and aldehyde dehydrogenase (AD) (Goldman-Rakic, 1998; Laatikainen et al., 2013; Marchese and Pani, 2002).

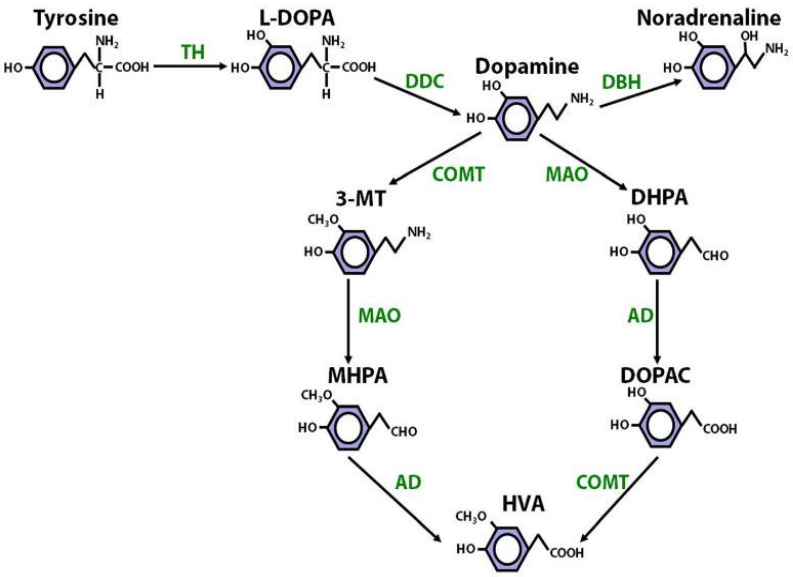


Figure 1.1 - The synthesis and degradation of dopamine.

Enzymes involved in the synthesis and catabolism of dopamine are highlighted in green. Dopamine is synthesised from tyrosine via L-DOPA, mediated by tyrosine hydroxylase (TH) and dopamine decarboxylase (DDC). Dopamine can be converted to noradrenaline, via the action of dopamine β-hydroxylase (DBH) or catabolised by the joint action of the enzymes COMT, monoamine oxidase (MAO) and aldehyde dehydrogenase (AH). Other abbreviations: 3-methoxytyramine (3-MT); 3,4 dihydrophenylacetaldehyde (DHPA); 3-methoxy-4-hydroxyphenlyacetaldehyde (MHPA) (Taken from (Laatikainen et al., 2013)).

1.1.1 Dopamine and cognition

The initial demonstration of the importance of PFC dopamine for working memory came by Brozoski et al., in 1979 (Brozoski et al., 1979). In this paper the authors demonstrated that dopamine depletion in the PFC of monkeys caused working memory impairments as severe as those found in monkeys with complete ablations of the PFC. Strikingly, performance of a non-PFC dependent task remained unaffected and the working memory impairments could be reversed by administering dopamine agonists. Furthermore, these working memory impairments were not observed in monkeys in which other neurotransmitters, such as serotonin, were depleted. Whilst the lesion affected both dopamine and noradrenaline, the role of dopamine was emphasised, since animals with large noradrenaline but small dopamine impairments remained unimpaired (Brozoski et al., 1979). Since then a wealth of evidence has accumulated implicating PFC dopamine in a range of cognitive functions such as working memory and cognitive control. These somewhat ill-defined terms generally refer to the functionally opposing computations of 1) "on-line" stabilization of task-relevant representations, and 2) flexible updating of those representations in response to novel information (Cools and D'Esposito, 2011).

1.1.1.1 *Inverted-U between dopamine and PFC-dependent function*

The relationship between dopamine and PFC-dependent function is complex. It has been proposed that the relationship between dopamine levels and PFC function is not linear, but instead resembles an 'inverted-U'-shape whereby either too little or too much dopamine signalling impairs cognitive performance (Error! Reference source not found.**,** Goldman-Rakic, 2000; Williams and Goldman-Rakic, 1995). First evidence came from initial studies by Sawaguchi and Goldman-Rakic, (1991) who showed that local PFC infusion of dopamine D1 receptor antagonists impaired working memory performance in a dose-dependent manner. The idea of a curve came from studies that showed that the a linear relationship between dopamine levels and PFC-dependent cognitive function did not fit the data (Goldman-Rakic, 2000; Williams and Goldman-Rakic, 1995). The author's iontophorized D1 receptor antagonists on to neurons in the dorsolateral PFC in chronic single-unit studies in monkeys performing working memory tasks. Dopamine appeared to exert its effects on working memory by modulating the activity of neurons exhibiting "memory fields" in the PFC. These neurons are spatially tuned and increase their firing during the delay period between target presentation and response. Failure of these cells to maintain their firing during the delay period is associated with incorrect behavioural response. Low level D1 antagonism of these neurons

potentiated the memory field: the neuron's firing during the delay period in increased and its spatial tuning is maintained. Conversely, excessive D1 antagonism caused non-specific inhibition of firing, presumably mediating the working memory impairments associated with excessive D1 receptor blockade. Therefore, D1 antagonists can selectively potentiate the 'memory fields' of prefrontal neurons which subserve working memory. Memory fields are most highly tuned at intermediate levels of DA receptor occupancy (Goldman-Rakic, 2000; Williams and Goldman-Rakic, 1995). More recently, Vijayraghavan et al., (2007) provided further evidence for the inverted-U shape relationship between dopamine and PFC-dependent function at the cellular level in behaving animals.

Since the early Williams and Goldman-Rakic study., (1995) in cells, behavioural studies conducted in monkeys, rats and mice performing PFC working memory tasks showed that activation of the dopamine D1 receptor produces an inverted "U"-shape dose/response curve, where either too little (Kozlov et al., 2001.; Sawaguchi and Goldman-Rakic, 1991; Seamans et al., 1998) or too much (Arnsten and Goldman-Rakic, 1998; Lidow et al., 2003; Zahrt et al., 1997) D1 receptor activity impairs performance on PFC-dependent cognitive tasks.

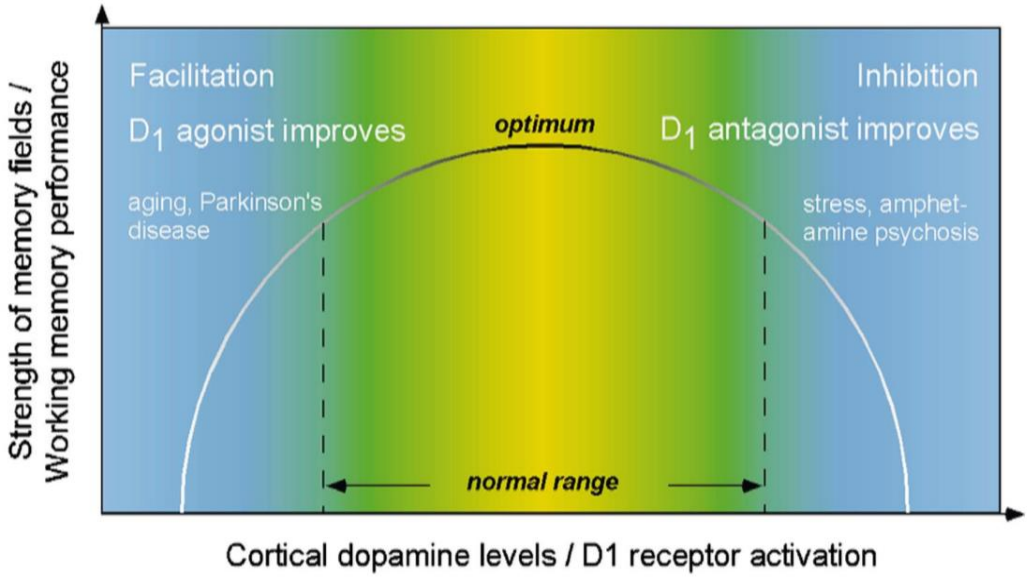


Figure 1.2 - The inverted U-shaped relationship between dopamine and PFC-function.

As first presented by Goldman-Rakic & Williams, (2000). PFC function is optimal at intermediate levels of dopamine (yellow region). PFC function is impaired in states of dopaminergic hypofunction, as in aged animals and patients with Parkinson's disease, and hyperfunction, as in stressed animals or during amphetamine-induced psychosis.

Further support for the inverted-U relationship between dopamine and PFC-dependent cognitive function comes from studying aging and stress. Administration of D1R agonists can ameliorate age related impairments in working memory (Cai and Arnsten, 1997). For example, aged monkeys were improved by low doses of a D1R agonist. However, higher doses worsened performance without any side effects, characteristic of the inverted "U" dose/response. Both the improvement at low doses and the impairment at high doses were reversed by coadministration of an D1R antagonist. Impairment in working memory can also be observed in rats and monkeys under conditions of stress (Arnsten and Goldman-Rakic, 1998; Murphy et al., 1996). As described in more detail later in this Chapter, acute stress results in endogenous dopamine released into the PFC. Stressor induced working memory deficits can be prevented by blocking the D1R to restore an optimal level of D1R stimulation by excessive dopamine (Murphy et al., 1996). Another line of evidence in support of an inverted-U comes from studies that investigated genetic influences on the relationship between dopamine and PFC-dependent cognitive function. I will summarise these findings in the next section of this Chapter, where I describe the effects of the COMT gene on behaviour (Section 1.2).

Although the evidence that supports the existence for an inverted-U relationship between dopamine levels and PFC-dependent cognitive function is quite strong in animals, these inverted-Us are much more difficult to study in humans. Indirect support for the hypothesis comes from studies of patients with Parkinson's disease (who have decreased dopamine levels due to cell loss in the substantia nigra), in which L-DOPA treatment improves working memory (Cools, 2001). However, the best human evidence for an inverted-U comes from studies of dopamine genetic variation and pharmacological manipulation (e.g. Egan et al., (2001) and Farrell et al., (2012)). I will describe these studies in the next section (Section 1.2).

In summary, dopamine appears to be critical for modulating PFC function with intermediate levels appearing to be optimal for working memory performance. These observations led to the 'inverted U' hypothesis, with genetic, pharmacological, pathological, and environmental factors affecting position on the curve. However, it should be noted that D1-mediated dopamine transmission is by no means the only important neurotransmitter system in this respect (Arnsten, 2004; Robbins, 2000). Thus, any investigation of PFC function should bear in mind the probable interactions between numerous neurotransmitter systems, as well as considering that the PFC functions as part of a widely distributed network involving a great number of cortical and subcortical regions whose activity is interdependent. Furthermore, the observation that the relationship between dopamine and cognitive function is nonlinear and inverted-U shaped, is an empirical one and provides a descriptive rather than a mechanistic account of the action of dopamine (Cools & D'Esposito, 2011).

Distinct optimum levels of dopamine exist for different cognitive functions. Manipulation of dopamine will have unpredictable cognitive consequences, depending on the type of task component under study, the brain region that is implicated, and the baseline levels of dopamine in that brain region (Cools & D'Esposito, 2011). In consequence, despite the attractiveness of the inverted U, it is difficult to test critically.

1.2 COMT

An example of a genetic factor that can affect the position on the 'inverted-U' curve is COMT. COMT is an enzyme important for methylating, and thereby degrading, a wide range of catechol substrates, mainly dopamine (Nnisto and Kaakkola, 1999.; Tunbridge et al., 2006; Witte and Flöel, 2012). In the PFC dopamine levels are influenced by COMT, and COMT modulates dopamine-dependent PFC functions (Papaleo et al., 2008; Tunbridge et al, 2004).

Where a person lies on the inverted-U shaped curve between dopamine levels and PFC function in any given environmental or genetic context, and what therefore the precise effect of COMT activity on PFC function will be, likely depends on multiple factors, including the precise phenotype being examined, state factors (for example, the amount of stress) and trait factors like the complex genetic background on which the COMT genotype is expressed (Craddock et al., 2006; Tunbridge et al., 2006).

1.2.1 COMT gene structure and expression

The gene for COMT has been localised to chromosome 22, band q11.2 (Grossman et al., 1992; Lundström et al., 1995; Tenhunen et al., 1994). It consists of six exons, the first two of which are non-coding, and encodes two transcripts, of 1.3kb and 1.5kb in humans, from two distinct promoters (Tenhunen et al., 1994). Two distinct allozymes arise from the COMT gene depending on the starting point of translation (the COMT gene has two AUG start codons) (Tenhunen et al., 1994). A soluble form of the protein, S-COMT, is located in the cytoplasm, whilst insoluble, MB-COMT is associated with membranes. The longer, 1.5kb transcript can encode both MB-COMT and S-COMT, whilst the shorter of the two transcripts only encodes S-COMT (Tenhunen et al., 1994).

Most human tissues express both the long and short COMT transcripts (at varying levels), with the exception of brain, in which only the longer transcript has been found (Hong et al., 1998; Tenhunen et al., 1994). MB-COMT is the predominant allozyme in the brain (particularly in the PFC) and, in comparison to most other tissues, there is a markedly reduced proportion of S-COMT, which

only accounts for 30% of cerebral COMT protein (Bonifácio et al., 2007; Chen et al., 2004; Karhunen et al., 1994; Matsumoto et al., 2003; Tenhunen et al., 1994; Tenhunen and Ulmanen, 1993). This indicates that the long COMT transcript can encode both forms (Tenhunen et al., 1994).

A number of putative regulatory elements have been discovered in the COMT gene which may explain the differential expression of the long and short transcripts in different tissues (Tenhunen et al., 1994). Significantly, the COMT gene contains oestrogen response elements (Xie et al., 1999) and oestradiol has been shown to down-regulate COMT expression in cell culture (Jiang, 2003), possibly explaining the decreased COMT activity found in women compared to men (Floderus et al., 1981; Harrison and Tunbridge, 2008). It might also be a factor contributing to the sex differences seen in emergence and clinical phenotype of some psychiatric disorders (Harrison and Tunbridge, 2008). Other factors such as the extent of DNA methylation may also play a part in regulating COMT expression (Nohesara et al., 2011; Swift-Scanlan et al., 2014).

Though MB-COMT and S-COMT have broadly the same sequences, their substrate affinities differ quite substantially. Despite having a lower capacity, MB-COMT has significantly higher affinity (approximately 10-fold) for dopamine than its soluble counterpart (Lotta et al., 1995). This could suggest why it is more highly expressed in the central nervous system (CNS), where it might be more suited to catabolising breakdown of catecholamine neurotransmitters at the concentrations present there. Thus, at brain concentrations of catecholamines MB-COMT is likely to be predominant (Roth, 1992).

1.2.2 COMT Val^{158}Met polymorphism

The COMT gene has a number of single nucleotide polymorphisms (SNPs) in its coding sequence. Of these, rs4680, results in a valine to methionine substitution at coding position 158 (Val^{158}Met) in COMT (corresponding to codon 108 in S-COMT) which influences enzyme activity. The ancestral COMT-Val allele has ~40% greater activity than the COMT-Met allele (Lachman et al., 1996; Chen et al., 2004; Tunbridge et al., 2006). The reason behind this difference in enzyme activity is thought to be the difference in thermostability between the two forms (Chen et al., 2004; Lotta et al., 1995; Weinshilboum and Dunnette, 1980). Met^{158}-MB-COMT has significantly lower thermostability than Val^{158}-MB-COMT (Chen et al., 2004; Lotta et al., 1995; Weinshilboum and Dunnette, 1980)

Since COMT-Val and COMT-Met are co-dominant, heterozygotes have an intermediate level of COMT activity (Chen et al., 2004). In Caucasian populations COMT-Val and COMT-Met are present in nearly equal frequencies (Palmatier et al., 1999). The allelic frequencies do differ

depending on which population is being studied. For example, in Asian populations, the COMT-Met allele is considerably less prevalent, with a frequency of only 25% (Palmatier et al., 1999).

In most regions of the human brain, dopamine transporters (DAT) are the predominant means of dopamine clearance from the synapse (Käenmäki et al., 2010). However, due to the relative sparsity of DAT in the PFC (Lewis et al., 2001; Sesack et al., 1998), COMT represents the principal mechanism of dopamine removal from the synapse in this region of the brain (Käenmäki et al., 2010; Tunbridge et al., 2004; Yavich et al., 2007).

1.2.3 COMT Val^{158}Met and behaviour

This genetically-influenced difference in COMT activity is reflected in differences in behaviour as well. Some previous research links the COMT-Met allele with better PFC-dependent performance and efficiency. (Egan et al., 2001) were the first to show this by demonstrating that COMT-Val allele is linked with relatively poorer performance on the Wisconsin Card Sorting Test (WCST) of executive function, with COMT-Met homozygotes performing better than COMT-Val homozygotes and heterozygotes showing intermediate performance (Egan et al., 2001). Their findings have been replicated by several studies (e.g. Diaz-Asper et al., 2008; Joober, 2002; Malhotra et al., 2002). Goldberg et al., (2003) extended these findings by showing that COMT-Val homozygotes had poorest performance on the N-back bask for working memory whilst COMT-Met homozygotes performed best, findings that were consistent in both the 1-back and 2-back conditions. However, associations are controversial. Two meta-analyses - (Barnett et al., 2008; Geller et al., 2017) - show no evidence for COMT Val^{158}Met effects on cognitive abilities (see below).

There are robust Val^{158}Met genotype effects on cortical activation and functional connectivity during PFC-dependent tasks, with the COMT-Met allele predicting a more efficient physiological response (Egan et al., 2001; Mier et al., 2010). Egan et al., (2001) demonstrated, that for a given level of N-back performance, COMT-Val homozygotes showed greater activation of the dorsolateral prefrontal and cingulate cortices than COMT-Met homozygotes (heterozygotes showing intermediate levels of activation). COMT-Val/Val individuals therefore seem to use their PFC relatively more “inefficiently” than COMT-Met carriers, i.e. they required greater prefrontal activation for a given level of performance. This is supported by a meta-analysis by (Mier et al., 2010) (however, again, see below). Furthermore, COMT Val^{158}Met also influences functional connectivity (FC) of the PFC at rest (Tunbridge et al., 2013): COMT genotype significantly modulated functional connectivity within the Executive Control Network (ECN - which included the head of the caudate, and anterior cingulate and frontal cortical regions). COMT-Val homozygotes showed

greater FC between a cluster within the left ventrolateral PFC and the rest of the ECN. Another imaging study investigated the effect of COMT genotype on the brain response to amphetamine, which blocks monoamine reuptake and therefore increases dopamine levels in the brain (Mattay et al., 2003). Differential effects of amphetamine on the different COMT genotypes were found: COMT-Val homozygotes showed significant improvements in prefrontal efficiency and WCST performance. In contrast, the prefrontal efficiency and performance of low activity COMT-Met homozygotes remained the same, or even deteriorated in the high working memory load (2-back) condition. However, a follow up study using a larger sample size failed to replicate this interaction (Wardle et al., 2013), again also see below.

Studies with transgenic mice support the hypothesis that low COMT activity is beneficial in terms of cognitive performance (Papaleo et al., 2008). The activity of wild type COMT is comparable to, or possibly greater than activity of the human Val isoform (Chen et al., 2004; Risbrough et al., 2014).

The Val^{158} allele might therefore impair prefrontal cognition and its physiological correlates by increasing prefrontal dopamine catabolism and therefore lowering dopamine levels. However, as already touched upon above, numerous studies fail to find a relationship between frontal cognitive measures and COMT genotype (different forms of working memory and executive function: (Ho et al., 2005; Szöke et al., 2006); meta-analyses: (Barnett et al., 2008; Geller et al., 2017). These inconsistencies may be due to different domains of working memory being studied, different versions of the tasks involved and their difficulty levels, or demographic differences, as gender-, age- and possibly IQ-related variation in COMT function exists (Farrell et al., 2012; Harrison and Tunbridge, 2008; Witte and Flöel, 2012).

1.2.4 COMT inhibition with tolcapone

COMT activity can be reduced using the selective, brain-penetrant COMT inhibitor tolcapone (chemical name 3,4-dihydroxy-4'-methyl-5-nitrobenzophenone), which has an elimination half-life of 2.0 ± 0.8 hours and produces about 70-80% inhibition for 4-6 hours after a single dose (Dingemanse et al., 1995; Jorga, 1998). It enhances dopamine neurotransmission by blocking the central methylation of dopamine into 3-methoxytyramine (Ceravolo et al., 2002; Jorga, 1998).

Tolcapone's inhibition is highly specific to COMT, and does not affect any of the other enzymes involved in the catabolism of catecholamines (Laatikainen et al., 2013; Tunbridge et al., 2006). Another advantage of tolcapone is that it has little effect on extracellular dopamine levels in other regions of the brain such as the striatum (Laatikainen et al., 2013; Li et al., 1998; Maj et al.,

1990), where there is a far higher density of DAT transporters. This means that the drug lacks abuse potential and psychostimulant effects. These properties make tolcapone a valuable research tool to investigate dopamine signalling in the PFC and it has been used in a number of studies to date.

COMT inhibition by tolcapone is shown to be beneficial to cognitive function in both wild type rodents (Barkus et al., 2016; Lapish et al., 2009; Tunbridge et al, 2004) and humans (Apud et al., 2007; Gasparini et al., 1997). In rat models, the drug has been shown to improve performance in a delayed spatial win-shift task (Lapish et al., 2009), to augment dopamine release in response to behaviourally salient stimuli (food) (Lapish et al., 2009), to improve extradimensional set shifting (Troudet et al., 2016; Tunbridge, 2004), and to enhance spatial working memory in a radial maze task (Liljequist et al., 1997). In humans, tolcapone has also demonstrated potential to enhance cognitive function. For example tolcapone improved attention and memory in Parkinson patients (Gasparini et al., 1997). However, as might be anticipated based on the inverted-U relationship between dopamine and cognitive function, cognitive enhancement by tolcapone seems to be COMT-genotype dependent, as discussed below.

1.2.5 COMT inhibition and behaviour

Following the inverted-U between dopamine levels and PFC-function, it would be predicted that tolcapone and the Val^{158}Met polymorphism would interact. At baseline, COMT-Val homozygotes have 'sub-optimal' PFC dopamine levels (when investigating in relationship to working memory performance, for other functions it may be optimal) and they can be pushed nearer to the peak of the inverted-U-shaped curve as a result of decreases in COMT activity by tolcapone treatment. COMT-Met homozygotes, on the other hand, have more optimal PFC dopamine levels at baseline and will be pushed to supraoptimal levels as a result of decreased COMT activity, impairing PFC function (Tunbridge et al., 2006). The study of Farrell et al., (2012) showed this very clearly: COMT-Met homozygotes outperformed COMT-Val homozygotes on the N-back task in the placebo group, while in the tolcapone group the opposite was the case: COMT-Met homozygotes showed poorer N-back performance than COMT-Val homozygotes (Farrell et al., 2012).

Other studies also show interactive effects of COMT genotype and inhibition on executive function and verbal episodic memory (Apud et al., 2007) and prepulse-inhibition (PPI), as well as further demonstrations of this relationship for N-back performance (Giakoumaki et al., 2008; Roussos et al., 2009). Apud et al., (2007) also showed effects of tolcapone on brain activity, with greater activation in brain regions subserving working memory (like the dorsolateral PFC) on

placebo compared with tolcapone, consistent with a positive effect of tolcapone on functional efficiency. However they did not find a COMT genotype drug interaction (Apud et al., 2007).

Furthermore, studies using a novel transgenic mouse model, engineered to express human-COMT on a COMT null background, indicate that the Met-COMT transgenic mice do not show the same improvements in cognitive function following tolcapone administration as their wild-type littermates (Barkus et al., 2016), in line with (Farrell et al., 2012). Therefore, in sum, tolcapone appears beneficial to cognitive function, but in a COMT genotype-dependent manner.

Before I move on describing the interactions between COMT genotype, COMT inhibition by tolcapone and stress, I will first give a brief introduction to the stress response.

1.3 The stress response

Stressors can be defined as certain physical and psychological events, either actual or anticipated, that threaten an organism's homeostasis (de Kloet et al., 2005; Ulrich-Lai and Herman, 2009). How the body responds to these stressors is called the stress response. In health, this well-coordinated stress response affects physiology, psychology and behaviour, and is orchestrated by the brain in order to effectively cope with homeostatic challenges (Ulrich-Lai and Herman, 2009). It serves as a vital adaptive mechanism by shifting available resources to a survival network (Hermans et al., 2014). The acute stress response is limited in both duration and amplitude to ensure that the individual returns to homeostasis during the recovery phase (de Kloet et al., 2005; McEwen and Gianaros, 2011). While the acute stress response is evolutionarily beneficial for the organism, prolonged or recurrent exposure to scenarios that trigger the stress response, or to extreme intense stressors, may lead to dysregulation of the stress system and serious metabolic, immunological and psychological dysfunction (de Kloet et al., 2005; Holsboer and Ising, 2010; Mcewen, 2004, 1998; Varese et al., 2012; Walker and Diforio, 1997).

Stressor-related information from all major sensory systems (for example, interoceptive cues, such as blood volume and osmolarity, and/or exteroceptive cues, such as the smell of a predator or negative social evaluation) is conveyed to the brain. As a result, behaviour is directed towards assessing the destabilising potential of the stressor. If the stressor fails to match some cognitive representation based on previous subjective experience (in other words, if the situation is perceived as stressful), the brain activates many neural and neuroendocrine systems to adapt to the demand and to minimize the net cost to the organism (de Kloet et al., 2005; Herman et al., 2003; Ulrich-Lai and Herman, 2009).

Central to the stress response are the activation of the autonomic nervous system (ANS) and the hypothalamic-pituitary-adrenal axis (HPA), with corticotrophin-releasing hormone (CRH) being a critical coordinator of these responses (Herman et al., 2003; Ulrich-Lai and Herman, 2009).

1.3.1 Autonomic nervous system

The ANS, consisting of sympathetic and parasympathetic arms, provides the most immediate response to stressor exposure. Activation of the sympathetic arm represents the classic 'fight or flight' response. It generally increases circulating levels of adrenaline (primarily from the adrenal medulla) and noradrenaline (primarily from sympathetic nerves). By exciting the cardiovascular system, the sympatho-adrenomedullary arm can rapidly (in seconds) increase heart rate (HR) and blood pressure (BP). Moreover, as a consequence of this autonomic activation, an increase in the sweat gland activity occurs (skin conductance (SC) activity). These reactions aim to prepare the individual to respond immediately. However, through simultaneous parasympathetic activation this excitation is only very short lived (de Kloet et al., 2005; Herman et al., 2003; Ulrich-Lai and Herman, 2009). Although adrenaline and noradrenaline cannot cross the blood-brain barrier, they exert indirect effects on the brain via the vagus nerve, resulting in the activation of noradrenergic brain stem nuclei (Williams, Men, and Clayton, 2000).

Next to blood pressure, heart rate and skin conductance, salivary alpha amylase (sAA – an oral cavity enzyme involved in the digestion of starch) has been identified as a possible biomarker of ANS reactivity to stressors, in particular as an indicator for sympathetic activity (Ditzen et al., 2014; Petrakova et al., 2017). Ditzen et al., (2014) showed that the increase of sAA was mediated via noradrenaline and adrenaline. These associations were stronger during stress than during rest. sAA release has moreover been correlated to other indicators of the sympathetic nervous system like left ventricular ejection time, heart rate, heart rate variability (LF/HF-ratio), systolic blood pressure and skin conductance (Ditzen et al., 2014; Nater et al., 2006; Nater and Rohleder, 2009; Petrakova et al., 2017). Furthermore, sAA and cortisol (marker of the HPA axis see below) are reliably associated, with sAA preceding cortisol release by approximately 14 minutes (Engert et al., 2011).

1.3.2 Hypothalamic-pituitary-adrenal (HPA) axis

The limbic-hypothalamic-pituitary-adrenal (HPA) axis (also sometimes called LHPA axis) is mediated largely by neurosecretory inputs to the anterior pituitary. The paraventricular nucleus (PVN) of the hypothalamus is the central feedback target receiving input from sensory relays (e.g. the

brainstem) and widespread regulatory limbic, paralimbic and prefrontal cortical regions (Herman et al., 2005; King and Liberzon, 2009). The activity of this axis is complex and thought to have two principal components that can interact and influence each other: baseline activity and responses to specific events/challenges/stressful events (de Kloet et al., 2005; Herman et al., 2003; King and Liberzon, 2009; Ulrich-Lai and Herman, 2009). Baseline activity is generally thought of as being under control of circadian rhythms. These rhythms involve cascades of "releasing" and "inhibiting" hormones which eventually leads to peripheral target organs to stimulate secretion of the hormonal end products – cortisol in humans and corticosterone in rodents. Cortisol levels have a distinct sharp rise at the time of awakening, followed by a steady decline over the course of the day, with the lowest levels in the early morning hours (Dedovic et al., 2009c; Herman et al., 2003; King and Liberzon, 2009).

The HPA axis can also be directly activated by stressors, which can be divided into different types. Reactive stressors are those that increase the demand on the system through a real sensory stimulus such as pain, bodily injury or an immune challenge while anticipatory stressors tap into innate or memory programs such as social challenges or unfamiliar situations (Dedovic et al., 2009c; Herman et al., 2003). Another differentiation is that of physical versus psychological stressors (Dickerson and Kemeny, 2004; Pacák and Palkovits, 2001). A physical stressor might be facing a situation with the anticipation of bodily injury (example: cold pressor test (Blandini et al., 1995), whilst an example of psychological stressor would be social evaluative treat (e.g. risk of humiliation). What these stressors have in common is that they all activate the HPA axis. As my thesis focusses on psychological stressors, I will only elaborate on those.

The psychological factors that most reliably activate the HPA axis are an atmosphere of high achievement, novelty, social evaluative threat and little or no controllability (Dickerson and Kemeny, 2004; King and Liberzon, 2009). Animal literature suggests that these psychological stressors do so by engaging limbic system regions, namely the hippocampus, the amygdala and medial PFC (mPFC) areas (Dedovic et al., 2009c; Herman et al., 2003; Pruessner et al., 2008).

When triggered, the PVN secretes CRH that synergistically acts with arginine-vasopressin (AVP) in the anterior pituitary to elicit adrenocorticotropin hormone (ACTH) that is released into the circulation (Holsboer, 2001). In addition, CRH and AVP function as neurotransmitters that induce complex behavioural effects such as anxiety, sleep and psychomotor changes (Keck, 2006). In the adrenal cortex, ACTH leads to the release of cortisol which further mediates the stress response through glucocorticoid receptors and mineralocorticoid receptors via both genomic and non-genomic effects (Makara, 2001). Corticosteroids (e.g. cortisol) have a multitude of biological effects in almost every tissue in the body. Peripheral effects include regulation of metabolism and

glucose deposition. There are also important effects on immune function as well as diverse effects on cardiovascular tone. The effects on the brain involve modulation of cognitive and emotional processing, social appraisal and decision making. This primary neuroendocrine stress response occurs with a slower timescale than the autonomic response, allowing for prolonged and amplified responses to stress (also on gene expression). Peak plasma levels occur after 15-30 minutes and slowly decline again to pre-stress levels 60-90 minutes later (de Kloet et al., 2005; Herman et al., 2003; King and Liberzon, 2009; Ulrich-Lai and Herman, 2009).

Next to this there is also top-down regulation by the limbic forebrain. Both psychogenic and systemic stimuli are processed in multiple limbic forebrain structures, - including the amygdala, the hippocampus and the PFC. These regions, which are also high in glucocorticoid receptors, receive associational information from subcortical and cortical areas that are involved in higher-order sensory processing and memory. They also receive ascending inputs from sites involved in attention and arousal. The limbic system therefore forms the interface between the incoming sensory information and the appraisal process of whether something will evoke a stress response or not. It moreover works in parallel to influence the activation of the HPA axis and probably performs similar functions in the autonomic responses to stressors. Thus there appears to be a "two-way traffic" between the LHPA axis and brain activity (de Kloet et al., 2005; Herman et al., 2003; King and Liberzon, 2009; Ulrich-Lai and Herman, 2009). As a result there will be an increase in arousal, alertness, vigilance, focussed attention and cognitive processing to deal with the potential treat (de Kloet et al., 2005; King and Liberzon, 2009; Ulrich-Lai and Herman, 2009). Stress elicited corticosteroids also have metabolic effects, e.g. by increasing plasma glucose concentrations which is beneficial when dealing with stressful situations. Cortisol provides negative feedback upon pituitary corticosteroids and exerts many effects on neural circuits that modulate cognitive and affective functions (Henckens et al., 2010; Lupien and Mcewen, 1997) and attenuate limbic and mPFC areas (Herman et al., 2005).

In sum, activation of the ANS is fast (within seconds of stressor presentation) but short lasting (minutes). Activation of the HPA axis on the other hand is slow (peaks about 20 minutes after stressor presentation), but longer lasting (hours) depending on stressor intensity. Moreover, the HPA axis and sympathetic system have largely complementary actions throughout the body, including energy mobilization and maintenance of blood pressure during the stress response. Catecholaminergic activity intensifies and extends the duration of the sympathetic response. CRF neurons of the hypothalamus sending fibres to the brain stem and locus coeruleus (both involved

in sympathetic regulation) represent a possible connection site between HPA axis and ANS (Engert et al., 2011).

There is a range of experimental/psychological stressors that can be used to induce a stress response. I will focus on VR stressors (Chapter 2) and the Montreal Imaging Stress Task (MIST) (Chapter 3) as these stressors are used in the studies presented in this thesis.

1.3.3 Stress and virtual reality

VR is increasingly being used to investigate and to treat psychological disorders, such as paranoia, social phobia, and acrophobia (Freeman et al., 2019, 2018; Gujjar et al., 2019; Kampmann et al., 2016). Several studies have also measured components of the stress response to different VR environments like height challenges (e.g. (Wilhelm et al., 2005)) or the virtual Trier Social Stress Test (e.g. (Kelly et al., 2007) (for review: (Diemer et al., 2014)). However, much remains unknown, especially regarding the physiological stress response. In Chapter 3 I will further elaborate on VR and the by VR induced stress response, and will present a novel VR stressor and its effect of working memory performance.

1.3.4 The MIST: measuring stress effects in MRI paradigms

Investigating the psychological stress response in the MRI scanner is not a straightforward task. As described before, important characteristics of psychological stressors that activate the HPA axis are an atmosphere of high achievement, novelty, social evaluative threat and little or no controllability (Dickerson and Kemeny, 2004; King and Liberzon, 2009). One of the best known and widely used laboratory stressors, the 'Trier Social Stress Test' (TSST) taps in to these characteristics by having subjects unexpectedly deliver a personally-salient public speaking task to an audience of non-responsive judges (and often a video camera) and perform mental arithmetic (serial subtractions by 13 from a four digit number) with critical feedback (Kirschbaum et al., 1993). In the neuroimaging environment, the subjects' position in the scanner makes this impossible; therefore the MIST was developed (Dedovic et al., 2005; Pruessner et al., 2008). The MIST requires the participant to perform computerised challenging mental arithmetic with an adaptive algorithm and a built-in negative social evaluation and relative uncontrollability component, and therefore fits (Dickerson and Kemeny, 2004) definition. The TSST consistently produces increases in cortisol about 200-400% above baseline (in men, whereas in women 50-150% changes are usually found) in about 70-80% of participants (Dedovic et al., 2005; Dickerson and Kemeny, 2004; Kirschbaum et

al., 1993; Kudielka et al., 2009), whilst the MIST typically increases cortisol 50-100% in about 50% of the participants, with the other 50% showing a cortisol decrease over the course of the experiment (Dedovic et al., 2005).

By using the MIST in fMRI and Positron emission tomography (PET) settings, Dedovic and others (Dedovic et al., 2005, 2009b, 2009c) showed that the induced cortisol response was associated with a deactivation of specific parts of the limbic system, including hypothalamus, hippocampus, amygdala, and medio-orbitofrontal cortex. Interestingly, cortisol non-responders fail to show this deactivation pattern, showing overall much weaker signs of signal reduction, especially in the hippocampus. A region of interest analysis showed that the degree of deactivation in the hippocampus was strongly correlated with the overall cortisol stress response (Pruessner et al., 2008). These findings suggest that the hippocampus may exercise a tonic inhibition of the HPA axis, which is removed upon stress perception allowing for the increase in cortisol secretion (Dedovic et al., 2009b). Furthermore, the MIST consistently seems to result in decreased activity in areas outside the limbic system as well, like the ventral striatum (Pruessner et al., 2008; van Oort et al., 2017). Conversely, increases in activity due to stress induced by the MIST are found in the frontal lobes as well, particularly the anterior cingulate cortex. Positive associations have been established between cortisol levels and activation in parietal, ventrolateral and dorsolateral prefrontal areas (Kern et al., 2008; Weerda et al., 2010). However, decreased cortisol secretion correlated with increases in activity in mPFC regions have also been found (Kern et al., 2008). Therefore, specific components of the PFC may play quite different roles in the regulation of cortisol secretion, and these may be stressor specific (Herman et al., 2005). In Chapters 3 and 5 I will further elaborate on the MIST, both in terms of behavioural responses (Chapter 3) and the effect of COMT genotype/inhibition in an MRI setting (Chapter 5). **Table 3.1** moreover gives an overview of studies using the MIST and their findings.

Many neurochemical messengers, like adrenaline, noradrenaline, dopamine, serotonin and glutamate also play an essential role in the stress response. These messengers work in different time frames and are differentially affected by the duration of stress (acute vs. chronic) (Hermans et al., 2014; Moghaddam, 2002; Vaessen et al., 2015). I will only focus on the role of dopamine in the next section since it is most pertinent to this thesis.

1.4 Interactions

1.4.1 Dopamine and stress

In animal models, the dopamine system has been shown to be consistently associated with the acute and chronic stress response (Pani et al., 2000). In rodents, increases in extracellular dopamine levels are specifically observed in the mPFC and to a lesser extent the striatum after pain (Abercrombie et al., 1989; Imperato et al., 1991) and social defeat (Tidey and Miczek, 1996). The striatum (consists of the caudate nucleus, putamen, nucleus accumbens and olfactory tubercle) receives inputs from prefrontal, limbic, motor and somatosensory cortices (Haber et al., 2000) and is involved in a broad range of neural processes involving cognition, decision making, reward processing as well as learning and execution of behaviour, movement and somatosensation (Joel and Weiner, 2000). Therefore, the striatum might also be involved in the fight-or-flight reaction (Vaessen et al., 2015).

In humans the dopaminergic (DA D2/3 radioligands measured by PET) stress response is dependent on the stressor source. In line with animal research, physiological stressors (i.e. pain or metabolic) are consistently associated with increased striatal dopaminergic activity. Studies find the cortisol response to be significantly correlated with dopamine release in the striatum, consistent with a facilitating effect of cortisol on dopamine neuron firing (Dedovic et al., 2005; Hernaus et al., 2013; Lataster et al., 2011; Nagano-Saito et al., 2013; Pruessner, 2004). Moreover, dopaminergic activity is positively associated with subjective stress ratings and heart rate (Nagano-Saito et al., 2013). The MIST however, does not consistently increase striatal dopaminergic activity but seems to increase dopaminergic activity in the mPFC (Hernaus et al., 2015; Lataster et al., 2011; Nagano-Saito et al., 2013; Vaessen et al., 2015) and temporal cortex (Hernaus et al., 2015) more reliably (suggested to be related to the magnitude of the evoked stress response). Therefore, it is suggested that across brain regions, stress related dopaminergic activity is correlated with the intensity of the stressor (Vaessen et al., 2015). Furthermore, several genetic polymorphisms (SNPs), rearing conditions and personality traits have been shown to modulate the dopaminergic stress response in striatal and extrastriatal regions, highlighting its variation and complexity (Vaessen et al., 2015).

The prominent role of dopaminergic activity in the mPFC during stress may serve modulatory purposes, regulating the more instinctive limbic and autonomic responses to stress (Vaessen et al., 2015). Animal studies examining the effects of stress in mPFC lesioned rodents seem to affirm this hypothesis (Deutch et al., 1990; King et al., 1997; Scornaiencki et al., 2009). In humans, the task-induced mPFC BOLD response predicts efficacy of the MIST in inducing stress (Dedovic et al., 2009b) while limbic activity is suppressed (Pruessner et al., 2008). mPFC

dopaminergic activity seems to be more directly related to the experience of stress, serving as a threat evaluation system, whilst striatal dopaminergic activity may be related to expectations about the stressor (Vaessen et al., 2015).

Prefrontal glutamate (Kegeles et al., 2000; Moghaddam, 2002; Poels et al., 2014) and prefrontal and brainstem noradrenaline (Belujon and Grace, 2015; Cabib and Puglisi-Allegra, 2012; Feldman and Weidenfeld, 2004; Sullivan and Dufresne, 2006) release may modulate stress-related cortical and striatal dopaminergic activity. Additionally, the endogenous opioid system is involved in both physiological (Bencherif et al., 2002; Zubieta, 2001) and psychological stress (Hsu et al., 2015, 2013). Therefore, we have to keep in mind that dopamine is not the only player in the stress response and that that the stressors used here (i.e. VR or MIST) likely influence additional pathways in our study.

1.4.2 COMT Val^{158}Met and stress

Similar to that observed for dopamine, an inverted-U relationship has also been suggested between stress level and cognitive performance, in which moderate levels of stress improve performance while mild and severe levels of stress do not (see **Figure 1.3**.). Yerkes and Dodson were the first to observe this relationship in rats (Yerkes and Dodson, 1908), but more recent animal studies also show this non-linear relationship (Akirav, 2004; de Kloet et al., 1999; Delarco et al., 2007; Diamond et al., 1992; Sandi et al., 1997). An inverted-U relationship can also be observed between acute stress/glucocorticoids and PFC-dependent cognitive performance in humans, again with moderate stress levels facilitating, and high levels impairing, cognitive function (Andreano and Cahill, 2006; Arnsten, 2009; Ossewaarde et al., 2011; Qin et al., 2012; Sandi and Pinelo-Nava, 2007).

Stress and dopamine signalling interact in complex ways; with regards to COMT, for example, acute stress elevates cortical catecholamines and affects working memory (Arnsten, 2009; Henckens et al., 2009; Nagano-Saito et al., 2013; Sandi, 2011; Schoofs et al., 2008; Schwabe et al., 2010). Consistent with this, there is some indication that COMT Val^{158}Met impacts on the cognitive, neural and physiological responses to acute stress (Buckert et al., 2012; Qin et al., 2012). Moreover, the inverted-U relation between stress and PFC dopaminergic functioning is suggested to be COMT-dependent (Hernaus et al., 2013).

It would be predicted that acute stress would be detrimental to COMT-Met homozygotes, by moving them to 'supra-optimal' dopamine levels, but enhance performance in COMT-Val homozygotes, by moving them closer to the peak (see **Figure 1.3**). Consistent with this, multiple genetic association studies show that acute stress seems to negatively impact on cognition and

emotion in COMT-Met subjects, whilst improving it in COMT-Val subjects. Buckert et al., (2012) show by using a social stressor (TSST for Groups) that verbal working memory performance under stress was significantly worse for COMT-Met homozygotes, as compared to COMT-Val homozygotes. There were no genotype differences in the evoked cortisol response (Buckert et al., 2012). These findings are in line with another recent study by Qin et al, (2012), who demonstrated that working memory accuracy was reduced by an acute stressor (a traumatic film) in COMT-Met homozygotes but was unimpaired (or slightly improved) in COMT-Val carriers. This interaction also extended to brain activation: stress decreased working memory-related activation in the PFC in COMT-Met homozygotes but increased it in COMT-Val carriers (Qin et al., 2012). The prediction that stress would be detrimental to COMT-Met homozygotes, by moving them to 'supra-optimal' dopamine levels, but enhance performance in COMT-Val homozygotes, by moving them closer to the peak of the inverted-U is consistent with data obtained in transgenic mice. COMT null mice (comparable to human COMT-Met) show exaggerated physiological responses to acute stress (used female mice only; exhibited a greater increase in corticosterone concentrations (Desbonnet et al., 2012)), whilst mice which overexpressed the COMT-Val variant showed a reduced physiological response to stress but disrupted cognitive functions compared to COMT-null mice (Papaleo et al., 2008).

Taken together, these data show that acute stress negatively impacts on cognition and emotion in COMT-Met subjects, whilst improving it in COMT-Val subjects. Therefore, overall, COMT-Val homozygotes appear more stressor-resistant, while carriers of the COMT-Met allele perform better on tasks indexing cognition (under normal non-stressful conditions).

1.5 Aims and objectives

COMT activity affects the inverted-U-shaped relationship between dopamine and PFC function. An inverted-U relationship also exists between acute stress and PFC-dependent cognitive performance. Despite the evidence that COMT genotype alters the cognitive and neural responses to stress, it is unknown whether this is modulated by COMT inhibition in humans. Moreover, there is evidence that the inverted-U relation between stress and PFC dopaminergic functioning is COMT-dependent. Clarifying these relationships could have significant implications in terms of understanding how real-world stressors might impact on therapeutic response to COMT inhibitors. For example, if stress and COMT inhibition negatively impact on working memory this may represent an undesirable side-effect of the drug. Understanding these interactions is also of neuroscientific interest, since it provides a useful test of the extent to which the inverted-U

relationships between stress and COMT with cognitive function overlap. Stress might be expected to push everyone to the right on the inverted-U (more dopamine) if the stress and dopamine curves are related. Therefore, under stress, tolcapone might be expected to impair PFC-dependent performance in both COMT-Val and COMT-Met homozygotes, in contrast to the genotype by drug interaction seen previously. The main study of this DPhil thesis will therefore investigate how COMT inhibition, COMT genotype, and acute stress, interact to affect dopamine-dependent PFC functions, both on behaviour and brain activity.

Before trying to answer this main question, I first describe the effects of a novel VR stressor in terms of physiological responses and its effect on working memory performance in Chapter 2. Chapter 3 sets the basis for the main study, by investigating the physiological and psychological effects of the MIST to validate it as a stressor in our hands and establish the testing-window (validate stressor in our hands in terms of both magnitude and duration). Moreover, as the N-back task for working memory will be used in the main study to assess the effects of stress on working memory performance, the effects of acute stress on performance of the N-back task was also included in this pilot. Chapter 4 details the methods used for the main MRI study, with the following three chapters describing the data from this study. The effects of COMT genotype and inhibition by tolcapone on resting state cerebral blood flow are presented in Chapter 5, whilst the effects of the same interaction on functional connectivity (before stress) is described in Chapter 6. In Chapter 7 the evidence for successfully inducing a stress response in the MRI study is presented together with the investigation of the interaction between COMT genotype and COMT inhibition on this evoked stress response (both in terms of physiological responses as on brain activity). Then in Chapter 8, I describe the effect of COMT inhibition, in Val and Met homozygotes subjected to an acute stressor (MIST), on working memory performance (N-back task) – both in terms of behaviour and the BOLD response. Finally, in Chapter 9 I discuss the overall findings plus implications of this thesis and propose extensions to this research.

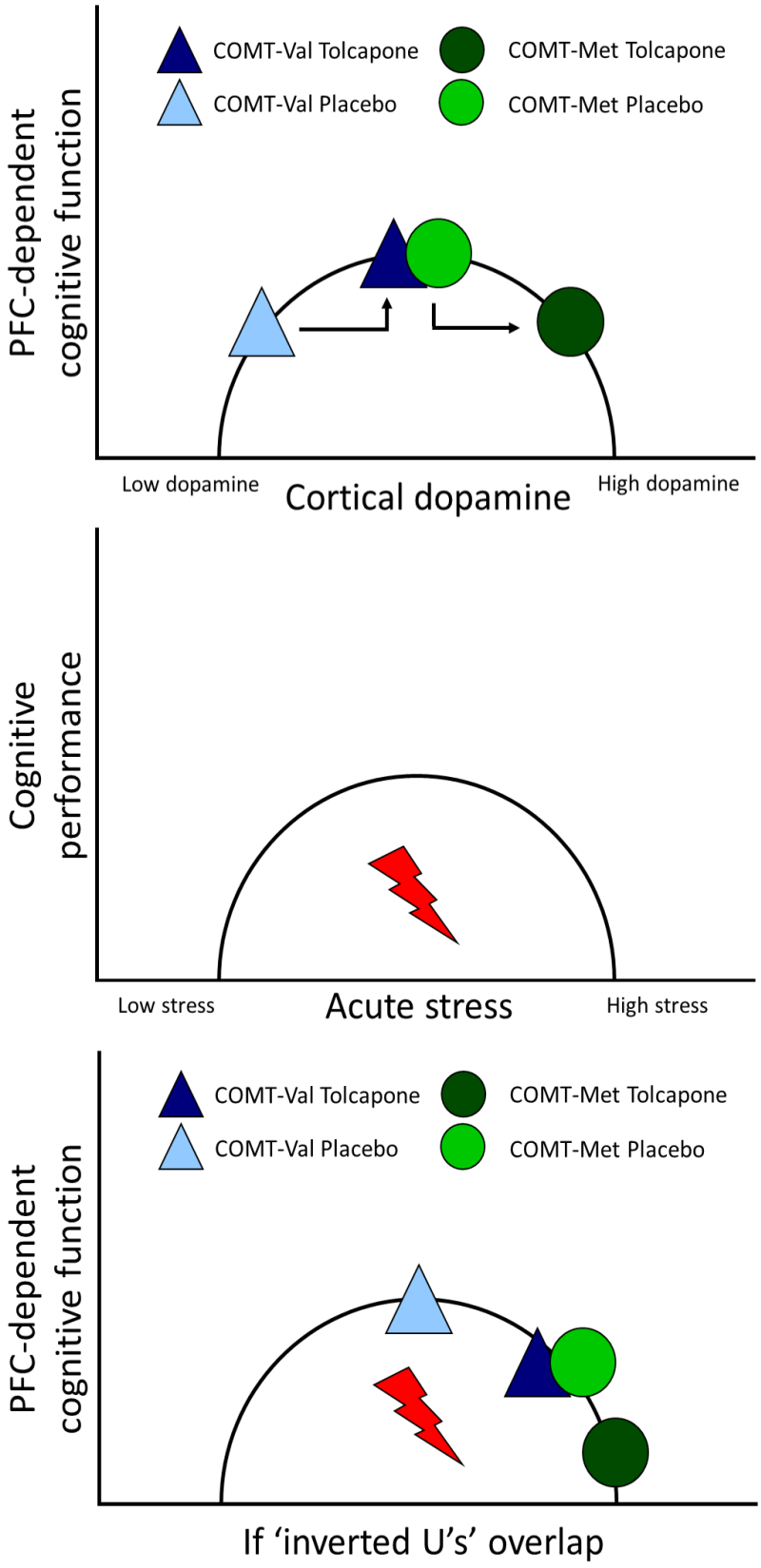


Figure 1.3 - Inverted-U's.

A) COMT genotype, inhibition, and dopaminergic inverted-U as presented by Farrell et al., (2012).
B) The inverted-U between acute stress and cognitive performance as first presented by Yerkes and Dodson (1908).
C) Position of COMT-Met and Val homozygotes when inverted-U's overlap.

Chapter 2 Physiological and psychological effects of a novel virtual reality stressor

The majority of this chapter has been submitted to the *Journal of Psychopharmacology (under review).*

2.1 Introduction

As outlined in Chapter 1, VR is increasingly being used to investigate and to treat psychological disorders, such as paranoia, social phobia, and acrophobia (Freeman et al., 2019, 2018; Gujjar et al., 2019; Kampmann et al., 2016). The immersive nature of VR can simulate key aspects of the condition of interest, whilst allowing full control over the environment and the opportunity to undertake more intensive investigations than is possible in the real-world situation. However, for a VR analogue to be effective, the environment must be sufficiently convincing for the participant to experience a high degree of presence (Sanchez-Vives and Slater, 2005). Thus, if VR is to be used for disorders in which stress or anxiety are a key component, or indeed as a means to induce acute stress (e.g. for use in experimental medicine studies), it is important to ensure that the VR environment produces a *bona fide* stress response, and to understand its nature, magnitude, and duration.

Several studies have measured components of the stress response to different VR environments (Diemer et al., 2014) but much remains unknown, especially regarding the physiological stress response. As well as there being inconsistencies, no study has examined the full range of standard stress indices, nor have they compared them using a *between-subjects design* in individuals randomised to a stressful vs. a control VR scenario: studies that have used control scenarios have examined the effect of control vs. stress scenarios using a *within-subjects* approach (e.g (Cleworth et al., 2012)). This information is critical if VR scenarios to be of value as laboratory-based stressors in experimental medicine studies, since both within- and between-subjects designs are in routine use.

In this chapter I compared a range of psychological and physiological stress indices between healthy individuals during a VR lift ride which is intended to be stressful, compared with a control VR lift ride. I predict that the stressful VR scenario would produce an acute sympathetic-mediated stress response (affecting pulse, blood pressure, skin conductance, and sAA) but, given the relatively brief duration of the stressor, that it would likely be insufficient to produce detectable elevations in cortisol. After the stressor, participants completed the N-back task of working memory, in light of prior data suggesting that acute stress can impact on memory performance

(Henckens et al., 2009; Schoofs et al., 2008; Schwabe et al., 2012) and because the N-back will be used in the main study of this thesis (Chapter 8) to assess the effects of stress on working memory performance.

The study presented here therefore aims to investigate whether *this novel virtual reality lift elicits a stress response in healthy male volunteers*. It is hypothesised that:

- **the stressor lift will cause a significant increase in sAA, blood pressure, pulse, skin conductance and subjective ratings of stress, but not in salivary cortisol, compared to the control lift.**

In this chapter, I aim to establish (a) the magnitude and (b) the duration of the stress response in the lift stressor vs. its control.

2.2 Methods

2.2.1 *Participants*

Ethical approval was granted by the Inter-Divisional Research Ethics Committee of the University of Oxford (MSD-IDREC-C2-2014-0022). Twenty-eight non-smoking, healthy men aged 18 to 45 years old were recruited by advertisement. All potential participants underwent initial telephone screening to establish inclusion and exclusion criteria. Mental health was assessed using the Structured Clinical Interview for DSM-IV. Exclusion criteria included: current or past history of psychiatric or neurological disorder; use of psychotropic medication or medication which may affect the stress response (e.g. corticosteroids, beta-blockers); a history of heart disease or hypertension; alcohol intake greater than 30 units/week; illicit drug use in the last three months, and an inadequate command of spoken English.

2.2.2 *Procedure*

On the day of the experiment, participants were assigned to the control or stress VR scenario by simple randomisation (coin toss) by me. All participants knew they were taking part in a study that involved a VR scenario that could potentially stress them, but no further details were given until they were debriefed following data collection. Participants were instructed not to have any food or caffeinated drinks after 1 pm, and attended the laboratory between 2 and 3pm, since cortisol levels are predicted to be most stable in the afternoon (Sin et al., 2017). Participants changed into a

motion-tracker VR suit and a blood pressure cuff was fitted. During a one-hour baseline period, they filled in several questionnaires: Rotter's Locus of Control scale, the Rosenberg self-esteem scale, and the National Adult Reading Test (NART), a measure of verbal IQ. Locus of control and self-esteem were measured since both have been reported to affect the magnitude of the response to an experimental stressor (Bollini et al., 2004; Pruessner et al., 1999). Participants were also asked how often they had been exposed to a VR environment. Participants were then randomly assigned to either the control or stressor version of the VR scenario, described below, before completing the N-back task (also described below). Following completion of the N-back task, participants remained in the laboratory for another hour, after which they were fully debriefed as to the nature and purpose of the experiment. A schematic of the experimental procedure is shown in **Figure 2.1a.**

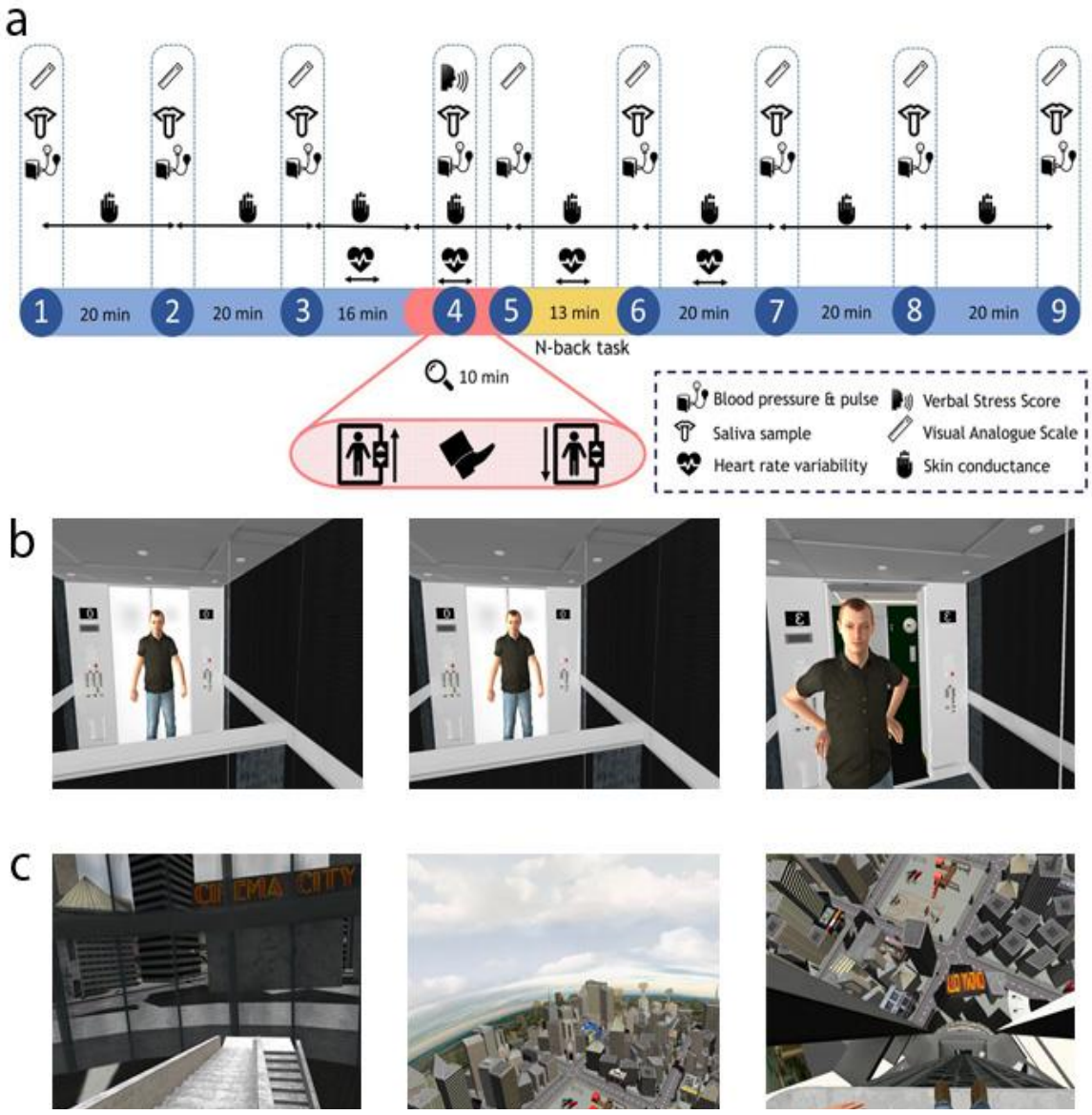


Figure 2.1 - Timeline of the experiment and VR lifts.

(a) Timeline of the experiment. (b) Images from the control lift. (c) Images from the stress lift. For details see text.

2.2.3 *Virtual reality*

Participants were immersed in the VR world via a head-mounted display (nVisor SX111 HMD) and velcro Optitrack suit (with 37 tracking markers) linked to a computer and tracking system (12 Intersense SoniStrip ceiling and an Intersense IS-900 SimTracker) (Freeman et al., 2016). The head-mounted display combined a 102-degree horizontal field of view and 64 degree vertical field of view with a high resolution (1280x1024). A stereo image was presented using a screen for each eye, updated at 60Hz. The Intersense SoniStrip ceiling and Intersense IS-900 SimTracker system combined an inertial and time of flight audio sensor to specify the viewer's position and orientation with six degrees of freedom. The resolution of the IS-900 was <0.75 mm, with an update rate of 180Hz, and latency of 4 msec. The computer running the application was custom built, and included a core i7 processor, and a NVIDIA GeForce GTX 780 ti graphics card with 3072MB of memory. This machine had 16GB RAM and an Asus Maximus VII Ranger motherboard. The tracking computer was a Dell T5500 workstation with a core i7 processor and 4GB RAM. Audio was rendered using the Realtek audio controller provided by the motherboard.

2.2.3.1 *Virtual reality environments*

There were two VR environments: an indoor closed lift (control condition) and an outdoor open platform lift (stress condition). For both scenarios, participants stood on a wooden platform (85 x 40 inches), whose edges corresponded to the edges of the VR lift platform. Both lift scenarios included two 15 second stops during the ascent and descent, and the sound of a lift played. The ascent and descent took 100 sec each; the total time of the VR paradigm was approximately 7.5 minutes.

The control scenario simulated a lift ride from a ground floor lobby up to the third floor; on arrival at the third floor, participants were instructed to step out of the lift and read the time on the clock in the hallway. The participant was alone, but was able to see his avatar's live mirror image via a 'mirror' on the back wall of the lift (**Figure 2.1b**). The stress scenario consisted of a VR journey on an open platform scaling the outside of a building, from the ground floor up to the top of a skyscraper, with an expanding view over the city (**Figure 2.1c**). Upon arriving at the top of the building, participants were instructed to step off the platform without hesitation. The edge of the platform corresponded to the edge of the virtual platform. Immediately after stepping out/off the lift, blood pressure and pulse rate (monitored for 30 seconds) were measured, and participants were asked to verbally rate how stressful they found the experience, on a scale from 0 to 10. In both scenarios, the lift then descended in a similar manner as it had ascended.

I recorded total movement (in metres) of each participant, to ensure that this was well-matched between the scenarios. For each of the 60 frames per second refreshes of the NVIS SX111 head mounted display, the position was read from the IS-900 tracker and written to an output data file, which was used to calculate the total movement of each participant.

2.2.4 *Measurements of stress response*

A range of psychological and physiological stress measures were taken throughout the experiment, as shown in **Figure 2.1a**. The first three time points (T1-3) were at 20-minute intervals in the hour prior to VR exposure; T4 occurred during the VR, immediately after the participant stepped off/out of the lift; T5 corresponded to the end of the VR; T6 was taken at the end of the N-back, and T7-T9 followed at 20-minute intervals over the subsequent hour.

Subjective reports of alertness, drowsiness, stress, happiness, sadness, anxiety and nausea were assessed using visual analogue scales (VAS) at all time points except T4, since at this time point the participant was immersed in the VR scenario. A verbal rating (from 0-10) of stress was taken at T4 but was analysed separately.

Cortisol and sAA were determined (by me, with additional help of Li Chen and Dr. Arne Mould) in saliva collected using salivettes (SalivaBio Oral Swab Saliva Collection Method, Salimetrics, Carlsbad, CA, US). Within four hours of collection, samples were centrifuged for 15 minutes at 3000rpm, aliquoted, and frozen at -20°C. Cortisol and sAA concentrations were determined (in duplicate) using either a competitive immunoassay (cortisol; Salimetrics Assay ID: 1-3002) or a kinetic enzyme assay (sAA; Salimetrics Assay ID: 1-1902). Intra-and inter-assay variability was <7% for cortisol and <11% for sAA.

Heart rate and skin conductance were continuously monitored throughout the experiment using Psychlab SC-EKG equipment at 500Hz. Heart rate ECG was measured using two standard dot snapper electrodes positioned under the right collar bone and left ribcage. QRS detection used the Pan and Tompkins's algorithm (Pan and Tompkins, 1985). From the heart rate data, heart rate variability (HRV) was calculated over four 5-minute periods (before VR, during VR, during N-back and after N-back). For clarity, I present root mean square of successive differences (RMSSD, in the time domain, as an index of short-range HRV) and low-frequency-high frequency ratio (LF-HF; in the frequency domain, which may reflect sympathetic modulations) as the main outcome measures (Camm et al., 1996). Skin conductance was measured using two 8-mm Ag/AgCl electrodes filled with isotonic electrolyte gel positioned on the index and middle finger of the non-dominant hand. Skin conductance was expressed as mean skin conductance level (μS) between the different data-

points. Blood pressure and pulse rate (monitored for 30 seconds) was measured with a standard blood pressure machine (OMRON).

2.2.5 *Tasks*

2.2.5.1 *N-back*

The N-back task imposes a parametric load on working memory. The version used here is relatively demanding (Farrell et al., 2012). It used three levels of complexity: 1-, 2- and 3- back, and a control task (0-back). Briefly, a number between 1 and 4 was randomly displayed on the computer screen (outside of the VR environment). For the 0-back condition, participants responded to the number showing on the screen by pressing the appropriate numerical button on the keyboard. For the 1-back, participants responded to the previous number on the screen, and so on for 2- and 3-back conditions. Each number was shown for 160msec, with an interval of 1640msec between numbers and 3000msec between blocks. Six blocks of each condition were run. Total duration was about 12 minutes. The primary performance measure was accuracy (correct responses); we also measured reaction time (RT) for correct trials. The task commenced within 2 minutes of completing the VR scenario, with a blood pressure reading and VAS rating taken in between (T5).

2.2.6 *Analyses*

Analyses were carried out using SPSS for Windows (Version 22, IBM SPSS Statistics). Data were expressed and analysed as a percentage of baseline, except for subjective stress-response ratings (since some participants endorsed zero values at baseline precluding normalisation). 'Baseline' was defined as measurement T3, as cortisol levels were anticipated to decline over the course of the study period, as the result of circadian variation and acclimatisation to the laboratory setting.

2.2.6.1 *Main analyses*

Since the autonomic stress response is brief, I pre-specified T4 (i.e. immediately after the acute stressor) as my primary time point of interest for blood pressure, pulse, sAA and (verbally reported) subjective ratings of stress and anxiety. Similarly, skin conductance and heart rate variability measures focussed on the period in the VR scenario as the main time interval of interest. The VAS 'Stressed' measure taken after the VR exposure (at T5), and the verbal 'Stressed' rating taken immediately after stepping off/out of the lift, were the primary psychological measures. In contrast, cortisol levels rise more slowly after stress, peaking after 20 minutes (Kudielka et al., 2009). Thus, I

defined T6, which occurred approximately 20 minutes after the VR scenario, as my primary time point of interest for cortisol levels. Values at these pre-determined time points were compared between conditions (control vs. stress) using t-tests or Mann-Whitney U tests as appropriate.
N-back data were analysed using repeated-measures analysis of variance (ANOVA), with level (0-3 back) as a within-subjects factor and group (stress or control) as the between-subjects factor.

2.2.6.2 *Exploratory analyses*

The effects of the VR environment on the psychological and physiological measures were explored using repeated-measures ANOVA with time as the within-subjects factor and group as the between-subjects factor. Raw data (rather than % baseline) and all time points (including the 3 baseline measures) were used for these analyses; VAS, cortisol, skin conductance and HRV measures were log-transformed as they were non-normally distributed. Huynh-Feldt correction was applied where data failed Mauchly's Test of Sphericity.

Correlational analyses (Spearman's rho, given the non-normal nature of many of the variables) were conducted to investigate the relationships between physiological and psychological variables, N-back performance, and personality characteristics. To limit the number of correlations examined, I focussed on the predetermined time points and measures included in the main analyses, with the additional of baseline (T3) VAS stress and anxiety scores, Rotter's Locus of Control and Rosenberg's Self-Esteem measures, and N-back % correct scores for each level.

2.3 Results

2.3.1 *Participants*

Participant demographics are given in **Table 2.1**. All participants completed the study. There were no group differences in the distance that participants moved within the VR scenarios, either overall or at the top of the lift (t's<0.75; p's>0.48). Due to technical difficulties, one participant (in the stress group) had missing ECG data, and three had missing skin conductance data. One participant (in the stress group) did not complete the N-back, and another did not complete VAS ratings at T5.

Table 2.1 - Demographic and personality measures

	Control Lift	Stress Lift
Number	13	15
Age (years)	23.9 ± 1.0	25.9 ± 1.2
NART	113 ± 2.4	111 ± 1.9
Locus of Control	75.4 ± 3.3	73.0 ± 3.5
Self-esteem	30.2 ± 1.8	30.2 ± 1.0
Computer literacy	5.1 ± 0.2	5.7 ± 0.3
Number of exposures to VR environment	1.4 ± 0.4	1.5 ± 0.5
Years in education	16.3 ± 0.9	18.4 ± 0.7

Values are mean ± SEM. NART: National Adult Reading Test; Locus of control: Rotter's Locus of Control Scale; Self-esteem: Rosenberg's Self-esteem Scale; Computer literacy + number of exposures to VR: Likert scale 1-7; Years in education from age 6.

2.3.2 *Main analyses*

The results of the group comparisons for stress measures at the predetermined time points are shown in **Figure 2.2**. As shown in **Table 2.2,** compared to the control, participants exposed to the stress VR scenario reported greater stress and anxiety. There was an increase in pulse and skin conductance, and changes in heart rate variability, but no change in blood pressure. Unexpectedly, exposure to the stress VR scenario was sufficient to increase salivary cortisol, compared to the control. The increase in sAA achieved trend-level statistical significance.

Table 2.2 - Effects of acute stress exposure in the VR scenario on physiological and psychological stress measures

	Control (n; mean ± SEM)	Stress (n; mean ± SEM)	Statistical test
VAS 'Stressed'	13; 1.1 ± 0.4	14; 2.8 ± 0.7	U=52; p=0.058
VAS 'Anxious'	13; 0.7 ± 0.3	14; 2.5 ± 0.6	U=40; p=0.013
Verbal 'Stressed' rating	13; 0.4 ± 0.2	15; 6.1 ± 0.7	U=5; p<0.001
Cortisol (% baseline)	13; 73.5 ± 9.6	15; 107.9 ± 10.2	t=-2.4; p=0.022
SAA (%baseline)	13; 108.7 ± 14.5	14; 161.9 ± 21.3	t=-2.0; p=0.056
Systolic BP (%baseline)	13; 105.2 ± 2.4	14; 108.6 ± 3.5	U=75; p=0.44
Diastolic BP (%baseline)	13; 115.0 ± 2.6	14; 118.3 ± 2.6	U=74; p=0.41
Pulse (%baseline)	13; 114.8 ± 4.9	14; 129.6 ± 7.1	U=45; p=0.026
Skin conductance	12; 106.4 ± 6.6	13; 149.6 ± 16.6	U=35; p=0.019
HRV: RMSSD (%baseline)	13; 96.7 ± 11.2	14; 167.2 ± 28.2	U=43; p=0.019
HRV: LF-HF ratio (%baseline)	13; 153.9 ± 33.8	14; 87.2 ± 10.9	U=45; p=0.025

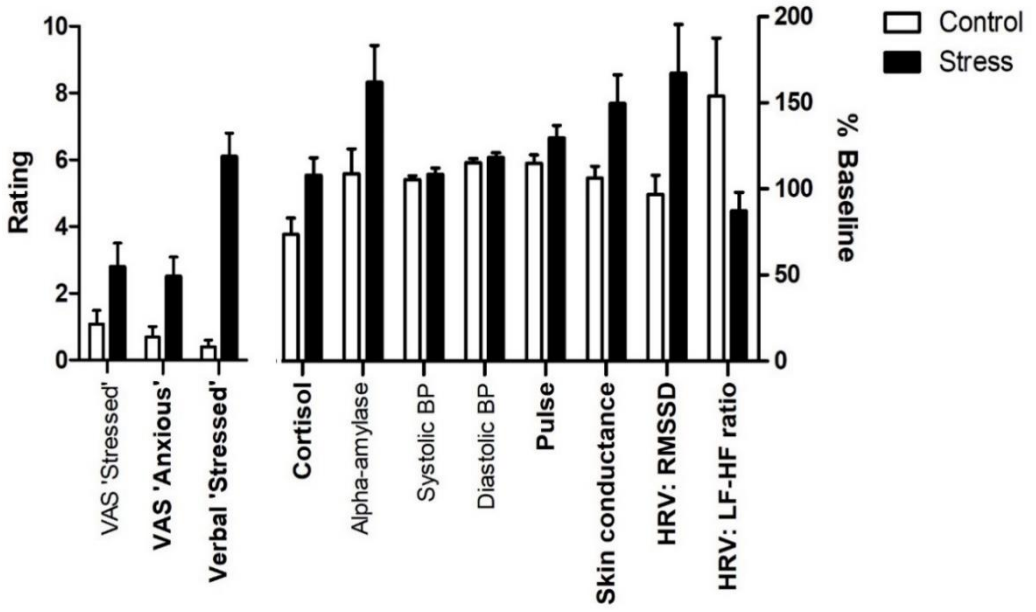


Figure 2.2 - Summary of main analyses.

Psychological and physiological measures of participants randomised to the control (open bars) or stress (closed bars) shown as means ± SEMs. Variables showing a group difference are highlighted with bold text (see **Table 2.2** for full statistical details).

In contrast to the physiological and psychological measures, there was no group difference in N-back performance **Table 2.3.** Thus, whilst there were main effects of level for the % correct trials ($F_{3,75}$=72.9; p<0.001), there was no effect of level on reaction time ($F_{3,75}$=1.4; p=0.27) and no main or interactive effects of group on either measure (F's<3.3; p's>0.57). There were no main or interactive effects for reaction time (F's<1.4; p's>0.26).

Table 2.3 - Effects of acute stress exposure in the VR scenario on N-back performance

	Control (Mean ± SEM)	Stress (Mean ± SEM)
0 back % correct	97.0 ± 0.6	97.5 ± 0.6
1 back % correct	84.4 ± 3.5	86.0 ± 3.3
2 back % correct	65.4 ± 5.0	70.2 ± 4.8
3 back % correct	52.4 ± 5.6	55.1 ± 5.4
0 back reaction time (msec)*	552.2 ± 35.8	539.6 ± 34.5
1 back reaction time (msec)*	491.9 ± 49.8	519.6 ± 49.8
2 back reaction time (msec)*	546.4 ± 57.7	590.7 ± 57.7
3 back reaction time (msec)*	553.2 ± 42.2	568.0 ± 40.7

*Reaction time calculated for correct trials only

2.3.3 *Exploratory analyses*

2.3.3.1 *HPA stress response*

In the control group, cortisol levels showed the predicted diurnal decrease over the course of the experiment; in contrast, cortisol levels remained relatively constant in the stress group (**Figure 2.3a**). Thus, there was a main effect of time ($F_{7,182}$=5.0; p=0.002), and a trend-level interaction between time and group ($F_{7,182}$=2.1; p=0.096) in the absence of a main effect of group ($F_{1,26}$=1.6; p=0.21). In contrast, there were no effects of time, group nor their interaction on amylase levels (**Figure 2.3b**; F's<1.7; p's>0.12).

2.3.3.2 *Autonomic stress response*

Blood pressure (systolic and diastolic), pulse rate and skin conductance increased during both VR scenarios (**Figure 2.3c-f**), reflected in main effects of time for these measures (F's>5.9; p's<0.001) in the absence of main or interactive effects of group (F's<1.3; p's>0.19). For heart variability, there was a main effect of time ($F_{3,75}$=3.6; p=0.025; **Figure 2.3g**) on the RMSSD measure, due to a decrease during the N-back epoch compared to the neighbouring time points (p's<0.014), but no main or interactive effects of group (F's<1.6; p's>0.2), nor were there any group or time effects on the LF-HF measure (F's<1.8 ; p's>0.15; **Figure 2.3h**).

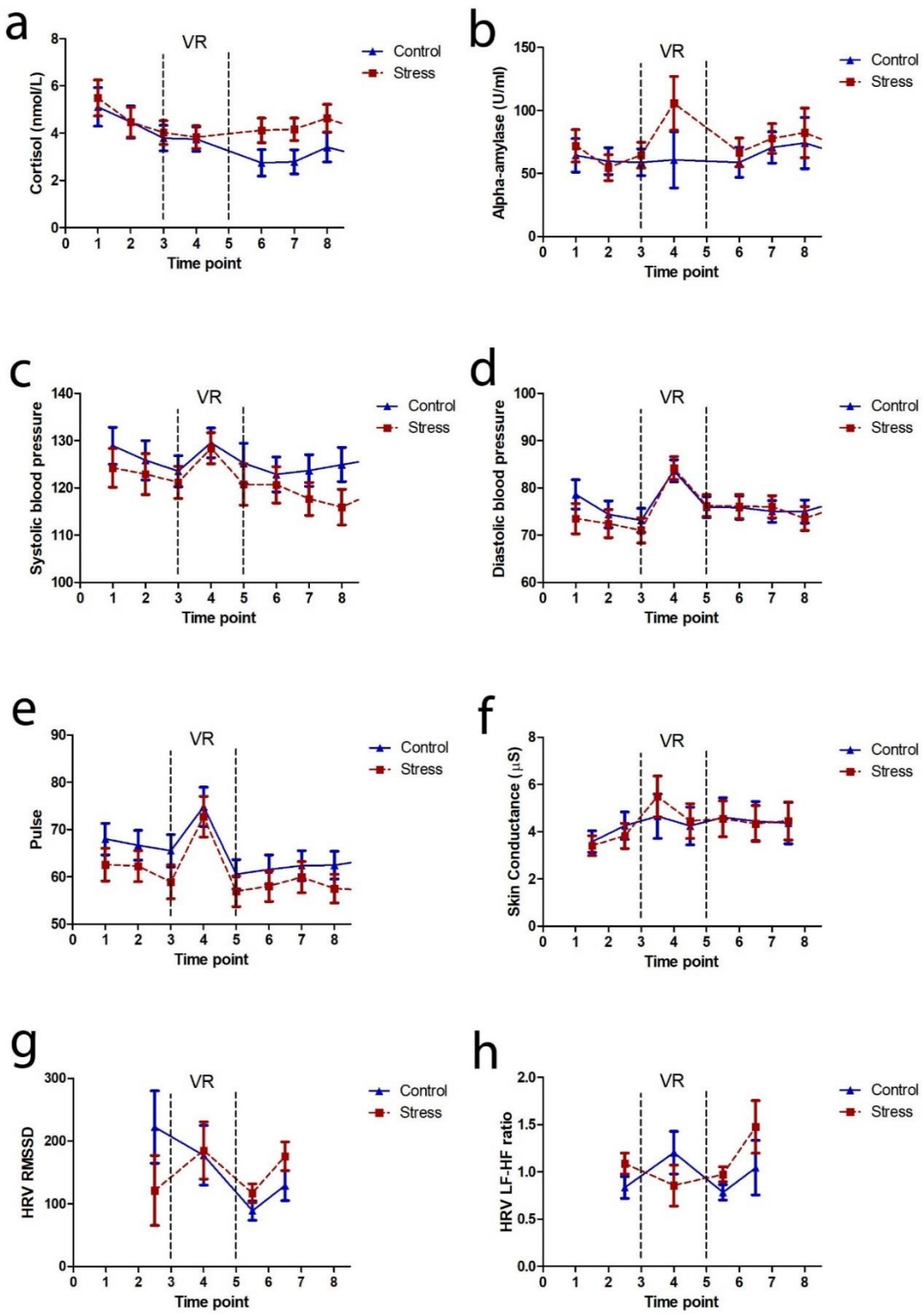


Figure 2.3 - Effects of acute stress exposure in the VR scenario on physiological stress measures.

Changes in (a) cortisol, (b) sAA, (c) systolic blood pressure, (d) diastolic blood pressure, (e) pulse rate, (f) skin conductance, and heart rate variability (g) RMSSD and (h) LF-HF ratio measures over the course of the experiment in those randomised to the control (blue triangles and solid lines) and stress (red squares and dashed lines) lift. Results are expressed as mean±SEM.

2.3.3.3 *Psychological stress response*

Several of the psychological variables showed evidence of being affected by the VR environment, in a group-dependent manner in some cases. 'Anxious' ratings were selectively increased in the stress group following VR exposure, reflected in a time by group interaction ($F_{7,175}$=2.5; p=0.036) that resulted from a group difference at T5 (post-VR; p=0.005) but not other time points (**Figure 2.4a**). There was also a main effect of time ($F_{7,175}$=6.6; p=<0.001) but no main effect of group ($F_{1,25}$=0.88; p=0.36). There was a main effect of time on 'Stressed' ratings ($F_{7,175}$=10.8; p=0.001). This resulted from higher ratings both after the VR and the N-back, compared to other time points (T5 differs from all other time points [p's<0.005], except T6 [p=0.62]; T5 differs from all other others [p's<0.026], except T6 and T1 [p=0.061] (**Figure 2.4b**). These data indicate that participants found both the VR (at least in the case of the stressful scenario, see above) and the N-back mildly stressful. Two other psychological ratings showed evidence of being slightly increased by VR exposure, namely 'Nausea' (Error! Reference source not found.**c**) and 'Alert' (**Figure 2.4d)**: there were main effects of time (F's>3.8; p's<0.003) but no main or interactive effects of group (F's<1; p's>0.4) for either. For both 'Nausea' and 'Alert' ratings, there was an increase from T3 (final baseline) to T5 (post-VR; p's<0.05). Finally, there was a main effect of time on VAS 'Sad' ratings ($F_{7,175}$=2.6; p=0.014; data not shown), that appeared to result from a gradual decrease in 'Sad' ratings across the testing session (no individual time point comparisons reached significance), in the absence of main or interactive effects of group (F's<1.2' p's>0.35). There were no main or interactive effects on ratings of 'Happy' (F's<1.2; p's>0.3; data not shown).

2.3.3.4 *Correlations*

Very few correlations were found between stress indices of different types in the dataset (**Table 2.4).** This applied both to a lack of correlations between psychological and physiological stress parameters, and also between different physiological measures.

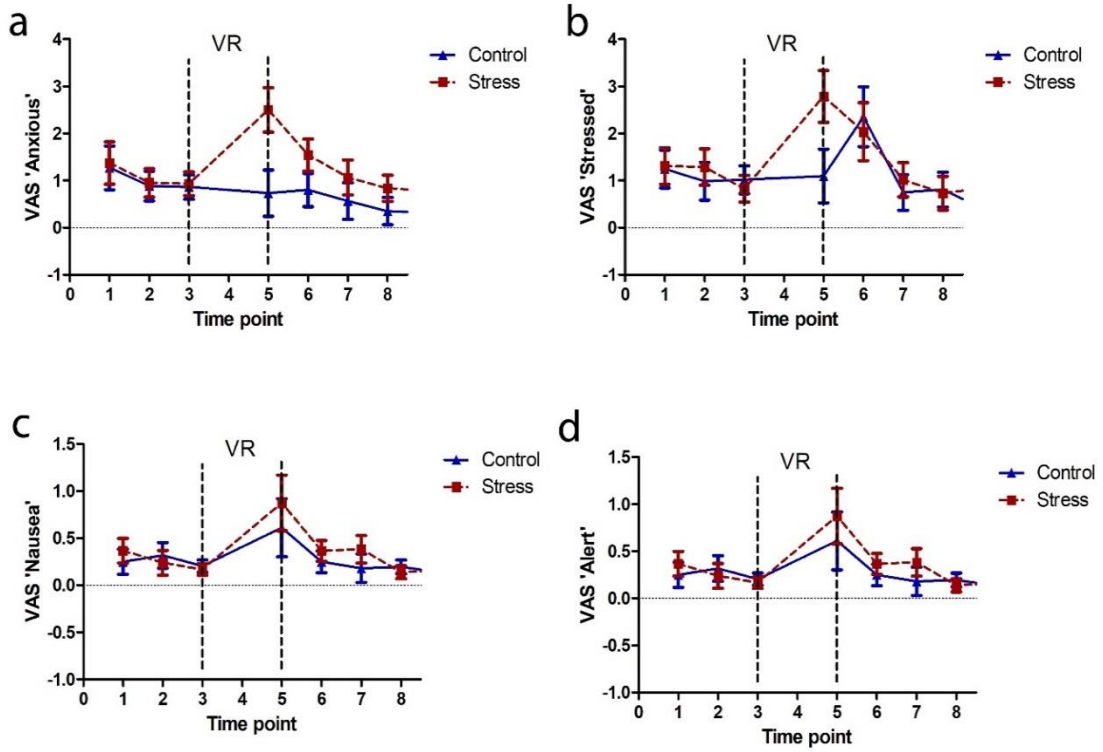


Figure 2.4 - Effects of acute stress exposure in the VR scenario on psychological stress measures.

Changes in VAS ratings of (a) 'Anxious', (b) 'Stressed', (c) 'Nausea' and (d) 'Alert' over the course of the experiment in those randomised to the control (blue triangles and solid lines) and stress (red squares and dashed lines) lift. Note that VAS ratings were not taken at T4 as participants were in the VR environment. Results are expressed as mean±SEM.

Table 2.4 - Correlations between different measures of the stress response, as induced by the VR scenario, and N-back performance.

		Self-esteem	Locus of control	Baseline VAS 'Stressed' Time point 3	Baseline VAS 'Anxious' Time point 3	Post-VR VAS 'Stressed' Time point 3	Post-VR VAS 'Anxious' Time point 4	Mid verbal 'Stressed'	Cortisol (% baseline) Time point 5	sAA (% baseline) Time point 4	Systolic BP (% baseline) Time point 4	Diastolic BP (% baseline)	Pulse BP (% baseline)	SC (% baseline)	HRV RMSSD (% baseline)	HRV (LF-HF ratio % baseline)	0 back (% correct)	1 back (% correct)	2 back (% correct)	3 back (% correct)
Self esteem	Spearman's rho	1.000	.688**	-.189	-.262	-.157	-.187	-.026	-.131	.138	-.043	-.229	-.045	.100	.192	-.359	.132	.387*	.061	-.112
	p value		.000	.335	.179	.436	.350	.896	.506	.483	.833	.250	.824	.636	.338	.066	.510	.046	.764	.579
Locus of control	Spearman's rho		1.000	-.312	-.328	-.273	-.260	-.086	-.069	-.201	-.201	-.044	-.118	.112	.178	-.090	.227	.433*	.217	.053
	p value			.106	.089	.169	.190	.663	.728	.305	.316	.827	.556	.594	.373	.656	.255	.024	.277	.793
Baseline VAS 'Stressed'	Spearman's rho			1.000	.761**	.665**	.612**	.138	-.371	-.189	.073	-.093	.151	.067	.239	-.183	.024	-.159	-.033	-.262
	p value				.000	.000	.001	.483	.052	.336	.716	.644	.451	.751	.230	.361	.907	.428	.869	.187
Baseline VAS 'Anxious'	Spearman's rho				1.000	.533**	.547**	.051	-.397*	-.027	.039	.079	-.046	-.057	.155	-.085	-.115	-.181	-.004	-.104
	p value					.004	.003	.797	.036	.892	.846	.695	.820	.786	.441	.674	.568	.366	.982	.606
Post-VR VAS 'Stressed'	Spearman's rho					1.000	.926**	.591**	-.058	.051	.130	-.279	.214	.167	.328	-.233	.102	-.196	.033	-.077
	p value						.000	.001	.773	.801	.527	.167	.295	.436	.102	.252	.621	.336	.872	.710
Post-VR VAS 'Anxious'	Spearman's rho						1.000	.587**	.079	.004	.072	-.295	.127	.262	.428*	-.344	.051	-.111	.101	.026
	p value							.001	.695	.986	.726	.143	.535	.216	.029	.085	.804	.589	.624	.899
Mid verbal 'Stressed'	Spearman's rho							1.000	.312	.359	.159	.067	.395*	.415*	.490**	-.360	.269	.108	.223	.157
	p value								.106	.061	.427	.740	.041	.039	.010	.065	.174	.594	.263	.435
Cortisol (% baseline)	Spearman's rho								1.000	.165	.108	.167	.439*	.393	.180	-.114	.047	-.032	-.114	-.002
	p value									.402	.591	.406	.022	.052	.369	.571	.815	.873	.572	.990
sAA (% baseline)	Spearman's rho									1.000	.262	.198	.106	.156	-.081	-.190	.050	.392*	.194	.159
	p value										.187	.323	.598	.456	.687	.341	.804	.043	.333	.429
Systolic BP (% baseline)	Spearman's rho										1.000	.329	.220	.341	.175	-.168	.011	.081	.192	.169
	p value											.094	.271	.103	.382	.403	.959	.695	.347	.408
Diastolic BP (% baseline)	Spearman's rho											1.000	.294	.100	.089	.049	.006	.171	.146	.273
	p value												.136	.642	.661	.809	.978	.404	.476	.177
Pulse BP (% baseline)	Spearman's rho												1.000	.362	.173	-.130	-.080	-.230	-.269	-.274
	p value													.082	.389	.518	.697	.259	.184	.176
SC (% baseline)	Spearman's rho													1.000	.447*	-.264	.102	.312	.042	.306
	p value														.029	.212	.629	.129	.841	.137

HRV RMSSD (% baseline)	Spearman's rho													1.000	-.700**	.308	-.009	.152	.145
	p value														.000	.126	.967	.459	.478
HRV LF-HF ratio (% baseline)	Spearman's rho														1.000	.285	-.007	.036	-.039
	p value															.158	.975	.860	.851
0-back (% correct	Spearman's rho															1.000	.497**	.444*	.423*
	p value																.008	.020	.028
1-back (% correct	Spearman's rho																1.000	.623**	.510**
	p value																	.001	.007
2-back (% correct	Spearman's rho																	1.000	.583**
	p value																		.001
3-back (% correct	Spearman's rho																		1.000
	p value																		

2.4 Discussion

This chapter's data show that the VR stress scenario increased pulse rate, skin conductance, salivary cortisol and perceived stress and anxiety, and altered heart rate variability but not blood pressure, compared to the control. SAA was numerically increased by exposure to the 'stress' scenario, compared to the control, but this did not reach formal statistical significance. Here, I comprehensively demonstrate physiological and psychological effects in individuals randomised to an active VR condition vs. a control VR condition. Thus, these findings underscore the utility of VR for inducing stress (and potentially other emotional states) for therapeutic and experimental purposes.

A number of previous studies have investigated the effect of VR environments on physiological stress measures but findings are mixed (reviewed in (Diemer et al., 2014). Several have used height as a stressor but most of these focussed on comparing responses between groups (e.g. comparing healthy participants with a clinical population). Thus, whilst numerical increases in skin conductance and/or heart rate were observed over the course of VR height exposure in some of these studies (Cleworth et al., 2012; Diemer et al., 2016; Meehan et al., 2002; Meehan et al., 2005; Seinfeld et al., 2016; Wilhelm et al., 2005), these were not always examined statistically and it is possible that these changes resulted from exposure to the VR environment rather than stress *per se*. Only a few groups have counter-balanced the order of control vs. stressful height exposure within-subjects, and findings are similarly mixed within these. Thus, one, in which healthy participants undertook a beam walk in the VR environment at ground level vs. at height, found changes in heart rate variability in the absence of effects on pulse or skin conductance (Peterson et al., 2018), whilst a second found changes in skin conductance but not pulse, when participants were asked to lean out over VR balconies of different heights (Simeonov et al., 2005). This chapter's results clearly demonstrate increases in a number of physiological and psychological markers of stress during VR height challenge using a randomised, between-subjects design. This approach, comparing active and control VR environments matched for movement demands, allows to disambiguate the effects of stress vs. non-specific components arising from the VR environment *per se*, as well as avoiding confounds due to cardiovascular demands and potential order effects.

A striking finding was that exposure to the stress VR paradigm was sufficient to induce changes in the HPA axis component of the stress response, *viz.* cortisol level. VR versions of the TSST, a widely-used psychosocial stressor, increase salivary cortisol levels (e.g. (Jönsson et al., 2010; Kelly et al.,

2007; Kothgassner et al., 2016), consistent with the robust cortisol response elicited by the face-to-face version (Kirschbaum et al., 1993). However, few VR studies using *non*-social stressors have investigated their effect on cortisol, and there is no clear evidence. Diemer and colleagues (Diemer et al., 2016) report that a subset of participants (20-30% of healthy controls, depending on the precise cut-off used) showed a cortisol response to a VR height challenge, but their results are difficult to interpret as they only report the proportion of responders and non-responders in their healthy control and acrophobia individuals and present data on cortisol levels 7 minutes post-exposure, likely prior to the peak cortisol response (Kudielka et al., 2009). Therefore, to my knowledge, this study is the first to demonstrate an increase in cortisol levels following a non-social VR stressor. I consider the finding somewhat surprising given the relatively brief nature of the lift stressor and the fact that the participants were all healthy controls. However, they provide further evidence for the utility of VR environments for inducing and modelling acute stress exposure in the laboratory setting.

I found no group difference in N-back performance, in contrast to some previous studies that demonstrate effects of stress on memory performance (Henckens et al., 2009; Schoofs et al., 2008). However, findings are mixed: whilst the majority of studies suggest that stress impairs working memory (Duncko et al., 2009; Gärtner et al., 2014; Luethi et al., 2009; Oei et al., 2006; Schoofs et al., 2008), some find a beneficial effect (Cornelisse et al., 2011; Stauble et al., 2013; Weerda et al., 2010) and others no differences (Hoffman, 2004; Kuhlmann, 2005; Smeets et al., 2006). These variable findings likely reflect the complex relationship between stress and memory. Thus, as well as different types of memory being differentially affected by stress (Cornelisse et al., 2011; Kuhlmann, 2005; Schwabe et al., 2012), there are important effects of, for example, gender (Cornelisse et al., 2011; Zandara et al., 2016) and the timing of the cognitive task relative to the stressor (Schwabe et al., 2012). It should be noted that this VR stress paradigm did not involve a social component and was relatively mild in nature, inducing only a relatively brief cardiovascular and cortisol response compared to, for example, the TSST (Allen et al., 2014), and so may have been insufficient to induce stress-related changes in working memory. However, whilst some previous studies have shown associations between stress-related cortisol changes and working memory performance (Schoofs et al., 2008), others have observed stress-related changes in working memory in the absence of group differences in cortisol levels (Duncko et al., 2009). Thus, although the findings suggest that mild stress does not affect working memory performance in young, healthy men, further studies are required to clarify the relationships between stressor, stress response, and working memory.

At first sight, the absence of correlations between different measures of the stress response may seem surprising. However, there is a substantial literature arguing against the 'stress response' as being a unitary construct, and weak or absent correlations between physiological and psychological measures of the stress response is a common finding both in experimental and naturalistic settings (Campbell and Ehlert, 2012; Dickerson and Kemeny, 2004; Wilhelm et al., 2005). This chapter's findings emphasise the value of examining multiple variables to establish a full picture, not least since different components of the stress response may impact differentially on outcomes of interest.

2.4.1 *Limitations*

This chapter's study has some limitations. Firstly, healthy young adult male volunteers were investigated only. Thus, it is not clear to what extent the findings can be generalised to females, other ages, or to patient groups (Cornelisse et al., 2011; Diemer et al., 2016). Secondly, the lift stressor was brief and relatively mild; therefore, the psychological and physiological effects observed are relatively modest in terms of magnitude and duration. Accordingly, it is not clear that these findings will be of relevance to situations of more extreme or prolonged stress. Broadly speaking, any attempt to extrapolate these findings should be mindful of the complex interplay between psychological and physiological effects of stress, its context, and the cognitive impacts (Schwabe et al., 2012).

2.4.2 *Conclusion*

In conclusion, I demonstrate that a VR environment can be used to induce a physiologically and psychologically relevant stress response. Therefore, my findings underscore the utility of scenarios of this type for therapeutic purposes, for example to allow individuals to experience an aversive environment in a controlled, safe setting as an adjunct or alternative means of delivering exposure therapy (Freeman et al., 2019). The fact that I observed a measurable stress response even in healthy individuals points to the potential of VR scenarios in an experimental medicine setting, both as a model in which to test putative anxiolytics and as a tool to investigate how stress might affect the therapeutic actions of drugs of interest. As VR scenarios become increasingly realistic and diverse, and the technology ever more cost-effective, its use in research and clinical settings will likely increase accordingly. My findings suggest that VR will be of utility in both situations.

Chapter 3 Physiological and psychological effects of the Montreal Imaging Stress Task (MIST)

3.1 Introduction

The over-arching aim of this thesis is to explore the impact of COMT genotype and pharmacological inhibition on cognitive function under conditions of stress. In Chapter 2, I demonstrated that a novel VR scenario is capable of inducing stress in a laboratory setting. However, effects on cortisol levels were small and relatively transient, making this paradigm unsuitable for use in my main study. Therefore, in the current chapter, I explored whether more robust physiological responses might be elicited by an alternative stressor: The Montreal Imaging Stress Test (MIST) (Dedovic et al., 2005).

The magnitude and duration of the physiological effects observed in Chapter 2 are not unusual. On average, psychological stressors have only a modest effect on cortisol levels (on average 0.31 standard deviations above baseline values), which investigators attribute (at least in part) to variability in the nature of the stressor employed, the sex of the subject and early life experience (Dedovic et al., 2009; Dickerson and Kemeny, 2004). However, tasks that include social-evaluative threat (in which others negatively judge performance, particularly when the outcome of the performance is uncontrollable) provoke larger and more reliable cortisol changes (both in terms of overall magnitude and in recovery trajectory) than stressors without these aspects (e.g. (Dickerson and Kemeny, 2004)). As outlined previously (see Chapter 1), the TSST, which combines public speaking with mental arithmetic, is the 'gold standard' laboratory-based stressor (Kirschbaum et al., 1993). Consistent with this, the TSST elicits the largest effect on cortisol levels (nearly twice as large as the effect sizes for other task categories), compared with other types of stressor, even when controlling for duration of the stressor. However, the 'classic' TSST cannot be administered in an MRI scanner and so it is not suitable for the main study proposed here. The robust effect of the TSST and related stressors have been attributed to outcome uncontrollability and social-evaluative threat; thus, Dickerson and Kemeny (2004) conclude that determinates of an increased cortisol response after psychological stress appear to consist of (a) a motivated performance task, (b) relative uncontrollability and (c) the presence of social evaluation. The MIST was developed as a scanner-compatible stressor designed to incorporate these key components.

The MIST requires performing computerised challenging mental arithmetic with an adaptive algorithm and a built-in negative social evaluation and relative uncontrollability

component, and therefore fits Dickerson and Kemeny, (2004)'s definition. The MIST is described in full in the methods section of this chapter.

The TSST consistently produces increases in cortisol about 200-400% above baseline, in about 70-80% of participants (Dedovic et al., 2005; Dickerson and Kemeny, 2004; Kirschbaum et al., 1993; Kudielka et al., 2009), whilst the MIST typically increases cortisol 50-100% for a duration of 20 – 60 minutes in about 50% of the participants (reflecting an inter-individual variability in reacting to a given stress stimulus (Dedovic et al., 2009b, 2009a). To attempt to control for this variability, (Pruessner et al., 2008) proposed to split participants up into cortisol 'responders' and 'non-responders'. Since the circadian rhythm of cortisol normally results in declining levels during the course of the day, (Pruessner et al., 2008) labels each subject that showed signs of cortisol decrease over the course of the experiment as a cortisol 'non-responder', and participants with increases as cortisol 'responders' (Pruessner et al., 2008). This change in cortisol is defined as AUC_G and AUC_I cortisol, of which I will give a full explanation in the methods section of this chapter.

To my knowledge, nine different studies have used the MIST to induce acute stress in either a behavioural or MRI setting relevant to this study so far (excluding studies conducted in patients, women or elderly participants only), as outlined in **Table 3.1**. Not all studies show a significant overall stress response, as defined by a statistically-significant increase in cortisol, nor do studies define their cortisol responders and non-responders according Pruessner et al., (2008)'s definition. Variability in the MIST response rate is therefore a possible explanation for the mixed findings in these studies (on either behavioural measures like working memory performance, or brain activity (Chapter 7)). Next to increases in cortisol, three studies also showed increases in heart rate and/or blood pressure during MIST exposure (Geva et al., 2014; Lederbogen et al., 2011; Orem et al., 2019) and increases in skin conductance (Geva et al., 2014; Orem et al., 2019).

In this study I investigated the physiological and psychological effects of the MIST, by comparing the stressor version of the MIST with its control. I aim to ensure that it acts as a robust stressor in our hands and in our target population, in order to validate it for use in our main imaging study. Specifically, I aimed to demonstrate that the MIST stress version shows clear effects on psychological and physiological stress measures compared to its control (which I cannot feasibly include in the main imaging study, given that it would double the size of the study), and to investigate the magnitude and duration of this stress in order to establish our testing-window. Moreover, as the N-back task for working memory will be used in this main study to assess the effects of stress on working memory performance, I examined the effects of acute stress induced by the MIST on N-back performance as well.

The study presented here therefore aims to investigate whether *conducting the MIST elicits a stress response in healthy male volunteers*. It is hypothesised that:

- **the stressor version of the MIST will cause a significant increase in salivary cortisol, blood pressure, pulse, skin conductance and subjective ratings of stress, compared to the control version of the MIST,**
- **and that this group difference will be greater than that observed for the VR stressor (Chapter 2), given the additional socioevaluative component of the MIST stressor (discussed in Chapter 9).**

In this chapter, I aim to establish (a) the magnitude and (b) the duration of the stress response in the MIST stressor vs. its control.

Table 3.1 - Behavioural and imaging studies that used the Montreal Imaging Stress Task to induce stress

Authors	Setting	Participants (age)	MIST procedure	Cortisol magnitude	Cortisol duration	Other physiological measures?
(Dedovic et al., 2005)	MRI: 1.5 Tesla	N = 22 healthy males (20-24)	Standard MIST Within subjects	Overall group Cortisol measure: raw values Baseline: ~6.5 nmol/l Post stress: ~10 nmol/l Magnitude: +54% Significant: yes	Cortisol increased for 40 minutes starting at baseline, however no statistical significance reported.	N/A
(Pruessner et al., 2008)	MRI: 1.5 Tesla	N = 40 20 males (23.35 ± 3.17) 20 females (22.75 ± 3.11)	Two runs of MIST completed over the course of 9 minutes. Within subjects	Overall group: Cortisol measure: raw values Baseline: ~5.5 nmol/l Post stress: ~6.8 nmol/l Magnitude: +24% Significant: yes Split by AUC_I, raw cortisol values nmol/l 21 responders: Baseline: ~5.5 Post stress: ~8.0 Magnitude: +45 19 non- responders: Baseline: ~5.5 Post stress: ~4.2 Magnitude: -24%	Cortisol increased for 30 minutes starting at baseline, however no statistical significance reported.	N/A
(Dedovic et al., 2009c)	MRI: 3 Tesla	N = 28 healthy males (23 ± 4.48)	Two runs of the EventMIST (event related fMRI design) Within subjects	Overall group Cortisol measure: raw values Significant: no Split by k-means cluster analysis, raw values nmol/l 7 responders: Baseline: ~4.2 Post stress: ~8.5 Magnitude: +102% 13 non- responders: Baseline: ~3.0 Post stress: ~3.0 Magnitude: 0%	Significant difference between responders and non-responders for 75 minutes starting at baseline.	Significant increase in state anxiety after MIST (overall group). Difference between responders and non-responders in locus of control but not self-esteem.
(Khalili-Mahani et al., 2010)	MRI 1.5 Tesla	N = 19 healthy males (20-28)	Standard MIST Within subjects	Overall group Significant: no Split by AUC_I, Raw values nmol/l 9 responders: Baseline: ~7.5 Post stress: ~15 Magnitude: +100% 10 non-responders: Baseline: ~11 Post stress: ~7 Magnitude: -37%	Cortisol increased in responders for 40 minutes starting at baseline, however no statistical significance reported.	N/A

(Lederbogen et al., 2011) Same subjects as (Boehringer et al., 2015)	MRI: 3 Tesla	N = 32 healthy 16 males 16 females (43.6±14.4)	Standard MIST Within subjects	Overall group Cortisol measure: raw values Baseline: 6.5±3.0 nmol/l Post stress: 14.8±10.9nmol/l Magnitude: +128% Significant: yes		Not specified Overall group	HR (BPM) Baseline: 68±6 Post: 73±9 Magnitude:+7% Significant: yes	BP (mmHG) Baseline: 124±13 Post: 136±15 Magnitude:+10% Significant: yes	Subjective: Baseline: 2.3±1. Post: 7.1±1.7 Magnitude: +209% Significant: yes
(Dedovic et al., 2014)	MRI: 1.5 Tesla	26 healthy controls (12 males; 14 females)	Modified MIST: added a 'no evaluation' block, to only capture the social evaluative threat component (not maths). Within subjects	Overall group Cortisol measure: raw values Baseline: ~3.3 nmol/l Post stress: ~3.3nmol/l Magnitude: 0% Significant: no		Cortisol decrease	N/A		
(Geva et al., 2014)	Behavioural	N = 29 healthy males (33 ± 10)	Two runs of 8 minute MIST Within subjects	Overall group Cortisol measure: Not specified Baseline: 529±321 Post stress: 889±818 Magnitude: =68% Significant: yes		Cortisol increased for 20 minutes starting at baseline.	SC: Baseline: 8.1±5.4 Post:10.7±5.1 Magnitude: =32% Significant: yes	HR: Baseline: 72.8 ±12 Post: 80.4±13.9 Magnitude: =10% Significant: yes	VAS stress: Baseline: 1.27±1.9 Post: 4.28±3.4 Magnitude: =237% Significant: yes
(Corbett et al., 2017)	Behavioural	N = 78 healthy males (20.31 ± 2.43) 39 stress group 39 control group	Standard MIST Between subjects	Stress group vs control group Decrease in cortisol for both groups Tertile split: Δcortisol 13 responders: Δcortisol = ~3 13 non-responders: Δcortisol=~-7.5 Control group: Δcortisol = ~-3 Magnitude: +140%		Duration of MIST measured only.	N/A		
(Orem et al., 2019)	MRI: 3 Tesla	239 healthy 126 males 113 females (19.44 ± 0.07)	Modified MIST: control vs. stress scan.	Stress MIST: Cortisol measure: raw values Baseline: 0.23±0.01 µg/dL Post stress: 0.20±0.01 µg/dL Magnitude: = -15% Significant: yes – decrease!		Cortisol decrease	SC: Control:0.40±0.03 Stress: 0.85±0.05 Magnitude: = +112% Significant: yes	HR (BBP): Control:66.9±0.91 Stress:72.3±1.11 Magnitude: = +8% Significant: yes	Subjective stress: Control:15.24±0.4 Stress: 26.1 ± 0.5 Magnitude: = +70% Significant: yes

3.2 Methods

In this study I investigated the physiological and psychological effects of the MIST, by comparing the stressor version of the MIST with its control, in healthy male volunteers. Moreover, I also examined the effects of acute stress as induced by the MIST on N-back performance.

3.2.1 *Participants*

Participants were recruited in an identical manner as in Chapter 2. All twenty-four participants knew they were taking part in a study that could potentially stress them, but all were told that they were in the control group.

3.2.2 *Procedure*

Participants were telephone screened prior to attendance, as described in Chapter 2. On the day of the experiment, participants were assigned to the either the control or stressor versions of the MIST based on Prof. Harrison's availability on that day, since he acted as the confederate.

Similar to as described in Chapter 2, to ensure that baseline cortisol levels were as consistent as possible, participants were instructed not to have any food or caffeinated drinks after 1 pm and attended the laboratory between 2 and 3pm. During a one-hour baseline period, they filled in several questionnaires: Rotter's Locus of Control scale, the Rosenberg self-esteem scale, and the NART. Locus of control and self-esteem were measured since both have been reported to affect the magnitude of the response to an experimental stressor (Bollini et al., 2004, Pruessner et al., 1999). Participants then did either the control or stressor versions of the MIST before completing the N-back task (see below). Following completion of the N-back task, participants remained in the laboratory for another hour, after which they were fully debriefed as to the nature and purpose of the experiment. A schematic of the experimental procedure is shown in **Figure 3.1**. Physiological measures of stress, including salivary-cortisol, heart rate (Psychlab), blood pressure and skin conductance (Psychlab) together with subjective stress and mood ratings, assessed using VASs, were recorded at 20 minutes intervals. VASs included ratings of alertness, drowsiness, stress, happiness, sadness, anxiety and nausea. This resulted in 9 data points over time in the MIST scenario (3 baseline measures, 3 taken during testing (during MIST, post-MIST and N-back), and 3 post-testing).

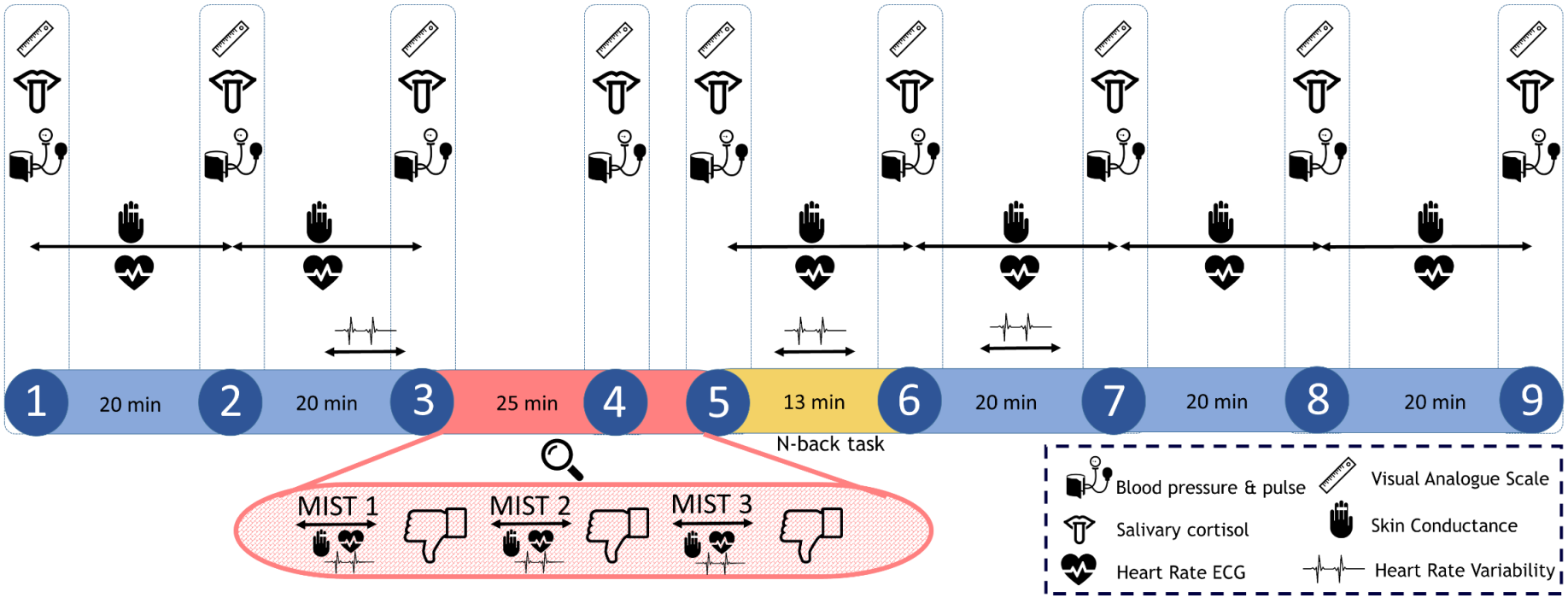


Figure 3.1 - Timeline of the experiment.

3.2.3 *Tasks*

3.2.3.1 *MIST*

The MIST is a task designed to induce psychological stress. It is presented as a series of computerised mental arithmetic challenges, along with (stress condition) or without (non-stress condition) social evaluative threat components that are presented by the investigators. For both groups, the participant's ability to perform mental maths is assessed by recording the average time needed to solve the mathematical problem at various difficulty levels. This averaged time is then used to set a default time limit for the experimental stressful condition. In this stressful condition, two performance indicators are shown. The participant is told that one indicates his performance, while the other indicates the performance that is required for the participant to be included in the study, which is 80-90% correct. Moreover, a time limit is enforced, with the exact time allowed depending on the participant's previous performance. To induce a high failure rate, the software is set to a time limit that is 10% less than the subject's average response time. In addition, the software continuously records the subject's average response time and the number of correct responses. If the subject answers a series of three consecutive trials incorrectly, the program increases the time limit to 10% more than the average time for the 3 correctly solved tasks. Conversely, if the subject answers a series of 3 consecutive tasks correctly, the program reduces the time limit for the following tasks by 10%. In this way a range of about 20% to 45% correct answers is enforced in the experimental stress condition. Participants are therefore never able to reach the instructed criterion levels. In addition, participants are given negative verbal feedback by the main investigator (me) after each 6 min session, telling them that they need to improve their performance to reach minimum performance requirements. The second round of feedback involved my supervisor (Prof. Harrison) providing additional negative feedback and discussing the participant's (poor) performance with me.

The stressor MIST consists of three 6-minute sessions, alternated with negative verbal feedback. Each session consists of two 1-minute control problems ('response not recorded'), alternated with two 2-minute stress problems ('response recorded') (control, stress, control, stress). Participants in the control condition also do three 6-minute sessions, but stay in the non-stressful condition without switching to the experimental stress condition (therefore no performance indicators are shown, nor is there a time limit enforced and all trials display 'response not recorded') and don't experience any negative feedback in between runs, but are given a short break of the same duration as the feedback in the stress condition.

In both conditions a rotary dial is shown on the screen which is used for submission of a response. Next to this rotary dial a text field is shown that provides feedback on the submitted

response ('correct', 'incorrect', 'not recorded', 'recorded'). Appendix I shows complete script and MIST examples.

3.2.3.2 *N-back*

The same N-back task was used as described in Chapter 2. The task commenced within 1-2 minutes of completing the MIST, with a blood pressure reading and VAS rating taken in between.

3.2.4 *Measurements of stress response*

Blood pressure, heart rate and skin conductance were measured as autonomic measures of stress. An increase of salivary cortisol was used as the primary measure of HPA axis stress.

A range of psychological and physiological stress measures were taken throughout the experiment, as shown in **Figure 3.1.**The first three time points (T1-3) were at 20 minute intervals in the hour prior to MIST exposure; T4 occurred during the second feedback period of the MIST (in which the investigator told the subject that the professor had to be contacted); T5 corresponded to the end of the MIST; T6 was taken at the end of the N-back, and T7-T9 followed at 20 minute intervals over the subsequent hour.

Salivary cortisol, blood pressure, heart rate, and skin conductance were determined as in Chapter 2. Subjective reports of alertness, drowsiness, stress, happiness, sadness, anxiety and nausea were assessed using VASs at all time points.

From the heart rate data HRV was calculated over six 6-minute periods (before MIST, MIST1, MIST2, MIST3, during N-back and after N-back). I present RMSSD, in the time domain (as an index of short-range HRV), and LF-HF-ratio in the frequency domain (which may reflect sympathetic modulations) as the main outcome measures (Camm et al., 1996).

3.2.5 *Analyses*

Analyses were carried out using SPSS for Windows (Version 22, IBM SPSS Statistics). Data were expressed and analysed as a percentage of baseline, except for subjective Stress ratings (since some participants endorsed zero values at baseline precluding normalisation in this manner). 'Baseline' was defined as measurement T3, as cortisol levels were expected to decline over the course of the study period, as the result of circadian variation and acclimatisation to the laboratory setting. Significance was set at $\alpha = .05$.

3.2.5.1 *Main analyses*

Since the autonomic stress response is brief, we pre-specified T4 (i.e. during the MIST) as our primary time point of interest for blood pressure, pulse, and subjective ratings of stress and anxiety. Similarly, skin conductance and heart rate and variability measures focussed on the period during the MIST scenario as the main time interval of interest. In contrast, cortisol levels rise more slowly after stress, peaking after 20 minutes (Kudielka et al., 2009). Thus, we defined T6, which occurred approximately 20 minutes after the MIST, as our primary time point of interest for cortisol levels. Values at these pre-determined time points were compared between conditions (control vs. stress) using t-tests or Mann-Whitney U tests as appropriate.

AUC_G and AUC_I measures for cortisol were calculated as described by (Pruessner et al., 2003) (See **Figure 3.2).** According to (Pruessner et al., 2003) these variables relate differently to psychological stress variables. AUC_G and AUC_I measures were calculated based on the individual's unique timings, rather than the mean intervals.

N-back data were analysed as in Chapter 2 (using repeated-measures ANOVA, with level (0-3 back) and block (0-6) as a within-subjects factors, and group (stress or control) as the between-subjects factor).

3.2.5.2 *Exploratory analyses*

The effects of the MIST on the psychological and physiological measures were explored using repeated-measures ANOVA with time as the within-subjects factor, and group as the between-subjects factor. Raw data (rather than % baseline) and all time points (including the 3 baseline measures) were used for these analyses; VAS, cortisol, skin conductance and HRV measures were log-transformed as they were non-normally distributed. Huynh-Feldt correction was applied where data failed Mauchly's Test of Sphericity. Planned post-hoc comparisons (defined as time points in main analyses) were explored regardless of overall significance. Moreover, MIST responders and non-responders were defined as by (Pruessner et al., 2008). Because of significant heterogeneity in the cortisol responses, participants who showed signs of cortisol increase over the course of the nine samples were differentiated from participants who showed a decrease in cortisol levels over the nine samples (AUC_I -cortisol). Since the circadian rhythm of cortisol normally results in declining levels during the course of the day, each subject that showed signs of cortisol decrease over the course of the experiment was labelled a non-responder, and participants with increases were labelled responder.

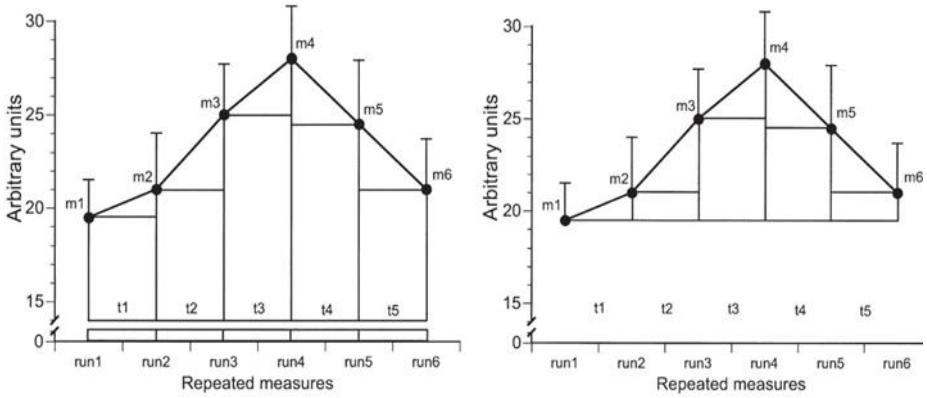


Figure 3.2 - Explanation of AUC_G and AUC_I.

Time course of an artificial dataset with six measurements; the triangles and rectangles illustrate the composition of the area under the curve. m_1 to m_6 denote the single measurements, and t_1 to t_5 denote the time interval between the measurements. Individual time intervals varied in our study and are not identical as in this example.

3.2.5.3 *Correlations*

Correlational analyses (Spearman's rho, given the non-normal nature of many of the variables) were conducted to investigate the relationships between physiological and psychological variables, N-back performance, and personality characteristics. To limit the number of correlations examined, we focussed on the predetermined time points and measures included in the main analyses, with the additional of baseline (T3) VAS stress and anxiety scores, Rotter's Locus of Control and Rosenberg's Self-Esteem measures, and N-back % correct scores for each level.

3.3 Results

3.3.1 *Participants*

Participant demographics are given in **Table 3.2.** All participants completed the study. The control and stress groups were well-matched in terms of demographics, including verbal IQ (as measured by the NART) and personality traits measures. Due to technical difficulties, one participant (in the stress group) had missing blood pressure and pulse data for the time point during the MIST, two (both stress group) had missing ECG data, one (stress group) had missing skin conductance data. One participant (in the control group) did not complete the N-back.

Table 3.2 - Demographic and personality measures.

	MIST Control	MIST Stress
Number	12	12
Ethnicity[a]	9C, 1I, 1P, 1A	10C, 2Ch
Age (years)	25.2 ± 1.0	25.6 ± 1.2
English first language?	4 No 8 Yes	4 No 8 Yes
NART	113 ± 1.2	108 ± 2.6
Locus of Control	73.6 ± 4.1	75.8 ± 2.1
Self-esteem	32.8 ± 1.2	33.5 ± 1.4
Years in education	18.3 ± 0.8	17.1 ± 0.9
Level of math education[b]	2G, 4A, 6D	4G, 4A, 4D

Values are mean ± SEM. NART, National Adult Reading Test; Locus of control, Rotter's Locus of Control Scale; Self-esteem, Rosenberg's Self-esteem Scale; Years in education from age 6. [a]C, Caucasian; Ch, Chinese; I, Indian; P, Pakistani; A, African Caribbean. [b]G, GCSE; A, A-levels; D, Degree.

3.3.2 *Analyses*

3.3.2.1 *Main analyses*

As shown in **Table 3.3** compared to the control, participants exposed to the stress MIST scenario reported greater stress and anxiety. There was an increase in salivary cortisol, systolic blood pressure, heart rate and changes in heart rate variability. Diastolic blood pressure and skin conductance only reached trend-significance. There were no group differences in any of these measures at baseline (p's>0.064) besides diastolic blood pressure (p=0.046).

Both area under the curve (AUC) measures (AUC_G (t_{13}=-3.2; p=0.007) and AUG_I (t_{22}=-3.41; p=0.002)) differed between conditions, with the stressor group having a greater cortisol response than the control group **Figure 3.3**).

Table 3.3 - Effects of acute stress exposure by the MIST on physiological and psychological stress measures

	Control (n; mean ± SEM)	Stress (n; mean ± SEM)	Statistical test
VAS 'Stressed'	12; 1.6 ± 0.3	12; 4.0 ± 0.8	U=34; p=0.028
VAS 'Anxious'	12; 1.1 ± 0.4	12; 2.9 ± 0.7	U=33; p=0.022
Cortisol (% baseline)	12; 91.1 ± 11.2	12; 191.8 ± 37.3	U=28; p=0.011
AUC_G cortisol (% baseline)	12; 161.0 ± 13.0	12; 301.2 ± 41.4	t=-3.2; p=0.007
AUC_I cortisol (% baseline)	12; 100.5 ± 12.1	12; 214.2 ± 39.0	U=29; p=0.013
Systolic BP (%baseline)	12; 100.5 ± 1.7	11; 108.9 ± 3.0	t=-2.4; p=0.024
Diastolic BP (%baseline)	12; 104.6 ± 2.2	11; 114.3 ± 5.0	U=32; p=0.085
Pulse blood pressure (%baseline)	12; 100.5 ± 2.2	11; 112.4 ± 7.0	U=35; p=0.056
Pulse ECG (%baseline)	12; 97.9 ± 0.9	10; 120.1 ± 10.4	U=22; p=0.012
Skin conductance (%baseline)	12; 91.6 ± 4.3	11; 110.6 ± 8.3	t=-3.0; p=0.010
HRV: RMSSD (%baseline)	12; 127.4 ± 22.2	9; 64.2 ± 13.1	U=22; p=0.023
HRV: LF-HF ratio (%baseline)	12; 114.7 ± 20.2	9; 174.1 ± 71.9	U=52; p=0.887

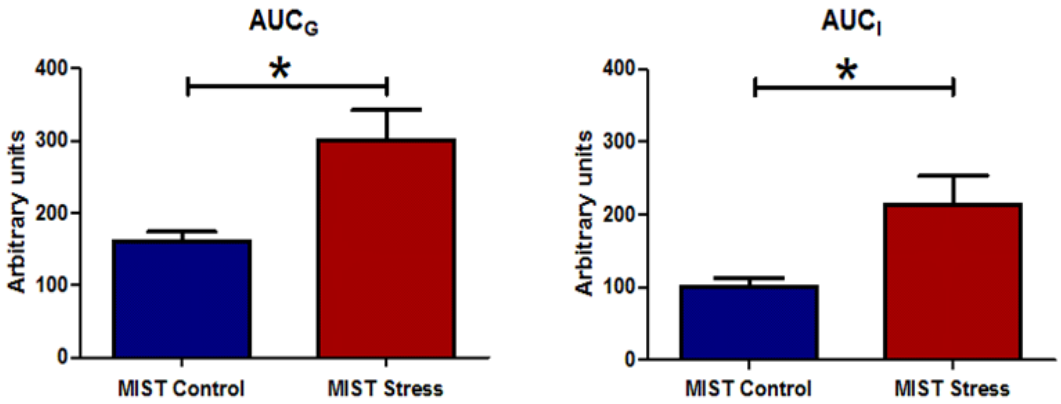


Figure 3.3 - Area under the curve cortisol data.

Both AUC_G (t_{22}=-3.2; p=0.007) and AUG_I (U=29; p=0.013) differ between conditions, with the experimental group having a higher stress response than the control group. Results are expressed as mean±SEM. *p<0.05.

N-back performance

In contrast to the physiological and psychological measures, there was no group difference in N-back performance. Thus, whilst there were main effects of level for the % correct trials ($F_{3,63}$=38.7; p<0.001) reflected by all participants performing worse on higher N-backs (p's<0.001), there was no effect of level on reaction time ($F_{3,63}$=0.26; p=0.851) and no main or interactive effects of group on either measure (F's<3.3; p's>0.57). There were no main or interactive effects for reaction time (F's<1.4; p's>0.26). See **Table 3.4** (overall results), Figure 3.4 (%-correct) and Figure 3.5 (reaction times).

Table 3.4 - Effects of acute stress exposure by the MIST on N-back performance

	MIST Control (Mean ± SEM)	MIST Stress (Mean ± SEM)
0 back % correct	95.5 ± 0.6	96.6 ± 1.0
1 back % correct	81.5 ± 4.5	86.4 ± 5.0
2 back % correct	69.2 ± 6.5	68.5 ± 9.3
3 back % correct	56.3 ± 6.4	54.9 ± 7.2
0 back reaction time (msec)	558.9 ± 37.8	563.7 ± 26.4
1 back reaction time (msec)	568.7 ± 58.9	578.1 ± 53.8
2 back reaction time (msec)	567.9 ± 52.8	578.1 ± 48.1
3 back reaction time (msec)	594.8 ± 55.9	583.9 ± 61.6
% - correct		
Main effect of level	$F_{3,63}$=38.7; p<0.001 Participants performed worse on higher load N-back stages (p's<0.001)	
No main effect of group	$F_{1,21}$=0.022; p=0.884	
No interaction of level * group	$F_{3,63}$=0.24; p=0.787	
Reaction time data	Reaction time calculated for correct trials only	
No main effect of level	$F_{3,63}$=0.26; p=0.851	
No main effect of group	$F_{1,21}$=0.03; p=0.956	
No interaction of level * group	$F_{3,63}$=0.047; p=0.986	

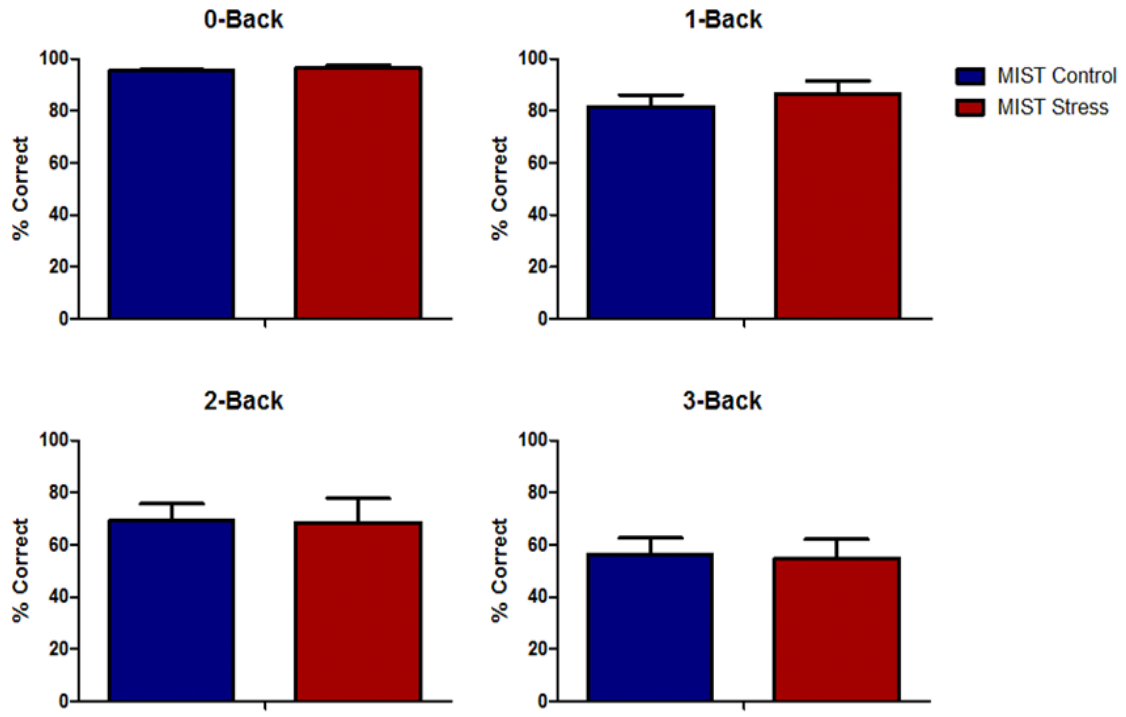


Figure 3.4 - Effects of acute stress exposure by the MIST on N-back performance (percentage correct).

(A) 0-back, (B) 1-back, (C) 2-back, (D) 3-back. There were no group differences in N-back performance (%-correct) for any of the levels (F's<1.23; p's>0.28). Results are expressed as mean±SEM.

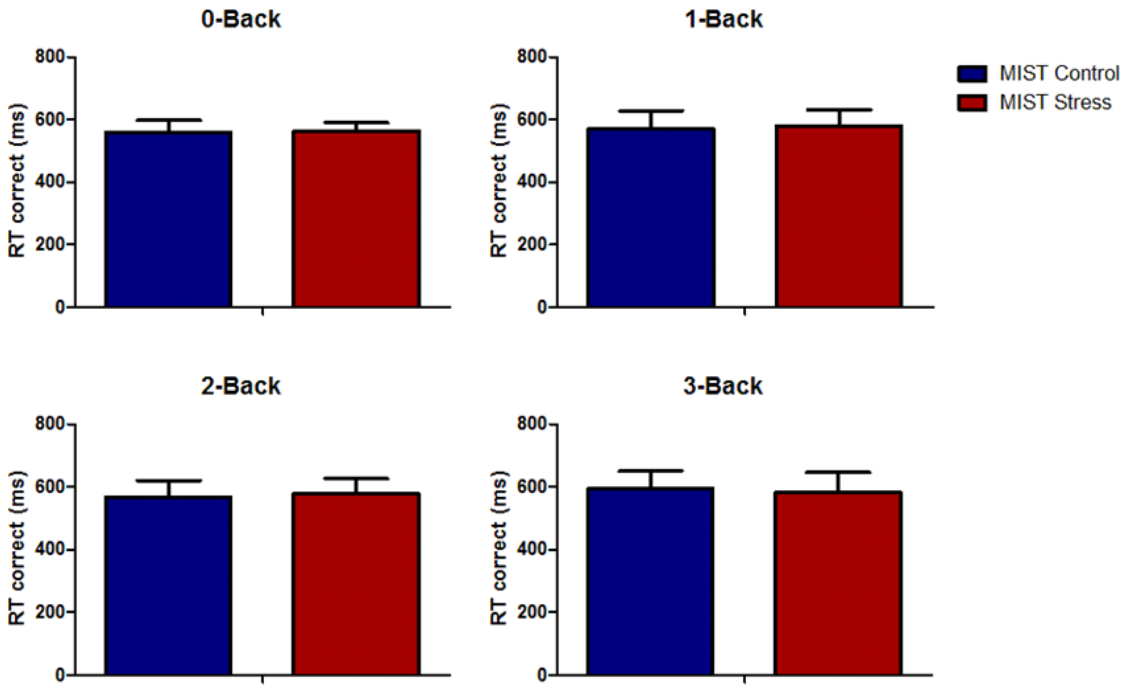


Figure 3.5 - Effects of acute stress exposure by the MIST on N-back performance (reaction times).

(A) 0-back, (B) 1-back, (C) 2-back, (D) 3-back. There were no group differences on N-back reaction times for any of the levels (F's<1.41; p's>0.176). Results are expressed as mean±SEM.

3.3.2.2 *Exploratory analyses*

Physiological measures of stress

Statistical results for the exploratory analyses are presented in **Table 3.5.**

In the control group, cortisol levels showed the predicted diurnal decrease over the course of the experiment; in contrast, cortisol levels increased in the stress group (**Figure 3.6a**). These numerical changes did not reach statistical significance in the full cohort, but did when only the responders were considered (**Table 3.5; Figure 3.6b).**

Blood pressure (systolic and diastolic – **Figure 3.6c+e**), pulse rate (via blood pressure (**Figure 3.6d** and ECG **Figure 3.6a**) and skin conductance (**Figure 3.6b**) increased during the stressor version of the MIST, reflected in main effects of group and/or time by group interactions in each case (**Table 3.5**). In contrast, there were no main or interactive effects involving group for either measure of heart rate variability (**Table 3.5; Figure 3.6c+d**).

Table 3.5 - Exploratory analyses - effects of acute stress by the MIST on physiological and psychological stress measures.

	Main effect of time	**Main effect of group**	**Interaction**	**Post-hoc**
VAS 'Stressed'	$F_{8,168}$=15.3; p<0.001	$F_{1,21}$=0.70; p=0.414	$F_{8,168}$=1.6; p=0.186	T4: p=0.020 T5: p=0.029
VAS 'Anxious'	$F_{8,176}$=12.0; p<0.001	$F_{1,22}$=0.70; p=0.447	$F_{8,176}$=3.7; p=0.003	T4: p=0.024 T5: p=0.003
Cortisol	$F_{8,176}$=2.0; p=0.115	$F_{1,22}$=0.08; p=0.778	$F_{8,176}$=1.8; p=0.154	-
Cortisol responders only	$F_{8,160}$=3.8; p=0.002	$F_{1,20}$=1.4; p=0.247	$F_{8,160}$=6.0; p<0.001	T6: p=0.035 T7: p=0.090 T8: p=0.042
Systolic BP	$F_{8,160}$=2.4; p=0.019	$F_{1,20}$=6.0; p=0.024	$F_{8,160}$=2.0; p=0.051	T4: p=0.008 T5: p=0.006 T7: p=0.040
Diastolic BP	$F_{8,160}$=7.0; p<0.001	$F_{1,20}$=5.0; p=0.036	$F_{8,160}$=2.9; p=0.004	T4: p=0.002 T5: p=0.010 T6: p=0.037 T7: p=0.046
Pulse BP	$F_{8,152}$=9.1; p<0.001	$F_{1,19}$=0.90; p=0.356	$F_{8,152}$=1.9; p=0.122	-
Pulse ECG	$F_{8,152}$=12.5; p<0.001	$F_{1,19}$=0.77; p=0.392	$F_{8,152}$=4.1; p=0.029	T4.5: p=0.059
Skin conductance	$F_{8,168}$=11.1; p<0.001	$F_{1,21}$=0.31; p=0.586	$F_{8,168}$=4.2; p=0.017	-
HRV: RMSSD	$F_{5,95}$=4.0; p=0.002	$F_{1,21}$=2.8; p=0.113	$F_{5,95}$=1.8; p=0.125	T4.5: p=0.018
HRV: LF-HF ratio	$F_{5,95}$=0.81; p=0.543	$F_{1,21}$=3.2; p=0.089	$F_{5,95}$=0.54; p=0.746	-

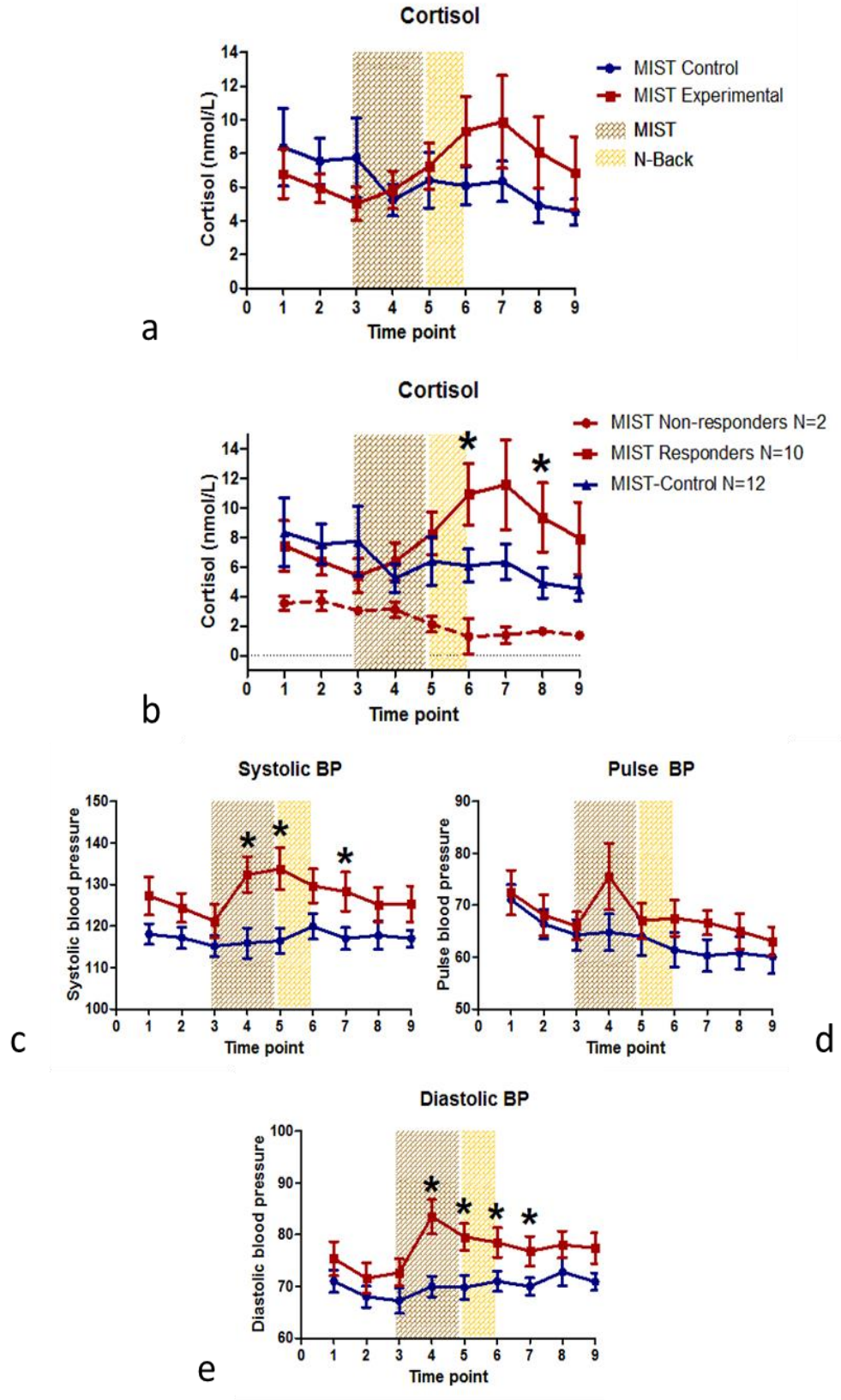


Figure 3.6 - Effects of acute stress exposure by the MIST on physiological stress measures – part 1.

Changes in (a) cortisol, (b) cortisol-responders, (c) systolic blood pressure, (d) pulse via blood pressure machine and (e) diastolic blood pressure measures over the course of the experiment in those randomised to the control (blue triangles and solid lines) and stress (red squares and solid lines) MIST. Results are expressed as mean±SEM. *p<0.05.

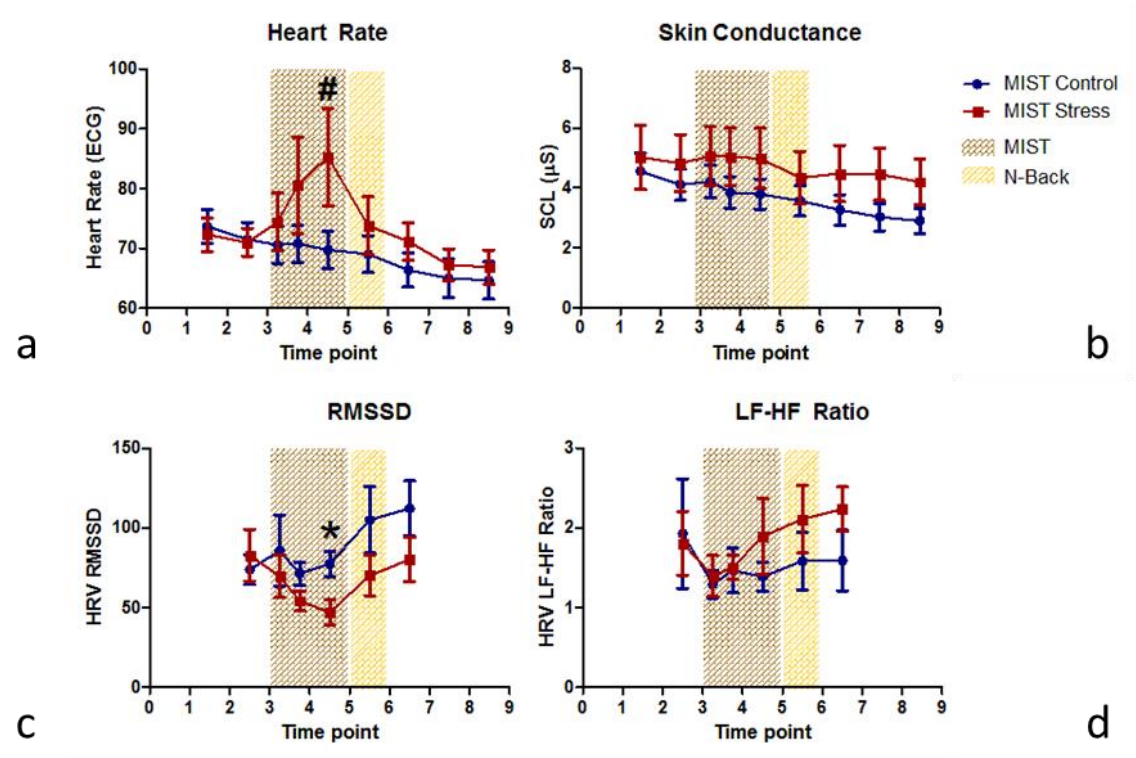


Figure 3.7 - Effects of acute stress exposure by the MIST on physiological stress measures – part 2.

Changes in (a) heart rate as measured by ECG, (b) skin conductance, heart rate variability RMSSD (c) LF-HF ratio (d), measured over the course of the experiment in those randomised to the control (blue triangles and solid lines) and stress (red squares and solid lines) MIST. Results are expressed as mean±SEM. *p<0.05 between groups, #p<0.06.

Subjective measures of stress

Although there was a main effect of time on 'Stressed' ratings ($F_{8,168}$=15.304, p<0.001), there were no main or interactive effects of group (Fs<1.6, p's>0.18). However planned LSD post-hoc comparisons showed significant group differences during (p=0.020) and immediately after the MIST (0.029) **(Figure 3.8a)**. In contrast, 'Anxious' ratings were selectively increased in the stress group following MIST exposure, reflected in a time by group interaction ($F_{8,176}$=3.7; p=0.03) that resulted from a group difference at T4 and T5 (during- and post-MIST; p=0.024 and p=0.03) but not at other time points **(Figure 3.8b**). There was also a main effect of time ($F_{8,176}$=112.0, p<0.001) but no main effect of group ($F_{1,22}$=0.60, p=0.447).

As presented in **Figure 3.8**, five other psychological ratings showed evidence of change over time, namely 'Nausea', 'Alert', 'Drowsiness', 'Sadness' and 'Happiness': there were main effects of time for 'Nausea', 'Alert' and 'Happiness' (F's>2.2; p's<0.047) but no main or interactive effects of condition (F's<1.4; p's>0.243). Both 'Drowsiness' and 'Sadness' ratings had trend interaction effects (F's>2.4; p's>0.052) but no main effects of time or group (F's<0.9; p's>0.110).

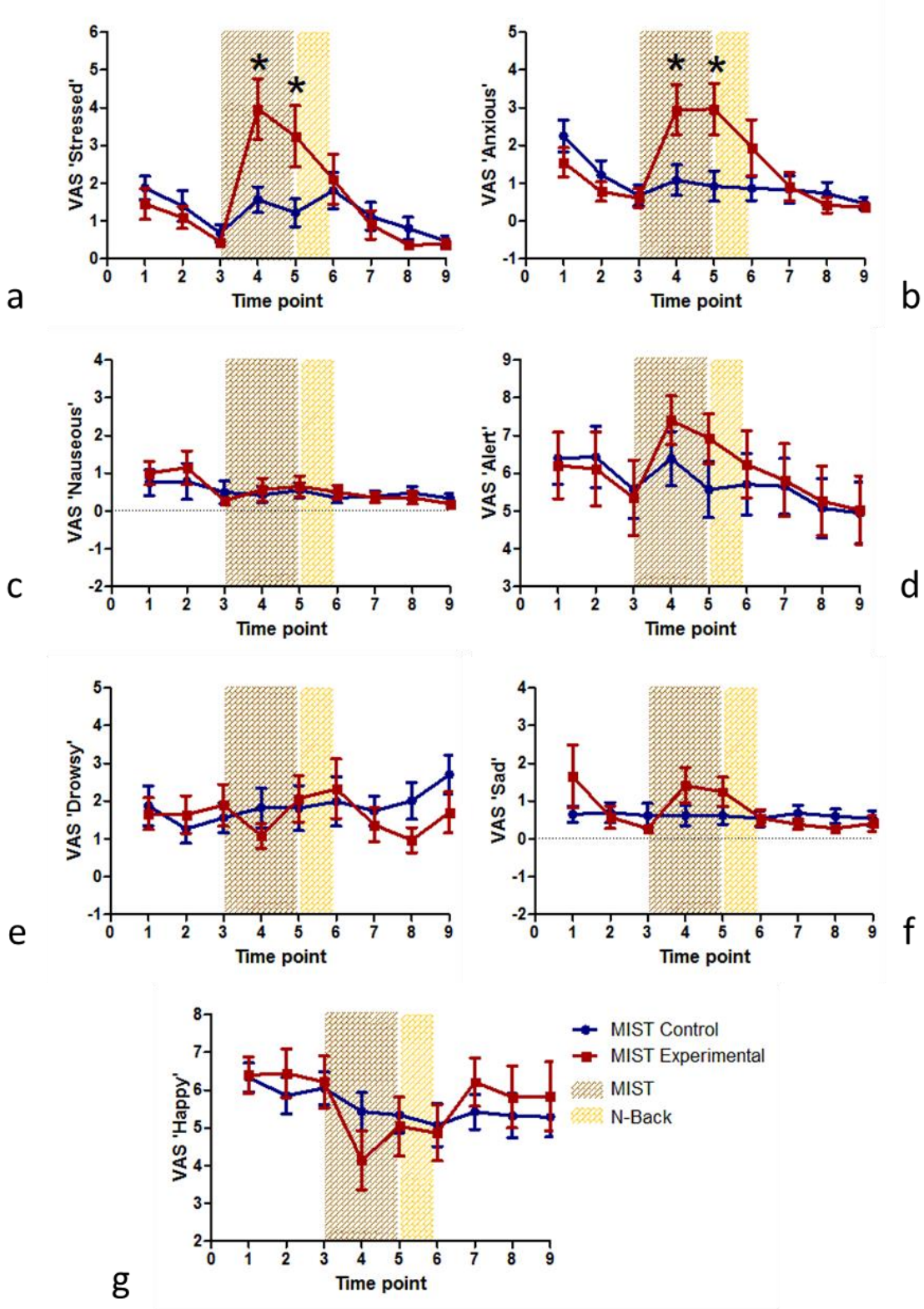


Figure 3.8 - Effects of acute stress exposure by the MIST on psychological stress measures.

Changes in VAS ratings of (a) 'Stressed, (b) 'Anxious, (c) 'Nauseous', (d) 'Alert', (e) 'Drowsy', (f) 'Sad') and (g) 'Happy' over the course of the experiment in those randomised to the control blue lines) and stress (red lines) MIST. Results are expressed as mean±SEM. *$p<0.05$ compared to baseline.

Correlations

Correlations between different variables are shown in **Table 3.6.** Whilst there were correlations between different aspects of a given measure (e.g. between %baseline cortisol and the AUC measures) there was little evidence of correlations between different components of the stress response. Notably, there were no correlations between subjective stress ratings (obtained during the MIST) and any of the concurrently-measured physiological variables (p's>0.14). These did exist for subjective anxiety ratings and cortisol ratings (%baseline cortisol6: rho=0.43, p=0.036, %baseline AUCi: rho=0.43, p=0.037). Moreover, cortisol levels also correlated with heart rate as measured by ECG (rho=0.63, p=0.002). Note, these correlations would not survive Bonferroni correction for multiple comparisons.

Most interestingly, there was a significant correlation between 1- and 2-back performance (%correct) and cortisol values (both %baseline cortisol on time point 6 and %baseline AUCi) across the whole cohort (1-back: rho= .48; p=.020; rho= .47; p=.023; 2back: rho= .59; p=.003; rho= .55; p=.007) which is presented in **Figure 3.9.**

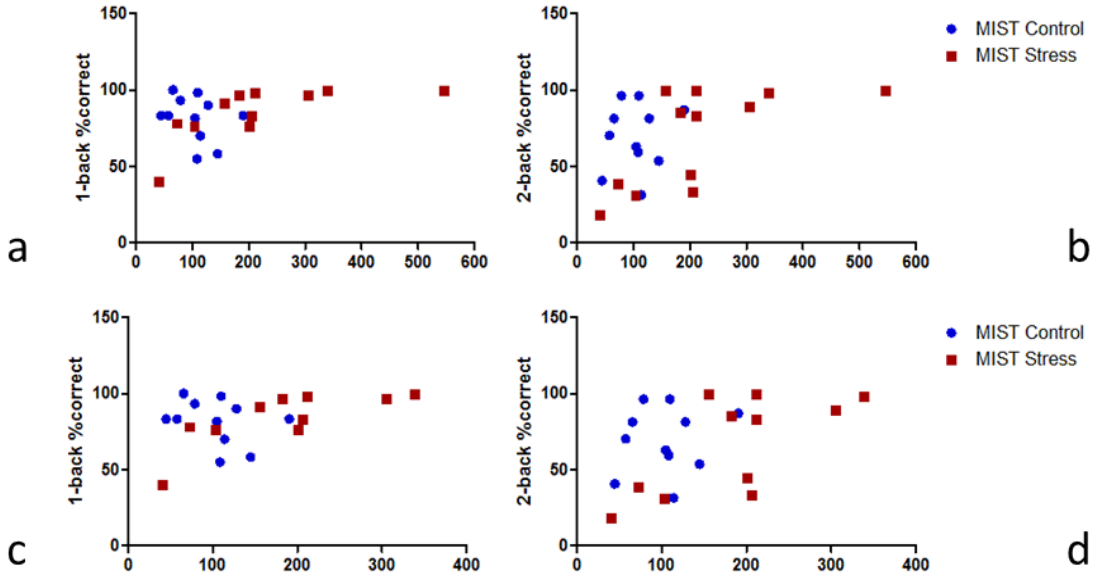


Figure 3.9 - Correlation between N-back performance and cortisol change.

Relationship between 1-back and 2-back performance (%-correct) and cortisol change (%baseline AUC_I). There was a significant correlation between 1-back (rho = 0.47; p=0.023) and 2-back performance and cortisol change across the whole cohort (rho = 0.55; p=0.007).
Correlation between 1-back (%-correct) and cortisol change (%baseline AUC_I) trend significant when removing highest value (rho=0.41, p=0.60). Still significant for 2-back (rho = 0.49; p=0.021).

Table 3.6 - Correlations between different measures of the stress response as induced by the MIST and N-back performance

		Self esteem	Locus of control	Baseline VAS 'Stressed' Time point 3	Baseline VAS 'Anxious' Time point 3	During MIST VAS 'Stressed' Time point 4	During MIST VAS 'Anxious' Time point 4	Cortisol (% baseline) Time point 6	AUCi cortisol (% baseline)	Systolic BP (% baseline) Time point 4	Diastolic BP (% baseline Time point 4	Pulse BP (% baseline Time point 4	SC (% baseline) Time point 4	HR (% baseline) Time point 4	HRV (RMSSD % baseline)	HRV (LF-HF ratio % baseline)	0 back (% correct)	1 back (% correct)	2 back (% correct)	3 back (% correct)
Self esteem	Spearman's rho	1.000	.046	-.165	-.333	-.285	-.172	.097	.064	.163	.236	.155	-.232	.045	-.071	.032	-.286	.187	.186	.140
	p value		.836	.452	.120	.187	.434	.661	.772	.468	.289	.492	.298	.847	.766	.892	.196	.406	.408	.534
Locus of control	Spearman's rho		1.000	.402	.302	.444	.393	-.133	-.043	-.068	.275	.175	-.008	.005	-.089	.076	.146	-.066	-.010	.099
	p value			.051	.151	.030	.058	.535	.843	.759	.204	.424	.971	.984	.703	.743	.505	.764	.963	.652
Baseline VAS 'Stressed' Time point 3	Spearman's rho			1.000	.697	.390	.311	-.171	-.009	-.327	.087	.297	-.004	.092	-.122	.455	-.158	-.115	-.246	-.055
	p value				.000	.059	.139	.425	.968	.127	.693	.169	.984	.683	.597	.038	.471	.602	.257	.805
Baseline VAS 'Anxious' Time point 3	Spearman's rho				1.000	.284	.398	-.183	-.121	-.180	-.015	.073	.016	.138	-.024	.392	-.257	-.177	-.313	-.172
	p value					.179	.054	.393	.574	.411	.944	.740	.942	.539	.917	.079	.237	.420	.147	.434
During MIST VAS 'Stressed' Time point 4	Spearman's rho					1.000	.753	.136	.165	-.106	.259	.276	.228	.327	-.311	.068	.268	.013	.012	.143
	p value						.000	.525	.440	.631	.234	.202	.295	.138	.169	.769	.217	.953	.958	.516
During MIST VAS 'Anxious Time point 4	Spearman's rho						1.000	.429	.428	-.056	.366	.398	.222	.517	-.381	.285	.233	.242	.345	.352
	p value							.036	.037	.798	.086	.060	.309	.014	.088	.211	.285	.266	.107	.099
Cortisol (% baseline) Time point 6	Spearman's rho							1.000	.958	.371	.184	.364	.158	.632	-.160	.017	.141	.481	.589	.290
	p value								.000	.082	.400	.088	.471	.002	.489	.942	.522	.020	.003	.180
AUCi cortisol (% baseline)	Spearman's rho								1.000	.331	.173	.364	.133	.614	-.222	.075	.140	.472	.548	.256
	p value									.123	.430	.088	.544	.002	.333	.746	.525	.023	.007	.239
Systolic BP (% baseline)	Spearman's rho									1.000	.521	.370	.185	.609	-.302	-.340	.062	.224	.002	.011
	p value										.011	.083	.411	.003	.195	.143	.783	.316	.994	.962
Diastolic BP (% baseline)	Spearman's rho										1.000	.672	.241	.387	-.457	.009	.042	.060	-.056	.031
	p value											.000	.280	.083	.043	.970	.854	.792	.804	.892
Pulse BP (% baseline)	Spearman's rho											1.000	.085	.495	-.272	.135	.058	.311	.114	.177
	p value												.706	.023	.246	.569	.797	.159	.614	.431

| | | |

3.4 Discussion

This study has two main findings. First, and most importantly, administration of the stress MIST led to robust increases in both physiological and subjective stress measures, compared to its control, consistent with its use as a laboratory-based stressor. Salivary-cortisol levels were increased to 150-200% of baseline in the stress vs. control group between 20 and 80 minutes after commencing the MIST. Blood pressure was elevated only transiently during the MIST in the stress vs. control group, to around 110% baseline. Heart rate, measured both by blood pressure pulse and ECG, also increased during the stress MIST only, to about 120% baseline. Skin conductance level in the stress group remained elevated compared to the control group over the whole task-period, with a maximum magnitude of about 110%. Subjective stress increased 2 to 4-fold during and immediately after the MIST in the stress MIST condition.

The stress responses I observed are similar in magnitude to other studies using the MIST (Dedovic et al., 2005) plus **Table 3.1**). According to (Dedovic et al., 2009b), the robust stress response induced by the MIST is driven by about 50% of the participants, reflecting an inter-individual variability in reacting to a given stress stimulus. Our data shows a higher response rate, with only 2 non-responders (non-responder defined as no clear cortisol increase (<5%) after the MIST) out of a total of 12 participants in the stressor condition. Interestingly, even though both physiological and subjective measures of stress increased significantly, there were no correlations between these variables. Thus, the MIST is suitable for use as the stressor in the imaging study of this DPhil project, which will further investigate the implications of these preliminary findings.

It should be noted that the largest study to date (126 males, 113 females; age 19.44 ± 0.07 years; range = 17–22 years) by Orem et al., (2019) (See Table 3.6) did not find a significant cortisol increase due to the MIST. However, the authors only reported the comparison of baseline cortisol levels with cortisol levels at the conclusion of the stress scan and so failed to take the delay in cortisol rise into account. In addition, stress tasks were performed both during both the morning and the afternoon, potentially adding further noise to the data (although the authors argue that including the time of day of sample collection did not alter the pattern of results). The authors speculated that the decrease in cortisol levels after the stress MIST could also be due to elevated baseline cortisol levels in anticipation of the fMRI scan.

Differences in MIST procedure between the Orem et al., (2019) study and mine (and that of Dodovic et al., 2005) might also explain the differences in cortisol response. Orem et al., (2019) compared a single eight-minute MRI scan session of control MIST with a single eight-minute MRI scan session of stress MIST. Prior to these scans, participants completed practice problems outside of the scanner and the investigators attempted to lower participant stress levels by telling them "It is OK if you do not answer all of the math problems correctly". In contrast, the investigators attempted to elevate stress levels prior to the stress scan by telling participants they must answer the questions correctly, and warning that if they did not perform as well as others in the study their data would not be used. Furthermore, during the Stress scan, the participants were given previously recorded negative auditory feedback. Failure was ensured by modulating the time in which the participant could respond in a stair-step manner such that on average participants answered approximately 50% of the problems correctly (compared to the 20-45% range in our procedure).

The MIST procedure used in our hands lasted longer (approximately 25 minutes) with additional moments of negative feedback. That Orem et al., (2019) did not find a significant cortisol response due to the MIST could therefore be due to differences in protocol. However, it is also possible that the MIST is not as robust a stressor as previously described. The conflicting findings therefore emphasise the importance of the pilot study described in this Chapter.

3.4.1 *Limitations of the MIST*

In the version of the MIST used in this study (and as in Chapter 7), control and stress blocks are not completely separable as it is likely that the stress induced during the stress block will "leak over" into the second control block. Moreover, the negative social evaluative threat induced during the feedback moments between runs might also influence the control blocks of the second and third run of the MIST. Therefore control blocks are not completely free from stress. In addition, cognitive load is different between control and stress blocks as the control questions are easier. These limitations should be taken into account when the MIST is used to study the effects of stress on brain activity (Chapter 7).

Secondary to the main results, the stress induced by the MIST did not influence working memory performance as N-back performance did not differ between stressed and control groups. However, interestingly, across all participants, the magnitude of the stress response, as indexed by cortisol, was correlated with 2-back performance, indicating that acute, mild stress (irrespective of the source – in this case MIST or N-back) might improve working memory performance. In contrast,

other studies using different laboratory stressors, like the TSST, show working memory impairments as a result of the stressor (Buckert et al., 2012; Schoofs et al., 2008). However, there is substantial evidence that stress, enhanced glucocorticoid levels and/or elevated sympathetic nervous system can have complex influences on memory performance, with both negative and positive effects observed in both humans and animals. This relationship seems to depend on the nature of the stressor and the memory process studied (Luethi et al., 2009; Sandi and Pinelo-Nava, 2007; Schoofs et al., 2008; Schwabe et al., 2010), as well as important effects of, for example, gender (Zandara et al., 2016, Cornelisse et al., 2011) and the timing of the cognitive task relative to the stressor (Schwabe et al., 2012). To date, as far as we know, no other studies have been conducted using the MIST to influence working memory performance. The increased cortisol dependent stress response induced by the MIST is modest, compared to the widely used TSST, which induces 2- to 4-fold elevations of cortisol (Kirschbaum et al., 1993). This difference in response magnitude is generally ascribed to multiple factors, including difference in the nature of the task (mental arithmetic versus public speaking) (Dedovic et al., 2005). Adding a further layer of complexity to the relationship between stress, cortisol and memory, whilst some previous studies have shown associations between stress-related cortisol changes and working memory performance (Schoofs et al., 2008), others have observed stress-related changes in working memory in the absence of group differences in cortisol levels (Duncko et al., 2009). Thus, although my findings suggest that mild stress does not affect working memory performance in young, healthy men, further studies are required to clarify the relationships between stressor, stress response, and working memory.

As in the previous chapter, I show an absence of correlations between different measures of the stress response. As discussed before, there is a substantial literature arguing against the 'stress response' as a unitary construct, and weak or absent correlations between physiological and psychological measures of the stress response is a common finding both in experimental and naturalistic settings (Dickerson and Kemeny, 2004; Mauss et al 2005; Campbell and Ehlert, 2012). My findings emphasise the value of examining multiple variables to establish a full picture, not least since different components of the stress response may impact differentially on outcomes of interest.

3.4.2 *Conclusion*

In conclusion, the MIST is suitable for use as the stressor in the imaging study of this DPhil project, as it induced robust and lasting changes in cortisol levels, providing an adequate testing window for the main fMRI study (see Chapter 6 and 7).

Chapter 4 Overall methods for imaging study

4.1 Introduction

The main study of this thesis was a randomised, double-blind, placebo-controlled, between-subjects study of the effects of COMT inhibition and genotype on cognitive function and brain activation under conditions of acute stress. The study was conducted in the 3T MRI scanner to allow brain perfusion (ASL), brain anatomy (structural MRI), and brain activity (both at rest with resting state fMRI, and during task-related fMRI) to be measured alongside behavioural performance. Methods that apply to all following chapters will be presented here. Methods that apply to each specific chapter only will be presented separately.

4.2 Methods

4.2.1 *Participants*

Ethical approval was granted by the Central University Research Ethics Committee (CUREC) of the University of Oxford (MSD-IDREC: R26521/RE006).

Non-smoking, healthy men, aged 18 to 40 years old were recruited by advertisement. Participants were genotyped for the Val^{158}Met polymorphism (see below). All potential participants (COMT Val^{158}Met homozygotes) underwent initial telephone screening to establish inclusion and exclusion criteria. Mental health was assessed using the Structured Clinical Interview for DSM-IV. Exclusion criteria included: current or past history of psychiatric or neurological disorder; use of psychotropic medication or medication that might affect the stress response (e.g. corticosteroids, beta-blockers); a history of heart disease or hypertension; current or past liver disease, or other significant current medical illness, alcohol intake greater than 30 units/week; smoker, currently or within past three months; illicit drug use in the last three months; MRI safety concerns or an inadequate command of spoken English. GPs were asked to check the participant's medical records to provide confirmation that they did not meet any of the exclusion criteria and that there were no medical reasons why it would be unsafe for them to take part in the study.

4.2.1.1 *Rationale for exclusion criteria*

Cigarette smoking has strong effects on basal and stress responsive LHPA function (Kirschbaum et al., 1992; Steptoe and Ussher, 2006) and nicotine interacts with COMT genotype to affect performance on cognitive tasks (Ashare et al., 2013; Loughead et al., 2009).

Over-40s were excluded because of possible aging effects on the neuropsychological tasks, and reported age x COMT genotype interactions (Harrison and Tunbridge, 2008).

Women were excluded from this study for three reasons: [1] COMT's activity and effects differ markedly between males and females, and COMT is affected by menstrual cycle and oral contraceptive use (Chen et al., 2004; Harrison and Tunbridge, 2008), [2] Oestrogen has known effects on HPA axis function (Kajantie and Phillips, 2006; Kudielka and Kirschbaum, 2005), which therefore complicates interpretation of the results. [3] Ethical concerns related to the administration of the COMT inhibitor tolcapone to a woman in whom there is a risk of pregnancy.

From the initial 474 study packs that were sent out, a group of 345 males were genotyped, of whom 174 were homozygotes (which is the expected proportion given 50% of the Caucasian population is heterozygote for COMT (genotypes were in Hardy-Weinberg equilibrium). After screening these homozygotes, 76 of them were eligible and were randomised into the study to either placebo or tolcapone (by Professor Harrison). Therefore, both the participants and I were blind to both genotype and drug allocation. Unblinding only occurred when all analyses (including MRI) were completed. Tolcapone + placebo capsules looked identical and were prepared before the start of the study by two researchers not involved in the study.

4.2.1.2 *COMT genotyping*

In order to provide DNA samples, men interested in participating were sent buccal swab kits. The kits consisted of two 2ml Eppendorf tubes (Sarstedt, UK) each containing a buccal/cervical swab brush (Morton Medical LTD) and clear instructions explaining how to collect the buccal cell samples (see Appendix). Participants were asked to slowly and firmly brush the inner surface of their cheek from top to bottom with the swab 15 times. Following collection of the sample, participants were instructed to return the buccal brush directly to the Eppendorf tube. The two samples were then placed into a labelled bag and sent back to the Department of Psychiatry where, upon arrival, they were stored in a freezer at -20°C until DNA extraction.

ChargeSwitch®gDNA Buccal Cell Kits were used to isolate genomic DNA from the samples according to the manufacturer's instructions (Invitrogen, Waltham, USA) by research technician, Li Chen. The purified DNA sample was then returned to a freezer for storage at -20°C. DNA was genotyped for Val^{158}Met using the appropriate Taqman SNP Genotyping Assay (TaqMan assay I.D.: C_25746809-

50, Applied Biosystems, Carlsbad, California), in duplicate, by a researcher not involved in the study (Dr. Arne Mould) to maintain blind. Genotype calls agreed in all cases.

4.2.1.3 *Sample size*

No meaningful power calculation is possible since there are no prior studies assessing the interaction of stress, COMT genotype and tolcapone upon brain activity or the behavioural tests that we will use. That is, even though this study follows a similar design as our previous one (Farrell et al., 2012), the experimental conditions are different because of the use of the stressor in this study. In Farrell et al., (2012) a group size of 15 provided >95% power to find both main effects and interactions at alpha=0.05. We have therefore made a pragmatic decision to use the same sample size as in the earlier study; this is also comparable to many other experimental medicine studies of this kind. A sample size of 18 allows for some dropout, and for potentially smaller effect sizes.

4.2.2 *Procedure*

As tolcapone absorption by the body is affected by food (Jorga et al., 2000; Jorga, 1998) and to keep cortisol levels as stable across participants as possible, participants were asked to eat a good breakfast and not to eat any more after 10:15 nor have any caffeinated drinks after that time.

Participants attended the MRI testing facility at 12:00 o'clock and testing was finished before 16:00 o'clock. Upon arrival, they were reminded of the study details and their right to withdraw before asking them to reconfirm their consent. All participants knew they were taking part in a study that that could potentially stress them, but as part of MIST introduction were told they were in the control group and were therefore not going to be stressed but had to perform simple arithmetic in the MRI scanner to stay awake. For the complete script see appendix II.

The timeline for the study is presented **Figure 4.1**.Baseline measures of stress (saliva sample + subjective stress) were taken prior to tolcapone/placebo administration (200mg by mouth). Tolcapone has an elimination half-life of 2.0 ± .8 hours, and the dose given produces 70%-80% peripheral blood COMT inhibition between 1 and 4 hours (Ceravolo et al., 2002; Dingemanse et al., 1995; Jorga, 1998). Therefore, scanning began 90 min after swallowing the capsule and lasted for about two hours.

During the 90-minute baseline period, participants filled in several questionnaires: Rotter's Locus of Control scale, the Rosenberg self-esteem scale, the NART, along with the State-Trait Anxiety Inventory (STAI) (Spielberger et al. 1983). Locus of control and self-esteem were measured since both have been reported to affect the magnitude of the response to an experimental stressor

(Bollini et al., 2004, Pruessner et al., 1999). The STAI assesses state anxiety (STAI-S) and trait anxiety (STAI-T). STAI-S can be defined as a transitory condition associated with subjective feelings of apprehension or tension, generally accompanied by intensified activity of the autonomic nervous system. STAI-T on the other hand can be defined as the enduring tendency of an individual to respond to perceived threats in the environment with anxiety (Spielberger et al. 1983).

Before participants entered the scanner, they changed into scrubs to make sure that their clothing was completely metal free. A radiographer confirmed MRI safety. If participants wore glasses, they were asked for their prescription so that MRI-safe goggles could be prepared to wear inside the scanner.

Once participants were in the scanner the following scans and tasks were run in order presented:

1) an ASL scan

2) a resting state scan

3) a structural scan

4) fMRI: administration of the stressor MIST

5) fMRI: N-back task

6) where time permitted, fMRI: the faces components of the emotional test battery (ETB, P1vital). However, 8 participants did not complete this task and is therefore not included in the current thesis.

During the scan protocol an eye-tracker monitored whether the participant's eyes were open (blinking normally). Following completion of scanning participants changed back into their normal clothes and were fully debriefed as to the nature and purpose of the experiment (including the deception regarding the use of the MIST to induce a stress response). They were asked to guess whether they had received tolcapone or placebo. The duration from arrival at the imaging centre to departure was about 4 hours, including ~85 mins in the MRI scanner.

A schematic of the experimental procedure is shown in **Figure 4.1**. Physiological measures of stress, including salivary cortisol and sAA, together with subjective stress and mood ratings, were recorded at 30 minute intervals throughout the experiment. To give participants the saliva swab, I entered the scanner room to place the swab inside the participant's hand. They were then asked to place the swab under their tongue, without moving their head (I piloted this procedure prior to commencing the study to ensure that it did not result in significant motion artefacts). After two minutes I collected the swab wearing sterile gloves.

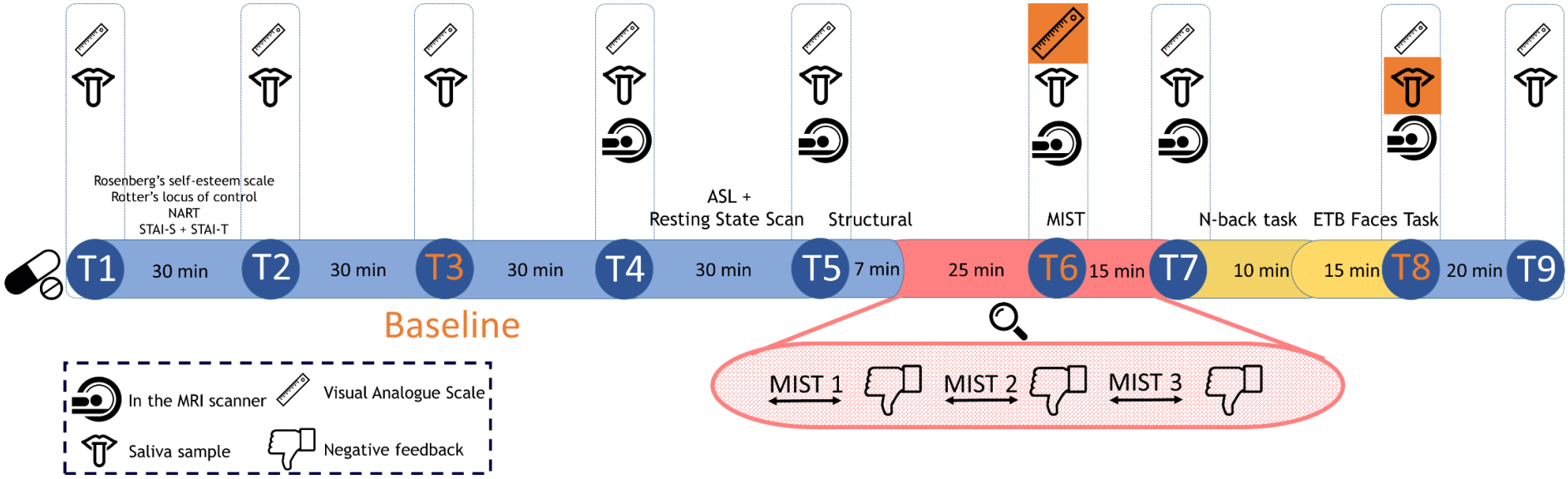


Figure 4.1 - Timeline of the imaging study.

VASs included ratings of alertness, drowsiness, stress, happiness, sadness, anxiety and nausea. Throughout the time the participant was in the scanner physiological measures of heart rate, skin conductance and breathing rate (all Biopac, Goleta, CA, US) were collected. VAS stress ratings were assessed via the scanner computer screen. This resulted in 9 data points over time (3 baseline-measures outside the scanner, 2 baseline measures inside the scanner, 3 taken during testing (during MIST, pre N-back and at the end of scanning), and 1 post-testing outside of the scanner after debriefing).

4.2.3 *Tasks*

The methods section of Chapter 7 describes the MRI scanner version of the MIST, and Chapter 8 describes the MRI scanner version of the N-back task.

4.2.4 *Behavioural / MRI analyses*

See each individual chapter for more details.

Chapter 5 The interaction between COMT genotype and COMT inhibition on cerebral blood flow and brain structure

5.1 Introduction

5.1.1 *Catecholamines and blood flow*

Blood flow to and from the brain is determined by multiple biomechanical, neurochemical, and physiological variables, and variations in cerebral blood flow (CBF) rate depend on blood viscosity, compliance of the blood vessels, structural remodelling of vascular beds as well as the levels and activity of multiple hormones and neurotransmitters that act as vasoconstrictors or vasodilators (Armulik et al., 2011; Hall et al., 2014; Henriksen et al., 2014; Iadecola, 2004; Nishijima et al., 2015; Raz et al., 2017).

Whilst catecholamines with α- or β-adrenergic agonist properties do not appear to significantly affect cerebral haemodynamics and metabolism, there is evidence that dopamine does have direct complex vasoactive effects on cerebral circulation (Azhan and Wong, 2012; Krimer et al., 1998; Ract et al., 2001; Tuor et al., 1986; Zeng et al., 2007). The question of whether dopamine contracts or relaxes blood vessels is not straightforward and depends on its location and concentration, and the presence of other neurotransmitters or receptor blockers (Cohen and Berkowitz, 1975; Edvinsson et al., 1978; Iadecola, 1998; Zeng et al., 2007). But dopaminergic axons have been shown to innervate the intraparenchymal micro vessels directly with vasoconstrictive responses in the cortical vasculature (Krimer et al., 1998).

5.1.2 *COMT and cerebral blood flow*

In Chapter 1 I outlined the evidence linking COMT Val^{158}Met with aspects of PFC activation and function (e.g. (Egan et al., 2001)). However, differences in dopamine availability between COMT-Val and Met homozygotes could result in differences in baseline perfusion, which could in turn explain differences in BOLD response.

COMT is expressed ubiquitously, including in the vasculature and could influence CBF via direct dopaminergic effects on vascular innervation. As described in Chapter 1, MB-COMT is the predominant allozyme in the brain (particularly in the PFC) and, in comparison to most other tissues, there is a markedly reduced proportion of S-COMT, which only accounts for 30% of cerebral

COMT protein (Bonifácio et al., 2007; Chen et al., 2004; Karhunen et al., 1994; Matsumoto et al., 2003; Tenhunen et al., 1994; Tenhunen and Ulmanen, 1993). In rats, COMT is expressed in perivascular astrocytes and capillary endothelia (Karhunen et al., 1995), as well as in the basilar artery tunica adventitia (Karhunen et al., 1994), and so is well-placed to contribute to the dopaminergic regulation of the cerebral microvasculature (Krimer et al., 1998). COMT's effects on CBF could also be more indirect, at a distance, whereby it only plays a role when high levels of dopamine are released.

Results of studies examining the effects of COMT Val-Met on blood pressure are mixed. Most show higher blood pressure in COMT-Met homozygotes, compared with COMT-Val carriers (Annerbrink et al., 2008; Htun et al., 2011; Kamide et al., 2007; Stewart et al., 2009; Yeh et al., 2010). However, one study also showed higher blood pressure in COMT-Val homozygotes, compared with Met carriers (Hagen et al., 2007).

Differences in regional cerebral blood flow (rCBF) between COMT-Val and Mets were indeed found by (Eisenberg et al., 2010) who measured rCBF via PET during rest in both men and women. COMT-Met allelic load positively correlated with rCBF in the left orbital cortex (BA47) and middle temporal gyrus (BA21), whilst COMT-Val allelic load positively correlated with rCBF in a cingulate gyrus region. No other regions showed significant COMT effects. Similarly, Thomason et al., (2009), using arterial spin labelling (ASL) magnetic resonance imaging, showed that children with different COMT polymorphisms do not differ in terms of their global perfusion values but show differences in regional perfusion. Specifically, Met-homozygotes had higher resting perfusion rates in frontal and temporal cortices, insula, caudate, brainstem and lateral cerebellum compared to COMT-Val homozygotes. However, Raz et al., (2017) observed higher overall CBF in adult COMT-Val homozygotes, compared with COMT-Met carriers, illustrated by an interaction between CBF, COMT and age (age-related slowing of flow rate was observed in COMT Val homozygotes only. Therefore, the influence of COMT on CBF may depend on age.

Finally, given that it inhibits COMT and increases dopamine availability, administration of tolcapone could also potentially influence CBF. There is evidence that dopamine agonists (Schouw et al., 2013) and antagonists (Fernández-Seara et al., 2011; Handley et al., 2013) influence regional CBF, although the effects of dopaminergic manipulations appear complex and non-linear (Dukart et al., 2018).To my knowledge no one has examined the effect of tolcapone on CBF to date.

5.1.3 *Arterial spin labelling*

ASL MRI is a non-invasive method for the quantification of blood flow/perfusion. It uses water protons in arterial blood as an endogenous diffusible tracer. Arterial blood water is magnetically tagged before it enters the tissue of interest (in this case the brain) by radiofrequency (RF) pulses. After a delay (called inversion delay (TI) in pulsed ASL (PASL) or post-labelling delay (PLD) in continuous ASL (CASL)) to allow labelled blood to flow into the brain tissue, labelled images (tag images) are acquired that contain signal from both labelled water and static tissue water. Separate control images are also acquired without prior labelling of arterial spins, in a temporally interleaved fashion. Subtraction of tag images from control images eliminates static tissue signal and the remaining signal is a relative measure of perfusion proportional to CBF / perfusion. Multiple labelled-control image pairs are acquired and averaged for the generation of CBF maps (Alsop et al., 2015).

ASL allows the quantification of rCBF in physiological units (ml of blood/100g of tissue/min), both at rest as well as during activation. Validation studies have shown that ASL measurement has excellent concurrent validity when correlated with rCBF measured by PET, the gold standard method to measure CBF (Donahue et al., 2006; Xu et al., 2009). The measurement of rCBF using ASL perfusion MRI provides a non-invasive means of quantifying regional brain function both at rest and in response to pharmacological or task-induced activation (Brown et al., 2007; Detre et al., 2009). ASL is more widely available, quicker, cheaper and safer (as not-invasive as no radioactive tracer needed) than ^{15}O-PET, and has been reported to be stable over time (Tjandra et al., 2005; Wang et al., 2003; Wu et al., 2011).

5.1.4 *COMT and brain structure*

As well as potentially being influenced by CBF, functional data could also be confounded by differences in grey matter (GM) anatomy between COMT-Val and COMT-Met homozygotes. The available literature suggests that COMT genotype does not influence GM anatomy (Barnes et al., 2012; Tunbridge et al., 2013; Zinkstok et al., 2008, 2006), but some studies have reported effects of Val^{158}Met on GM maps in healthy controls (Ohnishi et al., 2006; Rowe et al., 2010). Notably, links between COMT and GM volume may be confounded by age and sexually-dimorphic effects (Zinkstok et al., 2006) and may be more prominent in populations at risk for psychosis (McIntosh et al., 2007; Ohnishi et al., 2006).

Thus, in order to interpret functional MRI data, it is important to understand whether and how COMT genotype and/or inhibition influences CBF, as well as to investigate and control for any differences in GM density.

The aim of this chapter was therefore to:

- **Investigate whether there are group differences and/or an interaction between COMT genotype and tolcapone on CBF as measured by ASL.**
- **Assess GM T1 structural maps to investigate whether potential BOLD differences in connectivity or activity could be confounded by gross differences in GM anatomy between COMT-Val and COMT-Met homozygotes.**

5.2 Methods

5.2.1 *Participants, study design and procedure*

For information on participants, study design and procedure see Chapter 4. In brief, I conducted a randomised, double-blind, placebo-controlled, between-subjects study to investigate the effects of COMT inhibition and COMT genotype and their interaction on whole brain perfusion (as measured by ASL) and GM density (structural data analysed by voxel-based morphometry (VBM). Unblinding of treatment groups only occurred when data analysis was completed.

5.2.2 *Neuroimaging Protocol*

Scanning was performed at the Oxford Centre for Human Brain Activity (OHBA), University of Oxford, using a 3-Tesla Siemens Prisma scanner with a 32-channel head-coil. The neuroimaging protocol comprised functional and structural sequences as follows.

5.2.2.1 *Arterial Spin Labelling*

Whole-brain perfusion imaging was performed using Siemen's pASL product PICORE-Q2TIPS pulsed arterial spin labelling (ASL) with a 2D gradient spin echo readout (QUIPSS II (quantitative imaging

of perfusion using a single subtraction, version 2), thin slice TI1, periodic saturation (Q2TIPS) using a proximal inversion with a control for off-resonance effects (PICORE) labelling scheme).

ASL data were collected as tag-control pairs with a TI of 1.8 seconds and a bolus duration of 0.7 seconds (TR = 2500ms, TE = 12ms, FA 90°, field of view = 256mm, 13 slices, voxel dimensions = 4.0 x 4.0 x 8.0 mm, 241 volumes, acquisition time = 10min 7s).

5.2.2.2 *Structural MRI*

Structural scans were acquired via T1-weighted MR images (TR = 1900ms, TE = 3.97ms, flip angle = 8°, field of view = 192mm, voxel dimension = 1mm isotropic, acquisition time = 5min 31s). Participants were allowed to close their eyes but instructed not to fall asleep.

5.2.3 *Analysis methods*

Data were analysed using FSL (FMRIB Software Library v6.0) tools (https://fsl.fmrib.ox.ac.uk/fsl).

5.2.3.1 *Arterial Spin Labelling*

Distortion and motion corrected resting perfusion maps in units of mL·100g·min were calculated using Oxford_ASL (part of the Bayesian Inference for Arterial Spin Labelling (BASIL) tool, https://fsl.fmrib.ox.ac.uk/fsl/fslwiki/BASIL (Chappell et al., 2009) for each participant.

FSL's Anatomical Processing Script (FSL_Anat, https://fsl.fmrib.ox.ac.uk/fsl/fslwiki/fsl_anat) was used to pre-process each participant's high resolution T1 structural image (includes bias-field correction, brain extraction and registration to standard space via FMRIB's Linear Image Registration Tool (FLIRT) and FMRIB's Non-linear Image Registration Tool (FNIRT). As registration of ASL data to the structural image is difficult (the images are low resolution and with limited contrast) each subject's native perfusion image was registered to standard space via their calibration image and the warps created by FSL_Anat. A Gaussian smoothing kernel of 2.35 mm was applied to all the normalised images (to match functional data).

Data was interrogated using voxel-wise generalized linear model (GLM) permutation nonparametric testing (5,000 permutations) with randomise (FSL's tool for nonparametric permutation inference on neuroimaging data), correcting for multiple comparisons across space (cluster-based thresholding using TFCE and a family-wise error (FWE)-corrected cluster significance threshold of $p<0.05$ applied to the suprathreshold clusters). For completeness, uncorrected images with $p<0.005$ are also presented. This results in spatial maps characterising the between-subject/group differences. The GLM comparison included the groups of interest comparison

(COMT-Val-placebo, COMT-Val-tolcapone, COMT-Met-placebo, COMT-Met-tolcapone, and the interaction between those groups). Each of the contrasts of interest was tested for group averages and difference between groups.

To further visualise the results, individual Parameter Estimates (PE) values were extracted from their custom maps, using significant clusters as binary masks. These represent differences in blood flow between groups.

5.2.3.2 *Structural*

GM maps were assessed to investigate whether any genotype effects of functional connectivity were confounded by gross differences in GM anatomy between COMT-Val and COMT-Met homozygotes.

Structural data was analysed with FSL's tool for Voxel Based Morphometry (FSL-VBM, Douaud et al., 2007), an optimised VBM protocol (Good et al., 2001) carried out with FSL tools (Smith et al., 2004) using default settings as described at http://fsl.fmrib.ox.ac.uk/fsl/fslwiki/FSLVBM). In brief, structural images were brain-extracted and GM segmented before being registered to the MNI 152 standard space using non-linear registration (Andersson et al., 2007). The resulting images were averaged and flipped along the x-axis to create a left-right symmetric, study-specific GM template. Second, all native GM images were non-linearly registered to this study-specific template and "modulated" to correct for local expansion (or contraction) due to the non-linear component of the spatial transformation. The modulated GM images were then smoothed with an isotropic Gaussian kernel with a sigma of 3 mm. Finally, voxel wise GLM was applied using permutation-based non-parametric testing (5,000 permutations), correcting for multiple comparisons across space (cluster-based thresholding using TFCE and a family-wise error (FWE)-corrected cluster significance threshold of $p<0.05$ applied to the suprathreshold clusters).

This procedure results in spatial maps characterising the between-subject/group differences. The GLM comparison included the groups of interest comparison (COMT-Val-placebo, COMT-Val-tolcapone, COMT-Met-placebo, COMT-Met-tolcapone, and the interaction between those groups). Each of the contrasts of interest was tested for group averages and difference between groups.

5.3 Results

5.3.1 *Participants*

Participant demographics are given in **Table 5.1**. The total sample consisted of 17 COMT-Met placebo (aged 22.5 ± 1.0 years [mean ± SEM]), 20 COMT-Met tolcapone (aged 23.6 ± 1.5 years), 19 COMT-Val placebo (23.5 ± 1.1 years) and 20 COMT-Val tolcapone (25.0 ± 1.4 years) male homozygotes.

Table 5.1 - Participant demographics and personality measures

	COMT-Met Placebo	COMT-Val placebo	COMT-Met tolcapone	COMT-Val tolcapone
Number	17	19	20	20
Age (years)	22.5 ± 1.0	23.5 ± 1.1	23.6 ± 1.5	25.0 ± 1.4
NART predicted FS-IQ (non-native speakers excluded)	113.2 ± 1.1	112.2 ± 1.3	111.5 ± 1.2	113.3 ± 1.1
Baseline Locus of Control	73.8 ± 2.2	74.7 ± 2.6	76.0 ± 2.1	73.8 ± 3.1
Baseline Self-esteem	32.4 ± 1.4	31.9 ± 1.0	32.2 ± 0.8	32.0 ± 1.0
Baseline State	31.6 ± 2.1	31.0 ± 1.8	32.7 ± 1.3	29.8 ± 1.4
Baseline Trait	39.5 ± 2.6	39.2 ± 2.5	38.1 ± 1.7	35.7 ± 2.1
Ethnicity	Caucasian	Indian 1 Singapore 1 Indonesian 1 Brazilian 1 Pakistan 1	Caucasian	Chinese 1 Pakistan 1 Bangladeshi 1

Values are mean ± SEM. Locus of control: Rotter's Locus of Control Scale; Self-esteem: Rosenberg's Self-esteem Scale; Spielberger's State-Trait Anxiety Inventory

5.3.2 *Cerebral blood flow*

The results of the GLM showed between-group differences in resting brain perfusion (see **Table 5.2**). Significantly greater perfusion was observed in COMT-Val compared to COMT-Met homozygotes in two separate clusters in the right PFC. Cluster1 (t=3.88, p=0.0406, MNI peak voxel location: x=36, y=34, z=20, cluster size=274 voxels) extends into the right superior frontal and medial gyrus and includes the right dorsolateral PFC when looking at p=0.005 uncorrected (see

Figure 5.2a). Cluster 2 included the superior frontal gyrus and also included the right dlPFC (t=3.41, p=0.0497, MNI peak voxel location: x=24, y=52, z=28, cluster size=9 voxels), see **Figure 5.2b**.

Moreover, greater perfusion was also observed for placebo compared to tolcapone in three separate clusters (see **Figure 5.3**). The biggest cluster was found in the right parietal lobe, surrounding the post-central gyrus (t=4.99, p=0.041, MNI peak voxel location: x=20, y=-34, z=72, cluster size=1089 voxels). When looking at p=0.005 uncorrected this cluster extended into the right superior frontal and medial gyrus, and the superior parietal lobule. The other two clusters were found in the right superior parietal lobule (t=3.73, p=0.044, MNI peak voxel location: x=34, y=-48, z=36, cluster size=144 voxels) and right superior temporal gyrus (t=4.73, p=0.044, MNI peak voxel location: x=44, y=-30, z=0, cluster size=77 voxels) respectively. There was no significant interaction between COMT genotype and treatment on cerebral perfusion.

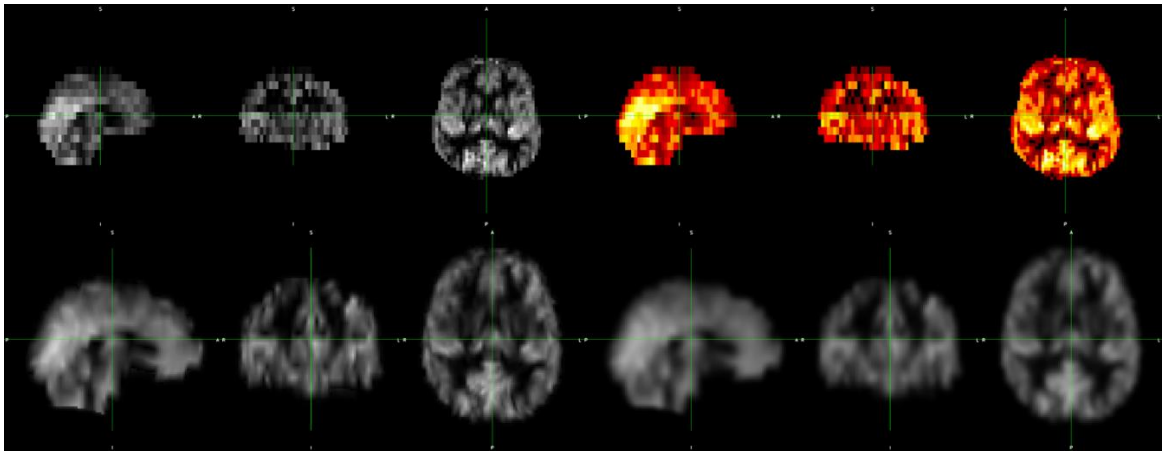


Figure 5.1 - Example of perfusion weighted images.

Top left: Example perfusion weighted image in native space. Top right: example perfusion weighed image in native space depicted in red. Bottom left: perfusion image registered to standard space. Bottom right: perfusion registered to standard space image smoothed with a Gaussian smoothing kernel of 2.35.

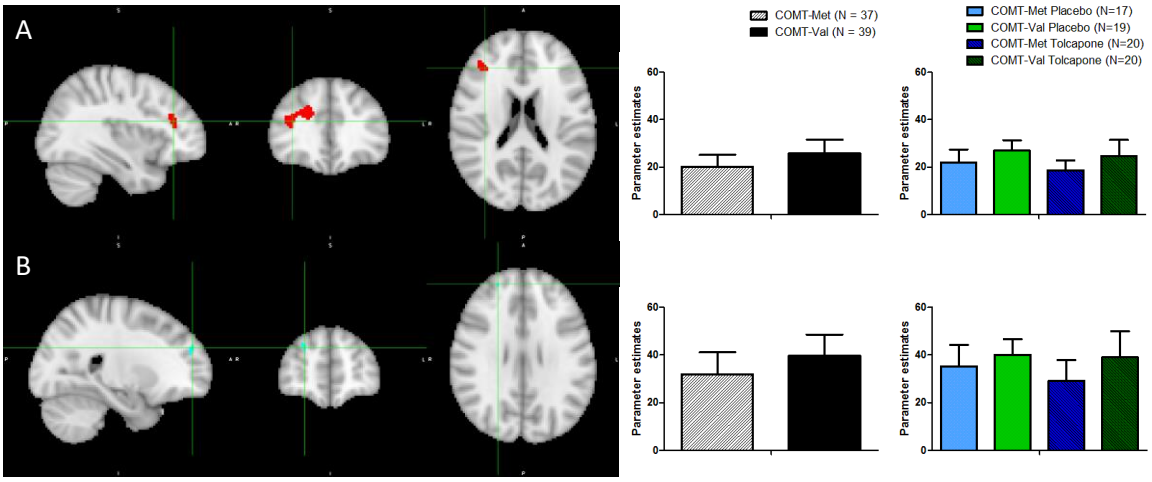


Figure 5.3 - Differences in cerebral blood flow between COMT-Val and COMT-Met homozygotes.

Significantly greater perfusion was observed in COMT-Val compared to COMT-Met homozygotes in two separate clusters in the right PFC. A = cluster 1 in red (MNI: x=36, y=34, z=20), B = cluster 2 in blue (MNI: x=24, y=52, z=28). Parameter estimates are presented on the right. Results were corrected for multiple comparisons by threshold-free cluster enhancement (TFCE) at FWE p=0.05. Error bars denote standard deviation.

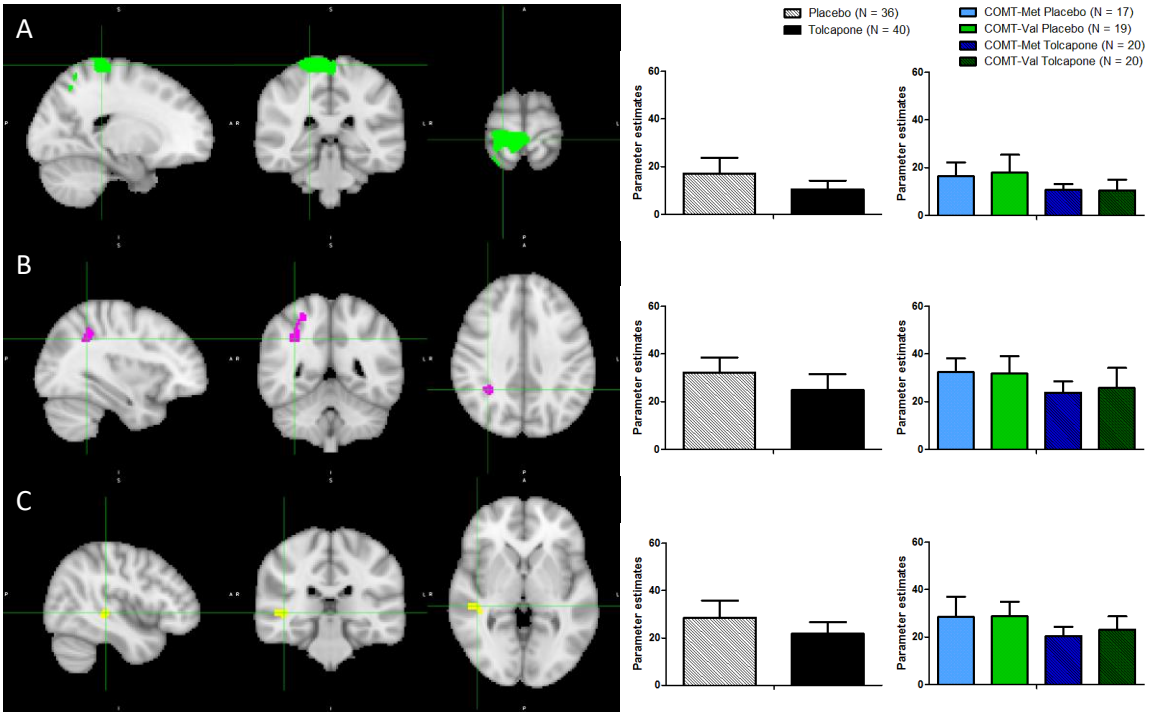


Figure 5.2 - Differences in cerebral blood flow between placebo and tolcapone.

Significantly greater perfusion was observed for homozygotes on placebo compared to tolcapone in three separate clusters (regardless of genotype). A = cluster 1 in green: x=20, y=-34, z=72. B = cluster 2 in purple: x=34, y=-48, z=36. C = cluster 3 in yellow: x=44, y=-30, z=0. Parameter estimates presented on the right. Results were corrected for multiple comparisons by threshold-free cluster enhancement (TFCE) at FWE p=0.05. Error bars denote standard deviation.

Table 5.2 - Significant effects of COMT genotype and tolcapone on cerebral blood flow. Results were corrected for multiple comparisons by TFCE at FWE p=0.05

CBF	**Brain area / Brodmann Area (BA)**	**Side**	**Cluster size**	**Voxel max**	**MNI max**	**t-score**	**p-value**
TFCE-corrected FWE P=0.05			**(voxels)**	**(x,y,z)**	**(x,y,z)**		
Main effect of gene							
COMT-Val > COMT-Met							
Cluster 1	Middle frontal and superior frontal gyrus, BA6, BA9 and BA32	R	274	27, 80, 46	24, 52, 28	3.88	0.041
Cluster 2	Superior frontal gyrus including BA9	R	9	33, 89, 50	36, 34, 20	3.41	0.050
Main effect of drug							
Placebo > tolcapone							
Cluster 1	Post-central gyrus, including BA3, BA4, BA5, BA6 and BA7	R	1089	35, 46, 72	20, -34, 72	4.99	0.023
Cluster 2	Superior parietal lobule, including BA7 and BA40	R	144	28, 39, 54	34, -48, 36	3.83	0.044
Cluster 3	Superior temporal gyrus BA22	R	77	23, 48, 36	44, -30, 0	4.73	0.040

5.3.3 *Structural differences*

GM maps were assessed to investigate whether any potential genotype effects of activity or functional connectivity could be confounded by gross differences in GM anatomy between COMT-Val and COMT-Met homozygotes. No significant voxel-wise differences in local GM volume were found between COMT-Met or COMT-Val homozygotes (results not shown).

5.4 Discussion

This study confirms that there are effects of both COMT genotype and tolcapone (but no interaction between them) on CBF as measured by ASL. COMT-Val homozygotes had greater cerebral perfusion in two clusters in the right the PFC (including the dlPFC) compared to COMT-Met homozygotes. Moreover, tolcapone reduced CBF compared to placebo, in three distinct clusters in including the right parietal lobe (surrounding the post-central gyrus), extending into superior frontal and medial areas and in the right superior temporal gyrus. However, I did not find an interaction between COMT-genotype and tolcapone. Nor were there genotype differences in brain structure, as assessed with FSL-VBM.

5.4.1 *COMT genotype*

These results are consistent with previous studies in that they are in the same direction (Val > Met; placebo > tolcapone) and in the same areas of the brain; however, the exact locations in which I observed these effects slightly differed from previous studies. Raz et al., (2017) showed greater global CBF in COMT-Val carriers compared to COMT-Met homozygotes. This study was conducted in young adults, like our study population, but included both men and women, a difference of note given effects of sex on CBF (Aanerud et al., 2017). Moreover, they used a different method to measure CBF (Phase Contrast Magnetic Resonance Imaging (PC-MRI) – which provides a method of MR angiography) and it is unclear how comparable ASL findings are to their result (Dolui et al., 2016). Eisenberg et al., (2010) measured CBF with PET during rest and found that COMT-Met allelic load correlated with rCBF in the left orbital cortex and middle temporal gyrus, whilst COMT-Val allelic load positively correlated with rCBF in cingulate gyrus region. Their study was conducted in men and women as well, with a wider age spread than my study (ages 20 –50, mean 28.7±7.5). My study is in contrast with (Thomason et al., 2009), who found higher CBF

(as measured by pASL) in regions important for cognitive processing in COMT-Met vs. COMT-Val homozygotes (e.g. prefrontal, temporal, and caudate). However, it should be noted that this study was conducted in children of both genders, in contrast to the adult, male sample studied here. Like sex, age also has effects on CBF (e.g. (Zhang et al., 2018)). Furthermore, the profound changes in COMT's activity and the dopamine system more generally across postnatal development makes extrapolating the findings of this study to adults difficult (Lewis, 1997; Tunbridge et al., 2006). A resting state study conducted by (Meyer et al., 2016) showed opposite effects of COMT genotype on resting state functional connectivity (see also Chapter 6) between adults (18-33 years, mean 24±2.6) and adolescents (14 year olds). Even though CBF and FC are two different measures, it is possible that age plays an important role in the effects of COMT genotype on perfusion as well. Raz et al., (2017) suggest that the effects of COMT genotype and dopamine on CBF are pleiotropic and linked with age. Younger adult COMT-Val homozygotes (lower available dopamine) evidence faster blood flow than COMT-Met carriers, but children and older adults who have lower dopamine levels than young and middle age adults may have a particularly significant reduction in blood flow rate.

5.4.2 *COMT inhibition by tolcapone*

Tolcapone reduced CBF compared to placebo, in three distinct clusters in including the right parietal lobe (surrounding the post-central gyrus), extending into superior frontal and medial areas and in the right superior temporal gyrus. This is in agreement with some studies who show direct vasoconstrictive effects of dopamine (e.g. (Krimer et al., 1998). However, I did not find an interaction between COMT-genotype and tolcapone. Therefore, these results show the complexity of dopamine's vasoactive properties. More dopamine, either due to the COMT- Met allele or tolcapone, results in less CBF, but their combined effects do not show any further significant decreases in CBF.

5.4.3 *Potential mechanisms*

The mechanism(s) by which COMT influences resting CBF remain obscure. Although COMT Val^{158}Met genotype shows associations with blood pressure (Annerbrink et al., 2008; Hagen et al., 2007; Htun et al., 2011)) it seems unlikely that the drug and genotype associated differences in regional CBF that we observe here result simply from these peripheral effects: firstly, because CBF is tightly autoregulated in normotensive individuals (Cipolla, 2009) and, secondly, because blood pressure effects on CBF would be expected to be global in nature. Moreover, tolcapone does not

affect blood pressure (Dingemanse et al., 1995). Whilst it is possible that the observed changes in CBF are indirect in nature, secondary to COMT-related differences neuronal activity, it is also plausible that they result from direct effects. Thus, at least in rats, COMT is expressed in perivascular astrocytes and capillary endothelia (Karhunen et al., 1995), as well as in the basilar artery tunica adventitia (Karhunen et al., 1994), and so is well-placed to contribute to the dopaminergic regulation of the cerebral microvasculature (Krimer et al., 1998). Taken together, these pieces of evidence suggest that our findings might result, at least in part, from direct effects of COMT on regional CBF.

A notable aspect of our findings is that drug and genotype influenced resting CBF in different regions. These findings, coupled with a lack of interactive effects, argue that the mechanisms underlying drug and genotype effects on CBF are distinct. The acute effects of COMT inhibition presumably reflect the localisation of perivascular COMT (which to our knowledge has not been studied systematically across the brain), perhaps coupled with heterogeneity in dopaminergic receptor distribution, and with possible regional variation in tolcapone penetrance into the brain parenchyma. In contrast, the most parsimonious explanation for the contrasting regional profile associated with the COMT Val^{158}Met polymorphism is that genotype effects are mediated, at least in part by compensatory changes, driven by the 'trait' differences that presumably result from COMT genotype. In this regard, it is notable that the effects of genotype are more prominent in frontal regions, in which genotype effects of COMT Val^{158}Met have been repeatedly demonstrated in BOLD fMRI studies (Egan et al., 2001; Mier et al., 2009; Tunbridge et al., 2013). It would be of interest to examine the effects of both acute and chronic tolcapone administration in one of the mouse models of the COMT-Val^{158}Met polymorphism, in order to better understand the molecular and cellular changes underlying effects of COMT on regional CBF (Barkus et al., 2016; Gogos et al., 1998; Risbrough et al., 2014).

5.4.4 *BOLD activations*

The size and extent of BOLD activations are directly influenced by the magnitude of resting brain perfusion, which essentially forms the baseline over which activation is measured. Therefore, mapping perfusion baseline within the same scan session might be useful for future BOLD fMRI studies comparing groups with differing neurotransmitter levels, particularly when those neurotransmitters are known to be vasoactive (Thomason et al., 2009). My findings highlight the importance of considering brain perfusion in studies examining brain activation determined using BOLD fMRI. Note that, whilst such differences could explain observed differences in the BOLD

response, they might also act to mask or reduce genuine drug or genotype effects on neuronal activation determined using this approach.

5.4.5 *Structural differences*

I compared GM maps between COMT-Val and COM-Met homozygotes and found no differences. This agrees with the available literature suggesting that COMT genotype does not influence GM anatomy (Barnes et al., 2012; Tunbridge et al., 2013; Zinkstok et al., 2008, 2006). However, some studies have reported effects of $Val^{158}Met$ on GM maps in healthy controls (Ohnishi et al., 2006; Rowe et al., 2010). Notably, links between COMT and GM volume may be confounded by age and sexually-dimorphic effects (Zinkstok et al., 2006) and may be more prominent in populations at risk for psychosis (McIntosh et al., 2007; Ohnishi et al., 2006). Therefore, my study cannot rule out effects of COMT on GM volume in less homogeneous populations. Accordingly, I will present further results corrected for GM maps.

5.4.6 *Limitations*

When interpreting the results, it has to be taken into account that the standard Siemens ASL method used for this study has a large voxel size and runs PICORE-Q2TIPS pulsed ASL. This ASL technique was the only one available at the time of starting at the OHBA 3T MRI scanner. Therefore, it was not possible to scan with the gold standard pseudo-continuous ASL (pcASL) (see (Alsop et al., 2015). Compared to the method used in this study, pcASL suppresses signal from static tissue, reduces motion artefacts and is therefore less sensitive to motion and physiological noise. Thus, pcASL would be more sensitive to measure regional changes in CBF as compared to our method. Replication of this ASL study with a more sensitive method would provide more information on the effects of COMT genotype and inhibition in smaller regions of interest as compared to a whole brain analysis.

5.4.7 *Conclusion*

In conclusion, COMT genotype and COMT inhibition influence CBF, but not GM density. However, effects of COMT on GM volume cannot be ruled out. Therefore, both CBF perfusion and GM maps were added as nuisance variables when analysing the functional data (for both resting state

functional connectivity (rsFC) presented in Chapter 6 as well as for task fMRI presented in Chapter 7 and 8). This to account for any potential differences explaining BOLD contrast differences and to be able interpret functional MRI data more confidently.

Chapter 6 The interaction between COMT genotype and COMT inhibition on resting state connectivity

6.1 Introduction

Much literature has highlighted the importance of COMT Val^{158}Met with respect to PFC activation and engagement of PFC networks during cognitively demanding tasks (**see Chapter 1**; and e.g. (Egan et al., 2001; Mier et al., 2010). However, less is known about the effects of COMT genotype and COMT inhibition on functional connectivity (FC) at rest (rsFC).

6.1.1 *Resting state analysis*

Patterns of spatial and temporal coherence in the spontaneous fluctuations in BOLD signal form functionally-relevant resting state networks (RSNs) in the brain (Biswal et al., 1995). The coherence of these is determined, at least in part, by genetic factors (Filippini et al., 2009; Glahn et al., 2010). Different statistical methods have been introduced to study these RSN's, like seed-based analysis, independent component analysis (ICA) and graph theory. These different kind of analysis approaches have in common that they assume that when two brain regions show similarities in their BOLD time-series that they are functionally connected. The differences between methods lie in the way these similarities are estimated and/or represented (Smitha et al., 2017).

In seed-based analysis, the linear correlation between a seed or region of interest (ROI) and all other voxels in the entire brain is estimated, thereby yielding a seed-based FC map. This method is entirely dependent on the user defined ROIs, therefore it is difficult to examine whole brain FC using this technique (Smitha et al., 2017). ICA however, is considered to be completely data driven without the need for a predefined seed or ROI (however, it remains partly subjective due to manual labelling of noise and signal components). Distinct resting state fMRI networks are extracted from the data by employing mathematical algorithms to decompose the signal from whole brain voxels to spatially and temporally independent components. These components describe the temporal and spatial characteristics of the underlying hidden networks. In contrast to seed analysis that finds the single interaction between the seed region and the brain, ICA investigates multiple simultaneous voxel to voxel interactions of distinct networks at the same time (Lee et al., 2013; Smitha et al., 2017). Graph theory methods on the other hand are not voxel based. Instead, the brain is defined abstractly as a network of nodes with edges connecting them. Nodes

are often anatomically defined regions, (ROIs) whereas edges typically carry weights describing the correlation or degree of connectivity between nodes. Connectional characteristics of the graph can then be computed. As these measures are network summary statistics they are further removed from the real data as compared to ICA defined networks (Lee et al., 2013; Smitha et al., 2017).

6.1.2 *Effects of COMT genotype on rsFC*

Most similar to the approach used to analyse the data for this chapter, Tunbridge et al., (2013) examined the effect of the Val^{158}Met polymorphism on FC at rest in healthy men with an ICA approach. COMT genotype was found to significantly modulate FC within the executive control network (ECN). The ECN is a PFC network implicated in a broad range of cognitive and emotional functions (Smith et al., 2009). The ECN found by Tunbridge et al., (2013) correlated moderately (r = 0.677) with that described by Smith et al, (2009) and comprised bilateral frontal regions (encompassing the anterior cingulate cortex, anterior insula, frontal pole, and parts of the inferior and middle frontal gyri) and the head of the caudate, as well as bilateral, anti-correlated areas within the middle temporal gyrus and superior parietal lobule. COMT-Val homozygotes showed greater FC than COMT-Met homozygotes between a cluster within the left vlPFC and the rest of the executive control network (ECN). Exploratory analyses revealed no effect of COMT genotype in any other RSNs (Tunbridge et al., 2013).

To my knowledge no other prior studies have investigated the impact of COMT Val^{158}Met genotype on connectivity at rest using a group ICA-style approach but approaches based on graph theory have been used (see this chapter's Discussion and **Table 6.5** for a summary overview). Studies using these other approaches implicated COMT to also modulate the rsFC of the Default Mode Network (DMN) (e.g. (Markett et al., 2016; Tian et al., 2013). The DMN includes the medial parietal (precuneus and posterior cingulate), bilateral inferior–lateral–parietal and ventromedial frontal cortex (Smith et al., 2009) and is most commonly seen as deactivating in task-based FMRI experiments. It is active when individuals are not focused on the external environment, for example when being engaged in internally focused tasks including autobiographical memory retrieval, envisioning the future, and conceiving the perspectives of others (Buckner et al., 2008).

In sum, the differences in PFC-dependent function between COMT-Val and COMT-Met homozygotes exist even at rest. However, COMT's effects on connectivity are complex, with the directionality depending on for example the brain areas and networks studied. To my knowledge

there is no previous literature that investigated the effects of COMT inhibition or its interaction with COMT genotype on rsFC.

The aim of this study was therefore to:

- **Investigate whether we can replicate the findings from (Tunbridge et al., 2013) and extend them by showing whether there is an interaction of COMT genotype and tolcapone on rsFC, by implementing two complementary neuroimaging analysis approaches:**
    - **whole brain analysis**
    - **seed analysis (with the left vlPFC and right dlPFC as seeds)**

6.2 Methods

6.2.1 *Participants, study design, and procedure*

For information on participants, study design and procedure see Chapter 4. In brief, I conducted a randomised, double-blind, placebo-controlled, between-subjects study to investigate the effects of COMT genotype (COMT-Val vs. COMT-Met) and COMT inhibition (through the administration of tolcapone vs. placebo) and their interaction on rsFC. Unblinding of treatment groups only occurred when data analysis was completed.

6.2.2 *Neuroimaging Protocol*

MRI environment and structural scan sequence are identical to described in Chapter 5.

6.2.2.1 *Resting-State fMRI*

Whole-brain resting-state imaging was performed using a gradient-echo EPI sequence (TR = 933 ms, TE = 33.40ms, flip angle = 60°, field of view = 192mm, voxel dimension = 2mm isotropic, multiband 6 acceleration factor interleaved, 650 volumes, acquisition time = 10 min 16s). Participants were instructed to stay still, to keep their eyes open looking at a white fixation cross presented on a black background, to blink normally, think of nothing in particular, and not to fall asleep. An eye-tracker camera was used to ensured participants had their eyes were open during scanning (allowed to blink normally).

Images were distortion corrected by an acquired fieldmap (echos at 4.92 and 7.38 ms, TR=482ms, flip angle = 46°).

6.2.3 *Analysis methods*

Data were analysed using FSL as described in Chapter 5. ICA analysis was unrestrained at subject level and restrained to 25 components at group level.

The primary RSNs of relevance given the previous literature (Liu et al., 2010; Tunbridge et al., 2013) are DMN and the ECN. Therefore, I focused on these RSNs as primary analyses.

6.2.3.1 *Pre-processing*

The structural anatomical scans were brain extracted using FSL's Brain Extraction Tool BET (Smith, 2002). Single subject functional MRI data were pre-processed and analysed using Multivariate Exploratory Linear Decomposition into Independent Components (Melodic version 3.15, part of FSL). Pre-processing involved a number of steps designed to reduce unwanted variability in the data and to improve the validity of statistical analysis. The following steps where therefore implemented for each subject: 1) Removal of non-brain structures using BET (Smith, 2002), 2) motion correction using FMRIB's Linear Image Registration Tool (MCFLIRT; (Jenkinson et al., 2002a), 3) distortion correction (fsl_prepare_fieldmap was used to generate the required input data), 4) spatial smoothing using a Gaussian kernel of FWHM 5mm, 5) grand-mean intensity normalisation of the entire 4D dataset by a single multiplicative factor and 6) high-pass temporal filtering cut-off = 150s (Gaussian-weighted least-squares straight line fitting, with sigma=75.0s). Furthermore, resting state specific pre-processing steps included masking of non-brain voxels; voxel-wise de-meaning of the data and normalisation of the voxel-wise variance. In addition, functional images were registered to their high resolution structural via the high contrast functional image and Boundary-Based Registration (BBR) using FLIRT (Jenkinson et al., 2002a; Jenkinson and Smith, 2001), and non-linear registration from structural to MNI [Montreal Neurological Institute (MNI)] standard space was then further refined using FNIRT nonlinear registration (Andersson et al., 2007a, 2007b), resampling resolution=2mm.

6.2.3.2 *ICA analysis*

Probabilistic ICA (Beckmann and Smith, 2004) implemented using FSL's MELODIC was used to analyse the resting state data.

First, pre-processed data were whitened and projected into a 91-dimensional subspace using probabilistic Principal Component Analysis (PCA) where the number of dimensions was estimated using the Laplace approximation to the Bayesian evidence of the model order (Beckmann and Smith, 2004; Minka, 2001).

The whitened observations were decomposed into sets of vectors which describe signal variation across the temporal domain (time-courses) and across the spatial domain (maps) by optimising for non-Gaussian spatial source distributions using a fixed-point iteration technique (Hyvarinen, 1999). Estimated Component maps were divided by the standard deviation of the residual noise and thresholded by fitting a mixture model to the histogram of intensity values (Beckmann and Smith, 2004).

Resting-state data were then denoised by ICA denoising using FMRIB's ICA-based Xnoiseifier (FIX) by manually creating a training dataset from five subjects in each group (N=20) randomly chosen by Prof. Harrison. Manual labelling of components was done by me and another independent researcher (Dr. Liliana Capitao) and then compared. A conservative approach was used in that if not agreed the component was included. Agreement rate was between 95 and 100% (average = 98.4%).

The pre-processed cleaned functional data were then temporally concatenated across subjects in order to create a single 4D dataset. Then, the (group-wise) concatenated multiple rs-fMRI datasets were decomposed using a group ICA to identify large-scale patterns of FC in the population of subjects (restrained to 25 components) as described previously (Filippini et al., 2009). Components corresponding to known RSNs were identified by eye and compared to previously published maps (Smith et al., 2009) using Pearson spatial cross-correlation.

The set of spatial maps from this group-average analysis was used to generate subject-specific versions of the spatial maps, and associated time series, using dual regression (Beckmann et al., 2009; Filippini et al., 2009). This is a two-step process. First, for each subject, the group-average set of spatial maps is regressed (as spatial regressors in a multiple regression) into the subject's 4D space-time dataset. This results in a set of subject-specific time series, one per group-level spatial map. Next, those time series are regressed (as temporal regressors, again in a multiple regression) into the same 4D dataset files (1 per original ICA map, with the fourth dimension being subject identification), resulting in a set of subject-specific spatial maps, one per group-level spatial map. These were then tested by a voxel-wise GLM based analysis for statistically significant differences between groups using nonparametric permutation testing (5,000 permutations) using FSL's randomise permutation-testing tool (Randomise). Cluster-based thresholding was applied, using TFCE and a family-wise-error corrected cluster significance threshold of $p<0.05$ applied to the

suprathreshold clusters. For completeness (and because previous studies also used less stringent statistical thresholds), uncorrected images with p<0.005 are also shown. GM maps and ASL maps were added as voxel-wise covariates (see below).

The GLM comparison included the groups of interest comparison (Val-Placebo, Val-Tolcapone, Met-Placebo, Met-Tolcapone), the mean activation across groups and the interaction between the groups. To further visualise the results, individual Parameter Estimates (PE) values were extracted from their custom maps, using significant clusters as binary masks.

Even though no voxel-wise differences in the local GM volume/topography were found (VBM results), GM images of each subject were extracted using Feat_GM_prepare and added to the model used to analyse the functional data to remove any potential structural differences explaining the BOLD contrast differences. Analogous to these GM maps, resting perfusion maps (ASL-data) were also used as covariates to account for differences in CBF between the groups.

All activations are reported using MNI coordinates.

6.2.3.3 *Seed based analysis*

Given the effects of COMT on ECN resting state connectivity as described by (Tunbridge et al., 2013), and the previous literature linking COMT with right dlPFC function, anatomical ROI analysis was conducted in addition to the whole brain ICA analysis. The ROI mask for the left vlPFC was defined by using a 10mm sphere centred around the peak coordinates (MNI x=-38, y=14, z=2) of the finding reported by (Tunbridge et al., 2013) from the MNI standard brain (**Figure 6.1**). The right dlPFC was defined by the coordinates of BA9 (MNI right dlPFC x=35, y=39, z=31) (Mier et al., 2010) and created from MNI standard brain, also with a 10mm sphere (**Figure 6.2**).

Seed masks were registered to EPI space. Connectivity was calculated as the correlation (both positive and negative) of time series for all other voxels in the brain within FEAT. WM and CSF masks were added as covariates of no interest. ASL and GM maps were also added again as nuisance variables.

I tested for group averages and differences between groups for each of the contrasts of interest. The Z statistic images were thresholded using clusters determined by Z>3.1, and a family-wise error–corrected cluster significance threshold of P<0.05 was applied to the superthreshold clusters. For completeness and to be able to compare with previous literature, clusters thresholded by Z>2.3 were again also depicted.

All activations are reported using MNI coordinates.

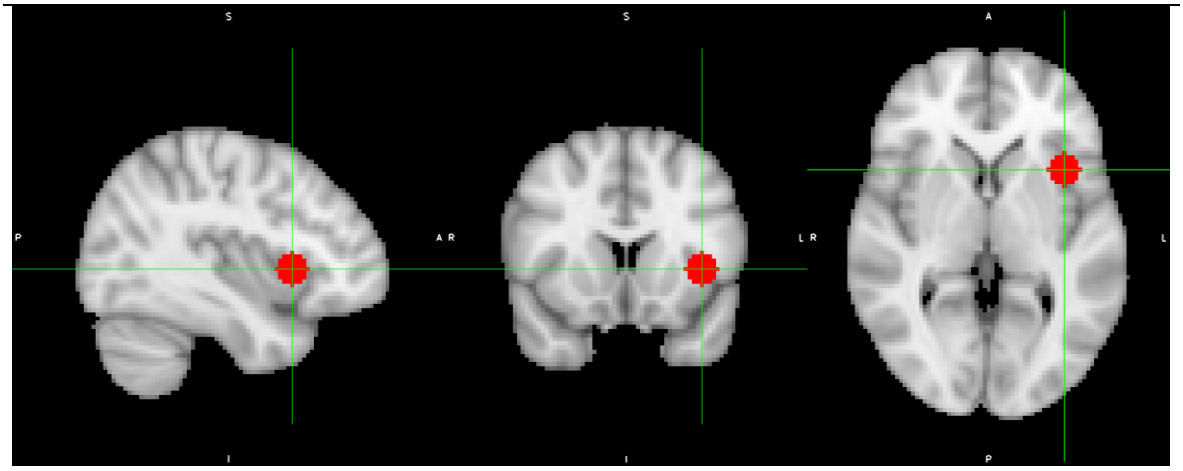


Figure 6.1 - Left vlPFC mask.

Left vlPFC mask, created with a 10mm sphere around the peak coordinates x=-38, y=14, z=2.

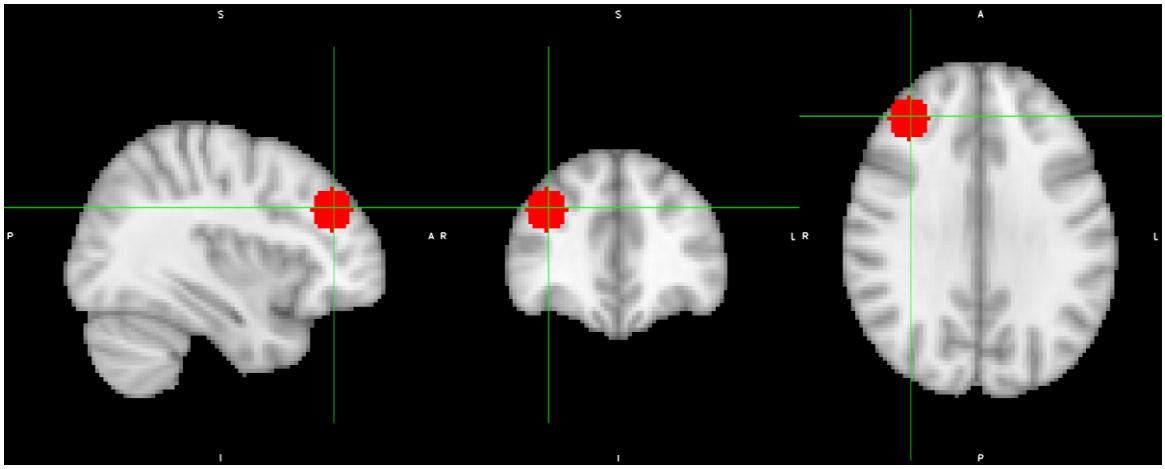


Figure 6.2 - Right dlPFC mask.

Right dlPFC mask, created with a 10mm sphere around the peak coordinates x=35, y=39, z=31.

6.3 Results

First, I will describe the found RSNs for the overall sample. Then, I will move on to describe the effects of COMT genotype and COMT inhibition on rsFC.

6.3.1 *Participants*

The same participants were studied as described in Chapter 5.

6.3.2 *Identification of resting state networks*

ICA was restricted to 25 components. Of these, 20 components were identified as RSNs (covering the majority of GM) and were evaluated further (**Table 6.1** and **Figure 6.3**). These networks corresponded to and overlapped with RSNs which have been described previously and show high stability over time (Beckmann et al., 2009; Smith et al., 2009). The other components reflected distinct artifacts resulting from scanner/multiband artifacts, head motion and physiological noise.

6.3.3 *Group differences in rsFC*

Voxel-wise comparisons of COMT-Val and COMT-Met homozygotes (regardless of treatment) showed a significant effect of COMT genotype on the FC of the anterior DMN (**Table 6.2**). Significantly greater temporal correlation (coherence) was observed for the COMT-Val homozygotes in a cluster in the right frontal pole (t=4.49, p=0.023, peak voxel location: x=20, y=48, z=22, cluster size=28 voxels, see **Figure 6.4**) with the rest of the DMN, compared to the COMT-Met homozygotes.

Table 6.1 - Resting state networks identified.

Component number	**Label as by (Smith et al., 2009)**	**Correlation with Smith et al., 2009**	**Labelled by visual inspection**
Comp0000	Visual lateral	0.65	Visual lateral
Comp0001	Visual medial	0.64	Visual medial
Comp0002	Frontoparietal	0.62	Frontoparietal left
Comp0003	Frontoparietal	0.64	Frontoparietal right
Comp0004	Visual medial / visual occipital pole	0.35 / 0.50	Visual medial / visual occipital pole
Comp0005			Parietal + motor
Comp0006			Salience
Comp0007	DMN / executive control	0.39 / 0.36	DMN anterior
Comp0008	Sensorimotor	0.31	Sensoriomotor
Comp0009			Language
Comp0010			Motor superior
Comp0011			Insula regions
Comp0012	Auditory	0.55	Auditory
Comp0013	DMN	0.30	DMN posterior / hippocampi
Comp0014	DMN	0.50	DMN precuneus
Comp0015	Executive control	0.55	Executive control
Comp0016			Cerebellum
Comp0017	Frontoparietal	0.35	Sensorimotor anterior
Comp0018	Visual occipital pole	0.55	Visual occipital pole
Comp0019			Left motor network

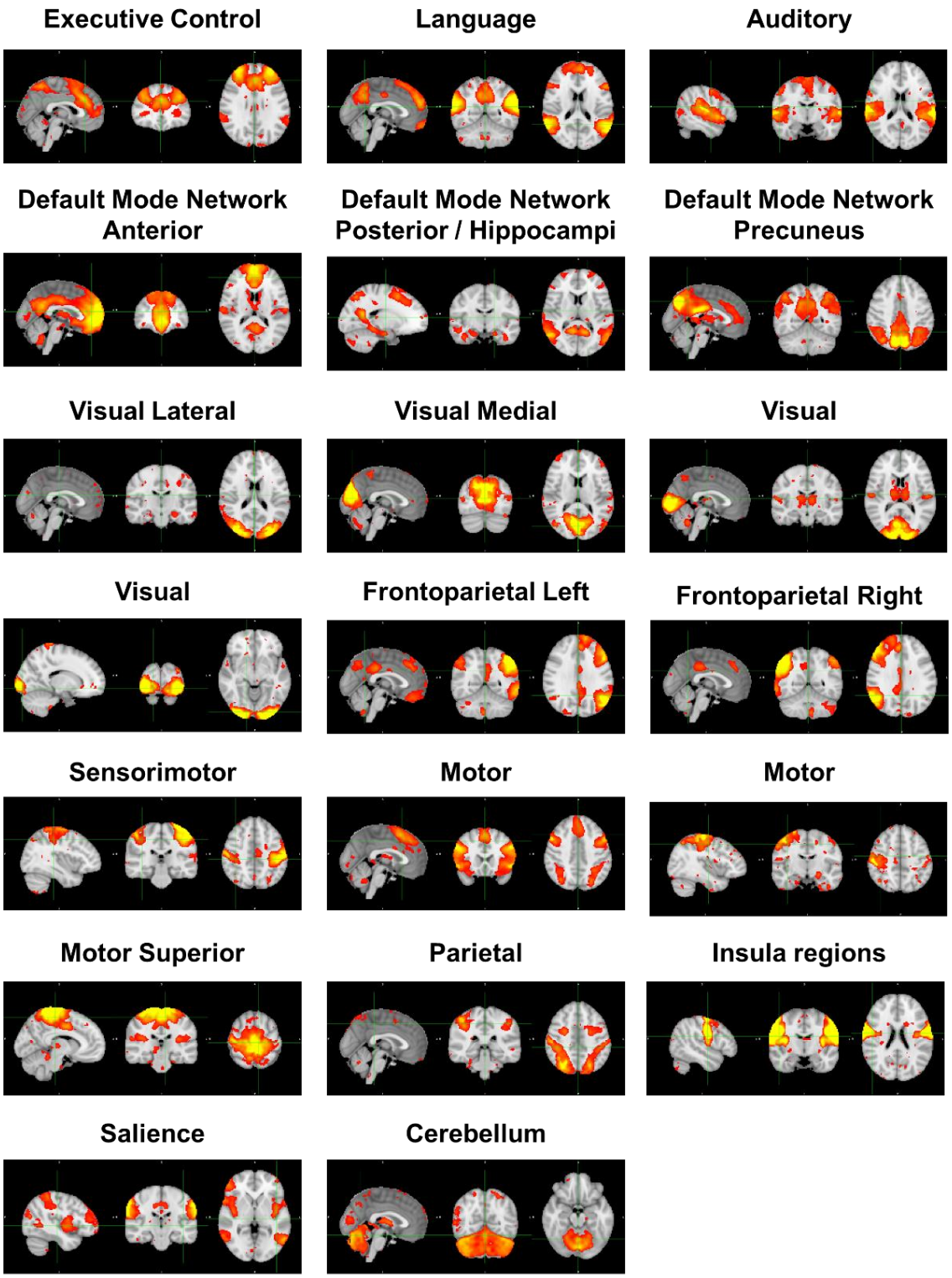


Figure 6.3 - Resting State Networks identified.

Axial, coronal and sagittal slices for the main resting state networks detected, overlaid onto the standard MNI brain.

When looking at p=0.005 uncorrected this cluster extended into the right superior frontal and medial gyrus. Exclusion of GM or perfusion covariates did not substantially alter the findings. There were no effects of treatment (tolcapone vs. placebo) nor an interaction between COMT genotype and treatment.

There were no effects of COMT genotype, COMT inhibition or their interaction on the rsFC of the ECN.

6.3.4 *Exploratory analyses*

Exploratory analyses of the other RSNs identified by the ICA revealed significant treatment effects (regardless of genotype) on the FC of the visual medial network, parietal motor network, language network and motor superior network (before correcting for multiple comparisons between RSNs). A significant interaction between genotype and treatment was found in the superior motor network (SMN) as well. Given findings from a previous MEG study, which implicated COMT in motor cortex activity (Tunbridge, personal communication), the effects of COMT inhibition (treatment effect) on the two motor networks are presented in more detail here as well. See **Table 6.2** and **Figure 6.5 and 6.6**.

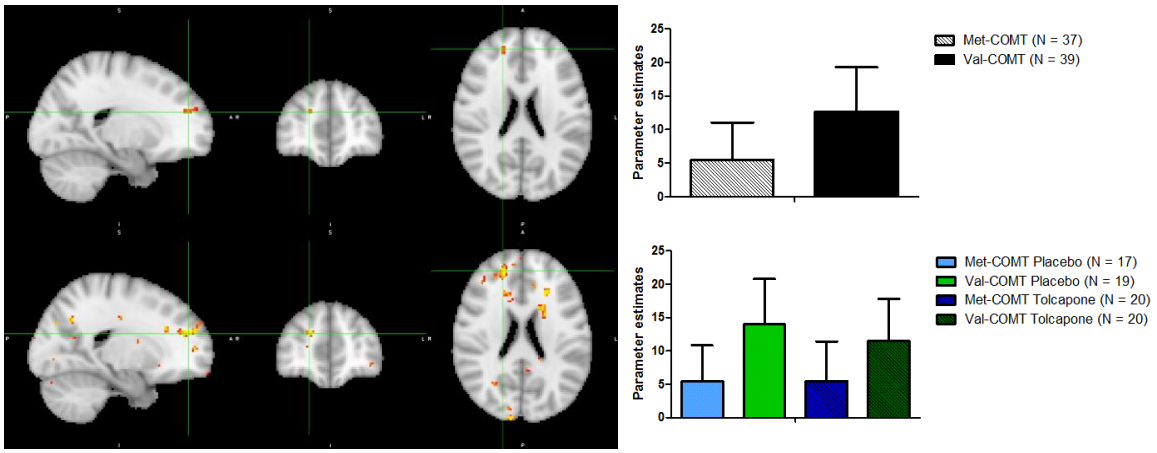


Figure 6.4 - The effect of COMT-genotype on anterior DMN functional connectivity.

Significantly greater temporal correlation (coherence) was observed for the COMT-Val homozygotes in a cluster in the right frontal pole (t=4.49, p=0.023, peak voxel location: x=20, y=48, z=22, cluster size=28 voxels) with the rest of the DMN, compared to the COMT-Met homozygotes. Results are shown TFCE-corrected with a family-wise error cluster significance level of p<0.05 (top figure), and p=0.005 uncorrected (lower figure). The bars on the right show mean parameter estimates from the significant cluster. Error bars denote standard deviation.

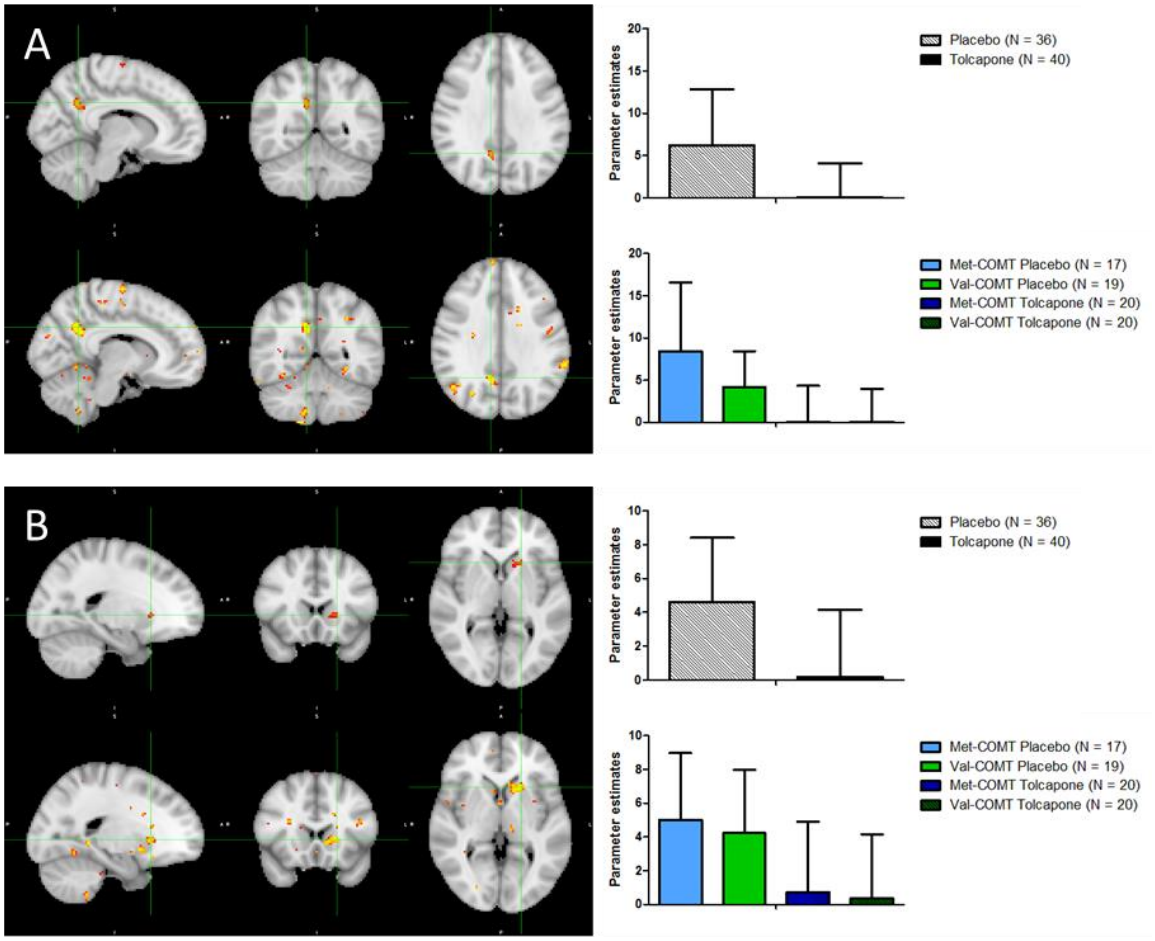


Figure 6.5 - Effect of COMT inhibition on Superior Motor Network (SMN) functional connectivity.

A: Greater FC for subjects on placebo compared to tolcapone between a cluster in the right precuneous cortex, extending into the posterior cingulate cortex and BA31 and the SMN (t=5.18, p=0.014, peak voxel location: x=10, y=-54, z=32, cluster size=56 voxels).

B: Greater FC for subjects on placebo compared to tolcapone between a cluster in the left caudate, extending into the right putamen and the SMN (t=4.46, p=0.033, peak voxel location: x=-20, y=18, z=2, cluster size=32 voxels).

Results are shown TFCE-corrected and with family-wise error cluster significance level of p<0.05 (top figure), and p=0.005 uncorrected (lower figure). The bars on the right show mean parameter estimates from the significant cluster. Error bars denote standard deviation.

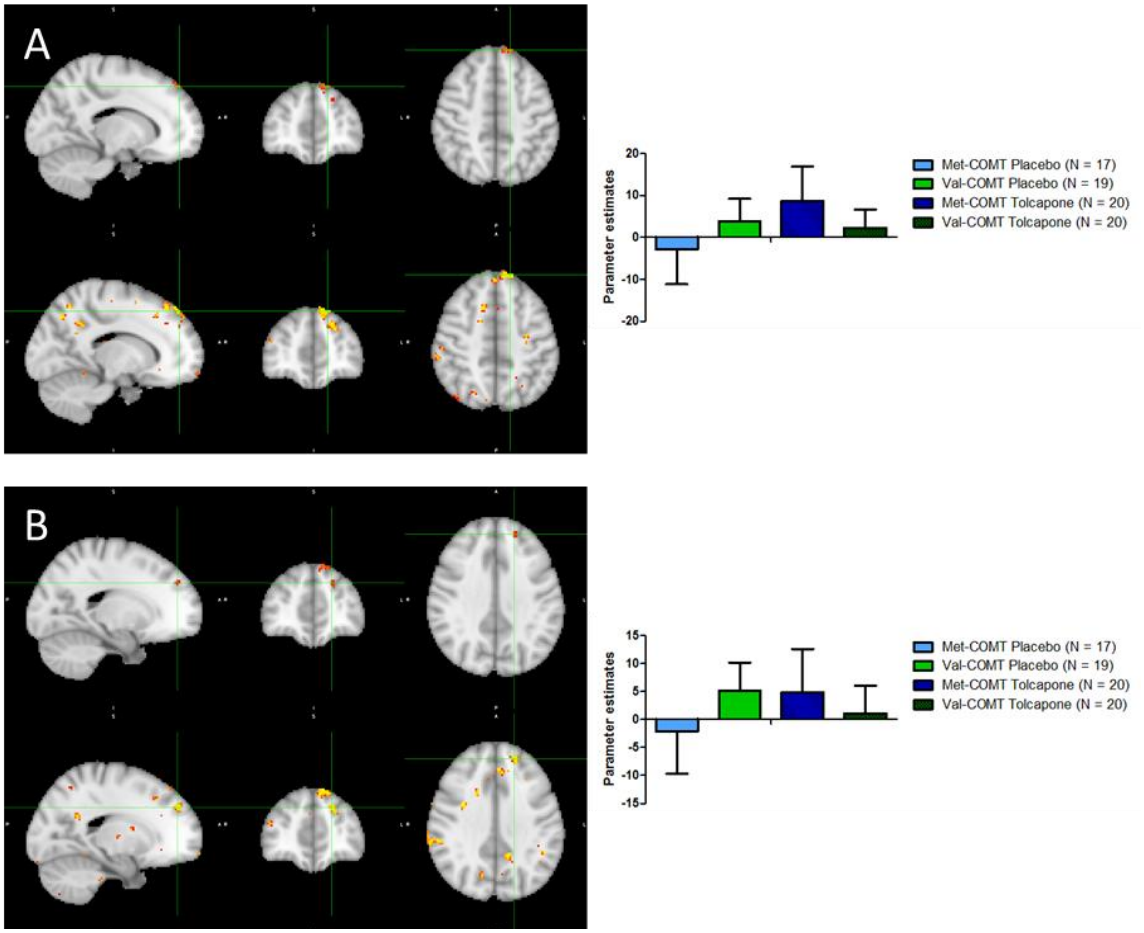


Figure 6.6 - Genotype by treatment interaction on SMN connectivity.

Genotype by treatment interaction on SMN connectivity. COMT-Val homozygotes had greater FC between two clusters in the left frontal pole extending into the superior frontal gyrus (BA8 and BA9) and the SMN compared to COMT-Met homozygotes on placebo. Tolcapone reversed this difference, increasing FC in these areas in COMT-Met homozygotes and decreasing connectivity in COMT-Val homozygotes, compared with their respective placebo groups (t=4.35, p=0.030, peak voxel location: x=-14, y=48, z=48, cluster size=14 voxels and (t=4.25, p=0.039, peak voxel location: x=-18, y=46, z=34, cluster size=13 voxels).

Results are shown TFCE-corrected and a family-wise error cluster significance level of p<0.05 (top figure), and p=0.005 uncorrected (lower figure). The bars on the right show mean parameter estimates from the significant clusters. Error bars denote standard deviation.

Table 6.2 - Effects of COMT genotype (COMT-Val vs. COMT-Met) and COMT inhibition (placebo vs. tolcapone) on resting state connectivity.

Resting State Data TFCE-corrected FWE cluster significance level of p<0.05		**Brain area / BA**	**Side**	**Cluster size (voxels)**	**Voxel max location (x,y,z)**	**MNI max (x,y,z)**	**t-score**	**p-value**
Component								
Comp001 Visual Medial								
Placebo>tolcapone	Cluster 1	Cuneal Cortex, BA18, extending into supra- and intra-calcarine cortex, BA17, occipital pole	L	180	47, 20, 45	-4, -86, 18	3.82	0.026
	Cluster 2	Cuneal Cortex, BA18	R	66	40, 25, 48	10, -76, 24	3.39	0.041
	Cluster 3	Precuneus Cortex, BA31,	R	14	42, 31, 51	6, -64, 30	3.48	0.041
	Cluster 4	Precnueus cortex, cuneal cortex, BA19	R	11	42, 24, 55	6, -78, 38	3.37	0.043
	Cluster 5	Intracalcarine cortex	R	2	33, 30, 41	24, -66, 10	3.56	0.047
Comp005 Parietal Motor								
Placebo>tolcapone	Cluster 1	Superior lateral occipital cortex	L	12	59, 26, 50	-28, -74, 28	4.93	0.021
Comp007 anterior DMN								
COMT-Val>Met	Cluster 1	Superior frontal gyrus extending into frontal pole	R	28	35, 87, 47	20, 48, 22	4.49	0.023
	Cluster 2	White matter. Corpus callosum, extending into the right caudate	R	16	39, 72, 44	12, 18, 16	4.24	0.032
	Cluster 3	Cingulate gyrus white matter	R	4	36, 77, 49	18, 27, 26	3.96	0.048
	Cluster 4	Superior frontal gyrus	R	2	39, 84, 53	12, 42, 34	4.18	0.048
Comp009 language								
Placebo>tolcapone	Cluster 1	Posterior cingulate gyrus, BA23, extending into the precuneous cortex	R	9	42, 38, 49	6, -50, 26	4.07	0.040

Comp0010 Motor superior								
Placebo>tolcapone	Cluster 1	Precuneous cortex, BA31, extending into posterior cingulate gyrus	R	56	40, 36, 52	10, -54, 32	5.18	0.014
	Cluster 2	Caudate extending into putamen	L	32	55, 72, 37	-20, 18, 2	4.46	0.033
	Cluster 3	Superior frontal gyrus, extending into supplementary motor gyrus and precentral gyrus, BA6	L	7	40, 58, 71	10, -10, 70	3.87	0.043
	Cluster 4	Lateral occipital cortex	L	5	21, 31, 54	48, -64, 36	4.13	0.047
	Cluster 5	White matter	R	3	62, 62, 30	-34, -2, -12	4.48	0.043
Genotype by treatment interaction	Cluster 1	Frontal pole, extending into superior frontal gyrus, BA8	L	54	52, 87, 60	-14, 48, 48	4.35	0.030
	Cluster 2	Frontal pole, extending into Superior frontal gyrus, BA9	L	13	54, 86, 53	-18, 46, 34	4.25	0.039
	Cluster 3	Superior frontal gyrus extending in to frontal pole, BA6	L	7	51, 80, 64	-12, 34, 55	4.16	0.042
Comp0018 Visual occipital pole								
Placebo>tolcapone	Cluster 1	Supracalcarine cortex, BA30, extending into cuneal cortex	R	2	55, 29, 44	-20, -68, 16	4.39	0.047

6.3.5 *Seed analysis*

Further to the whole brain ICA analysis, anatomical ROI analysis was also conducted with seeds in both the left ventrolateral and right dlPFC.

6.3.5.1 *Left vlPFC seed*

There were no significant main effects of COMT genotype nor treatment on this seed region. However, a significant COMT genotype by treatment interaction was found. Greater FC was found for COMT-Val homozygotes on placebo between the left vlPFC seed and two separate clusters compared to COMT-Met homozygotes on placebo. These two clusters included the left post-and pre-central gyrus (Z=4.32, p=0.002, peak voxel location: x=-54, y=-8, z=18, cluster size=127 voxels, **Table 6.3a and Figure 6.7a**) and the left anterior supramarginal gyrus extending into the post-central gyrus (Z=3.99, p=0.011, peak voxel location: x=-54, y=22, z=30, cluster size=93 voxels, **Table 6.3a and Figure 6.7b**). Tolcapone reversed this difference, increasing FC between these areas for COMT-Met homozygotes, and decreasing connectivity in COMT-Val homozygotes.

Complementary analysis

For completeness, data was also analysed for Z>2.3 p<0.05, as previous literature used this less stringent cluster-forming threshold. In addition to the interaction reported above, greater FC was also found for subjects on placebo compared to tolcapone between the left vlPFC and three different clusters. These clusters included: bilateral paracingulate gyrus (Z=3.57, p=0.0005, peak voxel location: x=-10, y=50, z=60, cluster size=463 voxels, **Table 6.3b**), left superior frontal gyrus extending into the frontal pole (Z=3.94, p=0.008, peak voxel location: x=-4, y=58, z=40, cluster size = 318 voxels, **Table 6.3b**) and bilateral paracingulate gyrus, extending into the frontal medial cortex (Z=4.47, p=0.012, peak voxel location: x=14, y=44, z=-4, cluster size=298 voxels, **Table 6.3b**). See **Table 6.3b** for more details.

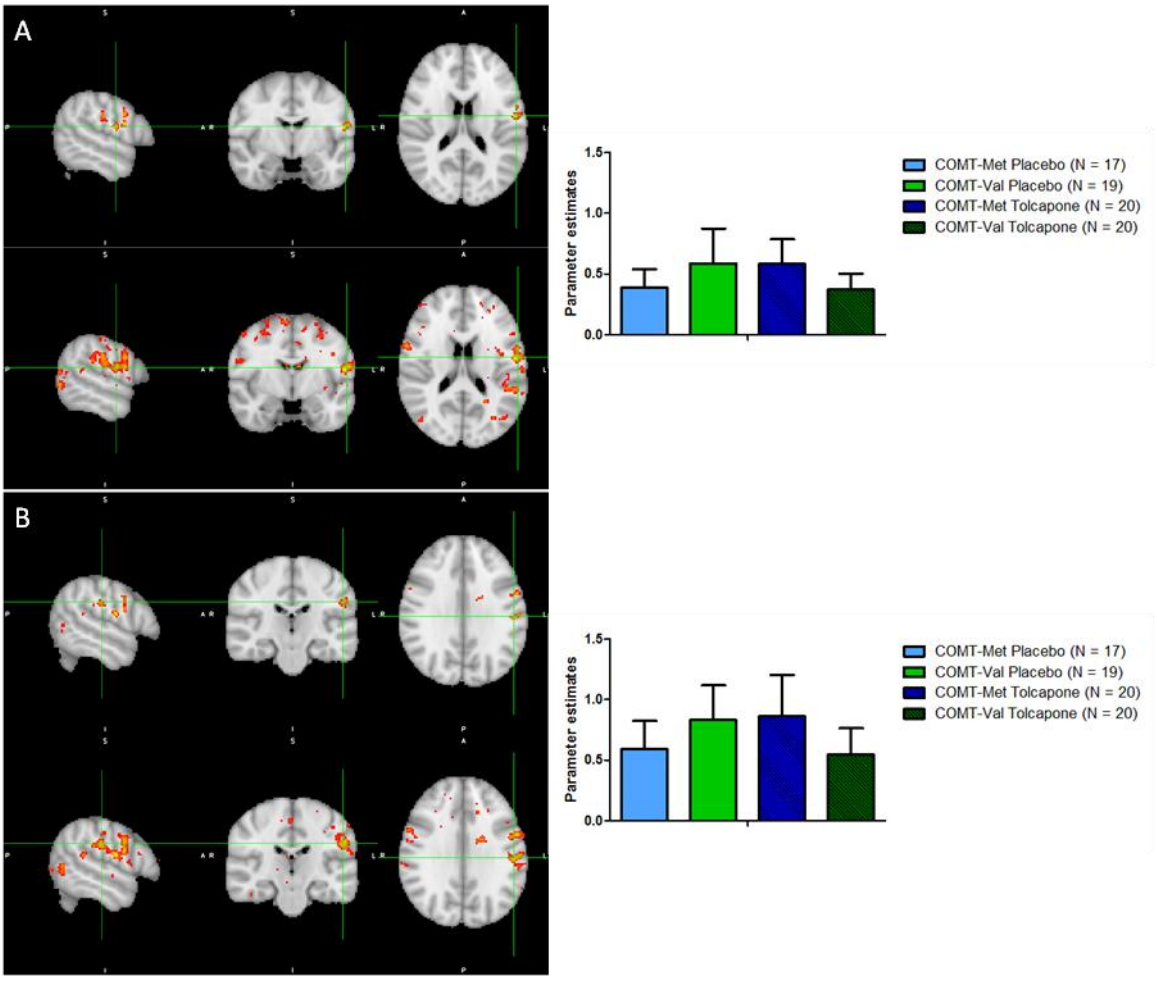


Figure 6.7 - COMT-genotype by treatment interactions for the left vlPFC-seed.

Greater FC for COMT-Val homozygotes on placebo between the left vlPFC seed and two separate clusters compared to COMT-Met homozygotes on placebo. Tolcapone reversed this difference, increasing FC between these areas for COMT-Met homozygotes, and decreasing connectivity in COMT-Val homozygotes, compared with their respective placebo groups.

A: Cluster 1: post-and pre-central gyrus, BA43, extending into BA6 and 9 (Z=4.32, p=0.002, peak voxel location: x=-54, y=-8, z=-18, cluster size=127 voxels).

B: Cluster 2: left anterior supramarginal gyrus, extending into post-central gyrus, BA2 and BA40 (Z=3.99, p=0.011, peak voxel location: x=-54, y=22, z=30, cluster size=93 voxels).

Images thresholded at Z>3.1 (top figure) and Z>2.3 (bottom figure), p<0.005 corrected. Right figure shows mean PEs from the significant cluster. Error bars denote standard deviation.

Table 6.3 - Left vlPFC seed connectivity.

Table 6.3a **Images thresholded at Z>3.1, p<0.005 corrected**		**Brain area / BA**	**Side**	**Cluster size (voxels)**	**Max voxel location (x,y,z)**	**MNI max (x,y,z)**	**Z-max**	**p-value**
Left vlPFC seed								
Positive correlation								
Negative genotype by treatment interaction								
	Cluster 1	Post- and pre- central gyrus, BA43, extending into BA6, and BA9	L	127	72, 59, 45	-54, -8, 18	4.32	0.002
	Cluster 2	Supramarginal gyrus, anterior, post-central gyrus, BA2 and BA40	L	93	72, 52, 51	-54, 22, 30	3.99	0.011
Table 6.3b **Images thresholded at Z>2.3, p<0.005 corrected**								
Left vlPFC seed								
Positive correlation								
Placebo>tolcapone	Cluster 3	Paracingulate gyrus, extending in BA9, BA10 and BA32	L+R	463	50, 88, 44	-10, 50, 16	3.57	0.0005
	Cluster 2	Superior frontal gyrus, frontal pole, BA8, edge of the brain BA6	L	318	47, 92, 56	-4, 58, 40	3.94	0.008
	Cluster 1	Paracingulate gyrus, frontal medial cortex, extending into BA10, BA11, and BA32	R+L	298	38, 85, 34	14, 44, -4	4.47	0.012

6.3.5.2 *Right dlPFC seed*

Greater FC was found for COMT-Met homozygotes as compared to COMT-Val homozygotes (regardless of treatment), between the right dlPFC cortex seed and the middle temporal gyrus, extending into the posterior supramarginal gyrus (Z=4.15, p=0.014, peak voxel location: x=71, y=40, z=38, voxel size=89 voxels, **Table 6.4 and Figure 6.8)**.

Moreover, a significant genotype by treatment interaction was found, driven by a greater connectivity between the right dlPFC seed and the middle temporal gyrus posterior extending into the inferior temporal gyrus posterior for COMT-Met homozygotes on placebo, compared to COMT-Val homozygotes on placebo, with tolcapone reversing this difference, increasing FC for COMT-Val homozygotes and decreasing it for COMT-Met homozygotes (Z=4.52, p=0.0009, peak voxel location: x=-60, y=-30, z=-18, voxel size=139 voxels, p=0.0009) (**Table 6.4 and Figure 6.9)**.

Complementary analysis

Again, for completeness, data was also analysed for Z>2.3 p<0.05 (See **Table 6.5**). In addition to the results described above, greater FC for COMT-Met homozygotes compared to COMT-Val homozygotes (regardless of treatment) were also found between the right dlPFC and occipital, parietal and frontal regions (see **Table 6.5b** for more details). Moreover, interactions between COMT genotype and COMT inhibition were now also found in areas including the precuneous and cerebellum. Furthermore, an interaction in the opposite direction (where tolcapone increased FC for COMT-Met homozygotes instead of COMT-Val homozygotes) was also found in the superior frontal gyrus extending into the supplementary motor area (see **Table 6.5b** for more details).

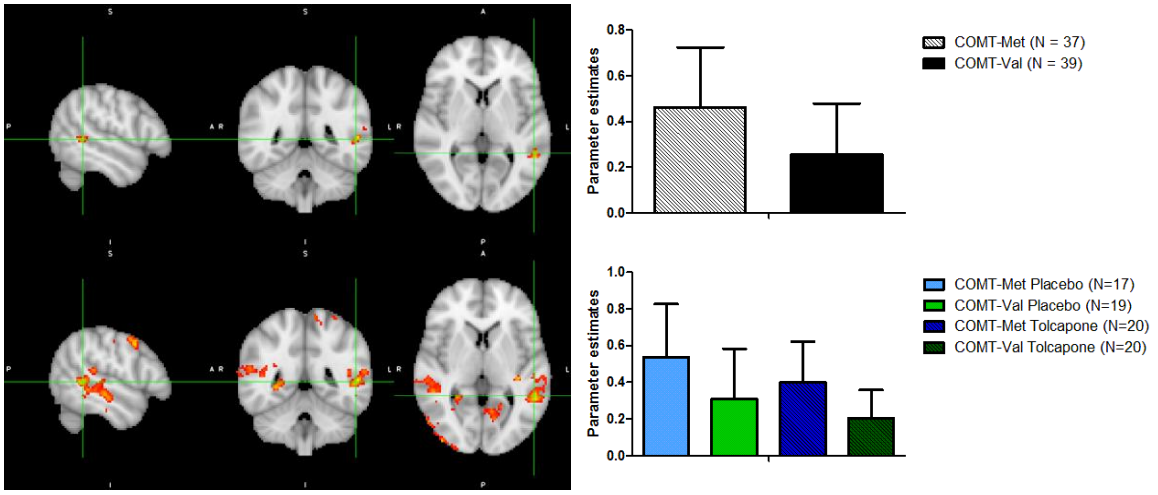


Figure 6.8 - Difference in FC between the right dlPFC for COMT-Met and COMT-Val homozygotes.

Greater FC was found for COMT-Met homozygotes as compared to COMT-Val homozygotes (regardless of treatment), between the right dlPFC seed and the left middle temporal gyrus, extending into the posterior supramarginal gyrus, Brodmann area 21 and 22 (Z=4.15, p=0.014, peak voxel location: x=71, y=40, z=38, voxel size = 89 voxels).

Images thresholded at Z>3.1 (top figure) and Z>2.3 (bottom figure), p<0.005 corrected. Right figure shows mean PEs from the significant cluster. Error bars denote standard deviation.

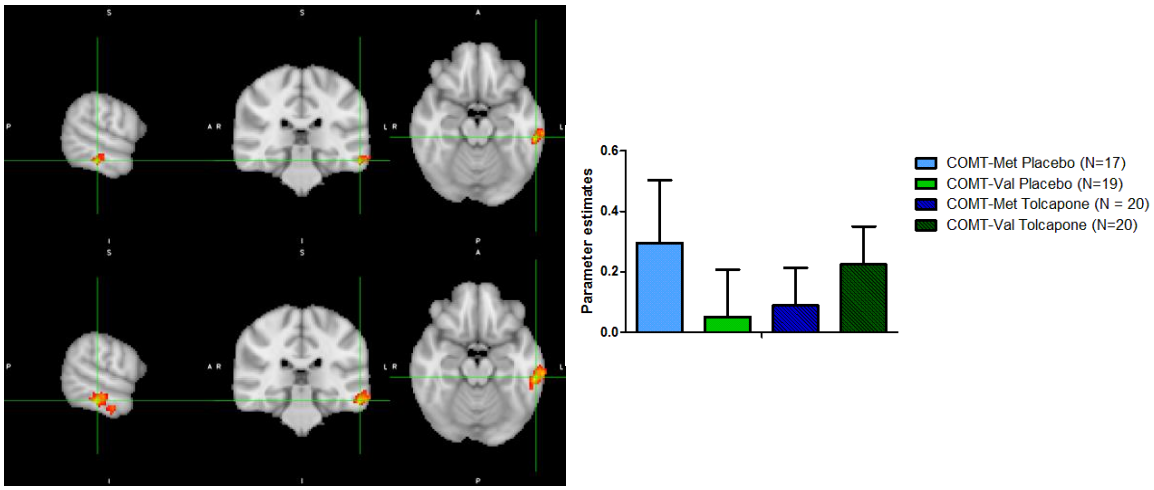


Figure 6.9 - Interaction effect on FC between the right dlPFC and the middle temporal gyrus.

COMT-Met homozygotes on placebo have greater FC between the dlPFC seed and the middle temporal gyrus posterior extending into the inferior temporal gyrus posterior, BA20 and BA21 compared to COMT-Val homozygotes on placebo, with tolcapone reversing this difference, increasing FC for COMT-Val homozygotes and decreasing it for COMT-Met homozygotes (t=4.52, p=0.0009, peak voxel location: x=-60, y=-30, z=-18, voxel size=139 voxels).

Images thresholded at Z>3.1 (top figure) and Z>2.3 (bottom figure), p<0.005 corrected. Right figure shows mean PEs from the significant cluster. Error bars denote standard deviation.

Table 6.4 – Right dlPFC seed connectivity.

Table 6.4a **Images thresholded at Z>3.1,** **p<0.005 corrected**		**Brain area / BA**	**Side**	**Cluster size (voxels)**	**Voxel max location (x,y,z)**	**MNI max (x,y,z)**	**Z-score**	**p-value**
Right DlPFC seed								
Positive correlation								
COMT-Met > Val								
	Cluster 1	Middle temporal gyrus, extending into the supramarginal gyrus posterior, BA21 and BA22	L	89	71,40,38	-52,-46,4	4.15	0.014
Positive COMT genotype by treatment interaction								
	Cluster 1	Middle temporal gyrus posterior extending into the inferior temporal gyrus posterior, BA20 and BA21	L	139	75,48,27	-60,-30,-18	4.52	0.0009
Table 6.4b **Images thresholded at Z>2.3,** **p<0.005 corrected**								
COMT-Met > Val								
	Cluster 1	Middle temporal gyrus, extending into the supramarginal gyrus posterior, BA21 and BA22, planum temporale BA42	L	1103	71,40,38	-52,-46,4	4.15	<0.001
	Cluster 2	Lateral occipital cortex inferior extending into superior, BA19, extending into angular gyrus, BA39, BA22, BA40 and middle temporal gyrus	R	890	21,22,41	48,-82,10	4.10	<0.001
	Cluster 3	Occipital pole, BA18, BA19, not connected to BA30, BA31, super and intracalcarine cortex, BA37, lingual gyrus, BA19	R	763	39,16,49	12,-94,26	4.13	<0.001
	Cluster 4	Intra and super calcarine cortex, precuneous cortex, BA30, lingual gyrus, BA18	L+R	711	51,30,42	-12,-66,-12	3.93	<0.001

	Cluster 5	Superior frontal cortex, BA8, extending into BA6	L+R	555	47,84,60	-4,42,48	3.96	<0.001
	Cluster 6	Pre-central gyrus, BA6, BA4, extending into middle frontal gyrus		456	63,59,57	-36,-8,42	4.02	<0.001
	Cluster 7	Post-central gyrus, extending into central opercular cortex, and parietal operculum cortex, supramarginal gyrus		415	22,53,52	46,-20,32	3.67	0.001
	Cluster 8	Pre-central gyrus, BA4, extending into post-central gyrus and superior parietal lobule BA5		257	52,49,72	-14,-28,72	3.40	0.03
Positive COMT genotype by treatment interaction								
	Cluster 1	Precuneous cortex, BA7, BA31, extending in cingulate posterior	L+R	437	50,32,51	-10,-62,30	3.77	<0.001
	Cluster 2	Middle temporal gyrus posterior extending into the inferior temporal gyrus posterior, BA20 and BA21	L	139	75,48,27	-60,-30,-18	4.52	0.001
	Cluster 3	Cerebellum pyramis gray matter, extending into the cerebellar tonsil and semi-lunar lobule	R	313	27,29,18	36,-68,-36	3.73	0.009
	Cluster 4	Cerebellum pyramis gray matter, extending intosemi-lunar lobule	L	245	60,22,18	-30,-82,-36	3.72	0.040
Negative COMT genotype by treatment interaction								
	Cluster 1	Superior frontal gyrus, BA6, extending in supplementary motor cortex	R+L	311	40,62,70	10,-2,68	3.61	0.009

6.4 Discussion

This chapter has three main findings: (1) COMT genotype modulates FC of the DMN, with significantly greater temporal correlation (coherence) for the COMT-Val homozygotes in a cluster in the right frontal pole with the rest of the DMN, compared to the COMT-Met homozygotes, (2) COMT inhibition influences rsFC of the visual medial network, parietal motor network, language network and motor superior network regardless of genotype. In particular, tolcapone decreased the FC between the SMN and a cluster in both the right parietal lobe and left striatum. (3) COMT genotype and COMT inhibition interact to influence the FC of the SMN. On placebo COMT-Val homozygotes had greater FC between this RSN and two clusters in the left PFC compared to COMT-Met homozygotes on placebo. Tolcapone reversed this difference, increasing FC in these areas in COMT-Met homozygotes whilst decreasing connectivity in COMT-Val homozygotes.

6.4.1 *Seed analysis*

Seed-based analysis revealed interaction effects of COMT genotype and COMT inhibition on FC between the left vlPFC and two independent clusters in the left parietal lobe, as well as a COMT genotype and tolcapone interaction modulating FC connectivity between the right DLPFC and a brain area in the left temporal cortex. Greater temporal coherence was found for COMT-Val homozygotes on placebo between the left vlPFC seed and a brain area surrounding the left post- and pre-central gyrus. Tolcapone reversed this difference, increasing FC between these areas for COMT-Met homozygotes, and decreasing connectivity in COMT-Val homozygotes. Conversely, tolcapone increased FC in COMT-Val homozygotes between the right dlPFC seed and a cluster in the middle temporal gyrus as compared to placebo, whilst it decreased FC for COMT-Met homozygotes compared to placebo. Therefore, the effects of COMT genotype and COMT inhibition on rsFC are not well defined and seem to depend on the specific RSN's and brain areas studied. COMT-Val and COMT-Met can be related to both increased and decreased FC, and tolcapone can reverse in either direction as well.

6.4.2 *Results in relationship to other analysis methods*

The same conclusion can be drawn when comparing previous literature studying the effect of COMT genotype on rsFC with other methods than ICA. **Table 6.5** gives a summary which does not show a clear consistent pattern of results. To complicate things even further, Meyer et al., (2016)

used a graph network analysis approach with the anterior mPFC as a seed and observed a significant age-dependent reversal of COMT Val^{158}Met effects on rsFC. COMT-Val homozygote adults exhibited increased FC between the anterior mPFC and ventrolateral as well as the dlPFC, and parahippocampal gyrus compared to COMT-Met homozygotes, whilst COMT-Val homozygote adolescents showed decreased connectivity for all reported regions (Meyer et al., 2016). Next to age, sex has also been shown to influence rsFC (Hjelmervik et al., 2014). Therefore, next to differences in method used to analyse the data, variation in age and gender also make comparing different studies that investigated the effect of COMT genotype on rsFC challenging. Even when analysis method used (ICA) and participant demographics are almost identical (young healthy men) (as with (Tunbridge et al., 2013) results can differ. I was unable to replicate Tunbridge et al., (2013) who showed increased rsFC for COMT-Val homozygotes between the left vlPFC and ECN compared to COMT-Met homozygotes. The left vlPFC mask used in the current study's seed analysis was based on the exact coordinates of Tunbridge et al., (2013). However, no COMT genotype related FC differences were found with regions of the ECN (parietal only).

In sum, COMT genotype influences the FC of frontal regions of the brain, though the exact clusters and direction of the findings do not show a consistent pattern. I could only speculate that the increased connectivities between DMN and PFC in the Val-homozygous group could possibly reflect a compensatory effect for the decreased prefrontal related connectivities or the recruitment of cognitive resources to maintain normal cognitive function. Moreover, COMT influenced dopamine signalling also seems to influence the connectivity from the prefrontal lobes to the posterior regions of the brain. Given the links between these frontal and parietal regions in for example working memory processing this might not be surprising (e.g. (Berryhill and Olson, 2008). Furthermore, the effects of COMT genotype on rsFC within the SMN are supported by a recent review of (Nogueira et al., 2019) who show that COMT genotype influences motor function. For example, spatial working memory could be the link as it has an important role in the initial phases of motor learning and in the learning rate in both visuomotor adaptation and sequential motor tasks (Nogueira et al., 2019).

6.4.3 *COMT inhibition*

No previous studies investigated the effect of COMT inhibition on rsFC. Therefore, my findings that tolcapone influences the FC of the visual medial network, parietal motor network, language network and motor superior network need to be replicated before conclusions can be drawn. There seems no reason to believe that COMT is expressed more in these regions than in the PFC. As I

corrected for CBF (however, note limitations of our method used) it is also unlikely that these results can be attributed to differences in CBF alone.

6.4.4 *Conclusion*

Resting state connectivities within the prefrontal lobes, and from the prefrontal lobes to the posterior regions, seem to be modulated by COMT. However, COMT's effects on connectivity are complex, with the directionality depending on for example the brain areas and networks studied. COMT's significance therefore extends beyond the dlPFC, and complex but subtle effects of genotype and inhibition are found. It is therefore difficult to delineate or predict exact functional correlates. Rather than grossly altering the overall extent of FC of the frontal cortex, COMT instead subtly modulates the precise neural circuitry used to process information.

Table 6.5 - Summary of previous literature studying the effects of COMT genotype on rsFC.

Authors	Method	Result
Tunbridge et al., 2013	ICA Males only	COMT-Val homozygotes greater FC between left vlPFC (left insula and inferior frontal gyrus) and ECN compared to COMT-Met homozygotes.
Meyer et al., 2016	Seed based analysis Males + females Adults + adolescents	COMT-Val homozygotes greater FC between anterior mPFC and vlPFC + dlPFC + parahippocampal gyrus compared to COMT-Met homozygotes.
Liu et al., 2010	Graph theory Males + females	COMT-Val homozygotes decreased FC between PFC and DMN compared to COMT heterozygotes. Specific areas: Left superior frontal cortex and anterior medial PFC; left superior frontal cortex and ventromedial PFC; left superior frontal cortex and posterior cingulate cortex; anterior medial PFC and posterior cingulate cortex; medial PFC and retrosplenial; ventral medial PFC and right inferior temporal cortex; left superior frontal cortex and left inferior temporal cortex; right inferior temporal cortex and retrosplenial. COMT-Val homozygotes greater connectivity between: left inferior temporal cortex and left parahippocampal gyrus; left inferior temporal cortex and right parahippocampal gyrus; left lateral parietal cortex and cerebellum, compared to COMT-heterozygotes.
(Tian et al., 2013)	Seed based analysis Males + females	Analysed and extracted GM volume differences between COMT-Val homozygotes and COMT heterozygotes and used these as seeds to compute FC with the rest of the brain. COMT-Val homozygotes decreased FC between right posterior cingulate cortex (DMN) and left medial frontal pole. The rsFC analysis revealed that both the PCC and mSFG were functionally correlated with brain regions of the default mode network (DMN). Both of these regions showed decreased rsFCs with different parts of the frontopolar cortex of the DMN in COMT-Val homozygotes compared to COMT heterozygotes (COMT-Val homozygotes decreased rsFC between the right PCC and the left medial frontal pole)
Markett et al., 2016	Eigenvector centrality (EC) derived from graph theory Males + females	COMT-Val homozygotes greater FC in key regions of the DMN (BA39, angular gyri, inferior parietal lobules, bilateral middle temporal gyri and dlPFC) compared to COMT heterozygotes. COMT-Val homozygotes decreased connectivity in somatomotor network (pre and postcentral gyri and paracentral lobule) compared to COMT-Met heterozygotes.

Chapter 7 The interaction between COMT genotype and COMT inhibition on the stress response and stress related brain activity

7.1 Introduction

In Chapter 3 I demonstrated that the MIST is suitable as a stressor to investigate the impact of COMT genotype and COMT inhibition on cognitive function under conditions of stress. In this chapter I will now present the findings of the MIST conducted in the MRI scanner and the effects that COMT genotype and COMT inhibition have on the elicited stress response, both in terms of physiological responses as well as on brain activity.

7.1.1 *MIST related brain activation*

A wide range of different brain areas seem to be engaged by the MIST. As also outlined in Chapter 1, by using the MIST in fMRI and PET settings, Dedovic and others (Dedovic et al., 2009b, 2009c, 2005) showed that the induced cortisol response was positively associated with a deactivation (control > stress contrast; see also methods section) of specific parts of the limbic system, including hypothalamus, hippocampus, amygdala, and medio-orbitofrontal cortex. Interestingly, cortisol non-responders fail to show this deactivation pattern, showing overall much weaker signs of signal reduction, especially in the hippocampus (Pruessner et al., 2008). The MIST seems to result in decreased activity in other brain areas as well. Conversely, increases in activity (stress > control contrast) have also been found. **Table 3.1** showed an overview of studies previously reporting the effects of the MIST on physiological responses. I present an overview of different brain areas being activated and deactivated in **Table 7.1**.

7.1.2 *Dopamine and stress*

Chapter 1 outlined the role of dopamine in the stress response. The MIST however, does not consistently increase striatal dopaminergic activity but seems to increase dopaminergic activity in the mPFC (Hernaus et al., 2015; Lataster et al., 2011; Nagano-Saito et al., 2013; Vaessen et al., 2015) and temporal cortex (Hernaus et al., 2015) more reliably (suggested to be related to the magnitude of the evoked stress response). Therefore, it is suggested that across brain regions, stress related dopaminergic activity is correlated with the intensity of the stressor (Vaessen et al., 2015). Moreover, the task-induced mPFC BOLD response predicts efficacy of the MIST for stress induction

(Dedovic et al., 2009b) in contrast with limbic activity being suppressed (Pruessner et al., 2008). mPFC dopaminergic activity seems to be more directly related to the experience of stress, serving modulatory purposes as a threat evaluation system (Vaessen et al., 2015). See **Table 7.2** for an overview of MIST dopamine PET studies and their results.

7.1.3 *COMT and stress*

Given the evidence that dopaminergic signalling is involved in the psychological stress response, it was hypothesized that COMT could have an effect on the PFC dopaminergic response to stress, influencing stress sensitivity. In line with this hypothesis, Hernaus et al., (2013) showed that COMT-Met carriers showed less [18F]-fallypride displacement than Val-homozygotes (therefore COMT-Val homozygotes had more dopamine release or a reduced dopamine degradation) in the left posterior superior and right inferior frontal gyrus as a result of the MIST. Additionally, COMT-Met-carriers experienced larger subjective stress responses than Val-homozygotes. The human stress response may therefore be mediated in part by COMT-dependent dopaminergic PFC activity and the inverted-U relation between stress and PFC dopaminergic functioning might be COMT-dependent (Hernaus et al., 2013).

In animal studies, transgenic mice overexpressing human COMT-Val polymorphism showed a blunted stress response, while COMT knock-out, “Met-like” mice exhibited increased stress response (Papaleo et al., 2008). There is some evidence for COMT genotype effects on the physiological and neural stress response in humans as well. Previous studies showed that COMT-Met homozygotes had greater cortisol responses after stress, but these studies were in patients, adolescents or children only (Armbruster et al., 2012; Jabbi et al., 2007; Oswald et al., 2004; Walder et al., 2010). Moreover, none of these studies induced stress with an acute laboratory stressor. They either conducted longitudinal studies taking normal life stressors into account or induced the stress response via pharmacological agents. In fact, a previous study that used the TSST to induce stress did not find any effects of COMT genotype on the stress response (Buckert et al., 2012).

To my knowledge there is no previous literature investigating the effects of COMT genotype, COMT inhibition or their interaction on stress-related brain activity or physiological changes induced by the MIST.

7.1.4 *Aims and predictions*

The main aim of this Chapter is to validate and to demonstrate the neural effects of the stress response induced by the MIST in the MRI scanner in our hands, needed to be able to investigate the interaction between COMT genotype, COMT inhibition and working memory under conditions of stress (Chapter 8). I predict that:

- **the MIST will cause a significant increase in salivary cortisol, sAA and subjective stress,**
- **and that similar brain regions will be engaged to those previously associated with acute mild stress as induced by the MIST (Table 7.1).**

Secondary to this main aim, as some literature suggested that the stress response may be mediated in part by COMT-dependent dopaminergic PFC activity, and that the inverted-U relationship between stress and PFC dopaminergic functioning might be COMT-dependent, I also explored whether COMT genotype and COMT inhibition impacted on the physiological and neural responses to acute stress (as induced by the MIST).

Table 7.1 - Overview of studies that used the MIST in an MRI setting, and their findings on brain activity in healthy volunteers.

Authors	MRI	Participants (age)	Brain areas activated / deactivated
(Dedovic et al., 2005)	1.5 Tesla	N = 22 healthy males (range: 20-24)	Contrast: stress > rest → activations in visual association cortices, angular cortex, sensory cortex, motor cortex, thalamus and caudate nucleus.
(Pruessner et al., 2008)	1.5 Tesla	N = 40 20 males (23.35 ± 3.17) 20 females (22.75 ± 3.11)	Contrast: stress > control → Activations in the left premotor area, the medial left PFC, bilaterally in the area of the cingulum/white matter and occipital cortex. Contrast control > stress → Deactivations in limbic system ventral striatum, hypothalamus, amygdala and hippocampus. Responding with a cortisol increase was associated with a decrease of activity in limbic system components. Cortisol non-responders: Contrast: control > stress → Deactivations in the medio-orbitofrontal cortex and temporal pole. Cortisol responders: Contrast: control > stress → Deactivations in right medio-orbitofrontal cortex / inferior frontal gyrus, temporal pole, left and right hippocampus, amygdala, hypothalamus, anterior cingulate cortex and dorsolateral PFC. Correlating the amount of deactivation with AUC_i cortisol showed significant correlation with deactivation in the hippocampus, but not with anterior cingulate.
(Dedovic et al., 2009c)	3 Tesla	N = 28 healthy males (23 ± 4.48)	Contrast: stress > control → Activation in the left ventrolateral PFC, occipital lobe, cerebellum, cingulum, bilateral anterior insula, right hippocampal tail + left hippocampal tail fimbria, inferior frontal gyrus / premotor gyrus and supramarginal/angular gyrus. Contrast: control > stress → Deactivations in bilateral frontal poles, left ventral medial and bilateral orbitofrontal cortex, left superior frontal gyrus, right hippocampus head, bilateral putamen, bilateral temporal poles, bilateral posterior insula, left dorsolateral PFC, bilateral posterior cingulate and bilateral precuneus.
(Khalili-Mahani et al., 2009)	1.5 Tesla	N = 19 healthy males (range: 20-28)	Contrast: stress > control → Deactivations in the medial orbitofrontal gyri, nucleus accumbens, anterior medial temporal area. Overall: correlation between left hippocampus deactivation and AUCi (r=0.47, p<0.04).
(Lederbogen et al., 2011) Same subjects as (Boehringer et al., 2015)	3 Tesla	N = 32 healthy 16 males 16 females (43.6 ± 14.4)	Contrast: stress > control → Activations in right temporoparietal junction, bilateral hypothalamus, anterior & posterior cingulate cortex, precuneus, right superior temporal sulcus, bilateral insular cortex, supplementary motor area, occipital cortex.
(Dedovic et al., 2014)	1.5 Tesla	26 healthy controls (12 males; 14 females) 23 subclinical depressed (12 males; 14 females)	Contrast: stress > no-evaluation maths → Activation in the right posterior mid-temporal gyrus, right posterior cingulate cortex, right mid-cingulate cortex, right cuneus and insula, right lingual gyrus, right cerebellum, left mid-cingulate cortex, left tempo parietal junction, left precentral gyrus, left postcentral gyrus, thalamus, bilateral temporoparietal junction and cerebellum. Contrast: no-evaluation maths > stress → 'Deactivations' in the right lateral orbitofrontal cortex and right subgenual anterior cingulate.
(Orem et al., 2019)	3 Tesla	239 healthy 126 males 113 females (19.44 ± 0.07)	Contrast: stress > control → fMRI signal within the dlPFC, dmPFC, posterior cingulate, hippocampus, and amygdala was positively related to SCR ($p < .05$, corrected). In addition, differential fMRI signal within the dlPFC, vmPFC, and cingulate cortex was positively related to subjective stress ratings ($p< .05$, corrected).

Table 7.2 - Overview of studies that used the MIST in a PET setting and measured dopamine release / CBF in healthy volunteers.

Authors	PET method	Participants (age)	MIST procedure	Significant cortisol response	Other measures	Brain areas
(Pruessner, 2004)	[11C]Raclopride	N = 10 5 high parental care, 5 low parental care 1 female 9 males (21-30)	Standard Rest and stress on two separate days.	Saliva Yes	Significant effects on state anxiety, VAS-Stress, HR, body temperature and skin conductance.	Stress increased extracellular levels of dopamine in bilateral ventral striatum in subjects reporting low parental care only. Cortisol response was significantly correlated with dopamine release in the ventral striatum, consistent with a facilitating effect of cortisol on dopamine neuron firing.
(Dedovic et al., 2005)	PET1: [11C]Raclopride Basal ganglia PET2: [H2^{15}O]	PET1: N = 10 1 female, 9 males (21-30) PET 2: N = 10 males, (20-25)	PET1: standard PET2: standard CBF	Saliva PET1: Yes PET2: Yes	NA	PET1: stress increased extracellular levels of dopamine in bilateral ventral striatum. PET2: increases in CBF in the area of the visual association cortex and angular gyrus.
(Pruessner et al., 2008)	[H2^{15}O)	N = 10 males (25.4 ± 2.5)	Standard CBF	Saliva Yes	N/A	Contrast: stress > control → no significant results. Contrast: control > stress → Deactivations → Reduced CBF in a network of structures linked to the limbic system, i.e. hippocampus and amygdala, ventral striatum, dorsal and ventral medial PFC including anterior cingulate cortex. Moreover, also deactivations bilaterally in the superior temporal gyrus and right superior insula. Responding with a cortisol increase was associated with a decrease of activity in limbic system components.
(Soliman et al., 2008)	[11C]Raclopride	N = 10 9 females 1 male (22 ± 1.1)	Three blocks of stress 12 min each (in four 3-min segments). Negative feedback after each 3-min segment. Vs. control blocks	Saliva Yes	Significant effects on state anxiety, VAS-stress, HR and EMG-response. No effects on SC.	No differences in dopamine release for the healthy controls.
(Lataster et al., 2011)	[18F]Fallypride	N = 12 (39.8 ± 15.8)	Standard vs control blocks	Blood Yes	Significant effects on subjective stress	Stress increased dopamine release throughout the PFC, with dopaminergic activity in bilateral ventromedial PFC being associated with subjectively rated experiences of psychosocial stress.
(Mizrahi et al., 2012)	[11C]-(+)-PHNO	N = 34 12 matched healthy controls 5 females 7 males	Standard vs control blocks	Saliva No	Significant effects on subjective stress	No differences in healthy controls. Positive association between dopamine release with stress-induced cortisol in associative striatum, sensorimotor striatum and whole striatum.

		(26.08 ± 3.83)				
(Suridjan et al., 2012)	[11C]-(+)-PHNO	N = 11 males (26 ± 3.87)	Standard vs control blocks	N/A	Significant effects on state anxiety	No differences in dopamine release. Neuroticism-related traits such as angry-hostility, vulnerability and depression were related to a blunted dopamine response in the D2-rich and D2/3-mixed regions.
Mizrahi et al., 2013	[11C]-(+)-PHNO	N = 12	Standard vs control blocks with control on separate day	Not reported	Significant effects on subjective stress and state anxiety	No differences in healthy controls.
(Hernaus et al., 2013)	[18F]Fallypride	N=12	Standard vs control, but longer duration (66 min of stress)	N/A	Significant effects on subjective stress	Same as Pruessner et al., 2004 and Lataster et al., (2011).
(Nagano-Saito et al., 2013)	18F]Fallypride	N = 11 males (18-30)	Six blocks of stress, 12 min each (in four 3 min segments) in a 3-hour PET scan. Negative feedback after each 3minute segment	Saliva No	Significant effects on subjective stress, HR and SC	Stress increased dopamine release in the dorsal part of the medial PFC corresponding to the rostal part of the cingulate motor zone. The greater the stress induced decrease in PET [18F]Fallypride the greater the stress induced increases in heart rate. ROI analysis a trend for decreases in [18F]Fallypride in the left caudate, right putamen, dmPFC, vmPFC, PCG and left and right thalami.

Note: Standard MIST as by Dedovic et al., 2005: rest vs. five 6-minute runs of stress, with negative feedback in between.
Standard MIST to measure CBF as by Dedovic et al., 2005: 3 consecutive sessions of stress, 3 consecutive sessions of control, and 3 consecutive rest sessions lasting 1 minute - counterbalanced among subjects. Repeated 9 times (3 times for each condition).
Non-stressed control: similar arithmetic task as in stress condition, but without time constraints, visible progress bar or negative verbal feedback.

7.2 Methods

I conducted a randomised, double-blind, placebo-controlled, between-subjects study of the effects of COMT genotype and COMT inhibition on physiological measures and brain activation under conditions of acute stress. As all of the participants did the stressor version of the MIST, control in this chapters stands for blocks with mental arithmetic without social evaluative treat.

7.2.1 *Participants, study design, and procedure*

For information on participants, study design and procedure see Chapter 4. Cortisol responders and non-responders were defined as in Chapter 3.

7.2.2 *Task - MIST*

The MRI scanner version of the MIST was similar to that employed in the pilot study (see Chapter 3), except that there was no control group (all participants performed the stressor version of the MIST). Moreover, 30 seconds of rest was added before each control block. These rest blocks showed the MIST starting screen without any mathematical equations. The control block in this study refers to the block where participants answered mental math questions when no performance indicators were shown, nor was a time limit enforced. Stress blocks were similar as in Chapter 3.

The total duration of each MIST session was 7 minutes. Each session consisted of two 30 seconds rest blocks, 1-minute control problems ('response not recorded'), alternated with two 2-minute stress problems ('response recorded') (rest, control, stress, rest control, stress). There were three MIST sessions in total, alternated with negative verbal feedback in between.

The verbal description of the MIST was also slightly adapted to make it fit with the MRI procedure. See appendix for full details (Appendix II). Briefly, as in the pilot, the first round of feedback focussed again on that participants had to improve their performance to reach minimum performance requirements. During the second round of feedback participants overheard a phone conversation between me (the main researcher) and the 'Professor' (the confederate: either Prof. Harrison, Prof. Tunbridge or Dr. Mould) providing additional negative feedback, and discussing the participant's (poor) performance. The confederate then attended the MRI-control room, where we further discussed the participants' poor performance, addressing the participant directly. The participant then undertook the last block of the MIST in the presence of the confederate. At the

end of the final block, the confederate then told the researcher that there was no time to try again and hope that some useful data were obtained and to come and discuss the participant's difficulties achieving criterion after the participant had gone (Appendix II).

7.2.3 *Measurements of stress response*

A schematic of the experimental procedure is shown in **Figure 4.1**. Physiological measures of stress, including salivary cortisol and sAA, together with subjective stress and mood ratings, were recorded at 30-minute intervals throughout the experiment. To give participants the saliva swab, I entered the scanner room to place the swab inside the participant's hand. They were then asked to place the swab under their tongue, without moving their head (I piloted this procedure prior to commencing the study to ensure that it did not result in significant motion artefacts). After two minutes I collected the swab wearing sterile gloves.

The first three time points (T1-3) were at 30 minute intervals in the 90 minutes prior to scanning; T4 occurred when the participants were just in the scanner (after localiser); T5 was between the resting state and structural scan; T6 corresponded to the time point during the second feedback period of the MIST (where investigator phoned confederate); T7 was taken at the end of the MIST right before the start of the N-back; T8 was the last time point taken at the end of scanning, and T9 followed after debriefing.

Subjective reports of alertness, drowsiness, stress, happiness, sadness, anxiety and nausea were assessed using VASs at time points outside of the scanner. In the scanner participants completed stress VASs only.

Cortisol and sAA levels were determined as in Chapter 2.

7.2.4 *Behavioural analyses*

7.2.4.1 *Main analysis – overall effects of the MIST*

To validate the overall stress response across participants, the effects of the MIST on the psychological and physiological measures were explored using repeated-measures ANOVAs with time as the within-subjects factor. Raw data (rather than % baseline) and all time points (including the 5 baseline measures) were used for these analyses; VAS, cortisol and sAA were log-transformed as they were non-normally distributed. Huynh-Feldt correction was applied where data failed Mauchly's Test of Sphericity.

7.2.4.2 *Main analyses – group differences*

Since the autonomic stress response is brief, T6 (i.e. during the MIST) was prespecified as primary time point of interest for sAA and subjective ratings of stress. In contrast, cortisol levels rise more slowly after stress, peaking after 20 minutes (Kudielka et al., 2009). Thus, T8, which occurred approximately 25 minutes after the MIST, was defined as the primary time point of interest for cortisol levels. Values at these pre-determined time points were compared between conditions (control vs. stress) using t-tests or Mann-Whitney U tests as appropriate.

7.2.4.3 *Exploratory analyses – group differences*

The effects of the MIST on the psychological and physiological measures were explored using repeated-measures ANOVAs with time as the within-subjects factor and genotype (COMT-Val or COMT-Met) and drug (placebo or tolcapone) as the between-subjects factors. Raw data (rather than % baseline) and all time points (including the 5 baseline measures) were used for these analyses; VAS, cortisol and sAA were log-transformed as they were non-normally distributed. Huynh-Feldt correction was applied where data failed Mauchly's Test of Sphericity. Planned post-hoc comparisons (defined as time points in main analyses) were explored regardless of overall significance.

7.2.4.4 *Correlations*

Correlational analyses were conducted (Spearman's rho, given the non-normal nature of many of the variables) to investigate the relationships between physiological and psychological variables, N-back performance (Chapter 8), and personality characteristics. To limit the number of correlations examined, we focussed on the predetermined time points and measures included in the main analyses, with the additional of baseline (T3) VAS stress and anxiety scores, Rotter's Locus of Control and Rosenberg's Self-Esteem measures, and N-back % correct scores for each level.

7.2.5 *Neuroimaging*

MRI scanner environment and protocol of structural scan identical to described in Chapter 5.

7.2.5.1 *Functional MRI protocol*

MIST

Functional imaging consisted of 72 T2-weighted echoplanar imaging (EPI) slices (TR = 1200ms,

TE=30ms, flip angle = 65°, field of view = 216mm, voxel size = 2*2*2 mm, 350 volumes, acquisition time 7min 28 seconds, multiband acceleration factor = 4, PAT GRAPPA acceleration factor = 2).

7.2.5.2 *MRI Analysis methods*

Data were analysed using FSL. The structural anatomical scans were brain extracted using BET (Smith, 2002). fMRI data were pre-processed and analysed using FEAT (FMRI Expert Analysis Tool), version 6.0, part of FSL. Pre-processing involved a number of steps designed to reduce unwanted variability in the data and to improve the validity of statistical analysis. The following steps where therefore implemented for each participant: 1) Removal of non-brain structures using BET (Smith, 2002), 2) motion correction using MCFLIRT (Jenkinson et al., 2002b)), 3) spatial smoothing using a Gaussian kernel of FWHM 5mm, 4) grand-mean intensity normalisation of the entire 4D dataset by a single multiplicative factor and 5) high-pass temporal filtering cut-off = 240s (Gaussian-weighted least-squares straight line fitting, with sigma=120.0s).

A custom 3 column format convolved with a gamma hemodynamic response function, and its temporal derivative was used to model the data. Brain activations and deactivations were specified as (Pruessner et al., 2008) and were as follows: deactivations = control blocks > stress blocks; activations = stress blocks > control blocks. Estimates of control vs rest and stress vs rest were also obtained for reference. I report deactivations to facilitate comparison with previous studies.

The stress blocks were modelled as two separate explanatory variables (EV's) to keep the length of the control block and stress block similar (1 minute). This to make sure the variance of the data was calculated over similar amounts of time for the different conditions.

In addition, functional images were registered to their high-resolution structural scan, via the high contrast functional image and BBR using FLIRT (Jenkinson et al., 2002b; Jenkinson and Smith, 2001). Non-linear registration from structural to MNI standard space was then further refined using FNIRT (Andersson et al., 2007a, 2007b], resampling resolution=2mm. These transformations into standard space were applied to images of contrasts of interest and their variances.

In the second level, the three MIST runs were combined by averaging the BOLD contrasts obtained from the first level analysis with a fixed effect analysis.

Higher level (group level) analysis was carried out using FMRIB's Local Analysis of Mixed Effects (FLAME). To reduce effects attributable to outliers, an automatic outlier deweighting tool was also applied. (Woolrich et al., 2004, 2001)

The general linear model (GLM) included the 4 groups (COMT-Met-Placebo, COMT-Met-tolcapone, COMT-Val-Placebo, COMT-Val-Tolcapone and their interactions). I tested for group

averages and differences between groups for each of the contrasts of interest. Significant activations were identified using cluster-based thresholding of statistical images with a height threshold of Z>3.1 and a family-wise error–corrected cluster significance threshold of p<0.05 was applied to the superthreshold clusters. Clusters thresholded by Z>2.3 are also reported for completeness and to be able to compare our results with previous studies who used this less stringent statistical threshold.

To further visualise the results, individual Parameter Estimates (PE) values were extracted from their custom maps, using significant clusters as binary masks.

All activations and deactivations are reported using MNI coordinates.

7.3 Results

In this chapter I investigated the stress response as induced by the MRI scanner version of the MIST, and the interaction between COMT genotype and COMT inhibition on this evoked stress response, both in terms of physiological responses (presented first) and brain activity (presented second).

7.3.1 *Participants*

Participant demographics are given in **Table 7.3**. The final sample consisted differed slightly from the sample presented in Chapter 5 and 6. Five participants did not complete the study for different reasons. There were scanner problems for two participants, one could not see the task as we were unable to correct vision (astigmatism), one participant panicked during the MIST procedure and therefore asked to stop, and finally one participant did not understand the task instructions even after explaining repeatedly (no button presses) therefore scanning was stopped.

7.3.2 *Physiological effects of the MIST - validation of the stress response*

Cortisol

As presented in **Figure 7.1a,** salivary cortisol levels for the whole group increased over time ($F_{8,536}$=17.3; p<0.001) – with significant differences between baseline (time point 3) and all other time points except 5 (p=0.053) and 6 (p=0.153). Cortisol levels show the expected delay in rise time after stress, indicating that participants overall showed a stress response (likely due to both the MRI scanner and the MIST).

Salivary amylase

Figure 7.1b shows that sAA levels changed significantly over time ($F_{8,512}$=39.1; p<0.001) with the highest amylase values for the time point after debriefing. However, planned post-hoc comparisons show sAA increases as a result of the MIST as well, with significant differences between pre and during (p<0.001) and pre and post-MIST (p<0.001).

Subjective stress

Subjective stress levels increased significantly over time ($F_{8,528}$=32.6; p<0.001), with significant differences between baseline (time point 3) and all other time points except time point 2. Therefore, subjective stress was increased due to both the MRI experience and the MIST (**see Figure 7.1c**).

Correlations

We found few significant correlations between stress indices of different types in our dataset (**Table 7.4**). This applied both to a lack of significant correlations between psychological and physiological stress parameters, and also between one physiological measure and another. Self-esteem correlated negatively with sAA levels during the MIST (rho = -0.290, p=0.016) but would not survive Bonferonni correction for multilpe comparisions. Notably, no correlations were found between cortisol response and self-esteem or locus and control (rho < 0.098, p > 0.465).

Table 7.3 - Participant demographics and personality measures.

	COMT-Met Placebo	COMT-Val placebo	COMT-Met tolcapone	COMT-Val tolcapone
Number	16	19	19	17
Age (years)	22.7 ± 1.0	23.6 ± 1.5	22.9 ± 6.0	25.3 ± 6.6
NART predicted FS-IQ (non-native speakers excluded)	113.7 ± 3.4	111.6 ± 5.7	112.2 ± 5.0	113.3 ± 4.3
Baseline Locus of Control	73.8 ± 2.3	74.7 ± 2.6	75.5 ± 2.1	72.1 ± 3.4
Baseline Self-esteem	32.2 ± 1.5	31.9 ± 1.0	31.7 ± 0.7	32.1 ± 1.2
Baseline State	31.8 ± 2.2	30.9 ± 1.8	33.3 ± 1.3	29.9 ± 1.5
Baseline Trait	39.9 ± 2.7	39.2 ± 2.5	38.5 ± 1.7	35.8 ± 2.4
Ethnicity	Caucasian	Indian 1 Singapore 1 Indonesian 1 Brazilian 1 Pakistan 1	Caucasian	Chinese 1 Pakistan 1 Bangladeshi 1

Values are mean ± SEM. Locus of control: Rotter's Locus of Control Scale; Self-esteem: Rosenberg's Self-esteem Scale; Spielberger's State-Trait Anxiety Inventory

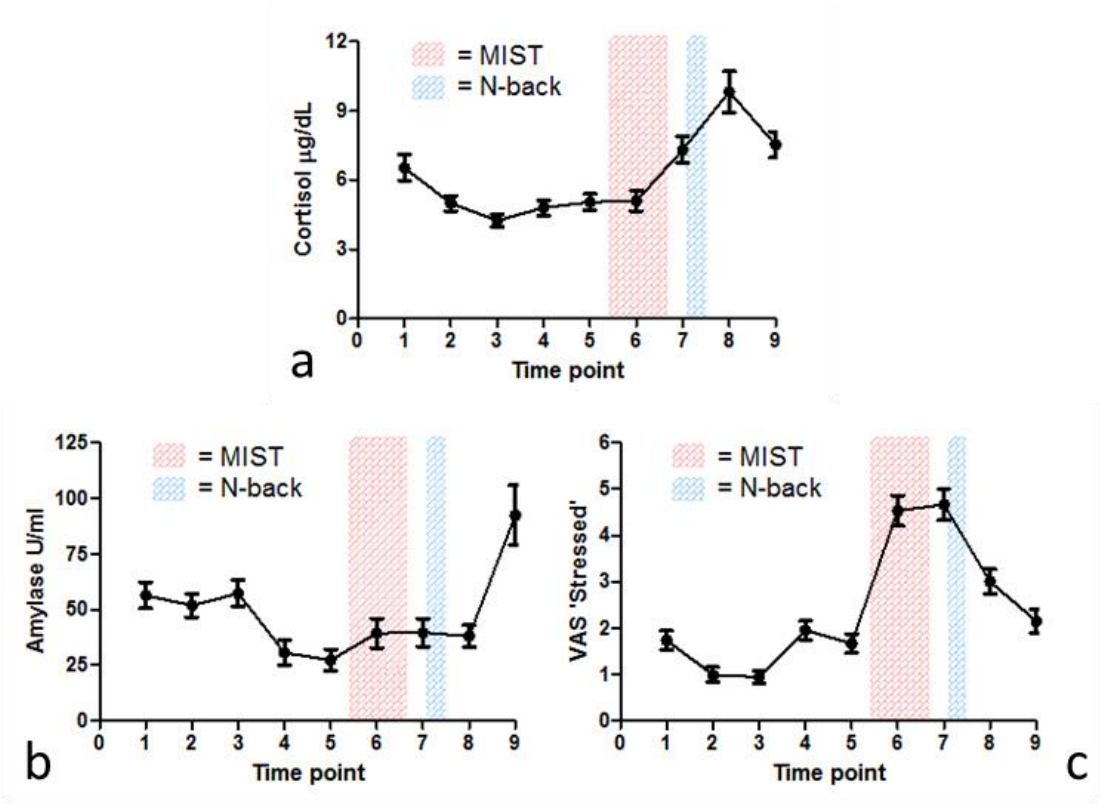


Figure 7.1 - Effects of acute stress exposure by the MRI MIST on physiological and psychological stress measures.

Significant changes in (a) cortisol, (b) sAA and (c) subjective stress over the course of the experiment. Error bars show SEM. For statistical tests see text above.

Table 7.4 - Correlations between different stress indices.

		Self esteem	Locus of control	Baseline VAS 'Stressed' Time point 3	During MIST VAS 'Stressed' Time point 6	Cortisol Time point 8	Cortisol (% baseline) Time point 8	sAA Time point 6	sAA (% baseline)	AUCi cortisol	AUCi cortisol (% baseline)
Self esteem	Spearman's rho	1.000	.320**	-.180	-.189	.045	.031	-.204	-.290*	.016	.089
	p value		.005	.123	.111	.706	.799	.092	.016	.895	.465
Locus of control	Spearman's rho		1.000	-.256*	-.029	.106	.107	.136	-.066	.089	.129
	p value			.027	.808	.380	.375	.265	.592	.466	.288
Baseline VAS 'Stressed' Time point 3	Spearman's rho			1.000	.309**	.024	-.041	-.004	-.054	.122	.043
	p value				.009	.846	.734	.972	.662	.316	.726
During MIST VAS 'Stressed' Time point 6	Spearman's rho				1.000	.178	.206	-.027	.029	.165	.196
	p value					.136	.084	.826	.815	.173	.103
Cortisol Time point 8	Spearman's rho					1.000	.802**	.046	.218	.859**	.692**
	p value						.000	.707	.072	.000	.000
Cortisol (% baseline) Time point 8	Spearman's rho						1.000	-.026	.015	.707**	.880**
	p value							.832	.900	.000	.000
sAA Time point 6	Spearman's rho							1.000	.541**	.096	.010
	p value								.000	.433	.934
sAA (% baseline)	Spearman's rho								1.000	.173	-.037
	p value									.156	.765
AUCi cortisol	Spearman's rho									1.000	.825**
	p value										.000
AUCi cortisol (% baseline)	Spearman's rho										1.000
	p value										

7.3.3 *Group differences – main analyses*

Salivary cortisol

As shown in **Table 7.5** and **Figure 7.2a**, there were no effects of COMT genotype, or tolcapone, nor an interaction between the two, on salivary-cortisol (F's<1.7; p>0.20). Moreover, area under the curve (AUC) measures for cortisol did not differ between groups (F's<2.0; p>0.16) either.

Salivary amylase

As shown in **Table 7.5** and **Figure 7.2b**, there were no effects of COMT genotype, or tolcapone, nor an interaction between the two on sAA (F's<1.2; p>0.27).

Subjective stress

As shown in **Table 7.5** and **Figure 7.2c**, COMT-Val homozygotes reported greater stress levels compared to COMT-Met homozygotes on placebo only (p=0.021), whilst tolcapone increased subjective stress levels in COMT-Met homozygotes only (0.018) (drug x genotype interaction: $F_{1,68}$=7.3; p=0.008).

7.3.4 *Group differences – exploratory analyses*

The results of the repeated measures ANOVA's are shown in **Table 7.6**. There were no effects of COMT genotype, or tolcapone, nor an interaction between the two on salivary cortisol or VAS-stress ratings, nor any interactions with time (F's<1.6; p>0.17).

There was a trend interaction between genotype and drug, with COMT-Met homozygotes showing higher sAA levels than COMT-Val homozygotes on placebo only ($F_{1,61}$=3.1; p=0.086). Planned post-hoc analyses of the time by genotype by drug interaction shows this genotype by drug interaction during the MIST (p=0.007).

Table 7.5 - Effects of acute stress exposure by the MRI MIST on physiological and psychological stress measures – main analyses

Time point of interest	COMT-Met placebo (Mean ± SEM)	COMT-Val placebo (Mean ± SEM)	COMT-Met Tolcapone (Mean ± SEM)	COMT-Val tolcapone (Mean ± SEM)	Univariate ANOVA	
Cortisol 8 (%Baseline)	227.6 ± 33.0	389.0 ± 80.9	209.1 ± 35.4	261.1 ± 55.5	No effect of genotype: No effect of drug: No interaction:	$F_{3,67}$=1.5; p=0.222 $F_{3,67}$=1.7; p=0.196 $F_{3,67}$=0.26; p=0.615
AUC_G (%Baseline)	451.3 ± 54.0	513.0 ± 64.0	421.9 ± 48.1	451.6 ± 64.3	No effect of genotype: No effect of drug: No interaction:	$F_{1,69}$=0.29; p=0.593 $F_{1,69}$=0.72; p=0.400 $F_{1,69}$=0.028 ; p=0.867
AUC_i (%Baseline)	264.1 ± 42.8	348.1 ± 64.0	264.1 ± 42.8	270.0 ± 59.3	No effect of genotype: No effect of drug: No interaction:	$F_{1,69}$=0.05; p=0.820 $F_{1,69}$=0.14; p=0.712 $F_{1,69}$=0.34 ; p=0.565
Amylase 6 (%Baseline)	73.3 ± 10.6	67.4 ± 13.3	74.3 ± 8.6	77.2 ± 13.2	No effect of genotype: No effect of drug: No interaction:	$F_{1,65}$=0.31; p=0.580 $F_{1,65}$=0.63 p=0.429 $F_{1,65}$=1.2; p=0.274
VAS Stress 6	4.0 ± 0.74	5.2 ± 0.51	5.3 ± 0.65	3.6 ± 0.62	No effect of genotype: No effect of drug: **Interaction:**	$F_{1,68}$=0.45; p=0.504 $F_{1,68}$=0.53; p=0.470 **$F_{1,68}$=7.3; p=0.008** **On placebo only, COMT-Vals more subjective stress than COMT-Mets (p=0.021)** **COMT-Mets only, tolcapone higher subjective stress than placebo (p=0.018)**

Table 7.6 - Effects of acute stress exposure by the MRI MIST on physiological and psychological stress measures – exploratory analyses

Exploratory analyses		
Cortisol		
Main effect of time	$F_{8,512}$ =17.5; p=<0.001	Significant differences between time point 3 (considered baseline) and all other time points besides time point 5 (p=0.053) and 6 (p=0.153).
No main effect of genotype	$F_{1,64}$=0.70; p=0.408	
No main effect of drug	$F_{1,64}$=0.21; p=0.646	
No interaction of genotype * drug	$F_{1,64}$=0.49; p=0.485	
No interaction of time * genotype	$F_{8,512}$ =1.6; p=0.174	
No interaction of time * drug	$F_{8,512}$ =1.2; p=0.327	
No interaction of time * genotype * drug	$F_{8,512}$ =1.2; p=0.314	
AUC_G		
No main effect of genotype	$F_{1,69}$=0.53; p=0.471	
No main effect of drug	$F_{1,69}$=2.0; p=0.164	
No interaction of genotype * drug	$F_{1,69}$=1.5; p=0.228	Trend: COMT-Vals on placebo > COMT-Vals on tolcapone (p=0.068)
AUC_I		
No main effect of genotype	$F_{1,69}$=0.53; p=0.471	
No main effect of drug	$F_{1,69}$=0.47; p=0.448	
No interaction of genotype * drug	$F_{1,69}$=0.003; p=0.953	
Amylase		
Main effect of time	$F_{8,488}$=38.5; p<0.001	Significant differences between time point 3 (considered baseline) and all other time points besides time point 1 (p=0.344) and 2 (p=0.106). Please note opposite direction → less sAA than baseline.
No main effect of genotype	$F_{1,61}$=1.4; p=0.238	
No main effect of drug	$F_{1,61}$=0.18; p=0.669	
Trend interaction of genotype * drug	**$F_{1,61}$=3.1; p=0.086**	**Mets > Vals, on placebo only**
No interaction of time * genotype	$F_{8,488}$=0.73; p=0.624	
No interaction of time * drug	$F_{8,488}$=1.2; p=0.315	
No interaction of time * genotype * drug	$F_{8,488}$=1.1; p=0.341	**On placebo, Mets > Vals, on time points 4 (p=0.035), 5 (p=0.045), 6 (p=0.007), 7 (p=0.036) and 8 (p=0.043).** **Tolcapone > placebo for Vals only, on time point 6 only (during MIST) (p=0.041).**
VAS Stressed		
Main effect of time	$F_{8,504}$=32.7; p<0.001	Significant differences between time point 3 (considered baseline) and all other time points besides time point 2 (p=0.800)
No main effect of genotype	$F_{1,63}$=0.19; p=0.666	
No main effect of drug	$F_{1,63}$=0.99; p=0.323	
No interaction of genotype * drug	$F_{1,63}$=0.93; p=0.338	
No interaction of time * genotype	$F_{8,504}$=0.59; p=0.712	
No interaction of time * drug	$F_{8,504}$=1.2; p=0.300	
No interaction of time * genotype * drug	$F_{8,504}$=1.7; p=0.135	

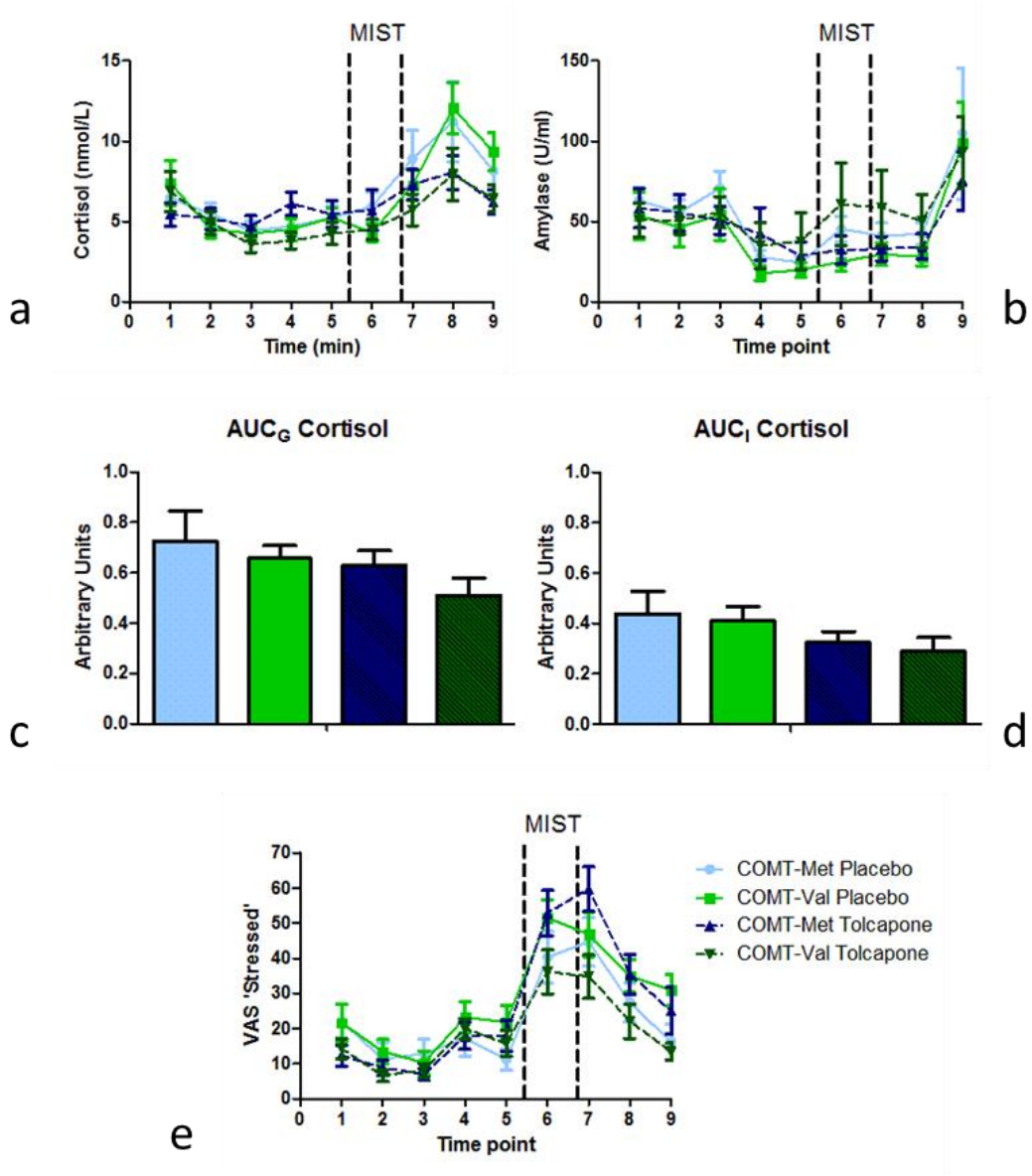


Figure 7.2 - Effects of COMT genotype and COMT inhibition on physiological and psychological stress measures.

Changes in (a) cortisol, (b) sAA, (c) AUC_G, (d) AUC_I and (e) subjective stress over the course of the experiment in COMT-Met homozygotes randomised to placebo (light blue) or tolcapone (dark blue), and COMT-Val homozygotes randomised to placebo (light green) or tolcapone (dark green). Error bars are SEM. For statistical tests see text and **Table 7.6.**

7.3.4.1 *Results in a subgroup of cortisol responders only*

As earlier in Chapter 3, the whole group was also split into participants with cortisol increases or decrease over the course of the experiment using the %baseline AUCi measure, as described in Chapter 3. In total, 57 participants were defined as such (14 cortisol non-responders). For one participant it was not possible to calculate AUC due to missing time points (not enough saliva) and therefore he was excluded from the analysis.

In the cortisol non-responder group, cortisol levels showed the predicted diurnal decrease over the course of the experiment; in contrast, cortisol levels increased in the cortisol responder group ($F_{8,400}$=27.1; p<0.001) (**Figure 7.3).**

Group differences in cortisol responders

As presented in **Table 7.7 and Figure 7.3**, as reflected in a trend genotype by drug interaction ($F_{3,52}$=4.0; p=0.052) cortisol levels were significantly higher for COMT-Val homozygotes on placebo as compared to COMT-Mets on placebo at time point 8 (p=0.005). Furthermore, COMT-Val homozygotes on placebo had higher cortisol responses than COMT-Val homozygotes on tolcapone, on time point 8 (p=0.031).

Only considering cortisol responders did not alter sAA or subjective stress levels (see **A**ppendix III).

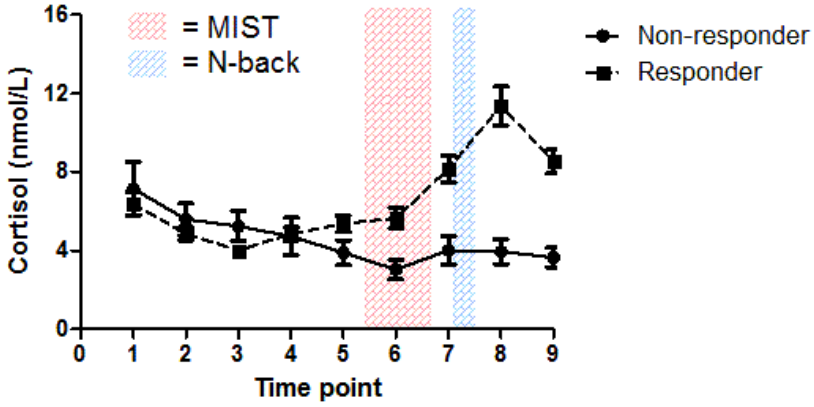


Figure 7.3 - Effects of acute stress exposure by the MRI MIST on cortisol levels in cortisol responders only. Cortisol levels in cortisol responders (dashed-line) and non-responders (solid-line).

Table 7.7 - Group differences in the effects of acute stress exposure in the MIST scenario on physiological and psychological stress measures in cortisol responders only.

Time point of interest **Cortisol responders only**	**COMT-Met placebo (Mean ± SEM)** **N = 15**	**COMT-Val placebo (Mean ± SEM)** **N = 15**	**COMT-Met Tolcapone (Mean ± SEM)** **N = 13**	**COMT-Val tolcapone (Mean ± SEM)** **N = 13**	**Univariate ANOVA**	
Cortisol 8 (%Baseline)	227.6 ± 32.9	483 ± 89.2	237.9 ± 38.3	274.4 ± 57.6	**Trend effect of genotype:** No effect of drug: **Trend interaction:**	$F_{3,52}$=3.9; p=0.054 COMT-Vals > COMT-Mets $F_{3,52}$=1.3; p=0.256 **$F_{3,52}$=4.0; p=0.052** **COMT-Val > COMT-Met homozygotes on placebo only (p=0.005)** **Placebo > tolcapone in COMT-Val homozygotes only (p=0.031)**
AUC_G (%Baseline)	466.4 ± 55.4	592.1 ± 67.2	512.2 ± 53.0	503.3 ± 71.4	No effect of genotype: No effect of drug: No interaction:	$F_{3,52}$=0.87; p=0.354 $F_{3,52}$=0.12; p=0.732 $F_{3,52}$=1.2; p=0.287
AUC_i (%Baseline)	275.1 ± 44.2	431.5 ± 65.5	296.4 ± 45.8	317.4 ± 66.3	No effect of genotype: No effect of drug: No interaction:	$F_{3,52}$=2.5; p=0.124 $F_{3,52}$=0.67; p=0.417 $F_{3,52}$=1.4; p=0.238 COMT-Val > COMT-Met homozygotes on placebo only (p=0.048)
Amylase 6 (%Baseline)					No effect of genotype: No effect of drug: No interaction:	$F_{1,51}$=0.054; p=0.817 $F_{1,51}$=0.051 p=0.823 $F_{1,51}$=1.8; p=0.189
VAS Stress 6					No effect of genotype: No effect of drug: **Interaction:**	$F_{1,52}$=0.23; p=0.635 $F_{1,52}$=0.80; p=0.377 **$F_{1,52}$=4.2; p=0.045** **On placebo only, COMT-Val > subjective stress than COMT-Met homozygotes (p=0.069)** **COMT-Met homozygotes only, tolcapone > subjective stress than placebo (p=0.018)**

Exploratory analyses		
Repeated measures ANOVA		
Cortisol		
Main effect of time	$F_{8,400}$=27.1; p<0.001	Significant differences between time point 3 (considered baseline) and all other time points
No main effect of genotype	$F_{1,50}$=0.181; p=0.673	
No main effect of drug	$F_{1,50}$=0.689; p=0.410	
No interaction of genotype * drug	$F_{1,50}$=0.187, p=0.667	
No interaction of time * genotype	$F_{8,400}$=1.8; p=0.120	
No interaction of time * drug	$F_{8,400}$=1.1; p=0.350	
Trend interaction of time * genotype * drug	$F_{8,400}$=2.15; p=0.069	**On placebo only, COMT-Val > COMT-Met homozygotes at time point 8 only (p=0.047)** **COMT-Val homozygotes only, placebo > tolcapone on time point 8 (p=0.024)**
Cortisol AUC_G		
No effect of genotype:	$F_{3,52}$=0.80; p=0.376	
No effect of drug:	$F_{3,52}$=1.6; p=0.214	
No interaction:	$F_{3,52}$=0.22; p=0.643	
Cortisol AUC_i		
No effect of genotype:	$F_{3,52}$=0.010; p=0.921	
No effect of drug:	**$F_{3,52}$=3.0; p=0.089**	Trend: placebo > tolcapone
No interaction:	$F_{3,52}$=0.52; p=0.475	Trend: effect of placebo only for COMT-Val homozygotes (p=0.089)

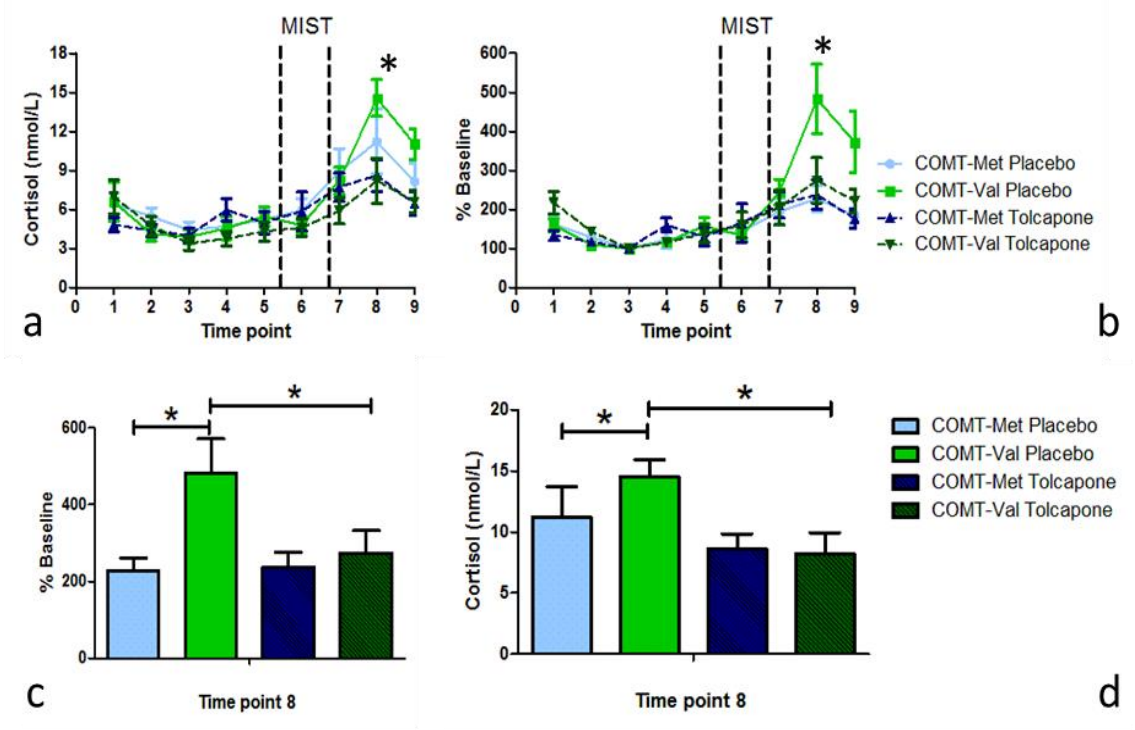


Figure 7.4 - Effects of COMT genotype and COMT inhibition on cortisol levels in cortisol-responders only.

COMT-Met homozygotes randomised to placebo (light blue) or tolcapone (dark blue), and COMT-Val homozygotes randomised to placebo (light green) or tolcapone (dark green). Error bars are SEM. *p<0.05.

7.3.5 *Imaging results*

As shown in the section above, administration of the MIST led to robust increases in salivary cortisol, sAA, and subjective stress in the overall group. No effects of COMT genotype, tolcapone, nor their interaction were observed for salivary-cortisol or sAA. Similarly, AUC measures for cortisol did not differ between groups either. In terms of subjective stress, COMT-Val homozygotes reported greater stress levels compared to COMT-Met homozygotes on placebo only, whilst tolcapone increased subjective stress levels in COMT-Met homozygotes only. These findings changed slightly when I considered cortisol responders only. Cortisol levels were significantly greater for COMT-Val homozygotes on placebo as compared to COMT-Mets on placebo at time point 8 (where cortisol levels were highest). Furthermore, there was a significant drug effect for COMT-Val homozygotes with those on tolcapone having a lower cortisol response than those on placebo, again on time point 8 only. In sum, the MIST induced significant levels of physiological stress. In the next section I will investigate the effects of the MIST on brain activity, and explore whether COMT genotype and COMT inhibition impacted on the neural responses to acute stress.

7.3.5.1 *fMRI*

Main effect of task (stress > control & control > stress)

In order to determine if the MIST engaged brain regions previously associated with acute mild stress, I compared neural activation in response to the stress blocks vs. control blocks (=activations) and control blocks vs. stress blocks (=deactivations). Significant activation and deactivations were observed in a network of areas that maps very closely to previous reports (**Table 7.1)** – including expected frontal, parietal and limbic regions**. Figure 7.5** and **Table 7.8** shows task activations and deactivations without the correction for CBF and GM differences (to be able to compare with previous literature), and **Figure 7.6** and **Table 7.9** with these maps added as nuisance variables (to show that expected frontal and limbic areas are still engaged). These findings therefore confirm that we engaged brain regions that are part of a network relevant to stress as a result of the MIST.

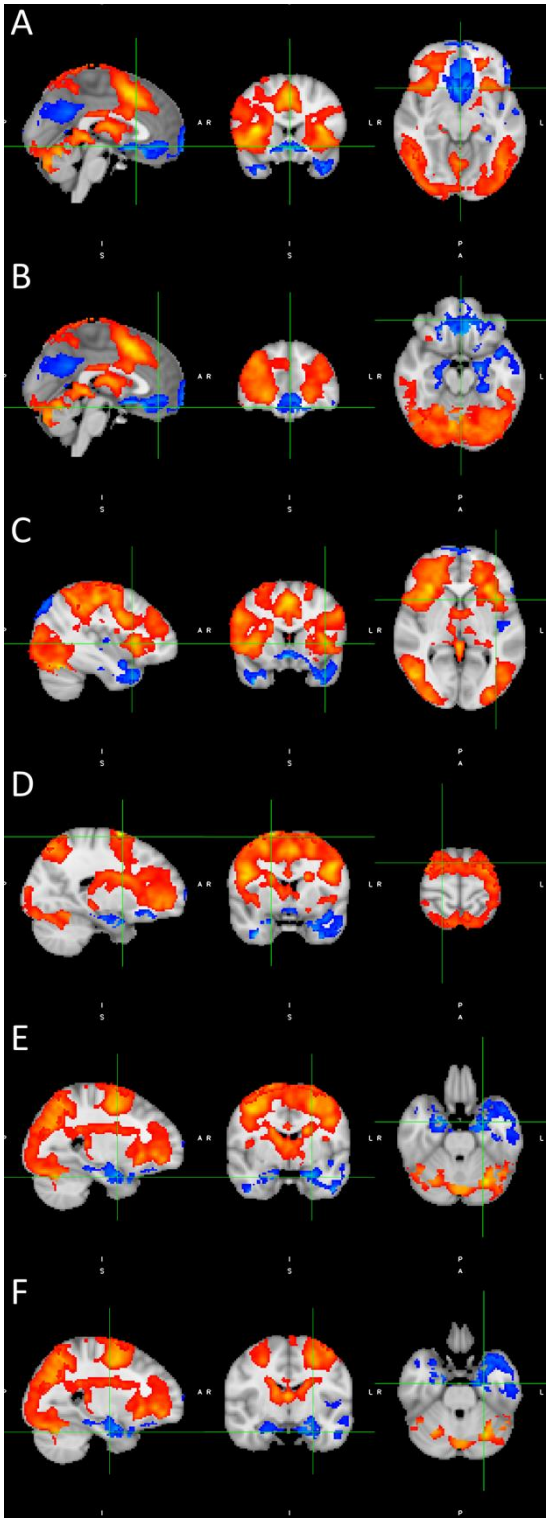


Figure 7.5 - Whole-brain fMRI MIST task activations and deactivations.

Sagittal, coronal and axial images depicting neural activation and deactivation. Main effect of task: across all groups, the stress blocks led to greater BOLD signal response compared to control blocks (red). Moreover, task deactivations (control > stress in blue) were also found. A = Anterior Cingulate, B = medial PFC, C = vlPFC, D = superior frontal gyrus region, E = left plus right hippocampus, F = left plus right amygdala. See table 7.8 for more details. Images thresholded at $Z>3.1$, $p<0.05$ corrected. Without CBF and GM maps as nuisance variables.

Table 7.8 - Whole brain fMRI MIST task activations and deactivations - without CBF and GM maps as nuisance variables. Results thresholded at Z>3.1, p<0.05 corrected.

MIST Threshold Z>3.1 p<0.05	**Brain area / Brodmann Area (BA)**	**Side**	**Cluster size (voxels)**	**Voxel max (x,y,z)**	**MNI max (x,y,z)**	**Z-score**	**p-value**
Task activation (stress > control)							
Mean across groups							
Cluster 1	Including ventral and dorsal medial frontal cortex, frontal orbital areas, middle temporal gyrus, pre- and supplementary motor-areas, angular gyrus, posterior cingulate gyrus, insular cortex, parietal regions (precuneus), lateral visual cortex, middle temporal gyrus, and subcortical regions like the thalamus and caudate	R+L	69506	28,74,40	34,22,8	9.46	<0.001
Task deactivation (control > stress)							
Mean across groups							
Cluster 1	Including anterior cingulate gyrus extending into BA25, subcallosal cortex, frontal medial cortex, paracingulate gyrus, BA11, BA32, BA24, frontal pole, left amygdala, left hippocampus, left BA28, left BA36, left BA13, parahippocampal gyrus, inferior temporal gyrus, middle temporal gyrus, BA25	L+R	5054	43,71,30	4,16,-12	8.99	<0.001
Cluster 2	Posterior cingulate gyrus, BA23, BA31, extending into precuneous cortex, BA18, cuneal cortex, occipital pole	L+R	1928	46,36,50	-2,-54,28	5.94	<0.001
Cluster 3	Lateral occipital cortex extending into BA19, BA39, angular gyrus, BA40	L	950	69,25,53	-48,-76,34	6.6	<0.001
Cluster 4	Temporal pole, BA38, extending into temporal fusiform cortex, right amygdala, right hippocampus, BA34	R	910	31,68,19	28,10,-34	6.38	<0.001
Cluster 5	Frontal orbital cortex, extending into inferior frontal gyrus, BA47, BA45, frontal pole	L	259	71,76,31	-52,26,-10	5.45	0.0043
Cluster 6	Heschl's gyrus, BA13, extending into insular cortex, planum polare	L	164	67,55,36	-44,-16,0	4.38	0.0343

Table 7.9 - Whole brain fMRI MIST task activations and deactivations - with CBF and GM maps as nuisance variables. Results thresholded at Z>3.1, p<0.05 corrected.

MIST Threshold Z>3.1 p<0.05, + GM + ASL maps	Brain area / Brodmann Area (BA)	Side	Cluster size (voxels)	Voxel max (x,y,z)	MNI max (x,y,z)	Z-score	p-value
Task activation (stress > control)							
Mean across groups							
Cluster 1	Superior parietal lobule, extending into supramarginal gyrus, angular gyrus, and BA40, BA7, lateral occipital cortex, BA19	L	750	60,40,55	-30,-46,38	5.89	<0.001
Cluster 2	Postcentral gyrus extending into BA40, BA3, BA6, precentral gyrus, BA3, superior frontal gyrus	L	548	76,46,67	-44,-34,62	5.08	<0.001
Cluster 3	Superior frontal gyrus, extending into pre-central gyrus, supplementory motor cortex, and middle frontal gyrus, BA6	R	456	35,64,72	20,2,72	6.83	<0.001
Cluster 4	Angular gyrus, BA40, superior parietal lobule, extending into BA7, and supramarginal gyrus, and lateral occipital cortex, precuneous cortex	R	455	24,38,63	42,-50,54	4.79	<0.001
Cluster 5	Inferior temporal gyrus, extending into temporal occipital fusiform cortex, extending into BA37 and BA20	R	329	22,38,29	46,-50,-14	5.08	0.0006
Cluster 6	Precuneous cortex, extending in to superior parietal lobule, BA7	L	230	45,46,76	0,-34,80	4.86	0.0049
Cluster 7	Lateral occipital cortex, extending into BA19, and occipital pole	R	230	29,27,48	32,-72,24	4.25	0.0049
Cluster 8	Cerebellum, extending into lateral occipital cortex, BA19,middle temporal gyrus, BA37	L	144	67,27,23	-44,-72,-26	4.61	0.0409
Task deactivation (control > stress)							
Mean across groups							
Cluster 1	Subcallosal cortex, BA25, extending into BA24, frontal orbital cortex, frontal medial cortex, anterior cingulate, cingulate gyrus, nucleus accumbens, paracingulate gyrus, BA32	L+R	1205	43,71,30	4,16,-12	6.79	<0.001
Cluster 2	Inferior temporal gyrus, extending into hippocampus, amygdala, middle temporal gyrus, BA21, extending into temporal fusiform cortex, extending into parahippocampal gyrus, temporal pole, BA38	L	441	68,62,16	-46,-2,-40	5.58	<0.001
Cluster 3	Temporal pole, BA38, extending into BA21, inferior temporal gyrus, extending into parahippocampal gyrus, temporal fusiform cortex, amygdala, hippocampus	R	256	28,68,17	34,10,-38	6.18	0.00273

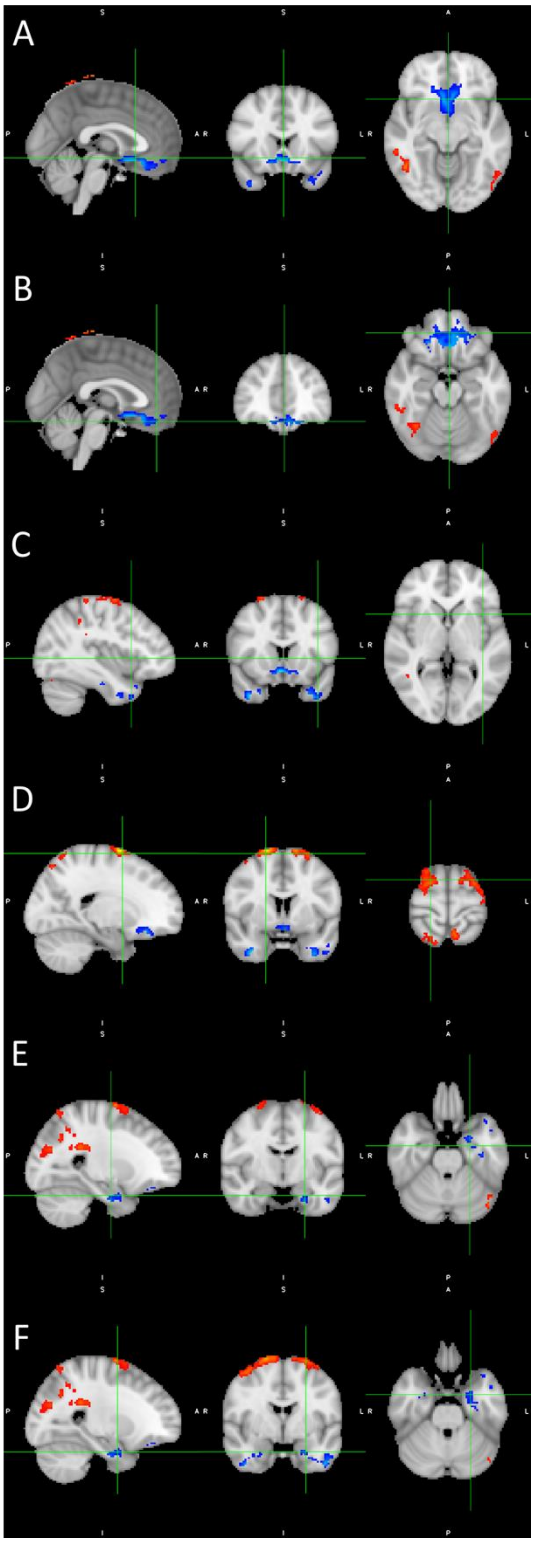


Figure 7.6 - Whole-brain fMRI MIST task activations and deactivations – with GM and CBF maps as nuisance variables.

Sagittal, coronal and axial images depicting neural activation and deactivation. Main effect of task: across all groups, the stress blocks led to greater BOLD signal response compared to control blocks (red). Moreover, task deactivations (control > stress in blue) were also found. A = Anterior Cingulate, B = medial PFC, C = vlPFC, D = superior frontal gyrus region, E = left plus right hippocampus, F = left plus right amygdala. See table 7.9 for more details. Images thresholded at $Z>3.1$, $p<0.05$ corrected. With CBF and GM maps as nuisance variables.

Group differences

As presented in **Figure 7.7**, a whole brain analysis (threshold Z>3.1, p<0.05, corrected) revealed greater BOLD activation in the COMT-Met homozygotes relative to COMT-Val homozygotes (regardless of treatment), in response to control versus stress blocks (greater deactivation due to stress), in a cluster located in the left inferior temporal gyrus (BA21), extending into the middle temporal gyrus (BA36) and the temporal fusiform cortex (Z=4.7, p<0.001, peak voxel: x=−52, y=−34, z=−16; Z=4.7, voxel size=456 voxels). Therefore, COMT-Met homozygotes have greater deactivations due to stress in these areas, compared to COMT-Val homozygotes.

When analysing at a less stringent threshold (Z>2,3, p<0.05 corrected) the results were similar, with additional deactivation patterns seen in the frontal orbital cortex and parietal cortex (supramarginal and post-central gyrus). There were no drug-related differences, nor interactive effects. Essentially the same results were obtained when only cortisol responders were considered.

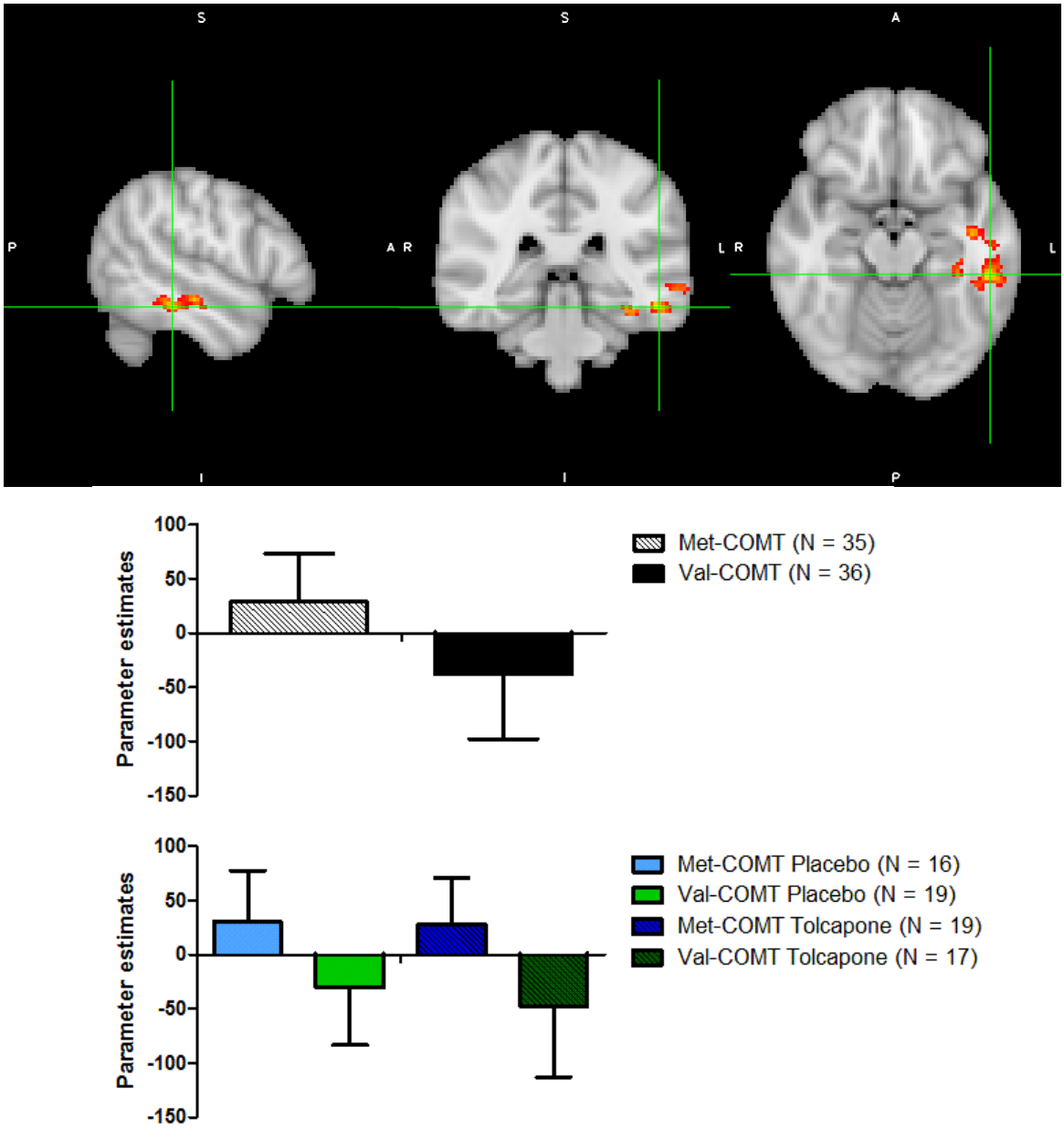


Figure 7.7 - Effects of COMT genotype on whole brain MIST deactivations (control MIST > stress MIST).

A main effect of genotype was found where COMT-Mets show greater deactivations in the left inferior temporal gyrus (BA21) extending into the middle temporal gyrus and temporal fusiform cortex (BA36), compared to COMT-Vals homozygotes (regardless of treatment) ($Z=4.7$, $p<0.001$, peak voxel: $x=-52$, $y=-34$, $z=-16$, $Z=4.7$, voxel size=456 voxels). Top image thresholded at $Z>3.1$, $p<0.05$ cluster corrected. Error bars showing standard deviation.

7.4 Discussion

This chapter has four main findings: (1) the MIST induced a robust stress response; (2) there were no effects of COMT or tolcapone on physiological stress indices when considering the whole sample; (3) COMT genotype and tolcapone interact to influence subjective stress ratings; (4) COMT genotype, but not tolcapone, influenced the effect of stress on brain activation.

7.4.1 *Validation of the MRI MIST*

Administration of the MIST led to robust increases in salivary cortisol, sAA and subjective stress. Moreover, similar brain regions to those previously associated with acute mild stress were engaged. Activity was observed in a network of areas that maps very closely to previous reports (**Table 7.1**), including the occipital fusiform gyrus, lateral occipital cortex, bilateral hippocampus, bilateral amygdala, cerebellum, thalamus, putamen, superior frontal gyrus, frontal orbital cortex, frontal pole, middle frontal gyrus, precentral and postcentral gyrus, insula and anterior cingulate. These findings therefore confirm that the MIST engaged brain regions that are part of a network relevant to stress and that the paradigm was effective in inducing both physiological and psychological stress in this sample of participants. The fact that the MIST was successful also validates its use to study the effects of stress on working memory performance (Chapter 8).

Salivary-cortisol levels were increased to 150-200% of baseline between 20 and 80 minutes after commencing the MIST. Salivary amylase levels were elevated only transiently by about 30%. Subjective stress increased 2 to 3-fold during and immediately after the MIST. The stress responses observed here are similar in magnitude to other studies using the MIST ((Dedovic et al., 2005); and **Table 3.1**). According to (Dedovic et al., 2009b), the robust stress response induced by the MIST is driven by about 50% of the participants, reflecting an inter-individual variability in reacting to a given stress stimulus. My data shows a higher response rate, with only 14 cortisol non-responders (non-responder defined as no clear cortisol increase (<5%) after the MIST as defined by percentage baseline AUCi)) out of a total of 71 participants (=80% cortisol responder rate).

Interestingly, even though both physiological and subjective measures of stress increased, there were few, if any, significant correlations between these variables. Self-esteem correlated negatively with sAA levels during the MIST, which means that participants who reported to have higher self-esteem showed a lower physiological stress response due to the MIST as measured by sAA only. However, no significant correlations were found between cortisol response and self-esteem or locus and control in contrast to those described previously (Bollini et al., 2004; Pruessner et al., 1999).

7.4.2 *Effects of COMT genotype and COMT inhibition on the stress response*

When considering all participants, no effects of COMT genotype, tolcapone, nor their interaction were observed for salivary-cortisol or sAA. Similarly, AUC measures for cortisol did not differ between groups. In terms of subjective stress, COMT-Val homozygotes reported greater stress levels compared to COMT-Met homozygotes on placebo only, whilst tolcapone increased subjective stress levels in COMT-Met homozygotes only.

These findings change slightly when I consider cortisol responders only. Cortisol levels were significantly greater for COMT-Val homozygotes on placebo as compared to COMT-Mets on placebo at time point 8 (where cortisol levels were highest). Furthermore, there was a significant drug effect for COMT-Val homozygotes with those on tolcapone having a lower cortisol response than those on placebo, again at time point 8. Considering cortisol responders only did not alter sAA or subjective stress ratings.

The finding that COMT-Val homozygotes report greater subjective stress levels than COMT-Met homozygotes stands in contrast to the previous literature, in which COMT-Val homozygotes appear more stress-resistant than COMT-Met homozygotes. However, these studies were conducted in diverse groups (in terms of age and diagnostic status) and none used the MIST to induce acute mild stress. (Collip et al., 2011; Jabbi et al., 2007; Oswald et al., 2004; Walder et al., 2010). It is possible that acute stress as induced by a laboratory stressor may alter the relationship between COMT and the stress response. Specifically, the MIST may have increased PFC dopamine levels of COMT-Val homozygotes over their optimum, potentially leading to a loss of stress-resistance (although does not explain why COMT-Mets have lower stress response levels).

At baseline (e.g. no stress or COMT inhibition by tolcapone) COMT-Val homozygotes have lower cortical dopamine levels than COMT-Met homozygotes due to higher enzyme activity. Hernaus et al., (2013) showed that PFC dopamine levels in COMT-Val homozygotes increased substantially after stress (either due to more dopamine release or reduced dopamine degradation) compared to both COMT-Met carriers and homozygotes (those did not differ from each other). In my study, on placebo, COMT-Val homozygotes had a higher cortisol response than COMT-Met homozygotes. Given that stress results in greater cortisol and cortical dopamine concentrations, it could be speculated that COMT-Val homozygotes therefore have overall higher dopamine levels than COMT-Met homozygotes under conditions of stress. Therefore, the effect of stress on dopamine release might be greater than the existing baseline genotype differences between COMT-Val and COMT-Met homozygotes. Tolcapone did not influence cortisol levels in COMT-Met homozygote, whilst it reduced cortisol levels in COMT-Val homozygotes (COMT-Val homozygotes on placebo higher cortisol response than COMT-Val on tolcapone). Therefore, in my study, even

higher levels of dopamine resulted in a lower cortisol response for COMT-Val homozygotes. It could therefore be speculated that more dopamine does not always lead to higher cortisol responses. As COMT-Met homozygotes on placebo had lower cortisol levels than COMT-Val homozygotes on placebo, it is unlikely that stress increased PFC dopamine levels of COMT-Val homozygotes over their optimum leading to a loss of stress-resistance (higher cortisol). Given the lack of a non-stress control group in my current design I was however unable to test this hypothesis directly. Therefore, further studies are required to fully characterise the impact of COMT on the acute stress response, and to investigate how these relationships may be changed in different groups of participants. Of course, other factors may also play a role, like for example environmental experiences which can directly activate or repress certain genes involved in stress reactivity/vulnerability to stress at the level of epigenetics (Ursini et al., 2011).

7.4.3 *Effects of COMT genotype and COMT inhibition on stress related brain activity*

To my knowledge this is the first study to investigate the interaction of COMT genotype, COMT inhibition and stress on brain activity. I found that COMT-Val homozygotes had greater de-activations due to stress compared to COMT-Met homozygotes, in the left temporal cortex. This area is believed to play a role in auditory processing and language, higher order ventral stream of visual processing, and memory. Previous studies linking the COMT Val^{158}Met polymorphism to the temporal cortex are limited. The middle temporal gyrus is part of the executive control network (ECN) as found by (Tunbridge et al., 2013). Taylor et al., (2007) showed that temporal lobe volumes but not caudate or cerebral volumes were smaller in COMT-Val homozygotes. However, the exact implications of these findings are currently still unknown.

7.4.4 *MRI scanner induced stress response*

The timing of the stress response observed in our study provides evidence that the MRI experience induces a robust stress response, both in terms of psychological responses (increase in both salivary cortisol but not sAA and subjective stress. Previous studies have found that the MRI environment directly increases cortisol levels even in the absence of any explicit stressor (Lueken et al., 2012; Muehlhan et al., 2011; Peters et al., 2011; Tessner et al., 2006). One study found that when the researchers administered a cognitive task (the continuous performance task; CPT) in the MRI scanner, the increase in cortisol in participants was greater than when they administered the CPT outside of the scanner (McCullough et al., 2015). However, we observed a further increase in stress

response after MIST, indicating that the stress induced in our study was not only MRI scanner related. Some studies have shown that the neuroendocrine stress response associated with the fMRI participation itself influences brain functioning (Kukolja et al., 2009; Muehlhan et al., 2011). These unintended effects of the scanner environment itself can act as a potential confounder in fMRI research.

7.4.5 *Salivary amylase*

The highest sAA response at the end of the experiment, right after debriefing was not anticipated (see Figure7.2b). (Nagy et al., 2015) speculate that the typical sAA increase post-stress might reflect a relief response, rather than a stress response (Nagy et al., 2015). It could therefore be speculated that this increase of sAA could be due to the debriefing (either as a response to being deceived by the experimenter or as a relief for the experience not being real). sAA might also be dependent on saliva flow rate. Stimulation of the saliva flow rate is mainly mediated by the parasympathetic nervous system, whilst stimulation of salivary proteins is generally ascribed to the sympathetic nervous system (Bosch et al., 2011; Nater et al., 2006). Therefore, sAA concentration may provide an overestimation of sAA secretion when salivary flow rate decreases (reflecting reduced PNS activation of the salivary glands – but may provide an underestimation when saliva flow rate increases. Further, experimental studies show that the sympathetic effects on sAA release are strongly moderated by concurrent PNS activity, a phenomenon denoted as 'augmented secretion' (Nagy et al., 2015).Therefore, it is believed that the parasympathetic nervous system might moderate the sAA response to stress. Rohleder et al., (2006) demonstrated that stress-induced increases in sAA levels were correlated with increases of amylase output but not with increases of flow rate suggesting that saliva flow rate is not a confounder of stress induced sAA activation and that valid sAA measures can be obtained with the use of salivettes (as in our study). It is possible that the increase is related to participants being thirsty at the end of the experiment. However, the time difference between the time of leaving the scanner and the last data point is only about 20 minutes. Thus, the reason for this late increase in sAA remains unclear.

7.4.6 *Limitations*

As in previous chapters (Chapter 2 and 3), few significant correlations between different measures of the stress response were found. As discussed before, there is a substantial literature arguing against the 'stress response' as being a unitary construct, and weak or absent correlations between

physiological and psychological measures of the stress response are a common finding both in experimental and naturalistic settings (Campbell and Ehlert, 2012; Dickerson and Kemeny, 2004; Wilhelm et al., 2005). Also, the findings of this study are subject to the limitations discussed in Chapter 2. Namely, it is not clear to what extent the findings can be generalised beyond young, healthy men (Cornelisse et al., 2011; Diemer et al., 2016) or to situations of more extreme or prolonged stress. Broadly speaking, any attempt to extrapolate our findings should be mindful of the complex interplay between psychological and physiological effects of stress, its context, and the cognitive impacts (Schwabe et al., 2012). Furthermore, as the control MIST is less difficult than the stress MIST, it is hard to differentiate between the effects of stress from those on cognitive load (Fechir et al., 2010).

Future replications using a larger sample size and a non-stress control group may further reveal and refine between-group similarities and differences. A final complication is the fact that acute psychosocial stress alters neurovascular coupling (Dunlop and Liston, 2018). Dunlop and Liston (2018) showed that psychological stress rapidly increased the latency of the haemodynamic response function (HRF) peak in cortical and limbic regions involved in stress response regulation, such that the blood oxygen level-dependent signal response to a mental arithmetic task was relatively sluggish and slower to respond than in an acute stress condition. This suggests that neurovascular coupling mechanisms linking changes in blood flow to neuronal activity demands may be disrupted by psychosocial stress. In the current study I modelled the temporal derivative of the task regressors to be able to at least partly account for these differences in HRF but a contribution from neurovascular coupling cannot be ruled out entirely.

7.4.7 *Conclusion*

In conclusion, the MIST paradigm implemented here was effective in inducing stress. Therefore, the results in this chapter validate the MIST as a stressor to investigate the effects of COMT genotype, COMT inhibition and their interaction on working memory performance and brain activity under conditions of stress (Chapter 8). My results do not support the hypothesis that COMT-Met homozygotes display a more sensitive biological stress response compared to COMT-Val homozygotes, nor that the stress response is (in part) regulated by COMT dependent dopaminergic PFC activity. However, given the lack of a non-stress control group in my current design, these conclusions need to be interpreted with caution and further research is therefore needed to fully test (or disprove) this hypothesis.

Chapter 8 The interaction between COMT genotype and COMT inhibition on working memory related brain activity and performance under acute stress

8.1 Introduction

8.1.1 *Interactions between COMT, COMT inhibition and stress*

Chapter 1 described the background for the main hypotheses of this chapter. In short, COMT activity affects the inverted-U-shaped relationship between dopamine and PFC dependent function (e.g. (Egan et al., 2001). Moreover, there is evidence that COMT genotype also alters the cognitive, neural and physiological responses to stress (Chapter 6 and e.g. (Buckert et al., 2012; Qin et al., 2012). An inverted-U relationship also exists between acute stress and PFC-dependent cognitive performance, with moderate stress levels facilitating, and high levels impairing, cognitive function (Andreano and Cahill, 2006; Arnsten, 2009; Ossewaarde et al., 2011; Qin et al., 2012; Sandi and Pinelo-Nava, 2007). Stress and dopamine signalling interact in complex ways; for example, acute stress elevates cortical catecholamines and affects working memory (Arnsten, 2009; Henckens et al., 2009; Nagano-Saito et al., 2013; Sandi, 2011; Schoofs et al., 2008; Schwabe et al., 2010). Despite the evidence that COMT genotype alters the cognitive, neural and physiological responses to stress it is unknown whether this is modulated by COMT inhibition in humans. Moreover, there is evidence that the inverted-U relation between stress and PFC dopaminergic functioning is COMT-dependent (Hernaus et al., 2013). Stress might be expected to push everyone to the right on the inverted-U (more dopamine) if the stress and dopamine curves are related.

Clarifying these relationships could have significant implications for understanding how real-world stressors might impact on the therapeutic response to COMT inhibitors. For example, if stress and COMT inhibition negatively impact on working memory this may represent an undesirable side-effect of the drug. Understanding these interactions is also of neuroscientific interest, since it provides a useful test of the extent to which the inverted-U relationships between stress and COMT with cognitive function overlap. In this chapter I investigated the interaction between COMT genotype, COMT inhibition and acute stress on working memory related brain activity and performance.

8.1.2 *Predictions*

Acute stress (as induced by the MIST) interacts with COMT genotype and COMT inhibition by tolcapone to influence

1. ***Working memory performance (as measured by the N-back task).***

I expect that the performance of COMT-Met homozygotes on placebo will be affected negatively by acute stress. I predict that the stress-induced dopamine increase in the PFC, combined with the high prefrontal baseline dopamine levels present in COMT-Met homozygotes should lead to supra-optimal PFC dopamine levels. On the other hand, COMT-Val homozygotes' performance should not be affected negatively by stress, but rather be improved through the heightened dopamine availability in PFC under stress (depending on the magnitude of effect), as these participants initially have a lower baseline level of prefrontal dopamine.

- **I therefore predict that in my study, after MIST exposure, COMT-Val homozygotes on placebo will perform better than COMT-Met homozygotes on the N-back task.**

On tolcapone however, dopamine levels will increase even further in the PFC, therefore causing even COMT-Val homozygotes to experience supra-optimal dopamine signalling.

- **I therefore predict that, under conditions of acute stress, the anticipated genotype x drug interactive effect on N-back performance (Farrell et al., 2012) will be lost: both COMT-Val and COMT-Met homozygotes are predicted to have worse working memory performance on tolcapone than on placebo.**

2. ***Brain activity (as measured by task fMRI)***

Previous literature showed that COMT-Val homozygotes have greater activity in the PFC for a given level of working memory performance, compared to COMT-Met homozygotes (e.g. (Egan et al., 2001), and that under conditions of stress COMT-Met homozygotes have greater PFC activations than COMT-Val carriers (Qin et al., 2012).

- **I predict that I will replicate these findings in participants on placebo (e.g. COMT-Met homozygotes will have greater PFC activations, compared to COMT-Val homozygotes).**
- **In contrast, I predict that participants on tolcapone will have further increases in PFC dopamine levels and therefore COMT-Val homozygotes will show similar brain activation to COMT-Met homozygotes.**

Table 8.1 - Hypotheses based on previous literature.

	Literature			**Current hypothesis**	
	COMT Untreated / placebo	*COMT Inhibition / tolcapone*	*COMT + Stress untreated*	*COMT + Stress + placebo*	*COMT + Stress + tolcapone*
Working memory performance	COMT-Met homozygotes perform better than COMT-Val homozygotes	COMT-Val homozygotes on tolcapone perform better than COMT-Met homozygotes on tolcapone	COMT-Val homozygotes perform better than COMT-Met homozygotes	COMT-Val homozygotes on placebo perform better than COMT-Met homozygotes Interaction of COMT genotype and drug	Both COMT-Val homozygotes and COMT-Met homozygotes will perform worse than on placebo Main effect of drug
Reference	e.g. Egan et al., 2001; Goldberg et al, 2003	e.g. Farrell et al., 2012	Buckert et al., 2012 Qin et al., 2012		
Brain activity (fMRI) in dlPFC during PFC-dependent cognitive task	COMT-Val homozygotes greater brain activity than COMT-Met homozygotes	Both COMT-Val homozygotes and COMT-Met homozygotes greater brain activity on tolcapone than compared to placebo	COMT-Met greater brain activity than COMT-Val	COMT-Met homozygotes greater brain activity than COMT-Val homozygotes Interaction or main effect of genotype	No differences in brain activity between COMT-Met homozygotes and COMT-Val homozygotes No differences
Reference	e.g. Egan et al., 2001; Mier et al., 2010; Qin et al., 2012	Apud et al., 2007	Qin et al., 2012		

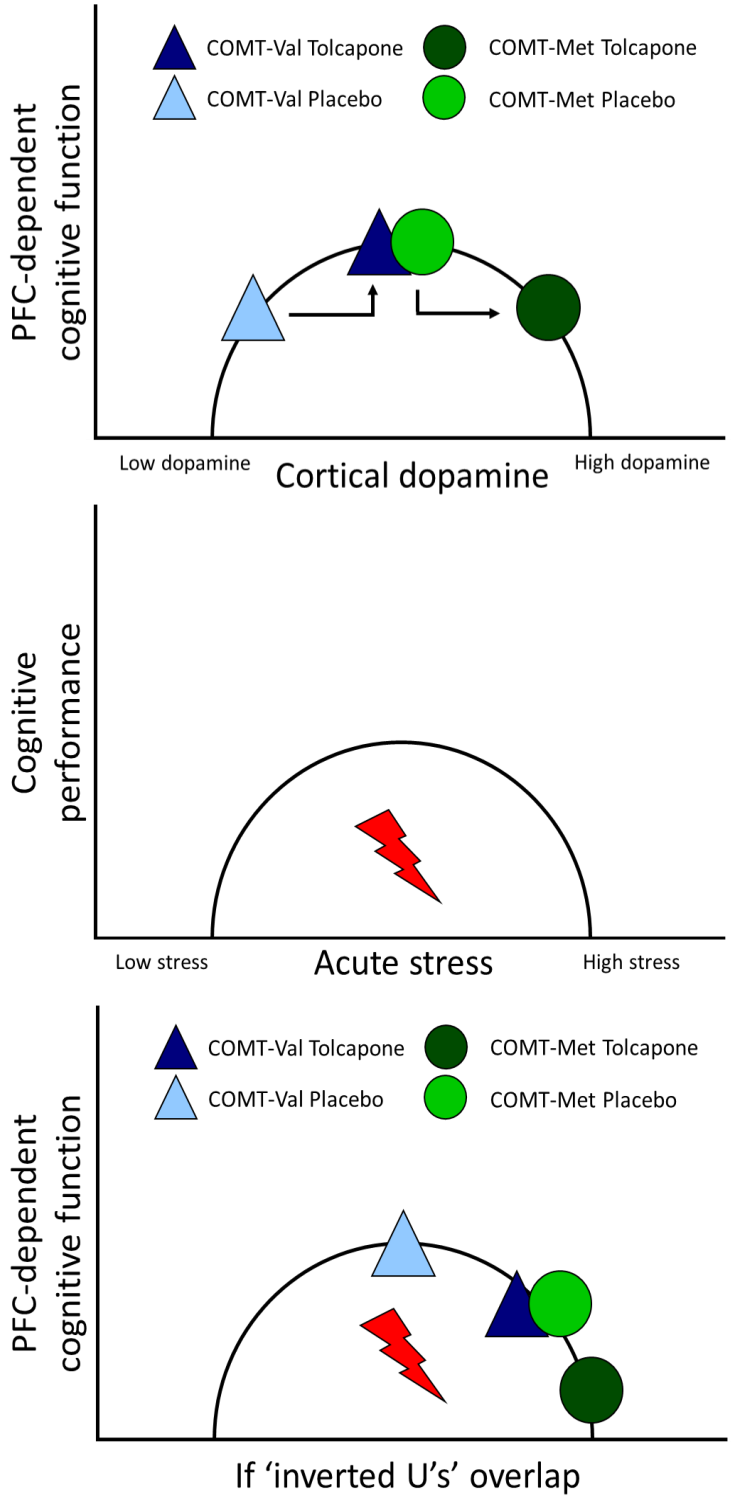


Figure 8.1 – Inverte1d-U's.

Top: Effect of tolcapone on the COMT-dependent dopaminergic inverted-U as presented by Farrell et al., (2012).
Middle: The inverted U between acute stress and cognitive performance as first described by Yerkes and Dodson (1908)
Bottom: Predicted position of COMT-Met and Val homozygotes when above inverted U's overlap.

8.2 Methods

I conducted a randomised, double-blind, placebo-controlled, between-subjects study of the effects of COMT inhibition and genotype on cognitive function and brain activation under conditions of acute stress.

8.2.1 *Participants, study design and procedure*

Participants, study design and procedures identical to Chapter 4.

8.2.2 *Task*

The N-back task employed was the same as the pilot study (see Chapter 3) but included only four blocks of each N-back condition (14 random numbers per block, each number was shown for 500msec, with an interval of 1500msec between numbers and 2500msec between blocks). The task began after the MIST, following a saliva collection and VAS rating. The total duration was approximately 7.5 minutes. The primary performance measure was accuracy (correct responses); I also measured reaction time (RT) for correct trials.

8.2.3 *Behavioural analysis*

N-back data were analysed using repeated-measures analysis of variance, with level (0-3 back) and block (1-4) as a within-subjects factors and genotype (COMT-Val or COMT-Met) and drug (placebo or tolcapone) as the between-subjects factors. Huynh-Feldt correction was applied where data failed Mauchly's Test of Sphericity. Post-hoc comparisons were explored regardless of overall significance.

8.2.4 *Neuroimaging Protocol and structural MRI*

MRI scanner environment and protocol of structural scan identical to described in Chapter 5.

8.2.4.1 *Functional MRI protocol*

N-back

Functional imaging consisted of 72 T2-weighted echoplanar imaging (EPI) slices (TR = 1200ms, TE=30ms, flip angle = 65°, field of view = 216mm, voxel size = 2*2*2 mm, 450 volumes, acquisition time 9min 28 seconds, Multiband acceleration factor = 4 interleaved, PAT GRAPPA acceleration factor = 2). Images were distortion corrected by an acquired fieldmap (echos at 4.92 and 7.38 ms, TR=482ms, flip angle = 46°).

8.2.4.2 *MRI analysis methods*

Functional data were pre-processed and analysed as in Chapter 6, with the following differences: N-back data were denoised (removal of noise due to movement, scanner or cardiovascular artifacts) by ICA denoising using FIX, by manually creating a training dataset from five subjects in each group (N=20, same participants as used to create a training data set in Chapter 6). Components were manually labelled by me; components were retained in cases where it was not clear whether or not they represented noise.

A high-pass temporal filtering cut-off = 150s (Gaussian-weighted least-squares straight line fitting, with sigma=75.0s) was used. A custom 3 column format convolved with a gamma hemodynamic response function, and its temporal derivative was used to model the data. The main contrast of interest was 2- back vs 0-back, but estimates of 0-back vs 2-back were also obtained for reference (but not 0-back vs rest, 1-back vs rest, 2-back vs rest and 3 -back vs rest as there was no rest block in the N-back task).

The general linear model (GLM) included the 4 groups (Val-Placebo, Val-Tolcapone, Met-Placebo, Met-tolcapone and their interaction). %Baseline_AUCi cortisol (see Chapter 3 and 6) was added as a co-variate of interest (was set as a contrast), and GM and ASL maps as nuisance variables. I tested for group averages and differences between groups for each of the contrasts of interest. The Z statistic images were thresholded using clusters determined by Z>3.1, and a family-wise error–corrected cluster significance threshold of P<0.05 was applied to the superthreshold clusters.

Small volume correction / pre-threshold masking

In addition to the whole brain analysis described in the previous section, I also used the right dlPFC mask (identical to the one used in Chapter 6) as a predefined region of interest. The small volume correction method restricts the search space for significant voxels only to those voxels within the mask, reducing the number of multiple comparisons and boosting statistical power. Again %baseline_AUC_i cortisol (see Chapter 3) was added as a covariate of interest, and GM and ASL maps as nuisance variables.

Finally, as a secondary analysis I also conducted the analyses described above in cortisol responders only (as defined by %baseline AUC_i see Chapter 3).

8.3 Results

First, I will present the effects of COMT genotype, COMT inhibition and stress as induced by the MIST on N-back performance after which I will present the effects on brain activity as measured by task fMRI.

8.3.1 *Participants*

Participant demographics are described in **Table 7.3.** One participant had to be excluded from the imaging analysis (COMT-Val homozygote on tolcapone) as two of his cortisol samples were missing (insufficient volume collected), making it impossible to calculate his %baseline AUC_i (this is a covariate in the analysis).

8.3.1.1 *Blinding*

The drug blind was maintained, with 50 of the 76 subjects thinking that they had received placebo (5 were not asked, 21 tolcapone (of whom 14 were actually given tolcapone) and the remainder placebo). When subjects were asked to give a percentage of how sure they were they received tolcapone on a scale from 0-100%, the overall percentage was 47% sure.

8.3.2 *Behavioural results*

8.3.2.1 *Group differences on N-back performance*

There were no group differences on N-back performance (F's < 2.1; p's >0.15). There were main effects of level for % correct trials ($F_{3,201}$=145.9; p=<0.001 reflected by all participants performing worse on higher N-backs (p's<0.001) except for 1-back vs. 0-back (p=0.454). Additionally, there was a main effect for level on reaction time (correct trials only - $F_{3,183}$=4.63; p=0.009): participants reacted slower during 3-back compared to 0-1-2-back (p's<0.031).

There were no main or interactive effects of group on either measure (F's<3.3; p's>0.57). Planned post-hoc analyses revealed a trend genotype difference. COMT-Met homozygotes performed better on the 3-back than the COMT-Val homozygotes ($F_{1,67}$= 3.89;p=0.053). There were no main or interactive effects for reaction time (F's<1.4; p's>0.26). See **Table 8.2**, **Figure 8.2** and **8.3**.

Table 8.2 - Effects of COMT genotype and COMT inhibition on N-back performance.

Reaction time calculated for correct trials only.

	COMT-Met placebo (Mean ± SEM) N = 16	COMT-Val placebo (Mean ± SEM) N = 19	COMT-Met Tolcapone (Mean ± SEM) N = 19	COMT-Val tolcapone (Mean ± SEM) N = 17
0 back % correct	94.3 ± 1.6	91.3 ± 4.1	93.1 ± 5.2	95.9 ± 1.0
1 back % correct	91.9 ± 3.7	89.9 ± 3.6	93.0 ± 1.4	94.6 ± 1.6
2 back % correct	78.8 ± 5.5	74.1 ± 2.8	76.1 ± 3.0	67.4 ± 5.0
3 back % correct	62.2 ± 6.1	52.3 ± 4.3	56.0 ± 4.5	45.9 ± 5.6
0 back reaction time (msec)	522.9 ± 42.5	517.1 ± 25.6	548.2 ± 32.5	487.4 ± 25.7
1 back reaction time (msec)	508.6 ± 50.1	460.0 ± 44.7	532.7 ± 50.2	504.8 ± 57.9
2 back reaction time (msec)	530.3 ± 57.6	451.1 ± 48.3	488.4 ± 38.3	596.7 ± 58.3
3 back reaction time (msec)	531.5 ± 65.1	566.2 ± 57.0	568.5 ± 55.2	722.6 ± 71.9
Performance % - correct				
Main effect of level		$F_{3,201}$=145.9; p=<0.001	Participants performed worse on higher N-backs (p's<0.001) except for 1-back vs. 0-back (p=0.454).	
No main effect of genotype		$F_{1,67}$=2.06; p=0.156		
No main effect of drug		$F_{1,67}$=0.29; p=0.592		
No interaction of genotype * drug		$F_{1,67}$=0.05; p=0.827		
Trend interaction of level * genotype		$F_{3,201}$=2.54; p=0.073	Effect of level was there for both genotypes. COMT-Met homozygotes performed better on the 3-back than the COMT-Val homozygotes (p=0.053).	
No interaction of level * drug		$F_{3,201}$=2.22; p=0.103		
No interaction of level * genotype * drug		$F_{3,201}$=0.50; p=0.640		
Reaction time data		Reaction time calculated for correct trials only		
Main effect of level		$F_{3,183}$=4.63; p=0.009	participants reacted slower during 3-back compared to 0-,1-, and 2-back (p's<0.031)	
No main effect of genotype		$F_{1,67}$=0.012; p=0.913		
No main effect of drug		$F_{1,67}$=0.77; p=0.385		
No interaction of genotype * drug		$F_{1,67}$=0.69; p=0.411		
Trend interaction of level * genotype		$F_{3,183}$=2.32; p=0.096	For COMT-Val homozygotes only: significant difference between 0-back and 3-back (p=0.006), between 1-back and 3-back (p=0.003), and between 2-back and 3-back (p=0.003).	
No interaction of level * drug		$F_{3,183}$=0.81; p=0.458		
No interaction of level * genotype * drug		$F_{3,183}$=1.59; p=0.205		

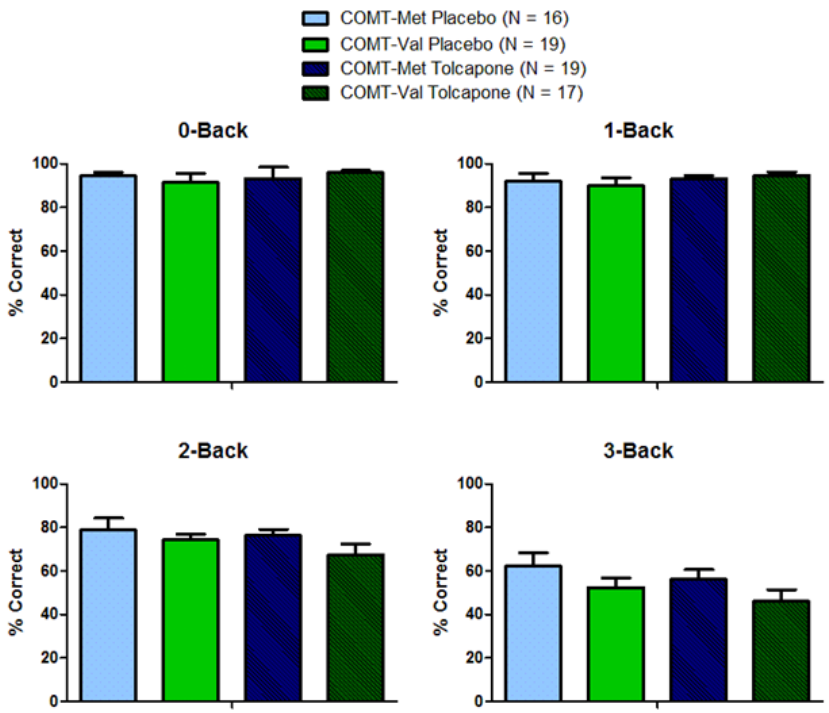


Figure 8.2 - Effects of COMT-genotype and tolcapone on N-back performance (percentage correct).

There were no significant group differences on N-back performance (F's < 2.1; p's >0.15). Results are expressed as mean±SEM.

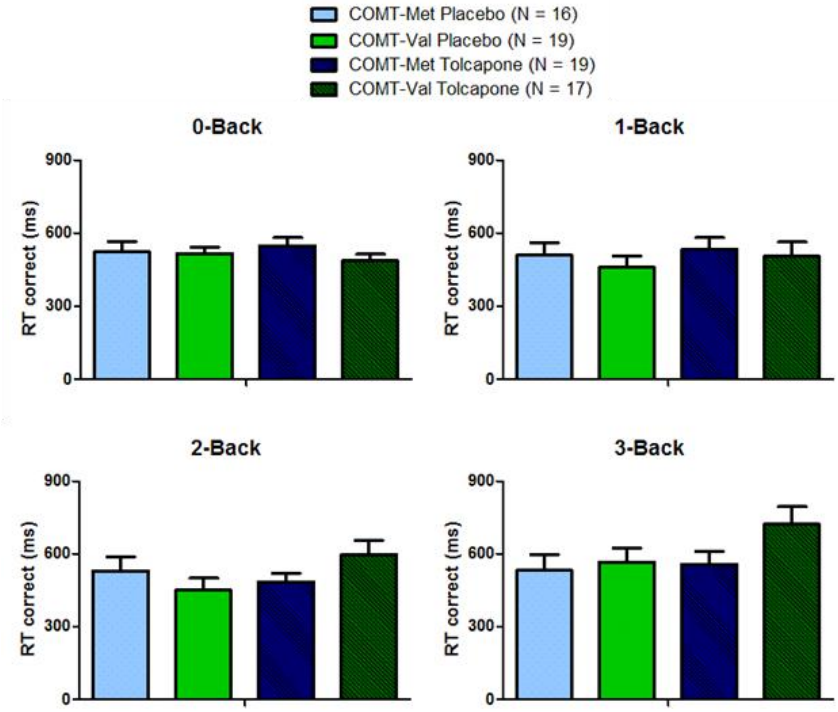


Figure 8.3 - Effects of COMT-genotype and COMT-inhibition on N-back reaction times.

There were no significant group differences on reaction times of the correct trials (F's < 0.77; p > 0.38). Results are expressed as mean±SEM

8.3.3 Group differences on N-back *performance* in cortisol responders

As presented in **Table 8.3** and **Figures 8.4** and **8.5**, when analysing the N-back data for cortisol responders only (as defined with %baseline AUC_i) there was a main effect of genotype for % correct trials ($F_{1,52}$=5.17; p=0.027) with COMT-Met homozygotes performing better than the COMT-Val homozygotes, but only during 2-back and 3-back, as reflected in a trend interaction of level and genotype ($F_{3,156}$=2.77; p=0.062). There was no main effect of drug ($F_{1,52}$=0.06; p=0.806) nor an interaction between genotype and drug ($F_{1,52}$=0.18; p=0.673).

There were main effects of level for the % correct trials ($F_{3,156}$=127.9; p=<0.001), and reaction time ($F_{3,144}$=5.68; p=0.003), but no interactive effects of group and drug on either measure (F's < 2.0; p's > 0.133). There were no main or interactive effects for reaction time (F's<0.6; p's>0.44), besides an interaction between genotype and level ($F_{3,144}$=4.42; p=0.012) driven by level effects.

Table 8.3 - Effects of COMT genotype and COMT inhibition on N-back performance in cortisol responders. Reaction time calculated for correct trials only.

	COMT-Met placebo (Mean ± SEM) N = 15	**COMT-Val placebo (Mean ± SEM) N = 15**	**COMT-Met Tolcapone (Mean ± SEM) N = 13**	**COMT-Val tolcapone (Mean ± SEM) N = 13**
0 back % correct	94.8 ± 1.7	91.2 ± 5.2	98.2 ± 0.7	95.3 ± 1.2
1 back % correct	94.0 ± 3.3	88.5 ± 4.5	92.6 ± 1.8	95.0 ± 1.5
2 back % correct	81.9 ± 4.7	73.8 ± 3.6	79.0 ± 3.4	68.1 ± 5.7
3 back % correct	65.2 ± 5.7	49.7 ± 5.2	57.9 ± 4.8	46.9 ± 5.9
0 back reaction time (msec)	534.7 ± 43.6	541.8 ± 28.9	576.3 ± 38.7	491.3 ± 32.3
1 back reaction time (msec)	517.3 ± 52.7	497.0 ± 52.4	572.7 ± 58.6	485.4 ± 57.5
2 back reaction time (msec)	498.2 ± 51.2	495.7 ± 55.7	500.5 ± 46.8	562.5 ± 55.5
3 back reaction time (msec)	492.4 ± 55.8	605.8 67.0	606.7 ± 71.7	729.5 ± 85.2
Performance % - correct				
Main effect of level		$F_{3,156}$=127.9; p=<0.001	Participants performed worse on higher N-backs (p's<0.001) except for 1-back vs. 0-back (p=0.061).	
Main effect of genotype		$F_{1,52}$=5.17; p=0.027	COMT-Met homozygotes performed better than COMT-Val homozygotes (p=0.027).	
No main effect of drug		$F_{1,52}$=0.06; p=0.806		
No interaction of genotype * drug		$F_{1,52}$=0.18; p=0.673	Trend: COMT-Met homozygotes performed better than COMT-Val homozygotes on placebo only (p=0.053).	
Trend interaction of level * genotype		$F_{3,156}$=2.77; p=0.062	Difference between COMT-Met homozygotes and COMT-Val homozygotes only on 2-back (p=0.036) and 3-back (p=0.019).	
No interaction of level * drug		$F_{3,156}$=1.96 p=0.142		
No interaction of level * genotype * drug		$F_{3,156}$=0.49; p=0.629		

Reaction time data	Reaction time calculated for correct trials only	
Main effect of level	$F_{3,144}$=5.68; p=0.003	Participants reacted slower during 3-back compared to 0-, 1-, and 2-back (p's<0.041).
No main effect of genotype	$F_{1,48}$=0.064; p=0.801	
No main effect of drug	$F_{1,48}$=0.62; p=0.437	
No interaction of genotype * drug	$F_{1,48}$=0.019; p=0.892	
Interaction of level * genotype	$F_{3,144}$=4.42; p=0.012	Driven by level effects. COMT-Met homozygotes faster on 1-back vs 2-back (p=0.039). COMT-Val homozygotes faster during 0-back vs 3-back (p=0.003), 1-back vs 3-back (p=0.001) and 2-back vs 3-back (p=0.001).
No interaction of level * drug	$F_{3,144}$=2.02; p=0.133	
No interaction of level * genotype * drug	$F_{3,144}$=0.55; p=0.598	

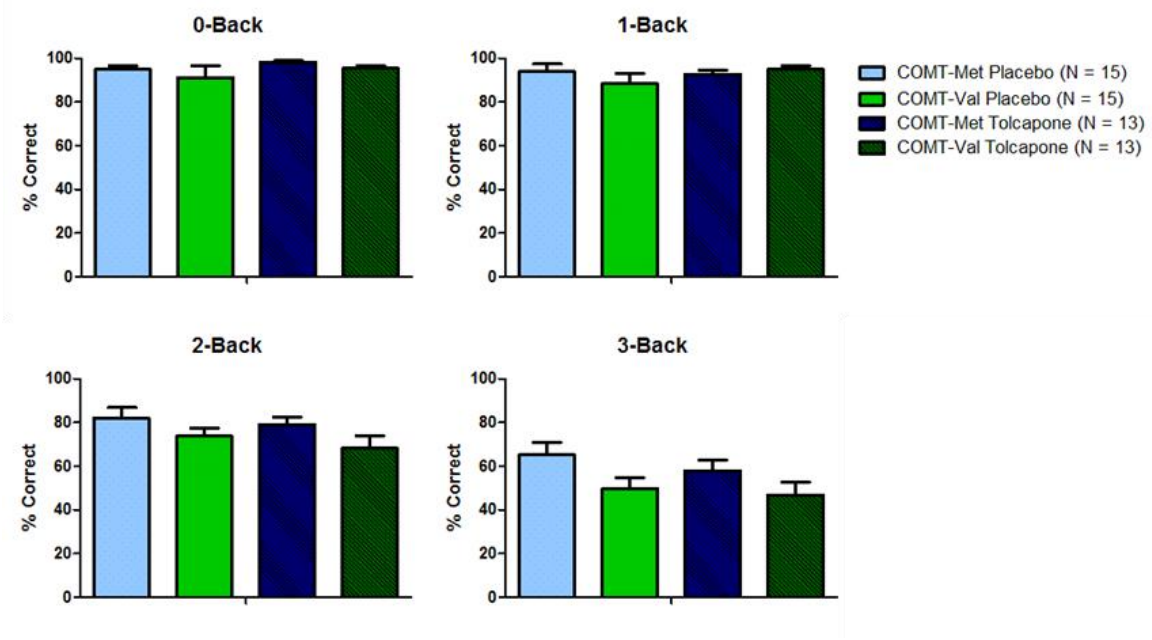


Figure 8.4 - Effects of COMT-genotype and tolcapone on N-back performance (%-Correct) in cortisol responders only.

There was a main effect of genotype for % correct trials ($F_{1,52}$=5.17; p=0.027) with COMT-Met homozygotes performing better than the COMT-Val homozygotes, but only during 2-back and 3-back, as reflected in a trend interaction of level and genotype ($F_{3,156}$=2.77; p=0.062). There was no main effect of drug ($F_{1,52}$=0.06; p=0.806) nor an interaction between genotype and drug ($F_{1,52}$=0.18; p=0.673). Results are expressed as mean±SEM.

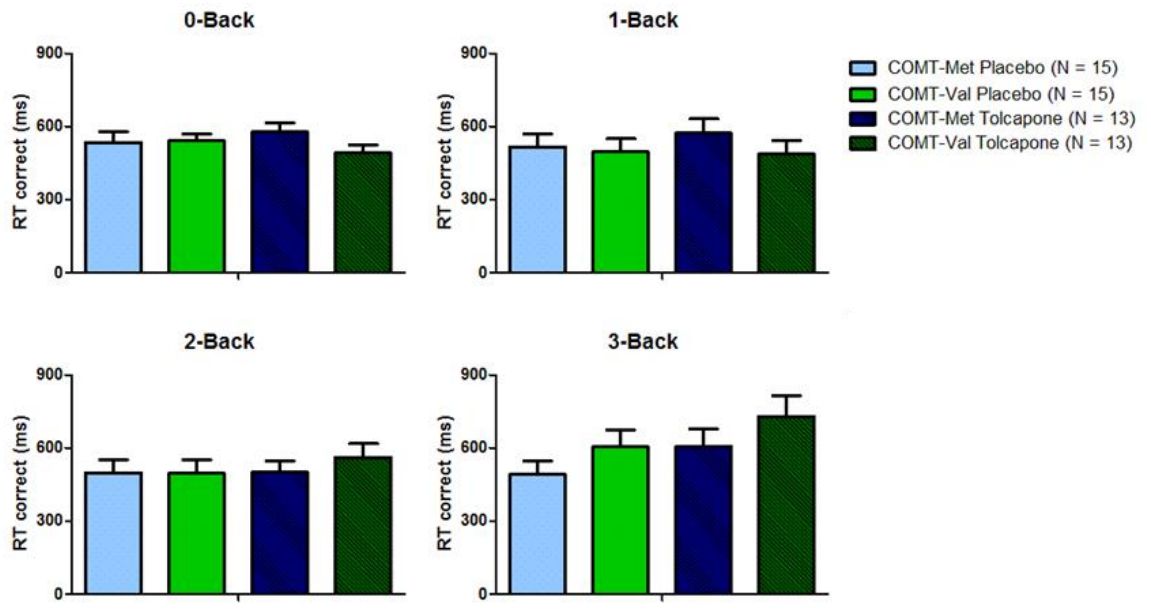


Figure 8.5 - Effects of COMT-genotype and tolcapone on N-back reaction times in cortisol responders only.

There were no effects of COMT-genotype and tolcapone nor an interaction on N-back reaction times for cortisol responders only (F's<0.6; p's>0.44). Results are expressed as mean±SEM.

8.3.4 *Imaging results*

In the previous section I showed that there were no effects of COMT genotype or COMT inhibition on working memory performance when considering the whole sample. However, when interrogating the data further, an effect of COMT genotype on working memory performance was found in cortisol responders only (i.e. when all subjects performed the N-back under condition of stress). Now I will present the effects of the MIST on brain activity during the N-back and again explore whether there are any effects of COMT genotype, COMT inhibition and their interaction.

8.3.4.1 *Main effect of task*

In order to determine if the N-back task engaged brain regions previously associated with working memory, I compared neural activation in response to 2-back vs. 0-back. Activity was observed in a network of areas that maps very closely to previous reports (Mier et al., 2010). As illustrated in **Table 8.4 and Figure 8.6**, the task activated the expected areas of interest (in red) including the right dorsolateral PFC, for 2-back vs 0-back (Z=11.40, p=<0.001, peak voxel location: x=27, y=73, z=38, cluster size=64733 voxels). There was also deactivation in default mode network (DMN) areas (significant activation in 0-back vs 2-back, in blue, such as the mPFC, posterior cingulate cortex, and the hippocampi) (Z=11.40, p=<0.001, peak voxel location: x=45, y=40, z=51, cluster size=43358

voxels). Together, these findings confirm that the N-Back task in our hands elicits activation of areas previously reported to support working memory.

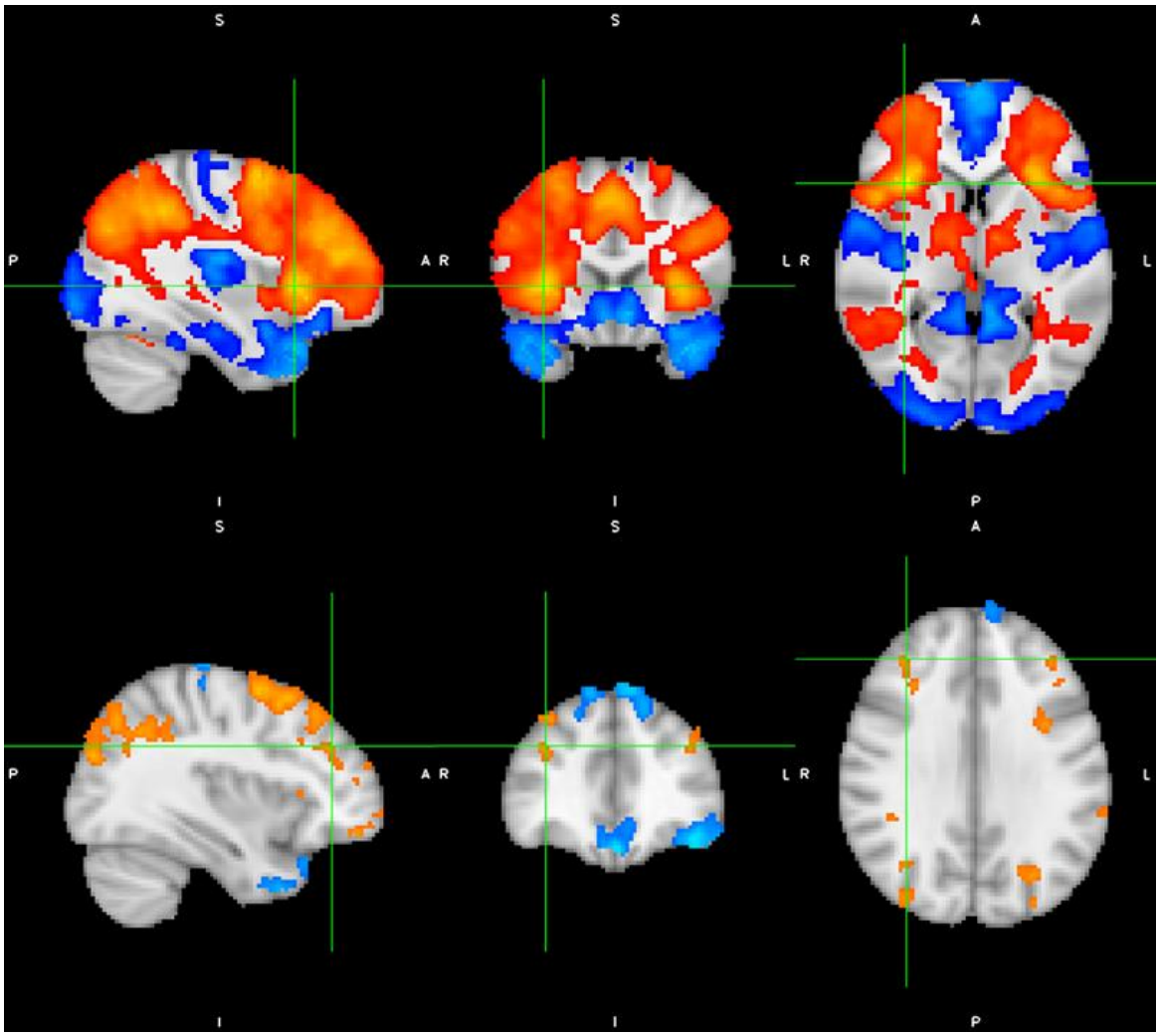


Figure 8.6 - Whole-brain fMRI MIST task activations and deactivations.

Sagittal, coronal and axial images depicting neural activation in response to 2-back vs 0-back across groups. Images thresholded at Z>3.1, p<0.05 corrected.
Top: Main effect of task: across all groups, 2-back led to greater (red) BOLD signal response including in the right dlPFC. Significant deactivations were found in for example the default mode network (DMN) areas (significant activation in 0-back vs 2-back, in blue).
Bottom: Same as top, but corrected for CBF and GM differences. Activations in the right dlPFC and deactivations in the mPFC remained significant. For more details see Table 8.5.

8.3.4.2 *Group differences*

Whole brain analysis

As presented in **Figure 8.7 and Table 8.6,** a whole brain analysis (threshold Z>3.1, p<0.05, corrected) revealed increased BOLD activation in the tolcapone group relative to the placebo (regardless of genotype) during 2-back (vs. 0-back) in seven different clusters, including the left caudate nucleus, left and right frontal areas and occipital gyrus. There were no genotype-related differences, nor interactive effects. Nor were there any genotype or drug related differences in the right dlPFC.

When analysing at a less stringent threshold (Z>2.3, p<0.05 corrected) results were similar but in larger clusters. Furthermore, two additional clusters were found for the tolcapone > placebo contrast (see **Table 8.6**).

Whole brain analysis, cortisol responders only

Results were similar when the functional data was analysed in cortisol responders only, though fewer clusters were found for the tolcapone > placebo contrast (3 instead of 7, cluster1: lateral occipital cortex, cluster2: superior frontal gyrus BA10 extending into frontal pole, cluster3: left caudate). There were no genotype-related differences, nor interactive effects (data not shown).

Table 8.4 - Whole brain fMRI N-back task activations and deactivations - without CBF and GM maps as nuisance variables.

ICA denoised N-back data Threshold 3.1 p<0.05	**Brain area / BA**	**Side**	**Cluster size (voxels)**	**Voxel max (x,y,z)**	**MNI max (x,y,z)**	**Z-score**	**p-value**
Task activation (2-back > 0-back)							
Mean across groups							
Cluster 1	Including middle + superior frontal gyrus extending into frontal pole, plus caudate, pallidum, thalamus, anterior cingulate gyrus, cerebellum	R+L	34008	30,67,65	30,8,58	9.81	<0.001
Cluster 2	Precuneous cortex, BA7, extending into lateral occipital cortex, inferior + middle temporal gyrus, angular gyrus	R+L	23346	41,30,63	8,-66,54	9.99	<0.001
Task deactivation (0-back < 2-back)							
Mean across groups							
Cluster 1	Posterior cingulate cortex, extending into precuneous cortex, mPFC, dlPFC + anterior cingulate gyrus, hippocampus, temporal occipital fusiform cortex	L+R	23553	47,36,46	-4,-54,20	9.68	<0.001
Cluster 2	Temporal pole	R	6472	24,70,16	42,14,-40	8.47	<0.001
Cluster 3	Occipital pole, extending into lateral occipital cortex	L+R	4200	54,13,43	-18,-100,14	6.59	<0.001
Cluster 4	Angular gyrus, lateral occipital cortex	L	813	70,32,53	-50,-62,34	7.47	<0.001
Cluster 5	Precentral + postcentral gyrus	L	276	56,49,75	-22,-28,78	5.22	<0.001

Table 8.5 - Whole brain fMRI N-back task activations and deactivations - with CBF and GM maps as nuisance variables.

ICA denoised N-back data Threshold Z>3.1, p<0.05	Brain area / BA	Side	Cluster size (voxels)	Voxel max (x,y,z)	MNI max (x,y,z)	Z-score	p-value
Task activation (2-back > 0-back), Mean across groups							
Cluster 1	Precuneous cortex, extending into lateral occipital cortex	L+R	3557	47,30,68	-4,66,64	6.33	<0.001
Cluster 2	Superior frontal gyrus, extending into middle frontal gyrus, BA6, supplementary motor cortex, BA9,frontal pole, middle frontal gyrus, BA10, BA8 and BA6	R+L	3290	38,64,72	14,2,72	7.28	<0.001
Cluster 3	Frontal pole, BA11 and BA10	R	316	33,85,28	24,44,16	5.75	<0.001
Cluster 4	Lateral occipital cortex, BA37, extending into inferior and middle temporal gyrus	R	210	19,26,31	52,-74,-10	4.64	<0.001
Cluster 5	White matter, Precentral gyrus, extending into inferior frontal gyrus	L	160	66,61,48	-42,-4.24	5.04	<0.001
Cluster 6	Frontal pole, middle frontal gyrus, BA8 and BA9	L	154	64,82,51	-38,38,30	4.19	<0.001
Cluster 7	BA37, lateral occipital cortex, middle temporal gyrus	L	145	72,31,37	-54,-64,2	5.49	<0.001
Cluster 8	Supramarginal gyrus, BA40, angular gyrus	R	103	18,44,66	54,-38,60	4.07	0.0074
Cluster 9	Insular cortex	R	79	30,73,41	30,20,10s	5.26	0.0289
Task deactivation (0-back < 2-back), Mean across groups							
Cluster 1	Frontal medial cortex, extending into frontal pole, BA11, paracingulate gyrus.	L+R	1147	44,84,26	2,42,-20	7.00	<0.001
Cluster 2	Superior frontal gyrus, BA6 and BA8	L+R	866	47,83,66	-4,40,60	6.43	<0.001
Cluster 3	BA38, Temporal pole, BA21	L	778	63,66,16	-36,6,-40	7.22	<0.001
Cluster 4	BA38, Temporal pole	R	492	25,69,16	40,12,-40	6.75	<0.001
Cluster 5	Frontal pole, frontal orbital cortex, BA47	L	355	65,82,28	-40,38,-16	6.63	<0.001
Cluster 6	Postcentral gyrus, BA3, BA4, precentral gyrus	R	244	22,52,68	46,-22,64	6.12	<0.001
Cluster 7	Occipital pole, BA17 and BA18	R	228	30,14,39	30,-98,6	5.14	<0.001
Cluster 8	Postcentral gyrus and precentral gyrus	R	223	32,49,74	26,-28,76	5.06	<0.001
Cluster 9	Occipital pole, BA17 and BA18	L	210	57,14,42	-24,-98,12	5.04	<0.001
Cluster 10	Postcentral gyrus and precentral gyrus	L	111	56,49,75	-22,-28,78	5.42	0.0048
Cluster 11	Middle + inferior temporal gyrus, BA21	L	87	75,55,28	-60,-16,-16	4.25	0.0182

Table 8.6 - Effects of COMT inhibition on working memory related brain activity - with CBF and GM maps as nuisance variables.

ICA denoised N-back data Threshold 3.1 p<0.05 + GM + CBF maps		**Brain area / BA**	**Side**	**Cluster size (voxels)**	**Voxel max location (x,y,z)**	**MNI max (x,y,z)**	**Z-score**	**p-value**
Tolcapone > placebo								
	Cluster 1	Left caudate extending in thalamus	L	195	50,60,44	-10.-6,18	5	<0.001
	Cluster 2	Frontal pole, extending into superior frontal gyrus, BA8	R	122	35,84,56	20,42,40	4.78	0.0027
	Cluster 3	Frontal orbital cortex, extending into BA47	R	107	28,75,29	34,24,-14	4.54	0.0060
	Cluster 4	Frontal pole, extending into BA10 and BA47	L	88	68,86,30	-46,46,-12	4.18	0.0172
	Cluster 5	Frontal pole, BA10	L	86	57,92,45	-24,58,18	4.89	0.0192
	Cluster 6	Lateral occipital gyrus, BA18 extending into BA19	L	75	64,20,34	-38-68,-4	4.26	0.0367
	Cluster 7	Superior frontal gyrus, BA6, extending into paracingulate gyrus and supplementary motor cortex	L	72	46,68,64	-2,10,56	3.96	0.0440
ICA denoised N-back data Threshold 2.3 p<0.05								
Tolcapone > placebo								
Additional clusters								
	Additional Cluster	Right caudate extending in thalamus and putamen and insular cortex	R	753	16,-18,20	37,54,46	4.03	<0.001
	Additional Cluster	Middle frontal gyrus, BA8, extending into precentral gyrus and inferior frontal gyrus	R	327	48,14,36	21,70,54	3.96	0.0088

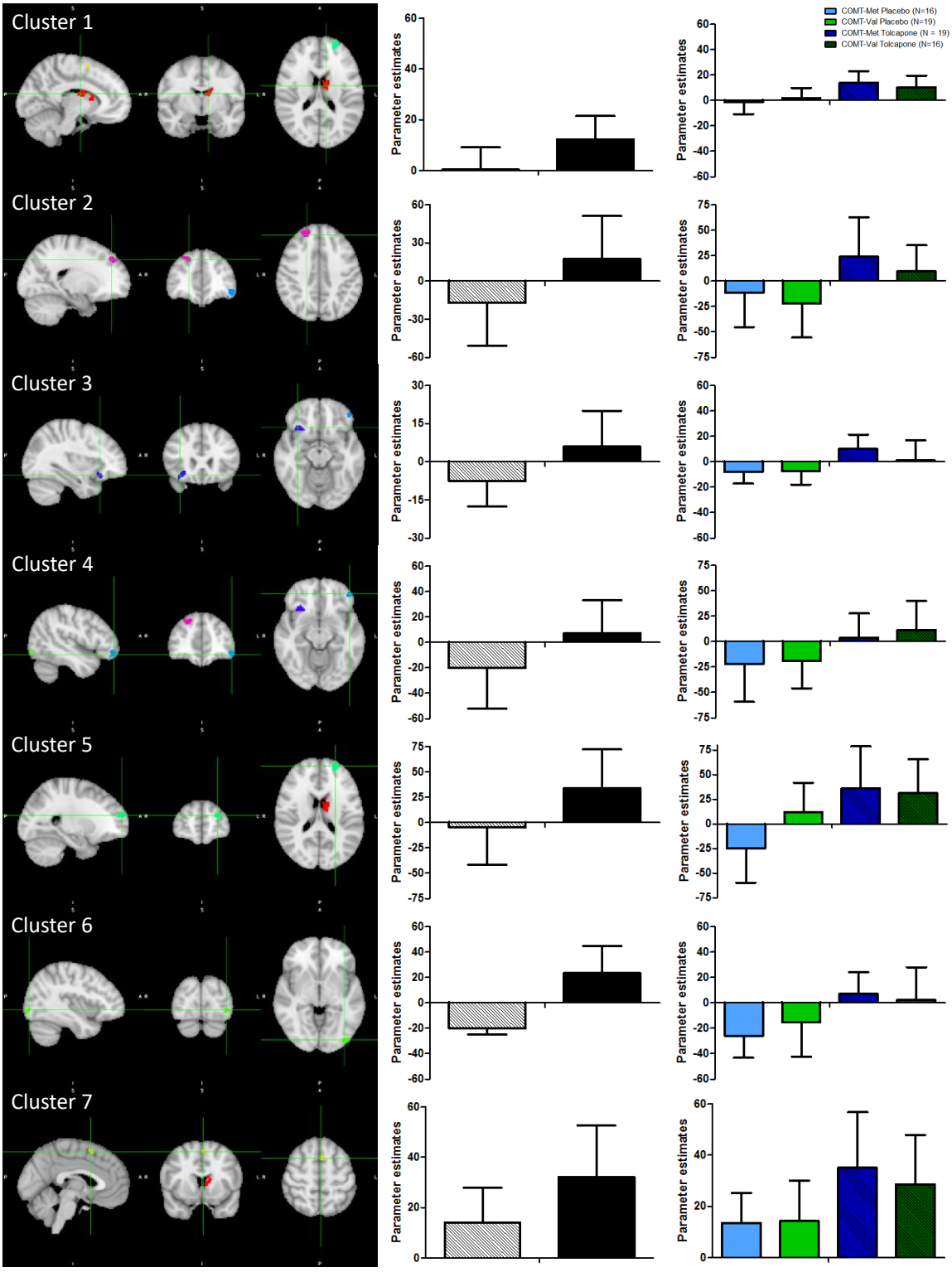


Figure 8.7 - Effects of COMT inhibition on whole brain working memory related activity.

Sagittal, coronal and axial images depicting neural activation in response to 2-back vs 0-back across groups. A main effect of drug was found where compared with placebo, participants on tolcapone showed greater activation in 7 different clusters. See Table 8.6 for full details. Images thresholded at Z>3.1, p<0.05 cluster corrected. Error bars showing standard deviation.

Region of Interest (ROI) analysis / small volume correction

When defining the right dlPFC mask as a ROI, there was a main effect of genotype, with COMT-Met homozygotes showing increased activation compared to COMT-Val homozygotes in the right dlPFC (Z= 3.23, p=0.0475, peak voxel location: x=40, y=40, z=30, cluster size=2 voxels). See **Figure 8.8.** When analysing at a less stringent threshold (Z>2,3, p<0.05 corrected) the cluster was larger but similar. There were no drug-related differences, nor interactive effects.

Region of Interest (ROI) analysis / small volume correction - cortisol responders only

There were no main or interactive effects for the ROI analysis in cortisol responders only. When setting a less stringent statistical threshold (Z>2,3, p<0.05 corrected) a drug effect was found where participants on tolcapone had a larger activation in the right dlPFC compared to both genotypes on placebo (Z=2.97, p=0.03, peak voxel location: x=40, y=44, z=24, cluster size=43 voxels, – data not shown).

8.4 Discussion

This chapter has two main findings: (1) there were no effects of COMT genotype or COMT inhibition on working memory performance when considering the whole sample, (2) both COMT genotype (ROI analysis) and COMT inhibition (whole brain) influenced working memory related brain activation. When interrogating the data further, an effect of COMT genotype on working memory performance was found in cortisol responders only (i.e. when all subjects performed the N-back

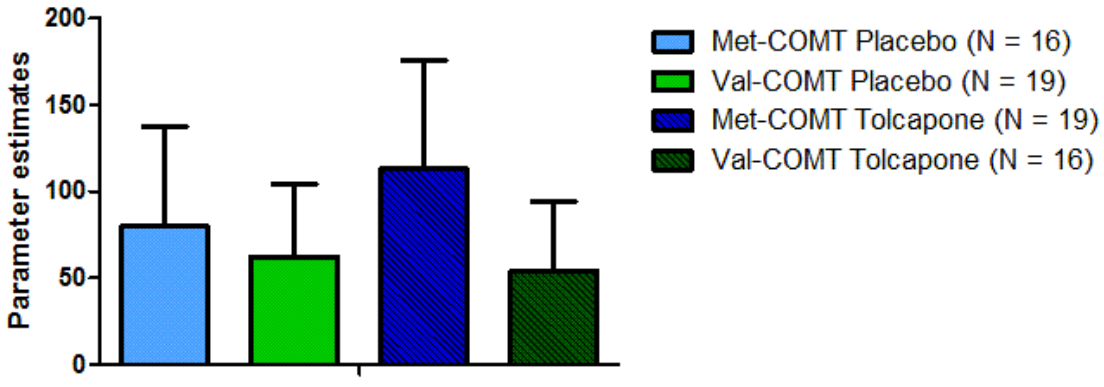


Figure 8.8 - Small volume correction / ROI analysis - right dlPFC.

2-back vs 0-back. Main effect of genotype: COMT-Met homozygotes showing greater activation compared to COMT-Val homozygotes in the right dlPFC. Images thresholded at Z>3.1, p<0.05 cluster corrected. Error bars showing standard deviation.

under condition of stress). See **Table 8.7** for an overview of findings of the previous literature, our hypotheses based on those, and our actual findings.

8.4.1 *Effects on working memory performance*

The main effect of N-back level indicated the presence of the predicted variation in performance according to working memory load, i.e. highest performance on the 0-back, and lowest on the 3-back condition. The trend genotype difference found for N-back performance in the whole sample, where COMT-Met homozygotes performed better than COMT-Val homozygotes, was more profound when only cortisol responders were considered. This genotype effect only seems to be present when subjects are on placebo (however, this should be interpreted with caution, as the interaction was only trend-level significant). I did not find any overall effects of tolcapone, nor any interactions, for working memory performance. Both COMT-Val and COMT-Met homozygotes performed similarly on tolcapone and placebo.

I predicted that acute stress would be detrimental to COMT-Met homozygote performance, by moving them to 'supra-optimal' dopamine levels, but would enhance performance in COMT-Val homozygotes, by moving them closer to the peak (as for example shown by Buckert et al., (2012) and Qin et al., (2012). I did not find this. My different results could be due to the fact that both of these previous studies used a different stressor (TSST for Groups or a traumatic film) to induce stress. Stressor related cortisol levels increased by either about 100% in the study done by Buckert et al., (2012) whilst cortisol levels remained the same in the Qin et al., (2012) study (control non-stress group showed a significant decrease in cortisol levels and therefore there was still an effect of stress), whilst the MIST in our hands increased cortisol levels by about 150-200%. Moreover, Buckert et al., (2012) studied both males and females and showed that cortisol levels were significantly higher for the males in their sample. Furthermore, these studies used a different version of the N-back task to asses working memory performance. The N-back used in our study requires participants to continually update their mental set while responding to previously seen stimuli, and has therefore been demonstrated to more reliably activate the PFC (Callicott, 1998).

Table 8.7 - Overview of predictions, hypotheses and actual findings.

	Literature			**Hypothesis**		**Findings**		**Findings in cortisol responders only**	
	COMT Untreated / placebo	*COMT Inhibition / tolcapone*	*COMT + Stress untreated*	*COMT + Stress + placebo*	*COMT + Stress + tolcapone*	*COMT + Stress + placebo*	*COMT + Stress + tolcapone*	*COMT + Stress + placebo*	*COMT + Stress + tolcapone*
Working memory performance	COMT-Met homozygotes perform better than COMT-Val homozygotes	COMT-Val homozygotes on tolcapone perform better than COMT-Met homozygotes on tolcapone	COMT-Val homozygotes perform better than COMT-Met homozygotes	COMT-Val homozygotes on placebo perform better than COMT-Met homozygotes Interaction of COMT genotype and drug	Both COMT-Val homozygotes and COMT-Met homozygotes will perform worse than on placebo Main effect of drug	COMT-Met homozygotes perform better than COMT-Val homozygotes when only cortisol responders are considered	No difference between COMT-Val and COMT-Met homozygotes nor compared to placebo	COMT-Met homozygotes performed better than COMT-Val homozygotes	No difference between COMT-Val and COMT-Met homozygotes nor compared to placebo
Brain activity (fMRI) in dlPFC during PFC-dependent cognitive task	COMT-Val homozygotes greater brain activity than COMT-Met homozygotes	Both COMT-Val homozygotes and COMT-Met homozygotes greater brain activity on tolcapone than compared to placebo	COMT-Met greater brain activity than COMT-Val	COMT-Met homozygotes greater brain activity than COMT-Val homozygotes Interaction or main effect of genotype	No differences in brain activity between COMT-Met homozygotes and COMT-Val homozygotes	COMT-Met greater brain activity than COMT-Val homozygotes in ROI analysis only	No differences between COMT-Met homozygotes and COMT-Val homozygotes nor compared to placebo	No differences between COMT-Met homozygotes and COMT-Val homozygotes	No differences between COMT-Met homozygotes and COMT-Val homozygotes nor compared to placebo

Sample sizes were roughly similar for previous studies compared to mine (Buckert et al., 2012): 15 COMT-Met homozygotes, 7 COMT-Val homozygotes and 17 COMT heterozygotes; (Qin et al., 2012): 17 COMT-Met homozygotes, 16 COMT-Val homozygotes, 14 females in total.

Other than the presence of a stressor and the study taking place inside an MRI scanner instead of a MEG scanner (participants sit upright in a MEG scanner, therefore perhaps less sleepy), our study is similar in terms of study population and N-back task to that of (Farrell et al., 2012). Farrell et al., (2012), found interactive effects of COMT genotype and COMT inhibition on N-back performance. In our current study we did not find any effects of tolcapone, nor an interaction with genotype: both our genotype groups performed similarly on placebo and tolcapone. As noted as a limitation before in Chapter 7, we do not have a control non-stress group in this study. Therefore, we do not know what the different starting positions were on the inverted-U curve between dopamine and PFC-dependent function for each group. I can only speculate that, in those on placebo, stress as induced by the MIST seemed to push everyone (presumably rightwards) closer to the peak of the inverted-U curve, given that (in cortisol responders only) COMT-Met homozygotes on placebo performed better under conditions of stress than COMT-Val homozygotes, but that these differences in performance disappear when dopamine levels are increased further by tolcapone. It is unclear why, if this explanation is correct, participants in the current study appeared to lie at different starting positions on the curve, compared to other studies studying these relationships. However, it is likely that many other factors (e.g. other genetic factors) play a role.

8.4.2 *Effects on working memory related brain activity*

The N-back task engaged similar brain regions to those previously associated with working memory, including the right dlPFC. Both COMT genotype (ROI analysis) and COMT inhibition (whole brain analysis) influenced working memory related brain activation, in the absence of interactions between them.

A whole brain analysis revealed greater BOLD activation in the tolcapone group, compared to placebo (regardless of genotype) in response to the 2-back (vs. 0-back) in multiple regions, including the left caudate nucleus, left and right frontal areas and occipital gyrus. There were no genotype-related differences, nor interactive effects at the whole brain level. Repeating this analysis in cortisol responders only did not reveal any differences. Our findings in the left and right caudate are perhaps unsurprising, given the use of COMT inhibitors for Parkinson's disease. The impact of tolcapone on dopamine levels has been well-studied in the striatum: in this region, COMT

inhibition typically has little or no effect on dopamine levels at baseline (given the relative abundance of synaptic dopamine transporters in that region in contrast to the PFC) (Laatikainen et al., 2013). Presumably, under baseline conditions, extracellular dopamine levels are regulated by uptake mechanisms, enzymatic degradation becoming significant only when dopamine release increases and the buffering capacity of the uptake mechanism is exceeded (like for example under conditions of stress as in our study). The effects of tolcapone in the frontal regions with a lack of COMT genotype effects could be explained by the same reasoning as above. Excess dopamine release due to the stressor in these regions for both genotypes.

8.4.3 *Effects on working memory related brain activity – right dlPFC*

When adding the right dlPFC mask as an a-priori selected region of interest, there was a small main effect of COMT genotype, with COMT-Met homozygotes showing increased activation compared to COMT-Val homozygotes. This effect of genotype disappeared when repeating this analysis in cortisol responders only (perhaps due to loss of power as less subjects in total) as we did not find any effects of COMT genotype or COMT inhibition during that analysis. When setting a less stringent statistical threshold however, a drug effect was found where participants on tolcapone had a larger activation in the right dlPFC compared to both genotypes on placebo. Used CBF maps as a covariate therefore unlikely that differences in CBF play a role, however, see limitations in Chapter 5 (possibility for additional differences in CBF for smaller regions).

(Egan et al., 2001) found that under normal conditions (i.e. not under conditions of stress) COMT-Val homozygotes showed greater activations in the dorsolateral PFC (defined as BA46; x=43, y=38, z=12) and anterior cingulate (BA32, x=6, y=60, z=8). Their study used a 1.5T scanner and a lower statistical threshold (uncorrected p=0.005 voxel-wise). Assuming that greater PFC activation for a given level of performance is indicative of 'PFC inefficiency', and that this measure is sensitive to stress, it would be predicted that under acute stress brain activity in COMT-Val homozygotes would decrease, whilst it would increase in COMT-Met homozygotes. This is indeed what we find. Moreover, the results from (Qin et al., 2012) are also consistent with our study. They demonstrated increased working memory-related activation in the right dlPFC by using a similar ROI analysis only considering that brain area due to a stressor (traumatic-film) (MNI coordinates: x=30, y=30, z=42) in COMT-Met homozygotes, but decreased activation in COMT-Val carriers (Qin et al., 2012). They used a 3T scanner and had similar statistical thresholds as we used in our study. Again, we did not find an interaction between COMT genotype and COMT inhibition on working memory related brain activity. The reasons for this are unclear. Therefore, future replications using a larger sample

size and a non-stress control group may further reveal and refine between-group similarities and differences.

8.4.4 *Conclusion*

In sum, neither COMT genotype nor COMT inhibition influenced working memory performance under conditions of stress in the whole sample. However, in cortisol responders only, in contrast to my predictions, COMT-Met homozygotes had better working memory performance than COMT-Val homozygotes. I did not find any overall effects of tolcapone, nor any interactions on working memory performance. In terms of brain activity, both COMT genotype (ROI analysis) and COMT inhibition (whole brain) influenced working memory related brain activation. Greater BOLD activation was found in the tolcapone group, compared to placebo (regardless of genotype) in multiple regions, including the left caudate nucleus, left and right frontal areas and occipital gyrus. There were no genotype-related differences, nor interactive effects at the whole brain level, but an ROI analysis in the dlPFC (the approach used in taken previous studies) indicated a main effect of genotype: COMT-Met homozygotes showed greater activation compared to COMT-Val homozygotes, consistent with earlier studies. Therefore, my results only partly support the hypothesis that the inverted-U relationships between stress and COMT with cognitive function overlap.

Stress and COMT inhibition did not interact to negatively impact on working memory performance. Therefore, my study does not provide evidence for undesirable side effects of clinically administered tolcapone. However, this study was done with a single dose of tolcapone in young healthy men without any existing working memory problems. Therefore, the apparent lack of interactive effects of stress and tolcapone should be interpreted with caution and may not extrapolate to the clinical situation. As I did not conduct a proper clinical trial the absence of an interaction between tolcapone and stress should be interpreted with caution.

Chapter 9 Overall Discussion

An inverted-U-shaped relationship exists between dopamine and PFC dependent cognitive function, whereby either too little or too much dopamine signalling impairs cognitive performance (as shown in for example for working memory performance). Genetic, pharmacological, pathological, and environmental factors can affect a person's position on the curve. In this thesis I explored three of these factors and their potential interactions: COMT genotype as a genetic factor, COMT inhibition by tolcapone as a pharmacological factor and acute stress as an environmental one. Interestingly, an inverted-U relationship also exists between acute stress and PFC-dependent cognitive performance, with moderate stress levels facilitating, and high levels impairing cognitive function. Despite there being some evidence that COMT genotype alters the cognitive and neural responses to stress, it is unknown whether this is modulated by COMT inhibition in humans. Moreover, there is evidence that the inverted-U relation between stress and PFC dopaminergic functioning is COMT-dependent. In this thesis I further explored these relationships.

In this final chapter I will give an overview of the main findings of this thesis. Then I will discuss strengths and limitations before concluding with suggestions for future work.

9.1 Summary of the main findings

There are many different kinds of laboratory-based stressors available to investigate the stress response in humans. I explored two - a novel VR stressor and the MIST - with the aim of establishing (a) the magnitude and (b) the duration of the stress response elicited by these stressors vs. their respective controls. As outlined in Chapter 2 and 3, both stressors induced a physiological and psychological stress response, however with a different magnitude and duration as summarised in **Table 9.1**. The MIST induced a stronger and longer lasting physiological response, whilst the VR lift seemed to induce higher subjective ratings of stress and anxiety. Specifically, in terms of induced cortisol response, this was more robust for the MIST, and lasted for the duration required to investigate the effects of stress on working memory performance. Therefore, these results validated the MIST as the stressor for the main study of this thesis. Similarly, administration of the MIST in the MRI scanner led to robust increases in both psychological and physiological stress indices (Chapter 8, see **Table 9.2**).

Table 9.1 - Comparison between the VR lift stressor and the behavioural MIST stressor in terms of physiological and subjective responses

	Stressor VR %-change compared to control	**Duration of significant /trend effect**	**Stressor MIST %-change compared to control**	**Duration of significant /trend effect**
VAS 'Stressed'	+157#	7 min	+150*	20 min
VAS 'Anxious'	+257*	7 min	+164*	20 min
Cortisol (% baseline)	+47*	20 min	+111*	80 min
Systolic BP (%baseline)	+3NS	-	+8*	20 min
Diastolic BP (%baseline)	+3NS	-	+9#	20 min
Pulse BP (%baseline)	+13*	7 min	+12*	20 min
Pulse ECG (%baseline)	+5NS	-	+23*	7 min
Skin conductance	+41*	7 min	+21*	20 min
RMSSD (%baseline)	+73*	7 min	-50*	30 min
LF-HF ratio (%baseline)	-43*	7 min	+52NS	-

*Indicates statistically significant; #indicates trend-level differences; NS indicates non-significant differences between control and stressor conditions

Table 9.2 - Magnitude and duration of stress response induced by MRI MIST

	MRI MIST %-change compared to baseline measure (time point 3)	**MRI MIST %-change compared to MRI baseline measure (time point 4)**	**Duration of significant effect**
VAS 'Stressed'	+ 374*	+ 137*	60 min
Cortisol (% baseline)	+140*	+ 114*	At least 45 min

*Indicates statistically significant differences between baseline and time point of interest

The remainder of the thesis focused on the effects of COMT genotype and inhibition, and their interaction, on behaviour and patterns of brain activity using MRI. A summary of the main findings of this MRI study is presented in **Table 9.3.**

In Chapter 5, I investigated whether there were group differences and/or an interaction between COMT genotype and tolcapone on CBF as measured by ASL, since such changes might confound later aspects of the study relying on the BOLD response. Consistent with the potential vasoconstrictive effects of dopamine, COMT-Val homozygotes had greater CBF in the PFC (including the dlPFC) compared to COMT-Met homozygotes. Moreover, tolcapone reduced CBF compared to placebo in three distinct clusters in the right parietal lobe. However, no interaction between COMT-

Table 9.3 - Summary of the main results of this thesis.

	Before stress induction ASL + rsFC (Chapter 5 and 6)	During stress induction MIST (Chapter 7)	After stress induction N-back (Chapter 8)
Main effects of genotype	**CBF:** COMT-Val homozygotes had greater CBF perfusion in the PFC (including the dlPFC) compared to COMT-Met homozygotes. **rsFC whole brain**: COMT-Val homozygotes had greater rsFC in a cluster in the right frontal pole with the rest of the DMN, compared to the COMT-Met homozygotes. **rsFC seed**: COMT-Met homozygotes had greater rsFC between the right dlPFC seed and the middle temporal gyrus, extending into the posterior supramarginal gyrus compared to COMT-Val homozygotes.	**Stress response**: no main effects of COMT genotype. **MRI whole-brain:** COMT-Met homozygotes showed greater stress induced deactivations in the left temporal cortex compared to COMT-Val homozygotes.	**N-back performance:** COMT-Met homozygotes performed better than COMT-Val homozygotes (significant in cortisol responders only). **MRI ROI:** COMT-Met homozygotes showed greater brain activation related to working memory performance compared to COMT-Val homozygotes in the right dlPFC.
Main effects of COMT inhibition / tolcapone / treatment	**CBF:** tolcapone reduced CBF compared to placebo in three distinct clusters in the right parietal lobe. **rsFC whole brain**: tolcapone influenced rsFC of the visual medial network, parietal motor network, language network and motor superior network regardless of genotype. In particular, tolcapone decreased the FC between the SMN and two clusters that included the right parietal lobe and left striatum.	**Stress response**: no main effects of tolcapone. **MRI whole brain**: no main effects of tolcapone.	**N-back performance**: no main effects of tolcapone. **MRI whole brain:** Homozygotes on tolcapone had greater brain activation related to working memory performance in 7 different clusters, including the left caudate nucleus, left and right frontal areas and occipital gyrus compared to participants on placebo. **MRI ROI:** cortisol responders with less stringent statistical threshold only: Participants on tolcapone had greater activation in the right dlPFC compared to both genotypes on placebo.
Interaction of COMT genotype and COMT inhibition	**CBF:** No interaction **rsFC whole brain**: COMT-Val homozygotes had higher FC between the SMN and two clusters in the left PFC compared to COMT-Met homozygotes on placebo. Tolcapone reversed	**Stress response:** COMT-Val homozygotes reported greater subjective stress levels compared to COMT-Met homozygotes on placebo only, whilst tolcapone increased subjective stress levels in COMT-Met homozygotes only.	**N-back performance:** No interaction effects **MRI whole brain**: No interaction effects **MRI seed**: No interaction effects

	this difference, increasing FC in these areas in COMT-Met homozygotes whilst decreasing connectivity in COMT-Val homozygotes. **rsFC seed:** greater FC was found for COMT-Val homozygotes on placebo between the left vlPFC seed and a brain area surrounding the left post-and pre-central gyrus and left anterior supramarginal gyrus. Tolcapone reversed this difference, increasing FC between these areas for COMT-Met homozygotes, and decreasing connectivity in COMT-Val homozygotes. **rsFC seed:** greater FC between the right dlPFC seed and a cluster in the middle temporal gyrus for COMT-Met homozygotes on placebo, compared to COMT-Val homozygotes on placebo, with tolcapone reversing this difference, increasing FC for COMT-Val and decreasing it for COMT-Met homozygotes.	**Stress response**: On placebo only, COMT-Met homozygotes had higher sAA levels during the MIST compared to COMT-Val homozygotes. **Stress response**: Cortisol responders only: Cortisol levels were significantly higher for COMT-Val homozygotes on placebo as compared to COMT-Mets on placebo at time point 8 only (where cortisol levels were highest). **Stress response:** COMT-Val homozygotes on tolcapone had a lower cortisol response than those on placebo when cortisol levels were highest (time point 8). **MRI whole brain**: No interaction effects.	
Conclusion	**CBF:** more dopamine, either due to the COMT- Met allele or tolcapone, results in less CBF, but their combined effects do not show any further significant decreases in CBF. **rsFC:** RSNs within the prefrontal lobes and the ones from the prefrontal lobes to the posterior regions, seem to be modulated by COMT influenced dopamine signalling.	Validated stress response to be able to investigate the interaction of COMT genotype, COMT inhibition, and their interaction on working memory performance and brain activity under conditions of stress (Chapter 7). No evidence for the idea that COMT-Met homozygotes display a more sensitive biological stress response compared to COMT-Val homozygotes, nor that the stress response is (in part) regulated by COMT dependent dopaminergic PFC activity.	Uncertain to what extend the inverted-U relationships between stress and COMT with cognitive function overlap. No indication that tolcapone interacts with stress to negatively impact on working memory performance.

genotype and COMT inhibition on CBF was found. These results show the complexity of dopamine's vasoactive properties. More dopamine, either due to the COMT- Met allele or tolcapone, results in less CBF, but their combined effects do not show any further significant decreases in CBF. Functional MRI data can also be confounded by differences in GM anatomy. Therefore, in order to interpret my functional MRI data more confidently, I investigated the potential effects on COMT genotype on GM density as well. However, after comparing GM maps between COMT-Val and COM-Met homozygotes no differences were found.

In Chapter 6 I demonstrated that COMT genotype influences FC at rest. rsFCs within the prefrontal lobes, and from the prefrontal lobes to posterior regions, were modulated by COMT. However, COMT's effects on connectivity were complex, with the directionality depending on the precise brain areas and networks studied. Delineating or predicting exact functional correlates is therefore difficult, although my data provide further evidence that COMT's significance extends beyond the dlPFC and that, rather than grossly altering the overall extent of FC of the frontal cortex, COMT seems to instead subtly tune neural circuitry.

As described in Chapter 7, in my hands, the MIST induced similar changes in brain activation to those reported in previous studies. There were no MIST related differences in physiological stress sensitivity between COMT-Met and COMT-Val homozygotes, nor between participants on placebo or tolcapone. However, there was an interaction between the two on subjective stress ratings: COMT-Val homozygotes reported greater subjective stress levels compared to COMT-Met homozygotes on placebo only, whilst tolcapone increased subjective stress levels in COMT-Met homozygotes only. In cortisol responders only, there were group differences on physiological stress: COMT-Val homozygotes on placebo had greater cortisol levels than both COMT-Met homozygotes on placebo and COMT-Val homozygotes on tolcapone. There were also genotype effects on stress-related brain activity: COMT-Val homozygotes had greater de-activations during the MIST in the left temporal cortex, compared to COMT-Met homozygotes. These findings stand in contrast to previous reports of greater stress sensitivity associated with the COMT-Met allele.

Finally, I investigated the effects of COMT genotype and COMT inhibition on working memory-related brain activity and performance under conditions of stress in Chapter 8. Neither COMT genotype nor COMT inhibition influenced working memory performance in the whole sample. However, in cortisol responders only, in contrast to my predictions, COMT-Met homozygotes had better working memory performance than COMT-Val homozygotes. I did not find any overall effects of tolcapone, nor any interactions on working memory performance. In terms of brain activity, both COMT genotype (ROI analysis) and COMT inhibition (whole brain) influenced working memory related brain activation. Greater BOLD activation was found in the tolcapone

group, compared to placebo (regardless of genotype) in multiple regions, including the left caudate nucleus, left and right frontal areas and occipital gyrus. There were no genotype-related differences, nor interactive effects at the whole brain level, but an ROI analysis in the dlPFC (the approach used in taken previous studies) indicated a main effect of genotype: COMT-Met homozygotes showed greater activation compared to COMT-Val homozygotes, consistent with earlier studies.

Across the thesis as a whole, I found variable relationships between the physiological stress response (indexed by cortisol) and working memory performance. In Chapters 2 and 3 I demonstrated that neither the VR stressor lift nor the MIST delivered outside the scanner influenced working memory performance, compared to their control conditions. However, when the MIST was delivered outside the scanner the magnitude of the cortisol response, was positively correlated with 2-back performance across all participants, indicating that acute, mild stress (irrespective of the source – in this case MIST or performance of the N-back) might enhance working memory performance. However, in contrast, when the MIST was delivered in the scanner there were *negative* correlations between the cortisol response and 1-back and 3-back (but not 2-back) performance (**see Table 9.4**). These variable findings likely reflect the complex relationship between stress and memory performance and are discussed further below.

Table 9.4 - Correlations between stress indices and N-back performance for the imaging study.

		Overall group (N=72)				Cortisol responders (N=56)			
		0-Back	1-back	2-back	3-back	0-Back	1-back	2-back	3-back
Self esteem	Spearman's rho	.026	.141	.119	.182	-.010	.069	.146	.167
	p value	.833	.242	.321	.129	.941	.613	.281	.220
Locus of control	Spearman's rho	.010	-.049	-.014	-.012	-.014	-.105	-.008	.035
	p value	.934	.686	.908	.922	.921	.443	.954	.796
Baseline VAS 'Stressed' Time point 3	Spearman's rho	-.006	.133	.130	.121	-.022	.195	.266	.244
	p value	.961	.274	.282	.317	.874	.154	.050	.072
During MIST VAS 'Stressed' Time point 6	Spearman's rho	-.096	-.145	.054	.115	-.133	-.094	.006	.086
	p value	.426	.228	.657	.339	.328	.492	.963	.527
Cortisol (% baseline) Time point 8	Spearman's rho	.119	-.245*	-.032	-.155	.065	-.395**	-.222	-.320*
	p value	.324	.039	.791	.197	.633	.003	.099	.016
sAA (% baseline) Time point 6	Spearman's rho	.284*	.066	-.129	-.109	.231	.096	-.086	-.038
	p value	.018	.590	.289	.371	.090	.485	.532	.784
AUCi cortisol (% baseline)	Spearman's rho	.232	-.137	.059	-.050	.230	-.220	-.092	-.175
	p value	.053	.257	.630	.679	.088	.103	.500	.197

9.2 Strengths and limitations

9.2.1 *Strengths*

In my thesis I investigated multiple physiological and psychological indices of the stress response. As discussed in Chapter 2, 3 and 8, very few (if any) correlations were found between indices of different types. Therefore, my findings emphasise the value of examining multiple variables to establish a full picture, not at least since different components of the stress response may impact differentially on outcomes of interest.

Many studies in neuroscience cannot be replicated. Differences in methodology between studies (e.g. in MRI parameters set, imaging analysis method used, different statistical threshold applied) are one potential explanation for this. In response, the neuroimaging field has adopted more stringent thresholds for statistical significance and demanded larger sample sizes. The sample size for my MRI study was considerably larger than many imaging studies, although clearly much smaller than large-scale 'big data' neuroimaging approaches. When examining a specific question, there is necessarily a trade-off between sample size (conducting very large experimental medicine studies is extremely expensive) and quality of data (large-scale datasets are necessarily broad in scope, rather than being tailored to a specific question). A strength of my study is that it was designed to address a single, specific question: the impact of COMT genotype and inhibition on brain activity and working memory performance under conditions of acute stress. My participants' demographics were well defined, as I was able to screen every participant myself. I have used a stringent statistical approach, by using the currently recommended statistical thresholds and including CBF and GM maps as covariates in all of my imaging analyses to account for possible confounding effects of these measures. I was blind to the different genotype and treatment groups in the imaging study until I completed all behavioural and MRI analyses, removing any potential for bias. None of the previous studies that I based my hypotheses on corrected for CBF, and only some corrected for potential GM differences. Therefore, I was able to interpret my data more confidently. It is possible that some of the functional effects found between COMT-Val and COMT-Met homozygotes in previous other studies could potentially be explained by differences in CBF.

9.2.2 *Limitations*

Firstly, only healthy young adult male volunteers were investigated. Not only do gender and age influence the physiological response to a stressor and its effect of the stressor on cognitive task

performance (Cornelisse et al., 2011; Schwabe et al., 2012; Zandara et al., 2016), but effects of age and gender have also been found on CBF and rsFC (Aanerud et al., 2017; Zhang et al., 2018; Hjelmervik et al., 2014). Moreover, COMT genotype and age interactions have also been reported (Harrison and Tunbridge, 2008). Furthermore, COMT's activity and effects differ markedly between males and females, and COMT is affected by menstrual cycle and oral contraceptive use (Chen et al., 2004; Harrison and Tunbridge, 2008). Thus, it is not clear to what extent the findings of this thesis can be generalised to females, other ages, or to patient groups.

Second, I only investigated the effects of stress on working memory performance. Other types of memory and other cognitive functions (like for example emotional processing and reward sensitivity) may be affected differently (e.g. Sandi and Pinelo-Nava, 2007; Berghorst et al., 2013).

Third, I only investigated two types of stressors. Different stressors may have different cognitive effects (as suggested by my findings here). Even when the overall stressor is the same (the MIST in my case), performing it inside or outside an MRI scanner environment (with almost all other factors held constant), seems to result in opposite effects on the correlation between cortisol response and working memory performance. Although my findings from Chapter 2 and 3 suggest that a mild stressor (either by a novel VR lift stressor or the behavioural version of the MIST) does not affect working memory performance in young, healthy men, further studies are required to further clarify the relationships between stressor type, the stress response(s), and working memory.

Fourth, the intensity of the stress response that I induced is considered to be relatively mild. To my knowledge, no other studies explored the effect of a VR stressor or the MIST (either behavioural or MRI version) on working memory performance. The increased cortisol-dependent stress response induced by the MIST is modest (although greater than the VR stressor), compared to the widely used TSST. Secondly, even though we had a significant higher number of cortisol responders in our studies compared to previously reported studies (about 80% in our study compared to 50% reported elsewhere) the psychological and physiological effects we observed are relatively modest in terms of magnitude and duration. Accordingly, it is not clear that these findings will be of relevance to situations of more extreme or prolonged stress in daily life. Adding a further layer of complexity to the relationship between stress, cortisol and memory, whilst some previous studies have shown associations between stress-related cortisol changes and working memory performance others have observed stress-related changes in working memory in the absence of group differences in cortisol levels. Therefore, differences in the overall magnitude of the induced cortisol response cannot be the only factor responsible for the found inverted-U between stress levels and cognitive performance (as discussed further below).

Fifth, I only studied one SNP in the COMT gene. Therefore, I cannot say anything about potential effects of other COMT haplotypes, potential gene by gene interactions (for example other genes involved in the regulation of dopamine in the brain), or potential epigenetic influences.

Sixth, the findings presented in this thesis examined a single 200mg dose of tolcapone only. Extrapolating to higher or repeated dosing is therefore not possible. Moreover, tolcapone was administered to young healthy men with no history of mental illness, or pre-existing impairments in working memory performance. Therefore, the apparent lack of interactive effects of stress and tolcapone should be interpreted with caution and may not extrapolate to the clinical situation. As I did not conduct a proper clinical trial the absence between an interaction between tolcapone and stress should be interpreted with caution.

Therefore, in sum, any attempt to extrapolate the findings of this thesis should be mindful of the complex interplay between psychological and physiological effects of stress, its context, its cognitive impacts and the population studied.

9.3 Future studies

Clearly, one could address one or all of the limitations described above in future studies. In this final section, I therefore focus on the extent to which my findings are, or are not, compatible with the inverted-U model(s), and the extent to which these models might be formally tested.

The majority of my findings are not compatible with a 'simple' inverted-U model, whereby stress acts only to increase central dopamine levels and thereby enhance (baseline) performance in COMT-Val homozygotes, and impairs it in COMT-Met homozygotes (**Figure 9.1**). My working memory ROI findings (in which dlPFC activation was greater in COMT-Met vs COMT-Val, and in tolcapone vs. placebo) are partially consistent with this model, if one assumes that greater activation is an index of PFC 'inefficiency'. However, I saw no interaction between COMT genotype and inhibition, which would have been expected in the case of a 'simple', single inverted-U. Furthermore, the effect that I found on working memory performance (COMT-Met homozygotes on placebo performed better than COMT-Val homozygotes on placebo, albeit only in cortisol responders) was also not in the expected direction for this model. My findings therefore argue against there being a single inverted-U, which can encompass both the effects of COMT and all of the effects of stress.

Since my findings argue against a single, dopaminergic inverted-U, they suggest that some of the cognitive the effects of stress are mediated by non-dopaminergic mechanisms. For example, glucocorticoids (e.g. cortisol) are found to be a common mediating mechanisms for both the facilitating and impairing actions of stress in different memory processes and phases (e.g. Sandi and Pinelo-Nava, 2007). Other neurotransmitters like noradrenaline (which is also suggested to have its own inverted-U relationship with PFC dependent cognitive function) have also been shown to influence cognitive performance after under conditions of stress (Birnbaum et al., 1999; Arnsten, 2000).

My findings demonstrate the challenges associated with studying these inverted-U relationships in humans, since they appear to be highly context-dependent. For example, other environmental and genetic factors than COMT genotype and stress could result into different starting positions on both curves. For example, age, pathology (like psychosis and ADHD) and even personality have been suggested (Tunbridge et al., 2006; Cools et al., 2007).

It is notable that the best evidence for the dopaminergic inverted-U came from studies in experimental animals in which these factors can be more tightly controlled (Goldman-Rakic, 2000; Williams and Goldman-Rakic, 1995). Understanding interactions between dopamine and stress are also challenging since, as I clearly demonstrate, the stress response is not a unitary concept. Thus, different components of the stress response may impact differentially on outcomes of interest and potentially lead to differences between studies: as outlined above, the relationships between cortisol levels and cognitive performance is far from clear. Studies in animal models may provide a way to clarify these interactions since, as well as the physiological measures collected here, central dopaminergic activity and corticosterone levels can be determined in behaving animals. However, animal models are unable to examine subjective stress and may be confounded by the fact that the measurements of stress (e.g. circulating corticosterone levels) may in themselves be stressful to the animal. Ultimately, untangling these relationships is likely to require a multidisciplinary approach.

Finally, whilst the inverted-U model(s) are physiologically valid and useful frameworks in which to interpret findings, they are also difficult to falsify. This is particularly the case in human studies, in which so many environmental and genetic factors cannot feasibly be controlled. These factors are particularly relevant for the main study described in this thesis which, for reasons of cost, did not

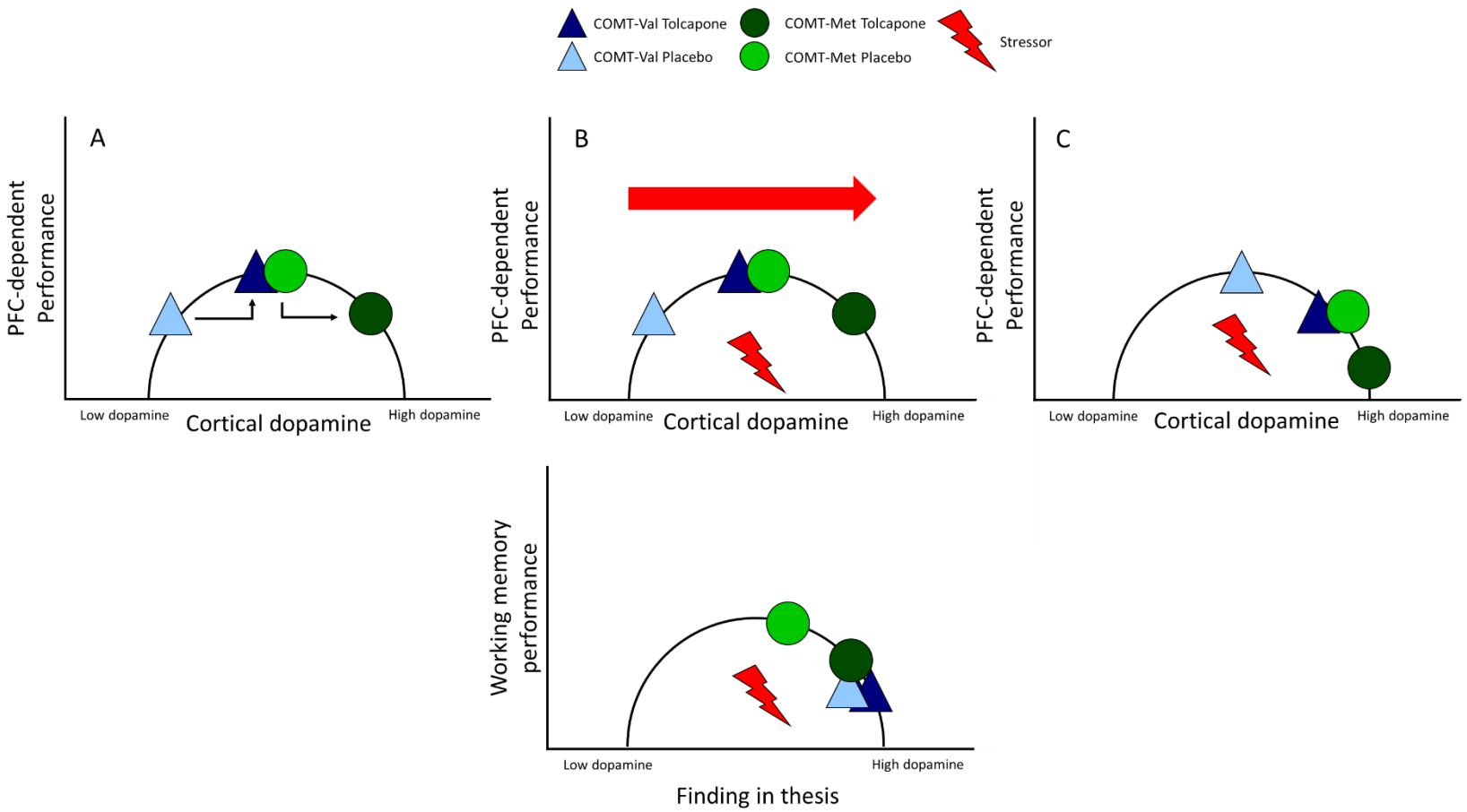


Figure 9.1 - Inverted-U's.

A) Effect of tolcapone on the COMT-dependent dopaminergic inverted-U as presented by Farrell et al., (2012).
B) Stress is predicted to push everyone to the right on the dopaminergic inverted-U if this inverted-U overlaps with the inverted-U between stress and cognitive performance.
C) Predicted position of COMT-Val and COMT-Met homozygotes on either placebo or tolcapone under conditions of stress.
D) Speculated result of this study.

include a no-stress control condition. This would certainly be worth considering in future studies, to help disentangle the complex relationships between dopamine, stress, brain activity and cognitive performance. However, this approach is unlikely to fully address the challenges associated with working within the framework of inverted-U type models. Ultimately, whilst these models are useful for formalising the relationships between different variables, it should always be acknowledged their predictive power is limited.

9.4 Broader considerations

Demonstrating genetic influences on behaviour using available neuroimaging metrics has proved difficult and inconsistent. Over the recent years it has become apparent that many of the studies linking single nuclear polymorphisms to complex brain phenotypes were not replicable (e.g. Meyer-Lindenberg et al., 2008; Avinun et al., 2018; Carter et al., 2017). This likely reflects the results of recent Genome Wide Association Studies (GWAS) which have revealed that complex phenotypes such as brain function are likely affected by many common polymorphisms, each with small effect sizes, typically accounting for <1% of the phenotypic variance. These effect sizes are much smaller than originally thought, demonstrating that most imaging genetics studies are far too under powered to detect true effects, likely explaining the lack of reproducibility within our field (Bogdan et al., 2017; Avinun et al., 2018; Carter et al., 2017).

These concerns apply to the imaging study presented in this thesis as well, making it perhaps not so surprising that we were not able to detect strong consistent results. However, in two respects, this study is arguably less affected by these concerns. First, because the COMT polymorphism is unequivocally functional; as recently confirmed by Tunbridge et al., (2019), it has a substantial (~30%) effect on COMT activity in brain. Second, my study also had a pharmacological as well as genetic variable, with tolcapone having an established and marked impact on COMT activity. Hence, we can conclude that cortical dopamine was impacted by both the genetic variant and the drug manipulation chosen, and thus that my research had a greater chance of producing positive results affecting the selected phenotypes than do most studies of this kind which use polymorphisms of unknown functionality and which lack a pharmacological element. Nevertheless, the power of these studies remains uncertain, and is likely to have been suboptimal. Such considerations should be taken more fully into account in any future studies.

9.5 Conclusion

In summary, I have shown that the existence of a single inverted-U (if indeed there is an inverted-U, given the difficulties proving these relationships as described in Chapter 1), which can encompass both the effects of COMT and the effects of stress is unlikely. In future it would be of interest to also study these inverted-Us by investigating how different forms of PFC dependent cognitive functions are affected by different kind of stressors (differing in type, duration and intensity) together with a non-stress control group. However, bearing in mind that some of the cognitive effects of stress are mediated by non-dopaminergic mechanisms, the context dependency of the different inverted-U relationships, the stress response not being a unitary concept and the need for multidisciplinary approaches and falsifiable hypotheses.

Appendix I Protocol for the behavioural MIST

Alright, now we will start with the pre-task in which you will have to solve simple mental math problems. On the screen you will see an image like this (show the examples). In the middle you will see the mental maths questions that you will have to answer (for example 2*3). There are two different kind of trials, green and red trials (show examples). Green trials are trials in which your response will not be recorded by us. You can see them as relaxation trials to give you little breaks during the task. The majority of the trials are red trials and these are the real deal. Therefore your answers on these trials will be recorded.

For both the green and red trials, there is a rotary dial to submit your response (0-9), and a text field that provides you feedback on the submitted response (correct, incorrect or timeout). For the red trials, there will also be 2 performance indicators, one for your own performance and one which shows the performance we expect you to achieve. I will come back to this expected performance in a bit. Note that during the green trials you will have more time to answer than during the real red trials and you will not see the performance indicators.

You select an answer by pressing these buttons on the keyboard (show them). Pressing the '/' key moves the highlighted number on the rotary dial clockwise, pressing the '.' Key will move it anti-clockwise. You submit your answer with the "' key. You will then see whether your answer was correct or incorrect. Then the next question will follow.

As I mentioned, during the green trials you will not see the time bar or any other performance indicators. However, during the real red trials you will see your own performance and the expected performance (which is to get about 80-90% correct in time). You'll need to reach this expected performance, otherwise I cannot use your data in my study, since it is very important that there is a standard performance across all participants to allow the data to be grouped. Try to perform the task as quickly and accurately as possible. I will be watching over your shoulder, particularly during the red trials, just in case you have any problems.

Ok, any questions? Then I will start the task now. The first few trials will be green, the ones that don't matter, to make you comfortable with the task. Once the screen turns red you will know we are in the collection phase, and that you have to step it up. Please really pay attention and answer as quickly and accurately as possible. Good luck!

Feedback:

<u>After 6 minutes:</u>

Marieke: Ok that was the first run. I am sorry but I have to stop the experiment here as well for a minute just to check. How are you doing? Is there a problem? Are you doing ok? Can you see the screen alright? Are the buttons responding when you press them? The reason why I am asking is that (as you may have noticed) you are not performing nearly as well as expected. You see the top bar? This compares your performance with the average performance of other participants that already did this task. Is there anything you need? Do you understand what you have to do? Briefly explain again: answer with these keys, as accurately as possible within the time limit.
Please try and improve your performance to reach minimum performance requirements, especially on the red trials! You know what to do now so hopefully it should go much better. Then we can move on to the main attention and memory task. Thank you!

<u>After 12 minutes.</u>

Marieke: I'm very sorry, the task stopped again, but this time it is for real. I do not want to be rude, but you are still performing below the expected performance. We would expect you to do better given your age and education levels. Are you feeling ok? Anything that happened this morning why you might not feel up for this?
Hmmm. Euhmm… Well the equipment seems to be working fine, you say you are doing ok, so everything seems to be alright. I never had this before where someone did not reach criterion. I don't really know what to do. I do not know why you are performing so poorly…….
If you don't mind, I will go and see my professor and ask him what he wants me to do. I really have to make sure that you perform on the minimum required level otherwise there is no point in proceeding as I will not be able to use your data in my thesis. But euhm, first let's do another measurement, in this way the study will be less affected by this forced break.
I will be right back. He might be in the clinic, he is a psychiatrist, then it will take a bit longer. Sorry again!
Marieke comes back in the room: Alright my professor thought it would be best if he would come down here himself to see. He will be here in a second as he had to finish what he was doing first. Let me collect the saliva swab and measure your blood pressure in the meantime.

Prof. Harrison knocks on door: Introduces himself and looks at the setup.
Prof. Harrison: So Marieke explained me that your performance is not as good as we expected it to be. The setup seems to be working fine. You said you did A level maths right? I think the reason why you are not performing well is that you make more errors than we expected. Your other fellow (students, same work etc.) participants performed really much better.

Marieke to professor: Do you think we could still use him as a participant for my thesis?
Prof. Harrison to Marieke: Well we could give him one more try. But he really does have to step it up! Your experiment really depends on him doing his best performance otherwise you cannot use the data and you will have to find someone else. You know time is ticking to finish in time right?
Marieke: Yes, thank you professor.
Prof. Harrison to Marieke: I will have to let the next patient know that I will be a bit delayed, but I believe this is important enough for me to stay and to watch him for a bit to see how he is doing for myself. I will be right back. Could you set the task up again? Professor leaves for 2 minutes.
Marieke to participant: alright, are you up for another try? I'm very sorry for this and for my professor being a bit harsh on you. I guess it is because I interrupted him in his clinic duties, but I really didn't know what to do. So please don't worry about it. Just try to answer as accurately and quickly as possible. I will stand behind you to see how you are performing and Professor Harrison will enter the room silently again in a bit.
Prof. Harrison enters room again without saying anything.

<u>After 18 minutes:</u>
Professor Harrison: Well let's end the task here. We have to give up and move on to the main task of this study. There is no point in continuing this math task. I will have to head back to the clinic now. Will you be alright from here on Marieke to get to the main task?
Marieke: Yes, thanks again professor! We can talk about this later to see if we can prevent this from happening again.

Prof. Harrison leaves.
Marieke: I am sorry for having to end the maths task. Hopefully you are still up for the main task of my study? It will be a task of attention and memory, so no more maths luckily.

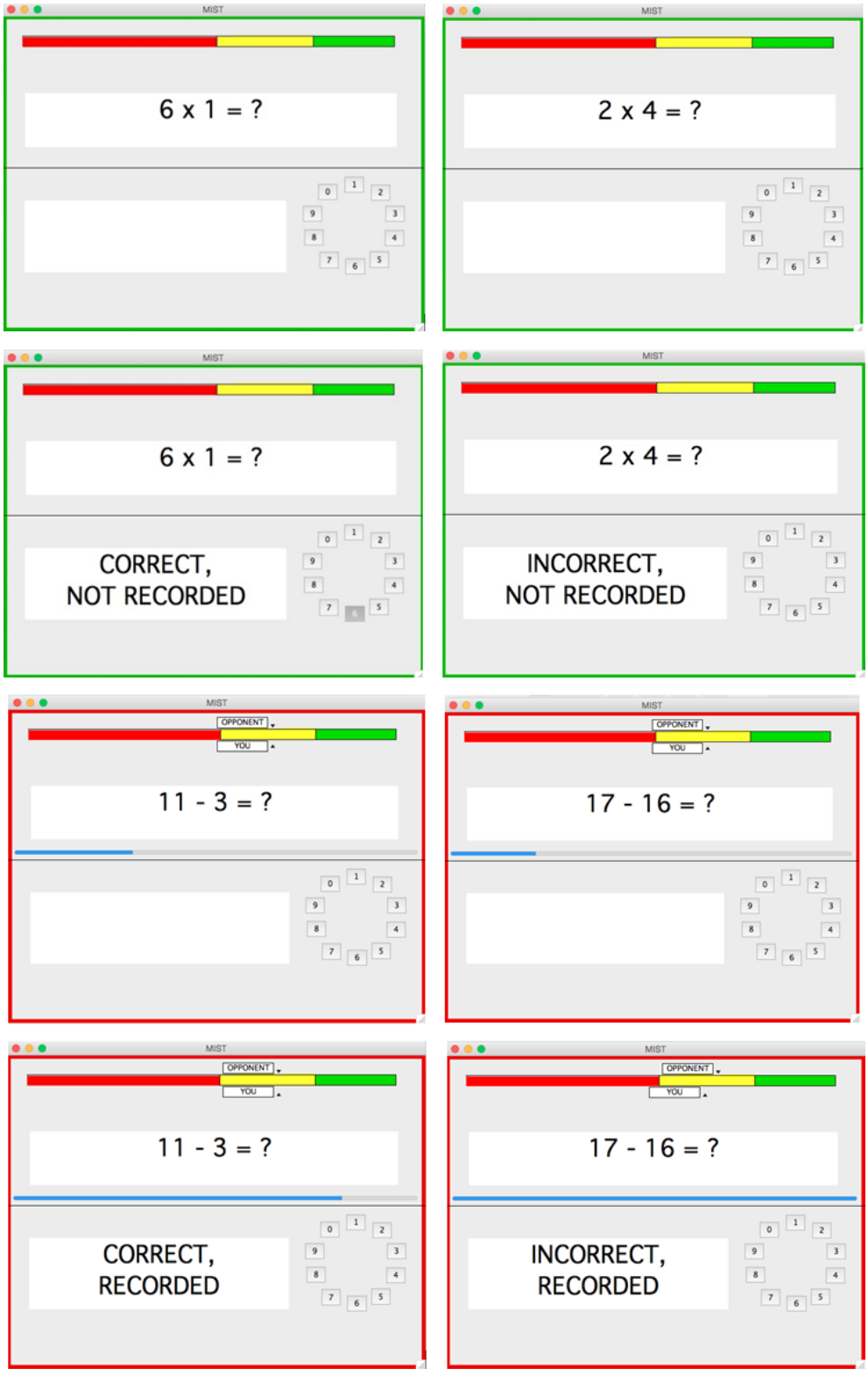


Figure I.1 - MIST examples

MIST control (green) and stress (red) trials, correct and incorrectly answered.

Appendix II Protocol for the MRI MIST

We will now start the first task. As I explained before, in this task you will need to answer the mental maths. For all trials, the first button will make the dial go left. The second button will make the dial go right. The third button will submit your answer. I will be watching your performance from over here in the control room. Any questions? Then I will start the task now. The first few trials will be green, the ones that don't matter, to make you comfortable with the task. Once the screen turns red you will know we are in the collection phase, and that you have to step it up. Please really pay attention and answer as quickly and accurately as possible. Good luck!

Feedback:

After 7 minutes:

Marieke: Ok that was the first run. I am sorry but I have to stop the experiment here as well for a minute just to check. Is there a problem? Are you doing ok? Can you see the screen alright? Are the buttons responding when you press them? The reason why I am asking is that (as you may have noticed) you are not performing nearly as well as expected. You remember the top bar? You'll need to reach this expected performance, otherwise I cannot use your data in my study. Do you understand what you have to do? Let me explain again then. → Briefly explain again: answer with these keys, as accurately as possible within the time limit.

Please try and improve your performance to reach minimum performance requirements, especially on the **red** trials! You know what to do now so hopefully it should go much better. Then we can move on to the next attention and memory task. Thank you!

After 14 minutes.

Marieke: I'm very sorry, the task stopped again, but this time it is for real. I do not want to be rude, but you are still performing below the expected performance. We would expect you to do better given your age and education levels. Are you feeling ok?

Hmmm. Euhmm… Well the task seems to be working fine, you say you are doing ok, so everything seems to be alright. I never had this before where someone did not reach criterion. I don't really know what to do. I do not know why you are performing so poorly…….

I think I will have to call my supervisor, Professor X, and ask him/her what he wants me to do. I really have to make sure that you perform on the minimum required level otherwise there is no point in proceeding as I will not be able to use your data in my thesis. Also my budget is limited as the MRI scans are really expensive. But euhm, first let's do another measurement, in this way the study will be less affected by this forced break.

OK now I'm going to try to call my supervisor. Hopefully he/she is able to answer. I'll be right back.

Let participant hear the phone conversation. Professor waiting in OHBA reception area.

Hi professor, this is Marieke speaking. Really sorry to bother you, but I am experiencing issues with our MRI study. For some reason the participant is not able to reach the criterion levels and I do not know what to do. Alright. Yes. Yes, I already gave him a second chance. I have never seen this before, not even during our pilot. Yes. Ok. I see. Yes. Alright, see you in a minute. Thank you so much!

Marieke to participant: Sorry to keep you waiting. Alright my supervisor thinks it would be best if he/she would come over here to check. He/she will be here shortly, once he's/she's finished with a clinical problem. Let me collect your saliva swab in the meantime.

Marieke: My supervisor is here now

Marieke: Hello Professor.

Professor: Good afternoon [participant name]. I understand there's a problem. I'm just going to discuss with my research assistant. So Marieke, what's the problem?

Marieke: Hello Professor. He is far from reaching the criterion. Even after trying for a second time. Let me show you his performance levels.

Professor: Ah, I see. You've checked that he's ok and that he can see the screen alright? How much maths has he done? You've set it up right for that? Had this happened before?

Marieke: No, this is the first time. Can we still use him as a participant or shall we abandon the study?

Professor: Hmmm. I guess we should give him one more try. I'll stay and watch him for a bit to see how he is doing for myself. Could you set the task up again?

Marieke to participant: Alright, are you up for another try? I'm really sorry for all of this. This never happened before. Erm…let me see….ermm…yes. Just try to answer as accurately and quickly as possible, especially on the red trials. Are you ready to start again? At least try to do better than before.

{Participant does MIST pt 3]

Professor: Hmm…I see what you mean Marieke. There's no time to try again, but I guess we may as well proceed to the next task and hope that we get some useful data from that one. We'll need to talk about this later….

Marieke: Sorry about the delay. Hopefully you are still up for the other tasks of my study? We will start the task of attention and memory, so no more maths, luckily…

Appendix III Group differences in the effects of acute stress exposure in the MIST scenario on sAA and subjective stress in cortisol responders only.

Amylase		
Main effect of time	$F_{8,384}$=31.9; p<0.001	Significant differences between time point 3 (considered baseline) and all other time points besides time point 1 (p=0.700), 2 (p=0.479) and 9 (p = 0.110).
No main effect of genotype	$F_{1,48}$=0.60; p=0443	
No main effect of drug	$F_{1,48}$=0.10; p=0.750	
No interaction of genotype * drug	$F_{1,48}$=3.0; p=0.090	
No interaction of time * genotype	$F_{8,384}$=0.33; p=0.992	
No interaction of time * drug	$F_{8,384}$=0.48; p=0.823	
No interaction of time * genotype * drug	$F_{8,384}$=1.4; p=0.208	On placebo, Met > Val on time point 4 (p=0.040) and 6 (p=0.023)
VAS Stressed		
Main effect of time	$F_{8,400}$=27.1; p<0.001	Significant differences between time point 3 (considered baseline) and all other time points besides time point 2 (p=0.998)
No main effect of genotype	$F_{1,50}$=1.1; p=0.304	
No main effect of drug	$F_{1,50}$=2.7; p=0.106	
No interaction of genotype * drug	$F_{1,50}$=0.87; p=0.356	
No interaction of time * genotype	$F_{8,400}$=0.29; p=0.681	
No interaction of time * drug	$F_{8,400}$=0.60; p=0.270	
No interaction of time * genotype * drug	$F_{8,400}$=1.1; p=0.339	

References

Aanerud, J., Borghammer, P., Rodell, A., Jónsdottir, K.Y., Gjedde, A., 2017. Sex differences of human cortical blood flow and energy metabolism. J. Cereb. Blood Flow Metab. 37, 2433–2440. https://doi.org/10.1177/0271678X16668536

Abercrombie, E.D., Keefe, K.A., DiFrischia, D.S., Zigmond, M.J., 1989. Differential Effect of Stress on In Vivo Dopamine Release in Striatum, Nucleus Accumbens, and Medial Frontal Cortex. J. Neurochem. 52, 1655–1658. https://doi.org/10.1111/j.1471-4159.1989.tb09224.x

Akirav, I., 2004. A Facilitative Role for Corticosterone in the Acquisition of a Spatial Task Under Moderate Stress. Learn. Mem. 11, 188–195. https://doi.org/10.1101/lm.61704

Allen, A.P., Kennedy, P.J., Cryan, J.F., Dinan, T.G., Clarke, G., 2014. Biological and psychological markers of stress in humans: Focus on the Trier Social Stress Test. Neurosci. Biobehav. Rev. 38, 94–124. https://doi.org/10.1016/j.neubiorev.2013.11.005

Alsop, D.C., Detre, J.A., Golay, X., Günther, M., Hendrikse, J., Hernandez-Garcia, L., Lu, H., MacIntosh, B.J., Parkes, L.M., Smits, M., van Osch, M.J.P., Wang, D.J.J., Wong, E.C., Zaharchuk, G., 2015. Recommended implementation of arterial spin-labeled perfusion MRI for clinical applications: A consensus of the ISMRM perfusion study group and the European consortium for ASL in dementia: Recommended Implementation of ASL for Clinical Applications. Magn. Reson. Med. 73, 102–116. https://doi.org/10.1002/mrm.25197

Andreano, J.M., Cahill, L., 2006. Glucocorticoid Release and Memory Consolidation in Men and Women. Psychol. Sci. 17, 466–470. https://doi.org/10.1111/j.1467-9280.2006.01729.x

Annerbrink, K., Westberg, L., Nilsson, S., Rosmond, R., Holm, G., Eriksson, E., 2008. Catechol O-methyltransferase val158-met polymorphism is associated with abdominal obesity and blood pressure in men. Metabolism 57, 708–711. https://doi.org/10.1016/j.metabol.2008.01.012

Apud, J.A., Mattay, V., Chen, J., Kolachana, B.S., Callicott, J.H., Rasetti, R., Alce, G., Iudicello, J.E., Akbar, N., Egan, M.F., Goldberg, T.E., Weinberger, D.R., 2007. Tolcapone Improves Cognition and Cortical Information Processing in Normal Human Subjects. Neuropsychopharmacology 32, 1011–1020. https://doi.org/10.1038/sj.npp.1301227

Armbruster, D., Mueller, A., Strobel, A., Lesch, K.-P., Brocke, B., Kirschbaum, C., 2012. Children under stress – COMT genotype and stressful life events predict cortisol increase in an acute social stress paradigm. Int. J. Neuropsychopharmacol. 15, 1229–1239. https://doi.org/10.1017/S1461145711001763

Armulik, A., Mäe, M., Betsholtz, C., 2011. Pericytes and the blood–brain barrier: recent advances and implications for the delivery of CNS therapy. Ther. Deliv. 2, 419–422. https://doi.org/10.4155/tde.11.23

Arnsten, A.F.T., 2009. Stress signalling pathways that impair prefrontal cortex structure and function. Nat. Rev. Neurosci. 10, 410–422. https://doi.org/10.1038/nrn2648

Arnsten, A.F.T., Goldman-Rakic, P.S., 1998. Noise Stress Impairs Prefrontal Cortical Cognitive Function in Monkeys: Evidence for a Hyperdopaminergic Mechanism. Arch. Gen. Psychiatry 55, 362–368. https://doi.org/10.1001/archpsyc.55.4.362

Arnsten, AmyF.T., 2004. Adrenergic targets for the treatment of cognitive deficits in schizophrenia. Psychopharmacology (Berl.) 174. https://doi.org/10.1007/s00213-003-1724-3

Ashare, R.L., Valdez, J.N., Ruparel, K., Albelda, B., Hopson, R.D., Keefe, J.R., Loughead, J., Lerman, C., 2013. Association of abstinence-induced alterations in working memory function and COMT genotype in smokers. Psychopharmacology (Berl.) 230, 653–662. https://doi.org/10.1007/s00213-013-3197-3

Azhan, A., Wong, F., 2012. Challenges in understanding the impact of blood pressure management on cerebral oxygenation in the preterm brain. Front. Physiol. 3. https://doi.org/10.3389/fphys.2012.00471

Barkus, C., Korn, C., Stumpenhorst, K., Laatikainen, L.M., Ballard, D., Lee, S., Sharp, T., Harrison, P.J., Bannerman, D.M., Weinberger, D.R., Chen, J., Tunbridge, E.M., 2016. Genotype-Dependent Effects of COMT Inhibition on Cognitive Function in a Highly Specific, Novel Mouse Model of Altered COMT Activity. Neuropsychopharmacology 41, 3060–3069. https://doi.org/10.1038/npp.2016.119

Barnes, A., Isohanni, M., Barnett, J.H., Pietiläinen, O., Veijola, J., Miettunen, J., Paunio, T., Tanskanen, P., Ridler, K., Suckling, J., Bullmore, E.T., Murray, G.K., Jones, P.B., 2012. No Association of COMT (Val158Met) Genotype with Brain Structure Differences between Men and Women. PLoS ONE 7, e33964. https://doi.org/10.1371/journal.pone.0033964

Barnett, J.H., Scoriels, L., Munafò, M.R., 2008. Meta-Analysis of the Cognitive Effects of the Catechol-O-Methyltransferase Gene Val158/108Met Polymorphism. Biol. Psychiatry 64, 137–144. https://doi.org/10.1016/j.biopsych.2008.01.005

Beckmann, C., Mackay, C., Filippini, N., Smith, S., 2009. Group comparison of resting-state FMRI data using multi-subject ICA and dual regression. NeuroImage 47, S148. https://doi.org/10.1016/S1053-8119(09)71511-3

Beckmann, C.F., Smith, S.M., 2004. Probabilistic independent component analysis for functional magnetic resonance imaging. IEEE Trans. Med. Imaging 23, 137–152. https://doi.org/10.1109/TMI.2003.822821

Belujon, P., Grace, A.A., 2015. Regulation of dopamine system responsivity and its adaptive and pathological response to stress. Proc. R. Soc. B Biol. Sci. 282, 20142516–20142516. https://doi.org/10.1098/rspb.2014.2516

Bencherif, B., Fuchs, P.N., Sheth, R., Dannals, R.F., Campbell, J.N., Frost, J.J., 2002. Pain activation of human supraspinal opioid pathways as demonstrated by [11C]-carfentanil and positron emission tomography (PET): Pain 99, 589–598. https://doi.org/10.1016/S0304-3959(02)00266-X

Berridge, K.C., Robinson, T.E., 1998. What is the role of dopamine in reward: hedonic impact, reward learning, or incentive salience? Brain Res. Rev. 28, 309–369. https://doi.org/10.1016/S0165-0173(98)00019-8

Berryhill, M.E., Olson, I.R., 2008. The right parietal lobe is critical for visual working memory. Neuropsychologia, Part Special Issue: What is the Parietal Lobe Contribution to Human Memory? 46, 1767–1774. https://doi.org/10.1016/j.neuropsychologia.2008.01.009

Biswal, B., Zerrin Yetkin, F., Haughton, V.M., Hyde, J.S., 1995. Functional connectivity in the motor cortex of resting human brain using echo-planar mri. Magn. Reson. Med. 34, 537–541. https://doi.org/10.1002/mrm.1910340409

Blandini, F., Martignoni, E., Sances, E., Bono, G., Nappi, G., 1995. Combined response of plasma and platelet catecholamines to different types of short-term stress. Life Sci. 56, 1113–1120. https://doi.org/10.1016/0024-3205(95)00048-B

Boehringer, A., Tost, H., Haddad, L., Lederbogen, F., Wüst, S., Schwarz, E., Meyer-Lindenberg, A., 2015. Neural Correlates of the Cortisol Awakening Response in Humans. Neuropsychopharmacology 40, 2278–2285. https://doi.org/10.1038/npp.2015.77

Bollini, A.M., Walker, E.F., Hamann, S., Kestler, L., 2004. The influence of perceived control and locus of control on the cortisol and subjective responses to stress. Biol. Psychol. 67, 245–260. https://doi.org/10.1016/j.biopsycho.2003.11.002

Bonifácio, M.J., Palma, P.N., Almeida, L., Soares-da-Silva, P., 2007. Catechol-O-methyltransferase and Its Inhibitors in Parkinson's Disease. CNS Drug Rev. 13, 352–379. https://doi.org/10.1111/j.1527-3458.2007.00020.x

Bosch, J.A., Veerman, E.C.I., de Geus, E.J., Proctor, G.B., 2011. α-Amylase as a reliable and convenient measure of sympathetic activity: don't start salivating just yet!

Psychoneuroendocrinology 36, 449–453. https://doi.org/10.1016/j.psyneuen.2010.12.019

Brown, G.G., Clark, C., Liu, T.T., 2007. Measurement of cerebral perfusion with arterial spin labeling: Part 2. Applications. J. Int. Neuropsychol. Soc. 13, 526–538. https://doi.org/10.1017/S1355617707070634

Brozoski, T., Brown, R., Rosvold, H., Goldman, P., 1979. Cognitive deficit caused by regional depletion of dopamine in prefrontal cortex of rhesus monkey. Science 205, 929–932. https://doi.org/10.1126/science.112679

Buckert, M., Kudielka, B.M., Reuter, M., Fiebach, C.J., 2012. The COMT Val158Met polymorphism modulates working memory performance under acute stress. Psychoneuroendocrinology 37, 1810–1821. https://doi.org/10.1016/j.psyneuen.2012.03.014

Buckner, R.L., Andrews-Hanna, J.R., Schacter, D.L., 2008. *The Brain's Default Network*: *Anatomy, Function, and Relevance to Disease*. Ann. N. Y. Acad. Sci. 1124, 1–38. https://doi.org/10.1196/annals.1440.011

Cabib, S., Puglisi-Allegra, S., 2012. The mesoaccumbens dopamine in coping with stress. Neurosci. Biobehav. Rev. 36, 79–89. https://doi.org/10.1016/j.neubiorev.2011.04.012

Cai, J.X., Arnsten, A.F.T., 1997. Dose-Dependent Effects of the Dopamine D1 Receptor Agonists A77636 or SKF81297 On Spatial Working Memory in Aged Monkeys 283, 7.

Callicott, J., 1998. Functional Magnetic Resonance Imaging Brain Mapping in Psychiatry: Methodological Issues Illustrated in a Study of Working Memory in Schizophrenia. Neuropsychopharmacology 18, 186–196. https://doi.org/10.1016/S0893-133X(97)00096-1

Campbell, J., Ehlert, U., 2012. Acute psychosocial stress: Does the emotional stress response correspond with physiological responses? Psychoneuroendocrinology 37, 1111–1134. https://doi.org/10.1016/j.psyneuen.2011.12.010

Ceravolo, R., Piccini, P., Bailey, D.L., Jorga, K.M., Bryson, H., Brooks, D.J., 2002. 18F-dopa PET evidence that tolcapone acts as a central COMT inhibitor in Parkinson's disease. Synapse 43, 201–207. https://doi.org/10.1002/syn.10034

Chappell, M.A., Groves, A.R., Whitcher, B., Woolrich, M.W., 2009. Variational Bayesian Inference for a Nonlinear Forward Model. IEEE Trans. Signal Process. 57, 223–236. https://doi.org/10.1109/TSP.2008.2005752

Chen, J., Lipska, B.K., Halim, N., Ma, Q.D., Matsumoto, M., Melhem, S., Kolachana, B.S., Hyde, T.M., Herman, M.M., Apud, J., Egan, M.F., Kleinman, J.E., Weinberger, D.R., 2004. Functional Analysis of Genetic Variation in Catechol-O-Methyltransferase (COMT): Effects on mRNA, Protein, and Enzyme Activity in Postmortem Human Brain. Am. J. Hum. Genet. 75, 807–821. https://doi.org/10.1086/425589

Cleworth, T.W., Horslen, B.C., Carpenter, M.G., 2012. Influence of real and virtual heights on standing balance. Gait Posture 36, 172–176. https://doi.org/10.1016/j.gaitpost.2012.02.010

Cohen, M.L., Berkowitz, B.A., 1975. Differences between the effects of dopamine and apomorphine on rat aortic strips. Eur. J. Pharmacol. 34, 49–58. https://doi.org/10.1016/0014-2999(75)90224-1

Collip, D., van Winkel, R., Peerbooms, O., Lataster, T., Thewissen, V., Lardinois, M., Drukker, M., Rutten, B.P.F., Van Os, J., Myin-Germeys, I., 2011. COMT Val158Met-Stress Interaction in Psychosis: Role of Background Psychosis Risk: Gene-Environment Interactions in Daily Life-A Replication. CNS Neurosci. Ther. 17, 612–619. https://doi.org/10.1111/j.1755-5949.2010.00213.x

Cools, R., 2001. Enhanced or Impaired Cognitive Function in Parkinson's Disease as a Function of Dopaminergic Medication and Task Demands. Cereb. Cortex 11, 1136–1143. https://doi.org/10.1093/cercor/11.12.1136

Cools, R., D'Esposito, M., 2011. Inverted-U–Shaped Dopamine Actions on Human Working Memory and Cognitive Control. Biol. Psychiatry 69, e113–e125. https://doi.org/10.1016/j.biopsych.2011.03.028

Corbett, B., Weinberg, L., Duarte, A., 2017. The effect of mild acute stress during memory consolidation on emotional recognition memory. Neurobiol. Learn. Mem. 145, 34–44. https://doi.org/10.1016/j.nlm.2017.08.005

Cornelisse, S., Joëls, M., Smeets, T., 2011. A Randomized Trial on Mineralocorticoid Receptor Blockade in Men: Effects on Stress Responses, Selective Attention and Memory. Neuropsychopharmacology 36, 2720–2728. https://doi.org/10.1038/npp.2011.162

Craddock, N., Owen, M.J., O'Donovan, M.C., 2006. The catechol-O-methyl transferase (COMT) gene as a candidate for psychiatric phenotypes: evidence and lessons. Mol. Psychiatry 11, 446–458. https://doi.org/10.1038/sj.mp.4001808

de Kloet, E.R., Joëls, M., Holsboer, F., 2005. Stress and the brain: from adaptation to disease. Nat. Rev. Neurosci. 6, 463–475. https://doi.org/10.1038/nrn1683

de Kloet, E.R., Oitzl, M.S., Joëls, M., 1999. Stress and cognition: are corticosteroids good or bad guys? Trends Neurosci. 22, 422–426. https://doi.org/10.1016/S0166-2236(99)01438-1

Dedovic, K., D'Aguiar, C., Pruessner, J.C., 2009a. What Stress Does to Your Brain: A Review of Neuroimaging Studies. Can. J. Psychiatry 54, 10.

Dedovic, K., Duchesne, A., Andrews, J., Engert, V., Pruessner, J.C., 2009b. The brain and the stress axis: The neural correlates of cortisol regulation in response to stress. NeuroImage 47, 864–871. https://doi.org/10.1016/j.neuroimage.2009.05.074

Dedovic, K., Duchesne, A., Engert, V., Lue, S.D., Andrews, J., Efanov, S.I., Beaudry, T., Pruessner, J.C., 2014. Psychological, endocrine and neural responses to social evaluation in subclinical depression. Soc. Cogn. Affect. Neurosci. 9, 1632–1644. https://doi.org/10.1093/scan/nst151

Dedovic, K., Renwick, R., Mahani, N.K., Engert, V., Lupien, S.J., Pruessner, J.C., 2005. The Montreal Imaging Stress Task: using functional imaging to investigate the effects of perceiving and processing psychosocial stress in the human brain. J Psychiatry Neurosci 30, 7.

Dedovic, K., Rexroth, M., Wolff, E., Duchesne, A., Scherling, C., Beaudry, T., Lue, S.D., Lord, C., Engert, V., Pruessner, J.C., 2009c. Neural correlates of processing stressful information: An event-related fMRI study. Brain Res. 1293, 49–60. https://doi.org/10.1016/j.brainres.2009.06.044

Delarco, A., Segovia, G., Garrido, P., Deblas, M., Mora, F., 2007. Stress, prefrontal cortex and environmental enrichment: Studies on dopamine and acetylcholine release and working memory performance in rats. Behav. Brain Res. 176, 267–273. https://doi.org/10.1016/j.bbr.2006.10.006

Desbonnet, L., Tighe, O., Karayiorgou, M., Gogos, J.A., Waddington, J.L., O'Tuathaigh, C.M.P., 2012. Physiological and behavioural responsivity to stress and anxiogenic stimuli in COMT-deficient mice. Behav. Brain Res. 228, 351–358. https://doi.org/10.1016/j.bbr.2011.12.014

Detre, J.A., Wang, J., Wang, Z., Rao, H., 2009. Arterial spin-labeled perfusion MRI in basic and clinical neuroscience: Curr. Opin. Neurol. 22, 348–355. https://doi.org/10.1097/WCO.0b013e32832d9505

Deutch, A.Y., Clark, W.A., Roth, R.H., 1990. Prefrontal cortical dopamine depletion enhances the responsiveness of mesolimbic dopamine neurons to stress. Brain Res. 521, 311–315. https://doi.org/10.1016/0006-8993(90)91557-W

Diamond, D.M., Bennett, M.C., Fleshner, M., Rose, G.M., 1992. Inverted-U relationship between the level of peripheral corticosterone and the magnitude of hippocampal primed burst potentiation. Hippocampus 2, 421–430. https://doi.org/10.1002/hipo.450020409

Diaz-Asper, C.M., Goldberg, T.E., Kolachana, B.S., Straub, R.E., Egan, M.F., Weinberger, D.R., 2008. Genetic Variation in Catechol-O-Methyltransferase: Effects on Working Memory in

Schizophrenic Patients, Their Siblings, and Healthy Controls. Biol. Psychiatry 63, 72–79. https://doi.org/10.1016/j.biopsych.2007.03.031

Dickerson, S.S., Kemeny, M.E., 2004. Acute Stressors and Cortisol Responses: A Theoretical Integration and Synthesis of Laboratory Research. Psychol. Bull. 130, 355–391. https://doi.org/10.1037/0033-2909.130.3.355

Diemer, J., Lohkamp, N., Mühlberger, A., Zwanzger, P., 2016. Fear and physiological arousal during a virtual height challenge—effects in patients with acrophobia and healthy controls. J. Anxiety Disord. 37, 30–39. https://doi.org/10.1016/j.janxdis.2015.10.007

Diemer, J., Mühlberger, A., Pauli, P., Zwanzger, P., 2014. Virtual reality exposure in anxiety disorders: Impact on psychophysiological reactivity. World J. Biol. Psychiatry 15, 427–442. https://doi.org/10.3109/15622975.2014.892632

Dingemanse, J., Jorga, K.M., Schmitt, M., Gieschke, R., Fotteler, B., Zürcher, G., Prada, M., van Brummelen, P., 1995. Integrated pharmacokinetics and pharmacodynamics of the novel catechol-O-methyltransferase inhibitor tolcapone during first administration to humans*. Clin. Pharmacol. Ther. 57, 508–517. https://doi.org/10.1016/0009-9236(95)90035-7

Ditzen, B., Ehlert, U., Nater, U.M., 2014. Associations between salivary alpha-amylase and catecholamines – A multilevel modeling approach. Biol. Psychol. 103, 15–18. https://doi.org/10.1016/j.biopsycho.2014.08.001

Dolui, S., Wang, Z., Wang, D.J., Mattay, R., Finkel, M., Elliott, M., Desiderio, L., Inglis, B., Mueller, B., Stafford, R.B., Launer, L.J., Jacobs, D.R., Bryan, R.N., Detre, J.A., 2016. Comparison of non-invasive MRI measurements of cerebral blood flow in a large multisite cohort. J. Cereb. Blood Flow Metab. 36, 1244–1256. https://doi.org/10.1177/0271678X16646124

Donahue, M.J., Lu, H., Jones, C.K., Pekar, J.J., van Zijl, P.C.M., 2006. An account of the discrepancy between MRI and PET cerebral blood flow measures. A high-field MRI investigation. NMR Biomed. 19, 1043–1054. https://doi.org/10.1002/nbm.1075

Douaud, G., Smith, S., Jenkinson, M., Behrens, T., Johansen-Berg, H., Vickers, J., James, S., Voets, N., Watkins, K., Matthews, P.M., James, A., 2007. Anatomically related grey and white matter abnormalities in adolescent-onset schizophrenia. Brain 130, 2375–2386. https://doi.org/10.1093/brain/awm184

Duncko, R., Johnson, L., Merikangas, K., Grillon, C., 2009. Working memory performance after acute exposure to the cold pressor stress in healthy volunteers. Neurobiol. Learn. Mem. 91, 377–381. https://doi.org/10.1016/j.nlm.2009.01.006

Dunlop, K., Liston, C., 2018. Stress response regulation and the hemodynamic response. Proc. Natl. Acad. Sci. 115, 10827–10829. https://doi.org/10.1073/pnas.1814592115

Edvinsson, L., Hardebo, J.E., Mcculloch, J., Owman, Ch., 1978. Effects of dopaminergic agonists and antagonists on isolated cerebral blood vessels. Acta Physiol. Scand. 104, 349–359. https://doi.org/10.1111/j.1748-1716.1978.tb06286.x

Egan, M.F., Goldberg, T.E., Kolachana, B.S., Callicott, J.H., Mazzanti, C.M., Straub, R.E., Goldman, D., Weinberger, D.R., 2001. Effect of COMT Val108/158 Met genotype on frontal lobe function and risk for schizophrenia. Proc. Natl. Acad. Sci. 98, 6917–6922. https://doi.org/10.1073/pnas.111134598

Eisenberg, D.P., Sarpal, D., Kohn, P.D., Meyer-Lindenberg, A., Wint, D., Kolachana, B., Apud, J., Weinberger, D.R., Berman, K.F., 2010. Catechol-O-methyltransferase Val158Met Genotype and Resting Regional Cerebral Blood Flow in Medication-Free Patients with Schizophrenia. Biol. Psychiatry 67, 287–290. https://doi.org/10.1016/j.biopsych.2009.08.039

Engert, V., Vogel, S., Efanov, S.I., Duchesne, A., Corbo, V., Ali, N., Pruessner, J.C., 2011. Investigation into the cross-correlation of salivary cortisol and alpha-amylase responses to psychological stress. Psychoneuroendocrinology 36, 1294–1302. https://doi.org/10.1016/j.psyneuen.2011.02.018

Farrell, S.M., Tunbridge, E.M., Braeutigam, S., Harrison, P.J., 2012. COMT Val158Met Genotype Determines the Direction of Cognitive Effects Produced by Catechol-O-Methyltransferase Inhibition. Biol. Psychiatry 71, 538–544. https://doi.org/10.1016/j.biopsych.2011.12.023

Fechir, M., Gamer, M., Blasius, I., Bauermann, T., Breimhorst, M., Schlindwein, P., Schlereth, T., Birklein, F., 2010. Functional imaging of sympathetic activation during mental stress. NeuroImage 50, 847–854. https://doi.org/10.1016/j.neuroimage.2009.12.004

Feldman, S., Weidenfeld, J., 2004. Involvement of Endogeneous Glutamate in the Stimulatory Effect of Norepinephrine and Serotonin on the Hypothalamo-Pituitary-Adrenocortical Axis. Neuroendocrinology 79, 43–53. https://doi.org/10.1159/000076044

Filippini, N., MacIntosh, B.J., Hough, M.G., Goodwin, G.M., Frisoni, G.B., Smith, S.M., Matthews, P.M., Beckmann, C.F., Mackay, C.E., 2009. Distinct patterns of brain activity in young carriers of the APOE- 4 allele. Proc. Natl. Acad. Sci. 106, 7209–7214. https://doi.org/10.1073/pnas.0811879106

Floderus, Y., Ross, S.B., Wetterberg, L., 1981. Erythrocyte catechol-O-methyltransferase activity in a Swedish population. Clin. Genet. 19, 389–392. https://doi.org/10.1111/j.1399-0004.1981.tb00731.x

Freeman, D., Bradley, J., Antley, A., Bourke, E., DeWeever, N., Evans, N., Černis, E., Sheaves, B., Waite, F., Dunn, G., Slater, M., Clark, D.M., 2016. Virtual reality in the treatment of persecutory delusions: randomised controlled experimental study testing how to reduce delusional conviction. Br. J. Psychiatry 209, 62–67. https://doi.org/10.1192/bjp.bp.115.176438

Freeman, D., Haselton, P., Freeman, J., Spanlang, B., Kishore, S., Albery, E., Denne, M., Brown, P., Slater, M., Nickless, A., 2018. Automated psychological therapy using immersive virtual reality for treatment of fear of heights: a single-blind, parallel-group, randomised controlled trial. Lancet Psychiatry 5, 625–632. https://doi.org/10.1016/S2215-0366(18)30226-8

Freeman, D., Lister, R., Waite, F., Yu, L.-M., Slater, M., Dunn, G., Clark, D., 2019. Automated psychological therapy using virtual reality (VR) for patients with persecutory delusions: study protocol for a single-blind parallel-group randomised controlled trial (THRIVE). Trials 20, 87. https://doi.org/10.1186/s13063-019-3198-6

Gärtner, M., Rohde-Liebenau, L., Grimm, S., Bajbouj, M., 2014. Working memory-related frontal theta activity is decreased under acute stress. Psychoneuroendocrinology 43, 105–113. https://doi.org/10.1016/j.psyneuen.2014.02.009

Gasparini, M., Fabrizio, E., Bonifati, V., Meco, G., 1997. Cognitive improvement during Tolcapone treatment in Parkinson's disease. J. Neural Transm. 104, 887–894. https://doi.org/10.1007/BF01285556

Geller, S., Wilhelm, O., Wacker, J., Hamm, A., Hildebrandt, A., 2017. Associations of the COMT Val 158 Met polymorphism with working memory and intelligence – A review and meta-analysis. Intelligence 65, 75–92. https://doi.org/10.1016/j.intell.2017.09.002

Geva, N., Pruessner, J., Defrin, R., 2014. Acute psychosocial stress reduces pain modulation capabilities in healthy men. PAIN® 155, 2418–2425. https://doi.org/10.1016/j.pain.2014.09.023

Giakoumaki, S.G., Roussos, P., Bitsios, P., 2008. Improvement of Prepulse Inhibition and Executive Function by the COMT Inhibitor Tolcapone Depends on COMT Val158Met Polymorphism. Neuropsychopharmacology 33, 3058–3068. https://doi.org/10.1038/npp.2008.82

Glahn, D.C., Winkler, A.M., Kochunov, P., Almasy, L., Duggirala, R., Carless, M.A., Curran, J.C., Olvera, R.L., Laird, A.R., Smith, S.M., Beckmann, C.F., Fox, P.T., Blangero, J., 2010. Genetic control over the resting brain. Proc. Natl. Acad. Sci. 107, 1223–1228. https://doi.org/10.1073/pnas.0909969107

Goldberg, T.E., Egan, M.F., Gscheidle, T., Coppola, R., Weickert, T., Kolachana, B.S., Goldman, D., Weinberger, D.R., 2003. Executive Subprocesses in Working Memory: Relationship to

Catechol- **O** -methyltransferase Val158Met Genotype and Schizophrenia. Arch. Gen. Psychiatry 60, 889. https://doi.org/10.1001/archpsyc.60.9.889

Goldman-Rakic, P., 2000. D1 receptors in prefrontal cells and circuits. Brain Res. Rev. 31, 295–301. https://doi.org/10.1016/S0165-0173(99)00045-4

Goldman-Rakic, P.S., 1998. The cortical dopamine system: role in memory and cognition. Adv. Pharmacol. San Diego Calif 42, 707–711.

Good, C.D., Johnsrude, I.S., Ashburner, J., Henson, R.N.A., Friston, K.J., Frackowiak, R.S., 2001. A Voxel-Based Morphometric Study of Ageing in 465 Normal Adult Human Brains. NeuroImage 14, 21–36. https://doi.org/10.1006/nimg.2001.0786

Grossman, M.H., n.d. Chromosomal Mapping of the Human Catechol-0-Methyltransferase Gene to 22qll .I eq11.2 4.

Gujjar, K.R., van Wijk, A., Kumar, R., de Jongh, A., 2019. Efficacy of virtual reality exposure therapy for the treatment of dental phobia in adults: A randomized controlled trial. J. Anxiety Disord. 62, 100–108. https://doi.org/10.1016/j.janxdis.2018.12.001

Haber, S.N., Fudge, J.L., McFarland, N.R., 2000. Striatonigrostriatal Pathways in Primates Form an Ascending Spiral from the Shell to the Dorsolateral Striatum. J. Neurosci. 20, 2369–2382. https://doi.org/10.1523/JNEUROSCI.20-06-02369.2000

Hagen, K., Pettersen, E., Stovner, L.J., Skorpen, F., Holmen, J., Zwart, J.-A., 2007. High Systolic Blood Pressure Is Associated With Val/Val Genotype in the Catechol-O-Methyltransferase Gene: The Nord-Trøndelag Health Study (HUNT). Am. J. Hypertens. 20, 21–26. https://doi.org/10.1016/j.amjhyper.2006.05.023

Hall, C.N., Reynell, C., Gesslein, B., Hamilton, N.B., Mishra, A., Sutherland, B.A., O'Farrell, F.M., Buchan, A.M., Lauritzen, M., Attwell, D., 2014. Capillary pericytes regulate cerebral blood flow in health and disease. Nature 508, 55–60. https://doi.org/10.1038/nature13165

Hamner, M.B., Diamond, B.I., 1993. Elevated plasma dopamine in posttraumatic stress disorder: A preliminary report. Biol. Psychiatry 33, 304–306. https://doi.org/10.1016/0006-3223(93)90302-T

Harrison, P.J., Tunbridge, E.M., 2008. Catechol-O-Methyltransferase (COMT): A Gene Contributing to Sex Differences in Brain Function and to Sexual Dimorphism in the Predisposition to Psychiatric Disorders. Neuropsychopharmacology 33, 3037–3045. https://doi.org/10.1038/sj.npp.1301543

Henckens, M.J.A.G., Hermans, E.J., Pu, Z., Joels, M., Fernandez, G., 2009. Stressed Memories: How Acute Stress Affects Memory Formation in Humans. J. Neurosci. 29, 10111–10119. https://doi.org/10.1523/JNEUROSCI.1184-09.2009

Henckens, M.J.A.G., van Wingen, G.A., Joels, M., Fernandez, G., 2010. Time-Dependent Effects of Corticosteroids on Human Amygdala Processing. J. Neurosci. 30, 12725–12732. https://doi.org/10.1523/JNEUROSCI.3112-10.2010

Henriksen, O.M., Jensen, L.T., Krabbe, K., Guldberg, P., Teerlink, T., Rostrup, E., 2014. Resting Brain Perfusion and Selected Vascular Risk Factors in Healthy Elderly Subjects. PLOS ONE 9, e97363. https://doi.org/10.1371/journal.pone.0097363

Herman, J.P., Figueiredo, H., Mueller, N.K., Ulrich-Lai, Y., Ostrander, M.M., Choi, D.C., Cullinan, W.E., 2003. Central mechanisms of stress integration: hierarchical circuitry controlling hypothalamo–pituitary–adrenocortical responsiveness. Front. Neuroendocrinol. 24, 151–180. https://doi.org/10.1016/j.yfrne.2003.07.001

Herman, J.P., Ostrander, M.M., Mueller, N.K., Figueiredo, H., 2005. Limbic system mechanisms of stress regulation: Hypothalamo-pituitary-adrenocortical axis. Prog. Neuropsychopharmacol. Biol. Psychiatry 29, 1201–1213. https://doi.org/10.1016/j.pnpbp.2005.08.006

Hermans, E.J., Henckens, M.J.A.G., Joëls, M., Fernández, G., 2014. Dynamic adaptation of large-scale brain networks in response to acute stressors. Trends Neurosci. 37, 304–314. https://doi.org/10.1016/j.tins.2014.03.006

Hernaus, D., Collip, D., Lataster, J., Ceccarini, J., Kenis, G., Booij, L., Pruessner, J., Van Laere, K., van Winkel, R., van Os, J., Myin-Germeys, I., 2013. COMT Val158Met Genotype Selectively Alters Prefrontal [18F]Fallypride Displacement and Subjective Feelings of Stress in Response to a Psychosocial Stress Challenge. PLoS ONE 8, e65662. https://doi.org/10.1371/journal.pone.0065662

Hernaus, D., Collip, D., Lataster, J., Viechtbauer, W., Myin, E., Ceccarini, J., Van Laere, K., van Os, J., Myin-Germeys, I., 2015. Psychotic reactivity to daily life stress and the dopamine system: A study combining experience sampling and [^{18}F]fallypride positron emission tomography. J. Abnorm. Psychol. 124, 27–37. https://doi.org/10.1037/abn0000010

Hjelmervik, H., Hausmann, M., Osnes, B., Westerhausen, R., Specht, K., 2014. Resting States Are Resting Traits – An fMRI Study of Sex Differences and Menstrual Cycle Effects in Resting State Cognitive Control Networks. PLoS ONE 9, e103492. https://doi.org/10.1371/journal.pone.0103492

Ho, B.-C., Wassink, T.H., O'Leary, D.S., Sheffield, V.C., Andreasen, N.C., 2005. Catechol-O-methyl transferase Val158Met gene polymorphism in schizophrenia: working memory, frontal lobe MRI morphology and frontal cerebral blood flow. Mol. Psychiatry 10, 287–298. https://doi.org/10.1038/sj.mp.4001616

Hoffman, R., 2004. The effect of acute stress on subsequent neuropsychological test performance (2003). Arch. Clin. Neuropsychol. 19, 497–506. https://doi.org/10.1016/j.acn.2003.07.005

Holsboer, F., 2001. Stress, hypercortisolism and corticosteroid receptors in depression: implicatons for therapy. J. Affect. Disord., KRAEPELIN SPECIAL ISSUE 62, 77–91. https://doi.org/10.1016/S0165-0327(00)00352-9

Holsboer, F., Ising, M., 2010. Stress Hormone Regulation: Biological Role and Translation into Therapy. Annu. Rev. Psychol. 61, 81–109. https://doi.org/10.1146/annurev.psych.093008.100321

Hong, J., Shu-Leong, H., Tao, X., Lap-Ping, Y., 1998. Distribution of catechol-O-methyltransferase expression in human central nervous system: NeuroReport 9, 2861–2864. https://doi.org/10.1097/00001756-199808240-00033

Howes, O.D., Kapur, S., 2009. The Dopamine Hypothesis of Schizophrenia: Version III--The Final Common Pathway. Schizophr. Bull. 35, 549–562. https://doi.org/10.1093/schbul/sbp006

Hsu, D.T., Sanford, B.J., Meyers, K.K., Love, T.M., Hazlett, K.E., Walker, S.J., Mickey, B.J., Koeppe, R.A., Langenecker, S.A., Zubieta, J.-K., 2015. It still hurts: altered opioid activity in the brain during social rejection and acceptance in major depressive disorder. Mol. Psychiatry 20, 193–200. https://doi.org/10.1038/mp.2014.185

Hsu, D.T., Sanford, B.J., Meyers, K.K., Love, T.M., Hazlett, K.E., Wang, H., Ni, L., Walker, S.J., Mickey, B.J., Korycinski, S.T., Koeppe, R.A., Crocker, J.K., Langenecker, S.A., Zubieta, J.-K., 2013. Response of the μ-opioid system to social rejection and acceptance. Mol. Psychiatry 18, 1211–1217. https://doi.org/10.1038/mp.2013.96

Htun, N.C., Miyaki, K., Song, Y., Ikeda, S., Shimbo, T., Muramatsu, M., 2011. Association of the Catechol-O-Methyl Transferase Gene Val158Met Polymorphism With Blood Pressure and Prevalence of Hypertension: Interaction With Dietary Energy Intake. Am. J. Hypertens. 24, 1022–1026. https://doi.org/10.1038/ajh.2011.93

Hyvarinen, A., 1999. Fast and robust fixed-point algorithms for independent component analysis. IEEE Trans. Neural Netw. 10, 626–634. https://doi.org/10.1109/72.761722

Iadecola, C., 2004. Neurovascular regulation in the normal brain and in Alzheimer's disease. Nat. Rev. Neurosci. 5, 347–360. https://doi.org/10.1038/nrn1387

Iadecola, C., 1998. Neurogenic control of the cerebral microcirculation: is dopamine minding the store? Nat. Neurosci. 1, 263–265. https://doi.org/10.1038/1074

Imperato, A., Puglisi-Allegra, S., Casolini, P., Angelucci, L., 1991. Changes in brain dopamine and acetylcholine release during and following stress are independent of the pituitary-

adrenocortical axis. Brain Res. 538, 111–117. https://doi.org/10.1016/0006-8993(91)90384-8

Jabbi, M., Korf, J., Kema, I.P., Hartman, C., van der Pompe, G., Minderaa, R.B., Ormel, J., den Boer, J.A., 2007. Convergent genetic modulation of the endocrine stress response involves polymorphic variations of 5-HTT, COMT and MAOA. Mol. Psychiatry 12, 483–490. https://doi.org/10.1038/sj.mp.4001975

Jenkinson, M., Bannister, P.R., Brady, M., Smith, S.A.C., 2002a. Improved Optimization for the Robust and Accurate Linear Registration and Motion Correction of Brain Images. NeuroImage 17, 825–841. https://doi.org/10.1006/nimg.2002.1132

Jenkinson, M., Bannister, P.R., Brady, M., Smith, S.A.C., 2002b. Improved Optimization for the Robust and Accurate Linear Registration and Motion Correction of Brain Images. NeuroImage 17, 825–841. https://doi.org/10.1006/nimg.2002.1132

Jenkinson, M., Smith, S., 2001. A global optimisation method for robust affine registration of brain images. Med. Image Anal. 5, 143–156. https://doi.org/10.1016/S1361-8415(01)00036-6

Jiang, H., 2003. Human catechol-O-methyltransferase down-regulation by estradiol. Neuropharmacology 45, 1011–1018. https://doi.org/10.1016/S0028-3908(03)00286-7

Joel, D., Weiner, I., 2000. The connections of the dopaminergic system with the striatum in rats and primates: an analysis with respect to the functional and compartmental organization of the striatum. Neuroscience 96, 451–474. https://doi.org/10.1016/S0306-4522(99)00575-8

Jönsson, P., Wallergård, M., Österberg, K., Hansen, Å.M., Johansson, G., Karlson, B., 2010. Cardiovascular and cortisol reactivity and habituation to a virtual reality version of the Trier Social Stress Test: A pilot study. Psychoneuroendocrinology 35, 1397–1403. https://doi.org/10.1016/j.psyneuen.2010.04.003

Joober, R., 2002. Catechol-O-Methyltransferase Val-108/158-Met Gene Variants Associated With Performance on the Wisconsin Card Sorting Test. Arch. Gen. Psychiatry 59, 662–663. https://doi.org/10.1001/archpsyc.59.7.662

Jorga, K., Fotteler, B., Banken, L., Snell, P., Steimer, J.-L., 2000. Population pharmacokinetics of tolcapone in parkinsonian patients in dose finding studies. Br. J. Clin. Pharmacol. 49, 39–48. https://doi.org/10.1046/j.1365-2125.2000.00113.x

Jorga, K.M., 1998. Pharmacokinetics, pharmacodynamics, and tolerability of tolcapone: A review of early studies in volunteers. Neurology 50, S31–S38. https://doi.org/10.1212/WNL.50.5_Suppl_5.S31

Käenmäki, M., Tammimäki, A., Myöhänen, T., Pakarinen, K., Amberg, C., Karayiorgou, M., Gogos, J.A., Männistö, P.T., 2010. Quantitative role of COMT in dopamine clearance in the prefrontal cortex of freely moving mice. J. Neurochem. 114, 1745–1755. https://doi.org/10.1111/j.1471-4159.2010.06889.x

Kajantie, E., Phillips, D., 2006. The effects of sex and hormonal status on the physiological response to acute psychosocial stress. Psychoneuroendocrinology 31, 151–178. https://doi.org/10.1016/j.psyneuen.2005.07.002

Kambeitz, J., Abi-Dargham, A., Kapur, S., Howes, O.D., 2014. Alterations in cortical and extrastriatal subcortical dopamine function in schizophrenia: systematic review and meta-analysis of imaging studies. Br. J. Psychiatry 204, 420–429. https://doi.org/10.1192/bjp.bp.113.132308

Kamide, K., Kokubo, Y., Yang, J., Matayoshi, T., Inamoto, N., Takiuchi, S., Horio, T., Miwa, Y., Yoshii, M., Tomoike, H., Tanaka, C., Banno, M., Okuda, T., Kawano, Y., Miyata, T., 2007. Association of genetic polymorphisms of ACADSB and COMT with human hypertension: J. Hypertens. 25, 103–110. https://doi.org/10.1097/HJH.0b013e3280103a40

Kampmann, I.L., Emmelkamp, P.M.G., Morina, N., 2016. Meta-analysis of technology-assisted interventions for social anxiety disorder. J. Anxiety Disord. 42, 71–84. https://doi.org/10.1016/j.janxdis.2016.06.007

Karhunen, T., Tilgmann, C., Ulmanen, I., Julkunen, I., Panula, P., 1994. Distribution of catechol-O-methyltransferase enzyme in rat tissues. J. Histochem. Cytochem. 42, 1079–1090. https://doi.org/10.1177/42.8.8027527

Keck, M.E., 2006. Corticotropin-releasing factor, vasopressin and receptor systems in depression and anxiety. Amino Acids 31, 241–250. https://doi.org/10.1007/s00726-006-0333-y

Kegeles, L.S., Abi-Dargham, A., Zea-Ponce, Y., Rodenhiser-Hill, J., Mann, J.J., Van Heertum, R.L., Cooper, T.B., Carlsson, A., Laruelle, M., 2000. Modulation of amphetamine-induced striatal dopamine release by ketamine in humans: implications for schizophrenia. Biol. Psychiatry 48, 627–640. https://doi.org/10.1016/S0006-3223(00)00976-8

Kelly, O., Matheson, K., Martinez, A., Merali, Z., Anisman, H., 2007. Psychosocial Stress Evoked by a Virtual Audience: Relation to Neuroendocrine Activity. Cyberpsychol. Behav. 10, 655–662. https://doi.org/10.1089/cpb.2007.9973

Kern, S., Oakes, T.R., Stone, C.K., McAuliff, E.M., Kirschbaum, C., Davidson, R.J., 2008. Glucose metabolic changes in the prefrontal cortex are associated with HPA axis response to a psychosocial stressor. Psychoneuroendocrinology 33, 517–529. https://doi.org/10.1016/j.psyneuen.2008.01.010

Khalili-Mahani, N., Dedovic, K., Engert, V., Pruessner, M., Pruessner, J.C., 2010. Hippocampal activation during a cognitive task is associated with subsequent neuroendocrine and cognitive responses to psychological stress. Hippocampus 20, 323–334. https://doi.org/10.1002/hipo.20623

Khalili-Mahani, N., Dedovic, K., Engert, V., Pruessner, M., Pruessner, J.C., 2009. Hippocampal activation during a cognitive task is associated with subsequent neuroendocrine and cognitive responses to psychological stress. Hippocampus 20, 323–334. https://doi.org/10.1002/hipo.20623

King, A.P., Liberzon, I., 2009. Assessing the neuroendocrine stress response in the functional neuroimaging context. NeuroImage 47, 1116–1124. https://doi.org/10.1016/j.neuroimage.2009.05.055

King, D., Zigmond, M.J., Finlay, J.M., 1997. Effects of dopamine depletion in the medial prefrontal cortex on the stress-induced increase in extracellular dopamine in the nucleus accumbens core and shell. Neuroscience 77, 141–153. https://doi.org/10.1016/S0306-4522(96)00421-6

Kirschbaum, C., Pirke, K.-M., Hellhammer, D.H., 1993. The 'Trier Social Stress Test' – A Tool for Investigating Psychobiological Stress Responses in a Laboratory Setting. Neuropsychobiology 28, 76–81. https://doi.org/10.1159/000119004

Kirschbaum, C., Wüst, S., Strasburger, C.J., 1992. 'Normal' cigarette smoking increases free cortisol in habitual smokers. Life Sci. 50, 435–442. https://doi.org/10.1016/0024-3205(92)90378-3

Kothgassner, O.D., Felnhofer, A., Hlavacs, H., Beutl, L., Palme, R., Kryspin-Exner, I., Glenk, L.M., 2016. Salivary cortisol and cardiovascular reactivity to a public speaking task in a virtual and real-life environment. Comput. Hum. Behav. 62, 124–135. https://doi.org/10.1016/j.chb.2016.03.081

Kozlov, A.P., Druzin, M.Y., Kurzina, N.P., Malinina, E.P., n.d. The Role of D1-Dependent Dopaminergic Mechanisms of the Frontal Cortex in Delayed Responding in Rats 7.

Krimer, L.S., Muly Iii, E.C., Williams, G.V., Goldman-Rakic, P.S., 1998. Dopaminergic regulation of cerebral cortical microcirculation. Nat. Neurosci. 1, 286–289. https://doi.org/10.1038/1099

Kudielka, B.M., Hellhammer, D.H., Wüst, S., 2009. Why do we respond so differently? Reviewing determinants of human salivary cortisol responses to challenge. Psychoneuroendocrinology 34, 2–18. https://doi.org/10.1016/j.psyneuen.2008.10.004

Kudielka, B.M., Kirschbaum, C., 2005. Sex differences in HPA axis responses to stress: a review. Biol. Psychol. 69, 113–132. https://doi.org/10.1016/j.biopsycho.2004.11.009

Kuhlmann, S., 2005. Impaired Memory Retrieval after Psychosocial Stress in Healthy Young Men. J. Neurosci. 25, 2977–2982. https://doi.org/10.1523/JNEUROSCI.5139-04.2005

Kukolja, J., Thiel, C.M., Fink, G.R., 2009. Cholinergic Stimulation Enhances Neural Activity Associated with Encoding but Reduces Neural Activity Associated with Retrieval in Humans. J. Neurosci. 29, 8119–8128. https://doi.org/10.1523/JNEUROSCI.0203-09.2009

Laatikainen, L.M., Sharp, T., Harrison, P.J., Tunbridge, E.M., 2013. Sexually Dimorphic Effects of Catechol-O-Methyltransferase (COMT) Inhibition on Dopamine Metabolism in Multiple Brain Regions. PLoS ONE 8, e61839. https://doi.org/10.1371/journal.pone.0061839

Lachman, H.M., Papolos, D.F., Saito, T., Yu, Y.-M., Szumlanski, C.L., Weinshilboum, R.M., 1996. Human catechol-O-methyltransferase pharmacogenetics: description of a functional polymorphism and its potential application to neuropsychiatric disorders. Pharmacogenetics 6, 243–250.

Lapish, C.C., Ahn, S., Evangelista, L.M., So, K., Seamans, J.K., Phillips, A.G., 2009. Tolcapone enhances food-evoked dopamine efflux and executive memory processes mediated by the rat prefrontal cortex. Psychopharmacology (Berl.) 202, 521–530. https://doi.org/10.1007/s00213-008-1342-1

Lataster, J., Collip, D., Ceccarini, J., Haas, D., Booij, L., van Os, J., Pruessner, J., Van Laere, K., Myin-Germeys, I., 2011. Psychosocial stress is associated with in vivo dopamine release in human ventromedial prefrontal cortex: A positron emission tomography study using [18F]fallypride. NeuroImage 58, 1081–1089. https://doi.org/10.1016/j.neuroimage.2011.07.030

Lederbogen, F., Kirsch, P., Haddad, L., Streit, F., Tost, H., Schuch, P., Wüst, S., Pruessner, J.C., Rietschel, M., Deuschle, M., Meyer-Lindenberg, A., 2011. City living and urban upbringing affect neural social stress processing in humans. Nature 474, 498–501. https://doi.org/10.1038/nature10190

Lee, M.H., Smyser, C.D., Shimony, J.S., 2013. Resting-State fMRI: A Review of Methods and Clinical Applications. Am. J. Neuroradiol. 34, 1866–1872. https://doi.org/10.3174/ajnr.A3263

Lewis, D.A., Melchitzky, D.S., Sesack, S.R., Whitehead, R.E., Auh, S., Sampson, A., 2001. Dopamine transporter immunoreactivity in monkey cerebral cortex: Regional, laminar, and ultrastructural localization. J. Comp. Neurol. 432, 119–136. https://doi.org/10.1002/cne.1092

Li, Y.-H., Wirth, T., Huotari, M., Laitinen, K., MacDonald, E., Männistö, P.T., 1998. No change of brain extracellular catecholamine levels after acute catechol-O-methyltransferase inhibition: a microdialysis study in anaesthetized rats. Eur. J. Pharmacol. 356, 127–137. https://doi.org/10.1016/S0014-2999(98)00524-X

Lidow, M.S., Koh, P.-O., Arnsten, A.F.T., 2003. D1 dopamine receptors in the mouse prefrontal cortex: Immunocytochemical and cognitive neuropharmacological analyses. Synapse 47, 101–108. https://doi.org/10.1002/syn.10143

Liljequist, R., Haapalinna, A., Ahlander, M., Hua Li, Y., Männistö, P.T., 1997. Catechol 0-methyltransferase inhibitor tolcapone has minor influence on performance in experimental memory models in rats. Behav. Brain Res. 82, 195–202. https://doi.org/10.1016/S0166-4328(97)80989-8

Lotta, T., Vidgren, J., Tilgmann, C., Ulmanen, I., Melen, K., Julkunen, I., Taskinen, J., 1995. Kinetics of Human Soluble and Membrane-Bound Catechol O-Methyltransferase: A Revised Mechanism and Description of the Thermolabile Variant of the Enzyme. Biochemistry 34, 4202–4210. https://doi.org/10.1021/bi00013a008

Loughead, J., Wileyto, E.P., Valdez, J.N., Sanborn, P., Tang, K., Strasser, A.A., Ruparel, K., Ray, R., Gur, R.C., Lerman, C., 2009. Effect of abstinence challenge on brain function and cognition in smokers differs by *COMT* genotype. Mol. Psychiatry 14, 820–826. https://doi.org/10.1038/mp.2008.132

Lueken, U., Muehlhan, M., Evens, R., Wittchen, H.-U., Kirschbaum, C., 2012. Within and between session changes in subjective and neuroendocrine stress parameters during magnetic resonance imaging: A controlled scanner training study. Psychoneuroendocrinology 37, 1299–1308. https://doi.org/10.1016/j.psyneuen.2012.01.003

Luethi, M., Meier, B., Sandi, C., 2009. Stress effects on working memory, explicit memory, and implicit memory for neutral and emotional stimuli in healthy men. Front. Behav. Neurosci. 2. https://doi.org/10.3389/neuro.08.005.2008

Lundström, K., Tenhunen, J., Tilgmann, C., Karhunen, T., Panula, P., Ulmanen, I., 1995. Cloning, expression and structure of catechol-O-methyltransferase. Biochim. Biophys. Acta BBA - Protein Struct. Mol. Enzymol. 1251, 1–10. https://doi.org/10.1016/0167-4838(95)00071-2

Lupien, S., Mcewen, B., 1997. The acute effects of corticosteroids on cognition: integration of animal and human model studies. Brain Res. Rev. 24, 1–27. https://doi.org/10.1016/S0165-0173(97)00004-0

Maj, J., Rogóż, Z., Skuza, G., Sowińska, H., Superata, J., 1990. Behavioural and neurochemical effects of Ro 40-7592, a new COMT inhibitor with a potential therapeutic activity in Parkinson's disease. J. Neural Transm. - Park. Dis. Dement. Sect. 2, 101–112. https://doi.org/10.1007/BF02260898

Makara, G.B., 2001. Non-genomic effects of glucocorticoids in the neural system Evidence, mechanisms and implications. Prog. Neurobiol. 24.

Malhotra, A.K., Kestler, L.J., Mazzanti, C., Bates, J.A., Goldberg, T., Goldman, D., 2002. A Functional Polymorphism in the COMT Gene and Performance on a Test of Prefrontal Cognition. Am. J. Psychiatry 159, 652–654. https://doi.org/10.1176/appi.ajp.159.4.652

Marchese, G., Pani, L., 2002. The role of limbic and cortical regions in schizophrenia: Focus on dopamine. Eur. Psychiatry 17, 349–354. https://doi.org/10.1016/S0924-9338(03)00078-6

Markett, S., Montag, C., Heeren, B., Saryiska, R., Lachmann, B., Weber, B., Reuter, M., 2016. Voxelwise eigenvector centrality mapping of the human functional connectome reveals an influence of the catechol-O-methyltransferase val158met polymorphism on the default mode and somatomotor network. Brain Struct. Funct. 221, 2755–2765. https://doi.org/10.1007/s00429-015-1069-9

Matsumoto, M., Weickert, C.S., Akil, M., Lipska, B.K., Hyde, T.M., Herman, M.M., Kleinman, J.E., Weinberger, D.R., 2003. Catechol O-methyltransferase mRNA expression in human and rat brain: evidence for a role in cortical neuronal function. Neuroscience 116, 127–137. https://doi.org/10.1016/S0306-4522(02)00556-0

Mattay, V.S., Goldberg, T.E., Fera, F., Hariri, A.R., Tessitore, A., Egan, M.F., Kolachana, B., Callicott, J.H., Weinberger, D.R., 2003. Catechol O-methyltransferase val158-met genotype and individual variation in the brain response to amphetamine. Proc. Natl. Acad. Sci. 100, 6186–6191. https://doi.org/10.1073/pnas.0931309100

McCullough, A.M., Ritchey, M., Ranganath, C., Yonelinas, A., 2015. Differential effects of stress-induced cortisol responses on recollection and familiarity-based recognition memory. Neurobiol. Learn. Mem. 123, 1–10. https://doi.org/10.1016/j.nlm.2015.04.007

Mcewen, B.S., 2004. Protection and Damage from Acute and Chronic Stress: Allostasis and Allostatic Overload and Relevance to the Pathophysiology of Psychiatric Disorders. Ann. N. Y. Acad. Sci. 1032, 1–7. https://doi.org/10.1196/annals.1314.001

Mcewen, B.S., 1998. Protective and Damaging Effects of Stress Mediators. N. Engl. J. Med. 9.

McEwen, B.S., Gianaros, P.J., 2011. Stress- and Allostasis-Induced Brain Plasticity. Annu. Rev. Med. 62, 431–445. https://doi.org/10.1146/annurev-med-052209-100430

McIntosh, A.M., Baig, B.J., Hall, J., Job, D., Whalley, H.C., Lymer, G.K.S., Moorhead, T.W.J., Owens, D.G.C., Miller, P., Porteous, D., Lawrie, S.M., Johnstone, E.C., 2007. Relationship of Catechol-O-Methyltransferase Variants to Brain Structure and Function in a Population at High Risk of Psychosis. Biol. Psychiatry 61, 1127–1134. https://doi.org/10.1016/j.biopsych.2006.05.020

Meehan, M., Insko, B., Whitton, M., Brooks, F.P., n.d. Physiological Measures of Presence in Stressful Virtual Environments 8.

Meehan, M., Razzaque, S., Insko, B., Whitton, M., Brooks, F.P., 2005. Review of Four Studies on the Use of Physiological Reaction as a Measure of Presence in StressfulVirtual Environments. Appl. Psychophysiol. Biofeedback 30, 239–258. https://doi.org/10.1007/s10484-005-6381-3

Meyer, B.M., Huemer, J., Rabl, U., Boubela, R.N., Kalcher, K., Berger, A., Banaschewski, T., Barker, G., Bokde, A., Büchel, C., Conrod, P., Desrivières, S., Flor, H., Frouin, V., Gallinat, J., Garavan, H., Heinz, A., Ittermann, B., Jia, T., Lathrop, M., Martinot, J.-L., Nees, F., Rietschel, M., Smolka, M.N., Bartova, L., Popovic, A., Scharinger, C., Sitte, H.H., Steiner, H., Friedrich, M.H., Kasper, S., Perkmann, T., Praschak-Rieder, N., Haslacher, H., Esterbauer, H., Moser, E., Schumann, G., Pezawas, L., 2016. Oppositional COMT Val158Met effects on resting state functional connectivity in adolescents and adults. Brain Struct. Funct. 221, 103–114. https://doi.org/10.1007/s00429-014-0895-5

Mier, D., Kirsch, P., Meyer-Lindenberg, A., 2010. Neural substrates of pleiotropic action of genetic variation in COMT: a meta-analysis. Mol. Psychiatry 15, 918–927. https://doi.org/10.1038/mp.2009.36

Minka, T.P., 2001. Automatic Choice of Dimensionality for PCA, in: Leen, T.K., Dietterich, T.G., Tresp, V. (Eds.), Advances in Neural Information Processing Systems 13. MIT Press, pp. 598–604.

Missale, C., Nash, S.R., Robinson, S.W., Jaber, M., Caron, M.G., 1998. Dopamine Receptors: From Structure to Function. Physiol. Rev. 78, 189–225. https://doi.org/10.1152/physrev.1998.78.1.189

Mizrahi, R., Addington, J., Rusjan, P.M., Suridjan, I., Ng, A., Boileau, I., Pruessner, J.C., Remington, G., Houle, S., Wilson, A.A., 2012. Increased Stress-Induced Dopamine Release in Psychosis. Biol. Psychiatry 71, 561–567. https://doi.org/10.1016/j.biopsych.2011.10.009

Moghaddam, B., 2002. Stress activation of glutamate neurotransmission in the prefrontal cortex: implications for dopamine-associated psychiatric disorders. Biol. Psychiatry 51, 775–787. https://doi.org/10.1016/S0006-3223(01)01362-2

Muehlhan, M., Lueken, U., Wittchen, H.-U., Kirschbaum, C., 2011. The scanner as a stressor: Evidence from subjective and neuroendocrine stress parameters in the time course of a functional magnetic resonance imaging session. Int. J. Psychophysiol. 79, 118–126. https://doi.org/10.1016/j.ijpsycho.2010.09.009

Murphy, B.L., Arnsten, A.F.T., Jentsch, J.D., Roth, R.H., 1996. Dopamine and Spatial Working Memory in Rats and Monkeys: Pharmacological Reversal of Stress-Induced Impairment. J. Neurosci. 16, 7768–7775. https://doi.org/10.1523/JNEUROSCI.16-23-07768.1996

Nagano-Saito, A., Dagher, A., Booij, L., Gravel, P., Welfeld, K., Casey, K.F., Leyton, M., Benkelfat, C., 2013. Stress-induced dopamine release in human medial prefrontal cortex- ^{18} F-Fallypride/PET study in healthy volunteers: Stress-Induced Dopamine Release in M PFC. Synapse 67, 821–830. https://doi.org/10.1002/syn.21700

Nagy, T., van Lien, R., Willemsen, G., Proctor, G., Efting, M., Fülöp, M., Bárdos, G., Veerman, E.C.I., Bosch, J.A., 2015. A fluid response: Alpha-amylase reactions to acute laboratory stress are related to sample timing and saliva flow rate. Biol. Psychol. 109, 111–119. https://doi.org/10.1016/j.biopsycho.2015.04.012

Nater, U., Lamarca, R., Florin, L., Moses, A., Langhans, W., Koller, M., Ehlert, U., 2006. Stress-induced changes in human salivary alpha-amylase activity—associations with adrenergic activity. Psychoneuroendocrinology 31, 49–58. https://doi.org/10.1016/j.psyneuen.2005.05.010

Nater, U.M., Rohleder, N., 2009. Salivary alpha-amylase as a non-invasive biomarker for the sympathetic nervous system: Current state of research. Psychoneuroendocrinology 34, 486–496. https://doi.org/10.1016/j.psyneuen.2009.01.014

Nishijima, Y., Akamatsu, Y., Weinstein, P.R., Liu, J., 2015. Collaterals: Implications in cerebral ischemic diseases and therapeutic interventions. Brain Res. 1623, 18–29. https://doi.org/10.1016/j.brainres.2015.03.006

Nnisto, P.T.M., Kaakkola, S., n.d. Catechol-O-methyltransferase (COMT): Biochemistry, Molecular Biology, Pharmacology, and Clinical Efficacy of the New Selective COMT Inhibitors 36.

Nogueira, N.G. de H.M., Bacelar, M.F.B., Ferreira, B. de P., Parma, J.O., Lage, G.M., 2019. Association between the catechol-O-methyltransferase (COMT) Val158Met polymorphism and motor behavior in healthy adults: A study review. Brain Res. Bull. 144, 223–232. https://doi.org/10.1016/j.brainresbull.2018.11.002

Nohesara, S., Ghadirivasfi, M., Mostafavi, S., Eskandari, M.-R., Ahmadkhaniha, H., Thiagalingam, S., Abdolmaleky, H.M., 2011. DNA hypomethylation of MB-COMT promoter in the DNA derived from saliva in schizophrenia and bipolar disorder. J. Psychiatr. Res. 45, 1432–1438. https://doi.org/10.1016/j.jpsychires.2011.06.013

Oei, N.Y.L., Everaerd, W.T.A.M., Elzinga, B.M., van Well, S., Bermond, B., 2006. Psychosocial stress impairs working memory at high loads: An association with cortisol levels and memory retrieval. Stress 9, 133–141. https://doi.org/10.1080/10253890600965773

Ohnishi, T., Hashimoto, R., Mori, T., Nemoto, K., Moriguchi, Y., Iida, H., Noguchi, H., Nakabayashi, T., Hori, H., Ohmori, M., Tsukue, R., Anami, K., Hirabayashi, N., Harada, S., Arima, K., Saitoh, O., Kunugi, H., 2006. The association between the Val158Met polymorphism of the catechol-O-methyl transferase gene and morphological abnormalities of the brain in chronic schizophrenia. Brain 129, 399–410. https://doi.org/10.1093/brain/awh702

Orem, T.R., Wheelock, M.D., Goodman, A.M., Harnett, N.G., Wood, K.H., Gossett, E.W., Granger, D.A., Mrug, S., Knight, D.C., n.d. Amygdala and Prefrontal Cortex Activity Varies With Individual Differences in the Emotional Response to Psychosocial Stress 9.

Ossewaarde, L., Qin, S., Van Marle, H.J.F., van Wingen, G.A., Fernández, G., Hermans, E.J., 2011. Stress-induced reduction in reward-related prefrontal cortex function. NeuroImage 55, 345–352. https://doi.org/10.1016/j.neuroimage.2010.11.068

Oswald, L.M., McCaul, M., Choi, L., Yang, X., Wand, G.S., 2004. Catechol-O-methyltransferase polymorphism alters hypothalamic-pituitary-adrenal axis responses to naloxone: a preliminary report. Biol. Psychiatry 55, 102–105. https://doi.org/10.1016/j.biopsych.2003.07.003

Pacák, K., Palkovits, M., 2001. Stressor Specificity of Central Neuroendocrine Responses: Implications for Stress-Related Disorders. Endocr. Rev. 22, 502–548. https://doi.org/10.1210/edrv.22.4.0436

Palmatier, M.A., Kang, A.M., Kidd, K.K., 1999. Global variation in the frequencies of functionally different catechol-O-methyltransferase alleles. Biol. Psychiatry 46, 557–567. https://doi.org/10.1016/S0006-3223(99)00098-0

Pani, L., Porcella, A., Gessa, G.L., 2000. The role of stress in the pathophysiology of the dopaminergic system. Mol. Psychiatry 5, 14–21. https://doi.org/10.1038/sj.mp.4000589

Papaleo, F., Crawley, J.N., Song, J., Lipska, B.K., Pickel, J., Weinberger, D.R., Chen, J., 2008. Genetic Dissection of the Role of Catechol-O-Methyltransferase in Cognition and Stress Reactivity in Mice. J. Neurosci. 28, 8709–8723. https://doi.org/10.1523/JNEUROSCI.2077-08.2008

Peters, S., Cleare, A.J., Papadopoulos, A., Fu, C.H.Y., 2011. Cortisol responses to serial MRI scans in healthy adults and in depression. Psychoneuroendocrinology 36, 737–741. https://doi.org/10.1016/j.psyneuen.2010.10.009

Peterson, S.M., Furuichi, E., Ferris, D.P., 2018. Effects of virtual reality high heights exposure during beam-walking on physiological stress and cognitive loading. PLOS ONE 13, e0200306. https://doi.org/10.1371/journal.pone.0200306

Petrakova, L., Boy, K., Mittmann, L., Möller, L., Engler, H., Schedlowski, M., 2017. Salivary alpha-amylase and noradrenaline responses to corticotropin-releasing hormone administration in humans. Biol. Psychol. 127, 34–39. https://doi.org/10.1016/j.biopsycho.2017.04.016

Poels, E.M.P., Kegeles, L.S., Kantrowitz, J.T., Slifstein, M., Javitt, D.C., Lieberman, J.A., Abi-Dargham, A., Girgis, R.R., 2014. Imaging glutamate in schizophrenia: review of findings and implications for drug discovery. Mol. Psychiatry 19, 20–29. https://doi.org/10.1038/mp.2013.136

Pruessner, J.C., 2004. Dopamine Release in Response to a Psychological Stress in Humans and Its Relationship to Early Life Maternal Care: A Positron Emission Tomography Study Using [11C]Raclopride. J. Neurosci. 24, 2825–2831. https://doi.org/10.1523/JNEUROSCI.3422-03.2004

Pruessner, J.C., Dedovic, K., Khalili-Mahani, N., Engert, V., Pruessner, M., Buss, C., Renwick, R., Dagher, A., Meaney, M.J., Lupien, S., 2008. Deactivation of the Limbic System During Acute Psychosocial Stress: Evidence from Positron Emission Tomography and Functional Magnetic Resonance Imaging Studies. Biol. Psychiatry 63, 234–240. https://doi.org/10.1016/j.biopsych.2007.04.041

Pruessner, J.C., Hellhammer, D.H., Kirschbaum, C., 1999. Low self-esteem, induced failure and the adrenocortical stress response. Personal. Individ. Differ. 27, 477–489. https://doi.org/10.1016/S0191-8869(98)00256-6

Pruessner, J.C., Kirschbaum, C., Meinlschmid, G., Hellhammer, D.H., 2003. Two formulas for computation of the area under the curve represent measures of total hormone concentration versus time-dependent change. Psychoneuroendocrinology 28, 916–931. https://doi.org/10.1016/S0306-4530(02)00108-7

Qin, S., Cousijn, H., Rijpkema, M., Luo, J., Franke, B., Hermans, E.J., Fernández, G., 2012. The effect of moderate acute psychological stress on working memory-related neural activity is modulated by a genetic variation in catecholaminergic function in humans. Front. Integr. Neurosci. 6. https://doi.org/10.3389/fnint.2012.00016

Ract, C., Vigué, B., Bodjarian, N., Mazoit, J.X., Samii, K., Tadié, M., 2001. Comparison of Dopamine and Norepinephrine after Traumatic Brain Injury and Hypoxic-Hypotensive Insult. J. Neurotrauma 18, 1247–1254. https://doi.org/10.1089/089771501317095287

Raz, N., Daugherty, A.M., Sethi, S.K., Arshad, M., Haacke, E.M., 2017. Age differences in arterial and venous extra-cerebral blood flow in healthy adults: contributions of vascular risk factors and genetic variants. Brain Struct. Funct. 222, 2641–2653. https://doi.org/10.1007/s00429-016-1362-2

Risbrough, V., Ji, B., Hauger, R., Zhou, X., 2014. Generation and Characterization of Humanized Mice Carrying COMT158 Met/Val Alleles. Neuropsychopharmacology 39, 1823–1832. https://doi.org/10.1038/npp.2014.29

Robbins, T.W., 2000. Chemical neuromodulation of frontal-executive functions in humans and other animals. Exp. Brain Res. 133, 130–138. https://doi.org/10.1007/s002210000407

Robinson, T.E., Berridge, second, n.d. The neural basis of drug craving: an ~~~~~tive~sensiti~atiun theory of addiction 45.

Rohleder, N., Wolf, J.M., Maldonado, E.F., Kirschbaum, C., 2006. The psychosocial stress-induced increase in salivary alpha-amylase is independent of saliva flow rate. Psychophysiology 43, 645–652. https://doi.org/10.1111/j.1469-8986.2006.00457.x

Roth, J.A., 1992. Membrane-bound catechol-O-methyltransferase: A reevaluation of its role in the O-methylation of the catecholamine neurotransmitters, in: Reviews of Physiology, Biochemistry and Pharmacology, Volume 120: Volume: 120, Reviews of Physiology, Biochemistry and Pharmacology. Springer Berlin Heidelberg, Berlin, Heidelberg, pp. 1–29. https://doi.org/10.1007/BFb0036121

Roussos, P., Giakoumaki, S.G., Bitsios, P., 2009. Tolcapone Effects on Gating, Working Memory, and Mood Interact with the Synonymous Catechol-O-methyltransferase rs4818C/G Polymorphism. Biol. Psychiatry 66, 997–1004. https://doi.org/10.1016/j.biopsych.2009.07.008

Rowe, J.B., Hughes, L., Williams-Gray, C.H., Bishop, S., Fallon, S., Barker, R.A., Owen, A.M., 2010. The val158met COMT polymorphism's effect on atrophy in healthy aging and Parkinson's disease. Neurobiol. Aging 31, 1064–1068. https://doi.org/10.1016/j.neurobiolaging.2008.07.009

Sanchez-Vives, M.V., Slater, M., n.d. From Presence Towards Consciousness 34.

Sandi, C., 2011. Glucocorticoids act on glutamatergic pathways to affect memory processes. Trends Neurosci. 34, 165–176. https://doi.org/10.1016/j.tins.2011.01.006

Sandi, C., Loscertales, M., Guaza, C., 1997. Experience-dependent Facilitating Effect of Corticosterone on Spatial Memory Formation in the Water Maze. Eur. J. Neurosci. 9, 637–642. https://doi.org/10.1111/j.1460-9568.1997.tb01412.x

Sandi, C., Pinelo-Nava, M.T., 2007. Stress and Memory: Behavioral Effects and Neurobiological Mechanisms. Neural Plast. 2007, 1–20. https://doi.org/10.1155/2007/78970

Sawaguchi, T., Goldman-Rakic, P.S., 1991. DI Dopamine Receptors in Prefrontal Cortex: Involvement in Working Memory 251, 5.

Schoofs, D., Preuß, D., Wolf, O.T., 2008. Psychosocial stress induces working memory impairments in an n-back paradigm. Psychoneuroendocrinology 33, 643–653. https://doi.org/10.1016/j.psyneuen.2008.02.004

Schwabe, L., Joëls, M., Roozendaal, B., Wolf, O.T., Oitzl, M.S., 2012. Stress effects on memory: An update and integration. Neurosci. Biobehav. Rev. 36, 1740–1749. https://doi.org/10.1016/j.neubiorev.2011.07.002

Schwabe, L., Wolf, O.T., Oitzl, M.S., 2010. Memory formation under stress: Quantity and quality. Neurosci. Biobehav. Rev. 34, 584–591. https://doi.org/10.1016/j.neubiorev.2009.11.015

Scornaiencki, R., Cantrup, R., Rushlow, W.J., Rajakumar, N., 2009. Prefrontal cortical D1 dopamine receptors modulate subcortical D2 dopamine receptor-mediated stress responsiveness. Int. J. Neuropsychopharmacol. 12, 1195. https://doi.org/10.1017/S1461145709000121

Seamans, J.K., Floresco, S.B., Phillips, A.G., 1998. D_1 Receptor Modulation of Hippocampal–Prefrontal Cortical Circuits Integrating Spatial Memory with Executive Functions in the Rat. J. Neurosci. 18, 1613–1621. https://doi.org/10.1523/JNEUROSCI.18-04-01613.1998

Seinfeld, S., Bergstrom, I., Pomes, A., Arroyo-Palacios, J., Vico, F., Slater, M., Sanchez-Vives, M.V., 2016. Influence of Music on Anxiety Induced by Fear of Heights in Virtual Reality. Front. Psychol. 6. https://doi.org/10.3389/fpsyg.2015.01969

Sesack, S.R., Hawrylak, V.A., Matus, C., Guido, M.A., Levey, A.I., 1998. Dopamine Axon Varicosities in the Prelimbic Division of the Rat Prefrontal Cortex Exhibit Sparse Immunoreactivity for the Dopamine Transporter. J. Neurosci. 18, 2697–2708. https://doi.org/10.1523/JNEUROSCI.18-07-02697.1998

Simeonov, P.I., Hsiao, H., DotsonM, B.W., Ammons, D.E., 2005. Height Effects in Real and Virtual Environments. Hum. Factors J. Hum. Factors Ergon. Soc. 47, 430–438. https://doi.org/10.1518/0018720054679506

Sin, N.L., Ong, A.D., Stawski, R.S., Almeida, D.M., 2017. Daily positive events and diurnal cortisol rhythms: Examination of between-person differences and within-person variation. Psychoneuroendocrinology 83, 91–100. https://doi.org/10.1016/j.psyneuen.2017.06.001

Smeets, T., Jelicic, M., Merckelbach, H., 2006. The effect of acute stress on memory depends on word valence. Int. J. Psychophysiol. 62, 30–37. https://doi.org/10.1016/j.ijpsycho.2005.11.007

Smith, S.M., 2002. Fast robust automated brain extraction. Hum. Brain Mapp. 17, 143–155. https://doi.org/10.1002/hbm.10062

Smith, S.M., Fox, P.T., Miller, K.L., Glahn, D.C., Fox, P.M., Mackay, C.E., Filippini, N., Watkins, K.E., Toro, R., Laird, A.R., Beckmann, C.F., 2009. Correspondence of the brain's functional architecture during activation and rest. Proc. Natl. Acad. Sci. 106, 13040–13045. https://doi.org/10.1073/pnas.0905267106

Smith, S.M., Jenkinson, M., Woolrich, M.W., Beckmann, C.F., Behrens, T.E.J., Johansen-Berg, H., Bannister, P.R., De Luca, M., Drobnjak, I., Flitney, D.E., Niazy, R.K., Saunders, J., Vickers, J., Zhang, Y., De Stefano, N., Brady, J.M., Matthews, P.M., 2004. Advances in functional and structural MR image analysis and implementation as FSL. NeuroImage 23, S208–S219. https://doi.org/10.1016/j.neuroimage.2004.07.051

Smitha, K., Akhil Raja, K., Arun, K., Rajesh, P., Thomas, B., Kapilamoorthy, T., Kesavadas, C., 2017. Resting state fMRI: A review on methods in resting state connectivity analysis and resting state networks. Neuroradiol. J. 30, 305–317. https://doi.org/10.1177/1971400917697342

Soliman, A., O'Driscoll, G.A., Pruessner, J., Holahan, A.-L.V., Boileau, I., Gagnon, D., Dagher, A., 2008. Stress-Induced Dopamine Release in Humans at Risk of Psychosis: a [11C]Raclopride PET Study. Neuropsychopharmacology 33, 2033–2041. https://doi.org/10.1038/sj.npp.1301597

Stauble, M.R., Thompson, L.A., Morgan, G., 2013. Increases in cortisol are positively associated with gains in encoding and maintenance working memory performance in young men. Stress 16, 402–410. https://doi.org/10.3109/10253890.2013.780236

Steptoe, A., Ussher, M., 2006. Smoking, cortisol and nicotine. Int. J. Psychophysiol. 59, 228–235. https://doi.org/10.1016/j.ijpsycho.2005.10.011

Stewart, S.H., Oroszi, G., Randall, P.K., Anton, R.F., 2009. COMT Genotype Influences the Effect of Alcohol on Blood Pressure: Results From the COMBINE Study. Am. J. Hypertens. 22, 87–91. https://doi.org/10.1038/ajh.2008.321

Sullivan, R.M., Dufresne, M.M., 2006. Mesocortical dopamine and HPA axis regulation: Role of laterality and early environment. Brain Res. 1076, 49–59. https://doi.org/10.1016/j.brainres.2005.12.100

Suridjan, I., Boileau, I., Bagby, M., Rusjan, P.M., Wilson, A.A., Houle, S., Mizrahi, R., 2012. Dopamine response to psychosocial stress in humans and its relationship to individual differences in personality traits. J. Psychiatr. Res. 46, 890–897. https://doi.org/10.1016/j.jpsychires.2012.03.009

Swift-Scanlan, T., Smith, C.T., Bardowell, S.A., Boettiger, C.A., 2014. Comprehensive interrogation of CpG island methylation in the gene encoding COMT, a key estrogen and catecholamine regulator. BMC Med. Genomics 7, 5. https://doi.org/10.1186/1755-8794-7-5

Szöke, A., Schürhoff, F., Méary, A., Mathieu, F., Chevalier, F., Trandafir, A., Alter, C., Roy, I., Bellivier, F., Leboyer, M., 2006. Lack of influence of COMT and NET genes variants on executive functions in schizophrenic and bipolar patients, their first-degree relatives and controls. Am. J. Med. Genet. B Neuropsychiatr. Genet. 141B, 504–512. https://doi.org/10.1002/ajmg.b.30352

Tenhunen, J., Salminen, M., Lundstrom, K., Kiviluoto, T., Savolainen, R., Ulmanen, I., 1994. Genomic organization of the human catechol O-methyltransferase gene and its expression from two distinct promoters. Eur. J. Biochem. 223, 1049–1059. https://doi.org/10.1111/j.1432-1033.1994.tb19083.x

Tenhunen, J., Ulmanen, I., 1993. Production of rat soluble and membrane-bound catechol *O* -methyltransferase forms from bifunctional mRNAs. Biochem. J. 296, 595–600. https://doi.org/10.1042/bj2960595

Tessner, K.D., Walker, E.F., Hochman, K., Hamann, S., 2006. Cortisol responses of healthy volunteers undergoing magnetic resonance imaging. Hum. Brain Mapp. 27, 889–895. https://doi.org/10.1002/hbm.20229

Thomason, M.E., Waugh, C.E., Glover, G.H., Gotlib, I.H., 2009. COMT Genotype and Resting Brain Perfusion in Children. NeuroImage 48, 217–222. https://doi.org/10.1016/j.neuroimage.2009.05.076

Tian, T., Qin, W., Liu, B., Jiang, T., Yu, C., 2013. Functional Connectivity in Healthy Subjects Is Nonlinearly Modulated by the COMT and DRD2 Polymorphisms in a Functional System-

Dependent Manner. J. Neurosci. 33, 17519–17526. https://doi.org/10.1523/JNEUROSCI.2163-13.2013

Tidey, J.W., Miczek, K.A., 1996. Social defeat stress selectively alters mesocorticolimbic dopamine release: an in vivo microdialysis study. Brain Res. 721, 140–149. https://doi.org/10.1016/0006-8993(96)00159-X

Tjandra, T., Brooks, J.C.W., Figueiredo, P., Wise, R., Matthews, P.M., Tracey, I., 2005. Quantitative assessment of the reproducibility of functional activation measured with BOLD and MR perfusion imaging: Implications for clinical trial design. NeuroImage 27, 393–401. https://doi.org/10.1016/j.neuroimage.2005.04.021

Troudet, R., Detrait, E., Hanon, E., Lamberty, Y., 2016. Optimization and pharmacological validation of a set-shifting procedure for assessing executive function in rats. J. Neurosci. Methods 268, 182–188. https://doi.org/10.1016/j.jneumeth.2015.08.012

Tunbridge, E.M., 2004. Catechol-O-Methyltransferase Inhibition Improves Set-Shifting Performance and Elevates Stimulated Dopamine Release in the Rat Prefrontal Cortex. J. Neurosci. 24, 5331–5335. https://doi.org/10.1523/JNEUROSCI.1124-04.2004

Tunbridge, E.M., Farrell, S.M., Harrison, P.J., Mackay, C.E., 2013. Catechol-O-methyltransferase (COMT) influences the connectivity of the prefrontal cortex at rest. Neuroimage 68, 49–54. https://doi.org/10.1016/j.neuroimage.2012.11.059

Tunbridge, E.M., Harrison, P.J., Weinberger, D.R., 2006. Catechol-o-Methyltransferase, Cognition, and Psychosis: Val158Met and Beyond. Biol. Psychiatry 60, 141–151. https://doi.org/10.1016/j.biopsych.2005.10.024

Tuor, U.I., Edvinsson, L., McCulloch, J., 1986. Catecholamines and the relationship between cerebral blood flow and glucose use. Am. J. Physiol.-Heart Circ. Physiol. 251, H824–H833. https://doi.org/10.1152/ajpheart.1986.251.4.H824

Ulrich-Lai, Y.M., Herman, J.P., 2009. Neural Regulation of Endocrine and Autonomic Stress Responses. Nat. Rev. Neurosci. 10, 397–409. https://doi.org/10.1038/nrn2647

Ursini, G., Bollati, V., Fazio, L., Porcelli, A., Iacovelli, L., Catalani, A., Sinibaldi, L., Gelao, B., Romano, R., Rampino, A., Taurisano, P., Mancini, M., Di Giorgio, A., Popolizio, T., Baccarelli, A., De Blasi, A., Blasi, G., Bertolino, A., 2011. Stress-Related Methylation of the Catechol-O-Methyltransferase Val158 Allele Predicts Human Prefrontal Cognition and Activity. J. Neurosci. 31, 6692–6698. https://doi.org/10.1523/JNEUROSCI.6631-10.2011

Vaessen, T., Hernaus, D., Myin-Germeys, I., van Amelsvoort, T., 2015. The dopaminergic response to acute stress in health and psychopathology: A systematic review. Neurosci. Biobehav. Rev. 56, 241–251. https://doi.org/10.1016/j.neubiorev.2015.07.008

van Oort, J., Tendolkar, I., Hermans, E.J., Mulders, P.C., Beckmann, C.F., Schene, A.H., Fernández, G., van Eijndhoven, P.F., 2017. How the brain connects in response to acute stress: A review at the human brain systems level. Neurosci. Biobehav. Rev. 83, 281–297. https://doi.org/10.1016/j.neubiorev.2017.10.015

Varese, F., Smeets, F., Drukker, M., Lieverse, R., Lataster, T., Viechtbauer, W., Read, J., van Os, J., Bentall, R.P., 2012. Childhood Adversities Increase the Risk of Psychosis: A Meta-analysis of Patient-Control, Prospective- and Cross-sectional Cohort Studies. Schizophr. Bull. 38, 661–671. https://doi.org/10.1093/schbul/sbs050

Vijayraghavan, S., Wang, M., Birnbaum, S.G., Williams, G.V., Arnsten, A.F.T., 2007. Inverted-U dopamine D1 receptor actions on prefrontal neurons engaged in working memory. Nat. Neurosci. 10, 376–384. https://doi.org/10.1038/nn1846

Walder, D.J., Trotman, H.D., Cubells, J.F., Brasfield, J., Tang, Y.-L., Walker, E.F., 2010. Catechol-O-methyltransferase modulation of cortisol secretion in psychiatrically at-risk and healthy adolescents: Psychiatr. Genet. 20, 166–170. https://doi.org/10.1097/YPG.0b013e32833a1ff3

Walker, E.F., Diforio, D., 1997. EF, Diforio D. Schizophrenia: a neural diathesis-stress model. Psychol Rev.

Wang, J., Aguirre, G.K., Kimberg, D.Y., Roc, A.C., Li, L., Detre, J.A., 2003. Arterial spin labeling perfusion fMRI with very low task frequency. Magn. Reson. Med. 49, 796–802. https://doi.org/10.1002/mrm.10437

Wardle, M.C., de Wit, H., Penton-Voak, I., Lewis, G., Munafò, M.R., 2013. Lack of Association Between COMT and Working Memory in a Population-Based Cohort of Healthy Young Adults. Neuropsychopharmacology 38, 1253–1263. https://doi.org/10.1038/npp.2013.24

Weerda, R., Muehlhan, M., Wolf, O.T., Thiel, C.M., 2010. Effects of acute psychosocial stress on working memory related brain activity in men. Hum. Brain Mapp. 31, 1418–1429. https://doi.org/10.1002/hbm.20945

Weinshilboum, R., Dunnette, J., 1980. Thermal stability and the biochemical genetics of erythrocyte catechol-O-methyltransferase and plasma dopamine-β-hydroxylase. Clin. Genet. 19, 426–437. https://doi.org/10.1111/j.1399-0004.1981.tb00740.x

Wilhelm, F.H., Pfaltz, M.C., Gross, J.J., Mauss, I.B., Kim, S.I., Wiederhold, B.K., 2005. Mechanisms of Virtual Reality Exposure Therapy: The Role of the Behavioral Activation and Behavioral Inhibition Systems. Appl. Psychophysiol. Biofeedback 30, 271–284. https://doi.org/10.1007/s10484-005-6383-1

Williams, C.L., Men, D., Clayton, E.C., 2000. The effects of noradrenergic activation of the nucleus tractus solitarius on memory and in potentiating norepinephrine release in the amygdala. Behav. Neurosci. 114, 1131–1144. https://doi.org/10.1037//0735-7044.114.6.1131

Williams, G.V., Goldman-Rakic, P.S., n.d. Modulation of memory fields by dopamine D1 receptors in prefrontal cortex 4.

Witte, A.V., Flöel, A., 2012. Effects of COMT polymorphisms on brain function and behavior in health and disease. Brain Res. Bull. 88, 418–428. https://doi.org/10.1016/j.brainresbull.2011.11.012

Woolrich, M.W., Behrens, T.E.J., Beckmann, C.F., Jenkinson, M., Smith, S.M., 2004. Multilevel linear modelling for FMRI group analysis using Bayesian inference. NeuroImage 21, 1732–1747. https://doi.org/10.1016/j.neuroimage.2003.12.023

Woolrich, M.W., Ripley, B.D., Brady, M., Smith, S.M., 2001. Temporal Autocorrelation in Univariate Linear Modeling of FMRI Data. NeuroImage 14, 1370–1386. https://doi.org/10.1006/nimg.2001.0931

Wu, W.-C., Jiang, S.-F., Yang, S.-C., Lien, S.-H., 2011. Pseudocontinuous arterial spin labeling perfusion magnetic resonance imaging—A normative study of reproducibility in the human brain. NeuroImage 56, 1244–1250. https://doi.org/10.1016/j.neuroimage.2011.02.080

Xie, T., Ho, S.-L., Ramsden, D., 1999. Characterization and Implications of Estrogenic Down-Regulation of Human Catechol- *O* -Methyltransferase Gene Transcription. Mol. Pharmacol. 56, 31–38. https://doi.org/10.1124/mol.56.1.31

Xu, G., Rowley, H.A., Wu, G., Alsop, D.C., Shankaranarayanan, A., Dowling, M., Christian, B.T., Oakes, T.R., Johnson, S.C., 2009. Reliability and precision of pseudo-continuous arterial spin labeling perfusion MRI on 3.0 T and comparison with ^{15} O-water PET in elderly subjects at risk for Alzheimer's disease. NMR Biomed. n/a-n/a. https://doi.org/10.1002/nbm.1462

Yavich, L., Forsberg, M.M., Karayiorgou, M., Gogos, J.A., Mannisto, P.T., 2007. Site-Specific Role of Catechol-O-Methyltransferase in Dopamine Overflow within Prefrontal Cortex and Dorsal Striatum. J. Neurosci. 27, 10196–10209. https://doi.org/10.1523/JNEUROSCI.0665-07.2007

Yeh, T.-K., Yeh, T.-C., Weng, C.-F., Shih, B.-F., Tsao, H.-J., Hsiao, C.-H., Chuang, F.-T., Hu, C.-Y., Chang, C.-Y., 2010. Association of polymorphisms in genes involved in the dopaminergic pathway with blood pressure and uric acid levels in Chinese females. J. Neural Transm. 117, 1371–1376. https://doi.org/10.1007/s00702-010-0492-6

Yerkes, R.M., Dodson, J.D., 1908. The relation of strength of stimulus to rapidity of habit-formation. J. Comp. Neurol. Psychol. 18, 459–482. https://doi.org/10.1002/cne.920180503

Zahrt, J., Taylor, J.R., Mathew, R.G., Arnsten, A.F.T., 1997. Supranormal Stimulation of D_1 Dopamine Receptors in the Rodent Prefrontal Cortex Impairs Spatial Working Memory Performance. J. Neurosci. 17, 8528–8535. https://doi.org/10.1523/JNEUROSCI.17-21-08528.1997

Zandara, M., Garcia-Lluch, M., Pulopulos, M.M., Hidalgo, V., Villada, C., Salvador, A., 2016. Acute stress and working memory: The role of sex and cognitive stress appraisal. Physiol. Behav. 164, 336–344. https://doi.org/10.1016/j.physbeh.2016.06.022

Zeng, C., Zhang, M., Asico, L.D., Eisner, G.M., Jose, P.A., 2007. The dopaminergic system in hypertension. Clin. Sci. 112, 583–597. https://doi.org/10.1042/CS20070018

Zhang, N., Gordon, M.L., Ma, Y., Chi, B., Gomar, J.J., Peng, S., Kingsley, P.B., Eidelberg, D., Goldberg, T.E., 2018. The Age-Related Perfusion Pattern Measured With Arterial Spin Labeling MRI in Healthy Subjects. Front. Aging Neurosci. 10. https://doi.org/10.3389/fnagi.2018.00214

Zinkstok, J., Schmitz, N., van Amelsvoort, T., de Win, M., van den Brink, W., Baas, F., Linszen, D., 2006. The COMT val158met polymorphism and brain morphometry in healthy young adults. Neurosci. Lett. 405, 34–39. https://doi.org/10.1016/j.neulet.2006.06.034

Zinkstok, J., Schmitz, N., van Amelsvoort, T., Moeton, M., Baas, F., Linszen, D., 2008. Genetic variation in COMT and PRODH is associated with brain anatomy in patients with schizophrenia. Genes Brain Behav. 0, 070514070132002- https://doi.org/10.1111/j.1601-183X.2007.00326.x

Zubieta, J.-K., 2001. Regional Mu Opioid Receptor Regulation of Sensory and Affective Dimensions of Pain. Science 293, 311–315. https://doi.org/10.1126/science.1060952